Investigation of the formulation, characteristics and performance of polymeric drug carrier particles intended for oral administration

A dissertation submitted for the degree of

Doctor of Philosophy

By

Adam Bohr

Department of Mechanical Engineering

University College London

Torrington Place, London WC1E 7JE

September 2013

Declaration

I, Adam Bohr, confirm that the work presented in this thesis is my own. Where information has been derived from other sources, I confirm that this has been indicated in the thesis.

Adam Bohr

ABSTRACT

Micro- and nanoparticles are being widely investigated for pharmaceutical purposes and are beginning to see application in clinical practice. There are numerous techniques to produce such therapeutic particles, including emulsion-based techniques and spray drying, each with their advantages. Electrospraying provides an alternative technique for preparing drug-loaded particles in the micro-scale with a good control of important particle characteristics, such as size and shape. In this work, electrospraying was used to investigate its potential for producing microparticles intended for oral administration of low solubility drugs. Different processing parameters including flow rate, solute concentration, drug loading and type of solvent and their influence on particle characteristics and drug release were studied using Celecoxib as a model drug and poly(lactic-co-glycolic acid) as a carrier material. The role of solvent mixtures were studied in detail with respect to particle characteristics and drug release kinetics and additional studies were performed for microparticles prepared with Celecoxib and the polymer Hypromellose Acetate Succinate.

The electrosprayed particles were then compared with particles prepared with spray drying using similar experimental conditions and their performance was tested.

Electrosprayed microparticles were prepared with diameters between 2-8 μm and a near-monodisperse size distribution was obtained in most cases. The morphology of the particles ranged from smooth and spherical to rough and non-spherical depending on parameters used and were mainly attributed the evaporation rate and solubility of solute in the solvents. They are different from the spray dried particles which were all smooth, spherical and with a broader size distribution. Electrosprayed particles also showed more porosity and a different drug distribution compared with spray dried particles. The drug molecules were in an amorphous form in particles prepared using both techniques

and remained stable after 8 months of storage. Drug release studies showed differences in release profiles depending on the parametric values. The drug release rates were directly related to the particle size, morphology, porosity and drug distribution observed and hence influenced by the studied process parameters. Spray dried particles generally had a slower drug release rate compared with electrosprayed particles attributed to differences in the particles characteristics observed.

The results indicated that electrospraying is an attractive technique for producing drug loaded microparticles that can be tailored towards an intended drug delivery application. Compared with the more conventional spray drying process it provides better control of particle characteristics and demonstrated its suitability for preparing particle-based solid dispersion formulations in which the drug is molecularly dispersed and is released in a sustained manner to potentially improve oral bioavailability of low solubility drugs.

TABLE OF CONTENTS

ABSTRACT ---------- **I**

TABLE OF CONTENTS ---------- **III**

ACKNOWLEDGEMENTS ---------- **X**

DEDICATION ---------- **XI**

PUBLICATIONS AND CONFERENCE PRESENTATIONS ---------- **XII**

LIST OF TABLES ---------- **XV**

LIST OF FIGURES ---------- **XVI**

LIST OF ABBREVIATIONS ---------- **XXIV**

LIST OF SYMBOLS ---------- **XXVI**

CHAPTER 1 - INTRODUCTION ---------- **1**

1.1 BACKGROUND ---------- 1

1.2 AIMS AND OBJECTIVES OF THIS RESEARCH ---------- 5

1.2.1 General aims ---------- *5*

1.2.2 Specific aims ---------- *6*

1.3 OUTLINE OF THE REPORT ---------- 6

CHAPTER 2 - LITERATURE REVIEW ---------- **8**

2.1 STRATEGIES TO IMPROVE ORAL FORMULATIONS OF POORLY SOLUBLE DRUGS ---------- 8

2.1.1 Introduction to strategies ---------- *8*

2.1.2 Dissolution rate ---------- *9*

2.1.3 Physical strategies ---------- *10*

2.1.4 Chemical strategies ---------- *12*

2.1.5 Formulation strategies ---------- *14*

2.1.6 Solid dispersions ---------- *16*

2.2 PREPARATION OF SOLID DISPERSIONS ---------- 17

2.2.1 Introduction to solid dispersions ----- *17*

2.2.2 Extended release solid dispersions ----- *18*

2.2.3 Methods for preparing solid dispersions ----- *19*

2.2.4 Particulate solid dispersions and particle engineering ----- *22*

2.3 SPRAY DRYING ----- 24

2.3.1 Principles of the spray drying process ----- *24*

2.3.2 Particle formation models for the spray drying process ----- *26*

2.3.3 Particle formation in spray drying ----- *28*

2.3.4 Parameters influencing particle properties in the spray drying process ----- *32*

2.4 ELECTROSPRAYING ----- 32

2.4.1 Principles of the electrospraying process ----- *32*

2.4.2 Cone-jet and spraying modes ----- *33*

2.4.3 Electrospraying setup ----- *36*

2.4.4 Particle formation models for the electrospraying process ----- *37*

2.4.5 Particle formation mechanisms with electrospraying ----- *38*

2.4.6 Parameters influencing jet stability and particle properties ----- *41*

2.4.7 Advantages and disadvantages of electrospraying ----- *47*

2.5 CHALLENGES IN FORMULATING SOLID DISPERSIONS ----- 48

2.5.1 Stability of solid dispersion ----- *48*

2.5.2 Dissolution and in vivo correlation of solid dispersions ----- *52*

2.5.3 Molecular dispersions, homogeneity and drug distribution ----- *55*

2.6 APPLICATIONS OF SPRAY DRYING AND ELECTROSPRAYING ----- 59

2.6.1 Formulation strategies for solid dispersions ----- *59*

2.6.2 Particle-based solid dispersions using spray drying ----- *64*

2.6.3 Control of particle characteristics with spray drying ----- *66*

2.6.4 Electrosprayed solid dispersions ----- *67*

2.6.5 Preparation of the final dosage form ----- *71*

2.7 DRUG RELEASE MODELS ----- 75

2.8 SUMMARY ----- 77

CHAPTER 3 - EXPERIMENTAL DETAILS ---- 78

3.1 MATERIALS ---- 78

3.1.1 Polymers ---- 78

3.1.2 Drug ---- 81

3.1.3 Solvents ---- 82

3.1.4 Miscellaneous materials ---- 84

3.2. PREPARATION AND CHARACTERIZATION OF SOLUTIONS ---- 84

3.2.1 Electrical conductivity: ---- 84

3.2.2 Surface tension measurements ---- 85

3.2.3 Viscosity ---- 85

3.2.4 Properties associated with viscosity ---- 85

3.2.5 Evaporation rate ---- 86

3.2.6 Solubility studies ---- 87

3.3 PARTICLE PREPARATION USING ELECTROSPRAYING ---- 87

3.4 PARTICLE PREPARATION USING SPRAY DRYING ---- 88

3.5 MICRONIZATION AND PREPARATION OF PHYSICAL BLEND ---- 90

3.5.1 Ball milling ---- 90

3.5.2 Physical blend ---- 90

3.6 CHARACTERIZATION OF PARTICLE SIZE AND MORPHOLOGY ---- 90

3.6.1 Size and morphology ---- 90

3.7 INNER STRUCTURE AND POROSITY OF PARTICLES ---- 92

3.8 CRYSTALLINITY AND PHYSICAL FORM OF PARTICLES ---- 93

3.8.1 Differential Scanning Calorimetry ---- 93

3.8.2 X-Ray Powder Diffraction ---- 94

3.8.3 Polarized light microscopy ---- 95

3.9 DRUG PHYSICAL STABILITY ---- 96

3.10 SURFACE CHEMICAL ANALYSIS AND DRUG DISTRIBUTION ---- 96

3.11 DRUG DETECTION ---- 97

3.11.1 Drug detection using UV-Vis spectroscopy and HPLC ---- 97

3.11.2 Drug entrapment efficiency----------*98*

3.12 DRUG RELEASE STUDIES----------98

3.12.1 Initial release study ----------*99*

3.12.2 Paddle drug release study----------*99*

CHAPTER 4 - ELECTROSPRAYING OF SOLID DISPERSIONS: THE INFLUENCE OF PROCESS PARAMETERS AND CONTROL OF PARTICLE CHARACTERISTICS AND DRUG RELEASE----------101

4.1 SELECTION AND CHARACTERIZATION OF DRUG AND CARRIER----------101

4.1.1 Selection and characterization of model drug----------*102*

4.1.2 Selection and characterization of polymer ----------*104*

4.1.3 Physical mixture of CEL and PLGA ----------*106*

4.2 PREPARATION AND CHARACTERIZATION OF SPRAYING SOLUTIONS----------108

4.2.1 Selection of solvent and preparation of solutions ----------*106*

4.2.2 Solubility of CEL and PLGA ----------*109*

4.2.3 Characterization of spraying solutions ----------*109*

4.3 ELECTROSPRAYING OF POORLY WATER-SOLUBLE DRUGS ----------114

4.3.1 Sprayability and particle collection----------*114*

4.3.2 Particle appearance and crystallization----------*115*

4.3.3 Physical form of CEL-loaded particles----------*117*

4.3.4 Comparison with micronized drug----------*120*

4.3.5 Drug release from drug-loaded PLGA particles ----------*121*

4.4 PARAMETRIC STUDY – DESIGN AND SETUP----------123

4.4.1 Design of study----------*123*

4.5 PARAMETRIC STUDY – PARTICLE CHARACTERISTICS----------126

4.5.1 Particle morphology----------*126*

4.5.2 Particle size ----------*131*

4.5.3 System yield and entrapment efficiency ----------*135*

4.5.4 Porosity and inner architecture----------*137*

4.5.5 Solid state form of CEL----------*140*

4.5.6 Physical stability----------*140*

4.6 Parametric Study – Drug release ---- 141

4.6.1 Solubility measurements ---- *141*

4.6.2 Drug release profiles ---- *143*

4.6.3 Drug release models ---- *149*

4.7 Particle elongation ---- 153

4.8 Summary ---- 156

CHAPTER 5 - ELECTROSPRAYING OF SOLID DISPERSIONS: THE INFLUENCE OF MIXED SOLVENT SYSTEMS ON PARTICLE FORMATION, PARTICLE CHARACTERISTICS & CONTROLLED DRUG RELEASE -158

5.1 Mixed solvent study – Characterization of solvents and solutions ---- 158

5.1.1 Selection of solvents ---- *159*

5.1.2 Design of study – solutions and samples ---- *160*

5.1.3 Characterization of spraying solutions ---- *160*

5.2 Mixed solvent study – Particle formation ---- 166

5.3 Mixed solvent study – Particle characteristics ---- 169

5.3.1 Particle size ---- *169*

5.3.2 Particle morphology and porosity ---- *170*

5.3.3 Particles porosity ---- *173*

5.3.4 Physical state of drug ---- *175*

5.4 Mixed solvent study – Drug distribution and Drug release ---- 176

5.4.1 Drug distribution in microparticles ---- *176*

5.4.2 Drug release from microparticles ---- *179*

5.4.3 Summary of study with mixed solvent system ---- *182*

5.5 Water-soluble microparticles – Introduction and setup ---- 184

5.5.1 Introduction to study ---- *184*

5.5.2 Experimental design ---- *185*

5.6 Water-soluble microparticles – Particle characteristics ---- 186

5.6.1 Particle morphology ---- *186*

5.6.2 Physical form of drug ---- *189*

5.6.3 Drug distribution ---- *190*

5.8 WATER-SOLUBLE MICROPARTICLES – DRUG RELEASE ---- 193

5.9 SUMMARY ---- 197

CHAPTER 6 - SPRAY DRYING OF SOLID DISPERSIONS: THE INFLUENCE OF MIXED SOLVENT SYSTEMS ON PARTICLE CHARACTERISTICS AND COMPARISONS WITH ELECTROSPRAYING ---- 199

6.1 SPRAY DRYING AND PARTICLE PREPARATION ---- 199

6.1.1 Introduction to setup and conditions with spray drying ---- 200

6.1.2 Spray drying of CEL-loaded PLGA particles – solutions and setup ---- 201

6.1.3 Characteristics of particles ---- 202

6.1.4 Drug release from microparticles ---- 206

6.2. SPRAY DRYING MIXED SOLVENT STUDY AND SOLUTION CHARACTERISTICS ---- 208

6.2.1 Introduction to spray drying of mixed solvent systems ---- 208

6.2.2 Setup and sample preparation ---- 208

6.2.3 Solubility and polymer configuration ---- 209

6.2.4 Evaporation study ---- 210

6.3 CHARACTERISTICS OF SPRAY DRIED PARTICLES ---- 213

6.3.1 Drug entrapment and moisture content of particles ---- 213

6.3.2 Morphology and size of particles ---- 213

6.3.3 Inner structure and porosity ---- 216

6.3.4 Solid state characterization of particles ---- 218

6.3.5 Drug distribution in particles ---- 220

6.4 DRUG RELEASE FROM SPRAY DRIED PARTICLES ---- 220

6.5 COMPARISON OF SPRAY DRIED AND ELECTROSPRAYED PARTICLES ---- 224

6.5.1 Particle size and size distribution ---- 224

6.5.2 Morphology and Porosity of particles ---- 226

6.5.3 Solid state characteristics of the particle based solid dispersions ---- 229

6.5.4 Drug distribution in particles ---- 231

6.5.5 Drug release ---- 233

6.6 ADDITIONAL REMARKS ON ELECTROSPRAYING AND SPRAY DRYING ---- 235

CHAPTER 7 - CONCLUSIONS AND FUTURE WORK ---------- 238

7.1 CONCLUSIONS ---------- 238

7.1.1 Electrospraying of solid dispersions ---------- 239

7.1.2 Parametric study on particle characteristics ---------- 239

7.1.3 Mixed solvent studies with electrospraying ---------- 242

7.1.4 Spray dried microparticles and comparisons with electrospraying ---------- 243

7.2 FUTURE WORK ---------- 246

7.2.1 Further investigation of the electrospraying particle formation process – A droplet study. - 246

7.2.2 Electrospraying of protein drugs and control of drug distribution. ---------- 247

7.2.3 Drug release kinetics from particles loaded with different drug molecules. ---------- 249

7.2.4 Drug transport studies and cellular uptake from microparticles ---------- 249

REFERENCES ---------- 251

ACKNOWLEDGEMENTS

I wish to thank my primary supervisor Prof. Mohan Edirisinghe as well as my secondary supervisor Dr. Eleanor Stride for their help, support and supervision during my project. I have been fortunate to have very knowledgeable supervisors during my PhD project and would like to especially acknowledge them for their time and effort putting together this project.

I further thank my two industrial supervisors Dr. Jakob Kristensen and Dr. Mark Dyas for their time and effort in this research project and would like to acknowledge their enthusiasm, support and guidance along the way.

I also want to thank the collaborators at the University of Copenhagen for letting me use their facilities during my time as a visiting student. I thank Dr. Mingshi Yang for providing knowledge on spray drying and letting me use their spray dryer, Dorthe Oerbaek for helping me out with different experimental methods and Professor Jukka Rantanen for letting me use their laboratory facilities in general.

I am grateful to the technicians Liselotte Hansen, Katja Hansen, Rikke Gormsen and Anne Raschkewitz as well as other colleagues at Veloxis Pharmaceuticals for all their help in using equipment and for their good company during my time at Veloxis. I wish to thank Dr. Steven Firth and Dr. Suguo Huo from UCL for helping me out with measurements using DSC and FIB-SEM, respectively. I would like to thank my colleagues and fellow PhD students at UCL for support and good company during my project.

Further, I thank the Danish Agency for Science, Technology and Innovation and Veloxis Pharmaceuticals A/S for financial support of this project. Lastly, I would like to thank My mother, father, sister, my girlfriend Sylvie and my friends who have given me support during my PhD studies.

DEDICATION

This dissertation is dedicated to

my loving parents, Yayoi and Henrik Bohr

and

my dear friend Simon Hede who passed away

during the preparation of this dissertation

PUBLICATIONS AND CONFERENCE PRESENTATIONS

Peer-reviewed journal papers:

1. Bohr A., Kristensen J., Stride E., Dyas M., and Edirisinghe M. (2011), Preparation of microspheres containing low solubility drug compound by electrohydrodynamic spraying. International Journal of Pharmaceutics, 412(1-2), 59-67.

2. Bohr A., Kristensen J., Dyas M., Edirisinghe M., and Stride E. (2012), Release profile and characteristics of electrosprayed particles for oral delivery of a practically insoluble drug. Journal of Royal Society Interface, 9, 2437-2449.

3. Bohr A., Yang M., Baldursdóttir S., Kristensen J., Dyas M., Stride E., and Edirisinghe M. (2012). Particle formation and characteristics of Celecoxib-loaded poly(lactic-co-glycolic acid) microparticles prepared in different solvents using electrospraying. Polymer. 53(15), 3053-3416.

4. Wan F.*, Bohr A.*, Maltesen MJ., Bjerregaard S., Foged C., Rantanen J., Yang M. (2012), Critical solvent properties affecting the particle formation process and characteristics of celecoxib-loaded PLGA microparticles via spray drying. Pharmaceutical Research 30, 1065-1076. * Co-first author

5. Bohr A., Boetker JP., Rades T., Rantanen J., Yang M. (2013), Application of spray drying and electrospraying/electrospinning for poorly water-soluble drugs: a particle engineering approach (Review article). Current Pharmaceutical Design, (In press).

Submitted journal papers:

- Bohr A., Wan F., Yang M., Kristensen J., Dyas M., Stride E., Baldursdòttir S., Edirisinghe M. (2013), Pharmaceutical microparticle engineering with electrospraying: the role of mixed solvent systems in particle formation and characteristics. (submitted to Pharmaceutical Research).

Peer reviewed conference proceedings:

- Bohr A., Edirisinghe M., Wan F., Kristensen J., Stride E., Yang M. (2012), Characteristics and drug release of drug-loaded microparticles prepared with different solvents using electrospraying. Proceedings of the 2nd Electron. Conf. Pharm. Sci.

Conference presentations:

- Bohr A., Kristensen J., Stride E., Dyas M., and Edirisinghe M. Microspheres with low solubility drug prepared by electrospraying. PhD Forum, Department of Mechanical Engineering, UCL, London, UK, Jun 2011. (oral presentation)

- Bohr A., Kristensen J., Stride E., Dyas M., and Edirisinghe M. Characteristics of electrosprayed microspheres containing low solubility drug. Pharmaceutical Solid State Research Cluster (PSSRC), Helsinki, Finland, Sep 2011. (oral presentation)

- Bohr A., Kristensen J., Stride E., Dyas M., Rantanen J., and Edirisinghe M. Electrospraying of Poly lactic-co-glycolic acid (PLGA) microspheres loaded with a BCS class II drug and optimization of the process conditions. American Association for Pharmaceutical Scientists (AAPS), Washington DC, USA, Oct 2011. (poster presentation)

- Bohr A., Kristensen J., Stride E., Dyas M., and Edirisinghe M. Drug-loaded microparticles prepared with different solvents using electrospraying. PhD Forum, Department of Mechanical Engineering, UCL, London, UK, Jun 2012. (oral presentation)

- Bohr A., Wan F., Kristensen J., Edirisinghe M., Yang M. Influence of solvents on the characteristics and drug release of microparticles prepared using electrospraying. Controlled Release Society Annual Meeting, Quebec, Canada, Jul 2012. (poster presentation)

- Bohr A., Kristensen J., Stride E., Dyas M., and Edirisinghe M. Characteristics of electrosprayed microspheres containing low solubility drug. Pharmaceutical Solid State Research Cluster (PSSRC), Lisbon, Portugal, Aug 2012. (oral presentation)

LIST OF TABLES

Table 3.1 Properties of solvents used for atomization of solutions. Values obtained from [Smallwood 1996]. 83

Table 4.1 Physical properties of solvents used to fabricate microparticles [Smallwood 1996]. * Relative to the evaporation rate of Butyl Acetate. 108

Table 4.2 Solubility of CEL and PLGA in solvents used in the study. 109

Table 4.3 Properties of solvents and solutions containing CEL or PLGA. 110

Table 4.4 Intrinsic viscosity and Martin constant of PLGA solutions. 112

Table 4.5 List of microparticle samples prepared. 125

Table 4.6 Characteristics of particle samples. 132

Table 4.7 Solubility of CEL in phosphate buffer containing different conc. of SLS… 142

Table 5.1 Physical properties of the solvents used to fabricate microparticles. Values in italic are adapted from [Smallwood 1996]. 159

Table 5.2 List of microparticle samples prepared. 161

Table 5.3 Electrical conductivity of solutions containing CEL or PLGA. 161

Table 5.4 Viscosity related properties of PLGA solutions with different solvent ratios. 163

Table 5.5 Particle samples prepared and their size, size distribution and drug entrapment efficiency. 170

Table 5.6. Surface chemical composition of CEL-loaded PLGA microparticles prepared at different drug loadings and with different solvent ratios. 177

Table 5.7 List of CEL-loaded HPMCAS microparticle samples prepared. 186

Table 5.8 Surface chemical composition of CEL-loaded HPMCAS microparticles prepared at different drug loadings and with different solvent ratios. 191

Table 5.9 Solubility of CEL and HPMCAS in solvent mixtures. Values are based on solutions with approximately 5% solute concentration and 20% CEL loading……192

Table 6.1 Composition of feed solutions spray dried and the operational values applied. 202

Table 6.2 Overview of solutions used for spray drying and their characteristics. 209

Table 6.3 Composition of feed solutions and physicochemical properties of CEL-loaded PLGA microparticles (5% solid concentration, 10% drug loading). Results denote mean ± SD (n = 3). 214

Table 6.4 Surface drug concentration of electrosprayed and spray dried particle samples prepared with 10% drug loading using solvent mixtures of ACE and MeOH.....232

LIST OF FIGURES

Figure 2.1 General spray drying setup and jetting process. 25

Figure 2.2 The drying stages of a liquid droplet with single solute and single solvent. 30

Figure 2.3 Overview of electrospraying atomization modes (A) adapted from [Jaworek and Krupa 1999] and illustration of cone-jet mode captured with CCTV camera (B)...34

Figure 2.4 General electrospraying setup with droplet formation, where *i* indicates the direction of the electric current, which is in the *nA* range, and *HV* is the high voltage power source with an electric potential, *U*, of several kV. 35

Figure 2.5 Schematic representation of forces in the liquid cone (A) (adapted from [Hartman *et al.* 1999b]) and axisymmetric (B) and lateral (C) instabilities of the liquid jet (adapted from [Cloupeau and Prunet-Foch 1994]). 39

Figure 2.6 Particle formation stages of droplets composed of a single solute and a single solvent, during electrospraying.....40

Figure 2.7 Encapsulation via Co-axial spraying (A) (adapted from [Jaworek 2008]), biphasic jetting via dual capillary (B) (adapted from [Roh *et al.* 2005]) and sketch of particles ideally formed by single (a), co-axial (b) and bi-phasic jet (c). 43

Figure 2.8 Representation of supersaturation in different systems, aqueous drug concentration versus time profile. 1: dissolution of pure crystalline drug, 2: dissolution of amorphous solid dispersion and 3: dissolution of amorphous solid dispersion under presence of precipitation inhibitor(s) (from [Warren et al. 2010]). 63

Figure 2.9 Example of spray dried particulate solid dispersions prepared using Netilmicin sulphate (A) [Vehring *et al.* 2007] and HPMC-AS with AMG 517 (B) [Kennedy *et al.* 2008].....65

Figure 2.10 Electrosprayed particles prepared with PCL (A) and PLGA (B) loaded with paclitaxel indicating different morphology [Xie *et al.* 2006b]. 70

Figure 2.11 High and low magnification SEM images of electrospun solid dispersion fibres composed from PVP K30 and ibuprofen (from [Yu *et al.* 2009]. 71

Figure 2.12 Multiple jet electrospraying setup built using a nozzle array system (A) (adapted from [Deng *et al.* 2006]) and a multi-hole injector (B) (adapted from [Bocanegra *et al.* 2005]).....75

Figure 3.1 Chemical structures of PLGA and its building blocks. 79

Figure 3.2 Chemical structure of HPMCAS (A) and chemical structure of CEL (B). ..80

Figure 3.3 XRD diffractogram of CEL crystal form I (A), II (B) and III (C). From [Chawla *et al.* 2003, Lu *et al.* 2006] 81

Figure 3.4 Schematic diagram of electrospraying setup (A), photographs of samples collected on aluminium foil (B) and in a glass vial (C). 88

Figure 3.5 Picture of Buchi spray dryer (A) and schematic image of spray drying mechanism (B) (adapted from Buchi B-290 catalogue). 89

Figure 3.6 Schematic view of inert loop closed circuit.....89

Figure 3.7 Sotax dissolution tester with 6 vessels. 100

Figure 4.1 Optical micrograph of crystalline CEL 102

Figure 4.2 DSC thermogram of CEL indicating melting endotherm. 103

Figure 4.3 XRPD spectrogram showing profile of crystalline CEL. 103

Figure 4.4 DSC thermogram of PLGA indicating glass transition event 105

Figure 4.5 XRPD spectrogram of PLGA. 106

Figure 4.6 DSC thermogram of PLGA and CEL physical mixtures at 1:4 ratio (A) and 1:1 ratio (B) indicating melting endotherm. 107

Figure 4.7 XRPD diffractogram of PLGA and CEL physical mixture. 107

Figure 4.8 Specific viscosity of ACE and ACN solutions as a function of PLGA concentration, including intrinsic viscosity (intercept with y-axis). 112

Figure 4.9 Evaporation of solutions at 25 ºC (A) and first derivative of evaporation curve (B) 113

Figure 4.10 Video camera image of stable cone-jet (A), microscopy image of PLGA particles on a glass slide (B) and particle drying and yield as a function of collection distance (C). 114

Figure 4.11 SEM images of CEL particles collected on glass slides without water (A and B) and with a thin layer of water (C) 115

Figure 4.12 SEM images of CEL-loaded PLGA particles prepared in ACE with varying drug loading. 0% CEL (A), 10% CEL (B), 20% CEL (C), 50% CEL (D) and SEM images of electrosprayed PLGA particles taken with low magnification (E). 116

Figure 4.13 Size distribution of electrosprayed PLGA microparticles prepared with 50% (A), 20% (B), 10% (C) and 0% drug loading (D) 117

Figure 4.14 DSC thermograms of unprocessed CEL powder (A), electrosprayed CEL microparticles (B), CEL-loaded PLGA microparticles prepared in ACE with 50% (C), 20% (D), 10% (E) and 0% (F) CEL-loading. 119

Figure 4.15 SEM image of ball milled CEL (A) and XRPD of ball milled CEL (B). . 121

Figure 4.16 Release of CEL from particles with 50% (solid line), 20% (dashed line) and 10% (dotted line) drug loading. Error bars indicate standard deviation from UV measurements. 123

Figure 4.17 Representative SEM images of different microparticle samples prepared in ACN: Samples N1(A), N2(B), N3(C), N4(D), N5(E), N6(F), N7(G), N8(H), N9(I), close-up of sample N3(J) and overview of sample N5(K). 127

Figure 4.18 Representative SEM images of different microparticle samples prepared in ACE: Samples A1(A), A2(B), A3(C), A4(D), A5(E), A6(F), A7(G), A8(H), A9(I), overview of sample A5(J). 128

Figure 4.19 Atomic Force Microscopy images of samples N2 (A) and A2 (B). 131

Figure 4.20 Mean diameter of particles prepared at different flow rates (A, B), solute concentrations (C) and drug loading (D, E). Error bars indicate standard deviation from the mean. 133

Figure 4.21 EDX spectra of a single CEL-loaded PLGA microparticle (A) and a blank area of same size beside the particle (B). Carbon peaks were cropped due to their height. 137

Figure 4.22 FIB/SEM images of microparticles showing the cross-sectional structure of sample N6 before (A) and after (B, C) milling, sample N5 (D), sample N2 (E), sample N1 (F), sample A5 (G) and sample A2 (H, I), sample A10 (J), and FIB beam images of samples N6 (K) and A10 (L). 138

Figure 4.23 XRPD diffractograms of particle samples prepared using electrospraying at different parametric conditions. Samples N1 (A), N2 (B), N4 (C), N5 (D), N6 (E), N7 (F). 140

Figure 4.24 XRPD diffractograms of microparticles taken during 8 months of storage. 141

Figure 4.25 Drug release profile of microparticles prepared with 5% solute concentrations, with 20% drug loading using ACE, measured over 24 hours in release medium with and without SLS. 143

Figure 4.26 Drug release profile of microparticles prepared with different solute concentrations, with 10% drug loading and at a flow rate of 30 µl/min, measured over 24 hours. Error bars indicate standard deviation. 144

Figure 4.27 Drug release profile of microparticles prepared with different drug loading at a flow rate of 30 µL/min, measured over 24 hours. 144

Figure 4.28 Drug release profile of microparticles prepared with ACN and with 7% solute concentration and 10% CEL at different flow rates measured over 24 hours. ... 145

Figure 4.29 Drug release profile of microparticles prepared with ACE at different solute conc. at a flow rate of 30 µL/min and 10% CEL 147

Figure 4.30 Drug release profile of microparticles prepared with ACN or ACE at 3% solute conc. and 10% or 30% CEL measured over 20 hours. 148

Figure 4.31 Drug release profile of microparticles prepared with ACN or ACE at 3% solute concentration and 10% or 30% CEL measured over 20 hours. 148

Figure 4.32 Selected drug release curves fitted to the Higuchi model. 150

Figure 4.33 Selected drug release curves fitted to the Higuchi model. 150

Figure 4.34 Selected drug release curves fitted to the modified Higuchi model. 151

Figure 4.35 A droplet (radius, 24 µm) during Coulomb instability elongates and fires lateral jets and returns to its original spherical shape. Images taken at time (in µs) 140 (A), 150 (B), 155 (C), 160 (D), 180 (E) and 210 (F) [Duft *et al.* 2003]. 154

Figure 4.36 Elongated particles produced from Titanium oxides using sol-gel reaction to capture shape during Coulomb instability [Adams and Brantner 2010]. 154

Figure 4.37 SEM images of particles prepared at 9% solute concentration (A, B) and particles prepared at 10% solute concentration (C, D, E). 155

Figure 5.1 Specific viscosity / PLGA concentration of spraying solutions plotted as a function of PLGA concentration. 162

Figure 5.2 Evaporation of solvent mixtures (A) and solutions (B) at 25 ºC and the first derivative of the evaporation curve for solvents (C) and solutions (D). 166

Figure 5.4 SEM images of microparticle samples, 10D100:0 (A), 10D90:10 (B), 10D75:25 (C), 10D69:31 (D), 20D100:0 (E), 20D90:10 (F), 20D75:25 (G), 20D69:31 (H) and overview of 10D100:0 (I). 171

Figure 5.5 Close-up SEM images of microparticle samples, 10D100:0 (A), 10D90:10 (B), 10D75:25 (C) and 10D69:31 (D). 172

Figure 5.6 FIB/SEM images of microparticles at progressing sections, samples 10D100:0 (A), 10D90:10 (B), 10D75:25 (C) and 10D69:31 (D). 174

Figure 5.7 XRPD patterns of pure CEL, PLGA and the physical mixture of these (A) and CEL-loaded PLGA microparticles prepared with different solvent ratios at 10% drug loading (B). 175

Figure 5.9 Drug release profile of microparticle samples 20D100:0, 20D90:10, 20D75:25, 20D69:31. 180

Figure 5.10 Representative SEM images of Electrosprayed microparticles loaded with 20% (w/w) CEL taken after drug release studies. Images represent samples 20D100:0 (A), 20D90:10 (B), 20D75:25 (C) and 20DD69:31 (D). 182

Figure 5.11 Particle formation process for solutions containing MeOH (A) and solution consisting of only ACE (B). 183

Figure 5.12 Representative SEM images of different microparticle samples: Samples AE100:0 (A), AE95:5 (B), AE85:15 (C), AE65:35 (D), AH95:5 (E), AH85:15 (F), AH65:35 (G), EH85:15 (H), EH65:35 (I), AEH70:15:15 (J), AEH50:25:25 (K), overview of sample AE85:15 (L) and overview of sample AH95:5 (M). 188

Figure 5.13 XRPD patterns of electrosprayed CEL-loaded HPMCAS particle samples, AE100:0 (A), AE95:05 (B), AE85:15 (C), AE65:35 (D), AH95:5 (E), AH85:15 (F), AH65:35 (G), EH85:15 (H), EH65:35 (I), AEH70:15:15 (J) and AEH50:25:25 (K). .189

Figure 5.14 DSC curves of selected CEL-loaded HPMCAS particles. 190

Figure 5.15 Drug release curves of CEL-loaded HPMCAS particles in H_2O. The smaller insert Figure shows drug release over a longer time interval.....194

Figure 5.16 Drug release curves of CEL-loaded HPMCAS particles and in phosphate buffer pH 6.8. 195

Figure 5.17 Drug release curves of CEL-loaded HPMCAS particles in phosphate buffer (pH 6.8) + 0.5% SLS.....196

Figure 6.1 Particles prepared with ACE at 3 ml/min and 40 ºC outlet temperature. ...201

Figure 6.2 Representative SEM images of spray dried microparticles prepared in ACN (A, B) and ACE (C, D) prepared with an outlet temperature of 30 ºC. 203

Figure 6.3 FIB/SEM images of spray dried microparticles prepared in ACN. The numbers indicate progression through the sample. 204

Figure 6.4 FIB/SEM images of spray dried microparticles prepared in ACE. The numbers indicate progression through the sample. 204

Figure 6.5 DSC curves of spray dried particles, prepared in ACE (A) and ACN (B). 205

Figure 6.6 XRPD curves of spray dried particles prepared in ACE (A) and ACN (B). 206

Figure 6.7 Drug release profile of microparticles prepared with 5% solute concentration and 20% drug loading in ACE or ACN, using spray drying and electrospraying, measured over 20 hours. Error bars indicate the standard deviation from the mean. ...207

Figure 6.8 Estimation of the evaporation rates of the pure solvent mixtures (A) and the spraying solutions (B) performed at 30 °C. Results denote mean values for evaporation rate (n = 3). 210

Figure 6.9 Representative SEM images of spray dried PLGA microparticles loaded CEL, samples SD100:0 (A), SD90:10 (B), SD75:25 (C) and SD69:31 (D). 215

Figure 6.10 Viscosity of PLGA solutions with different solvent ratios as a function of concentration 216

Figure 6.11 Representative FIB/SEM images of PLGA microparticles loaded with 10% (w/w) CEL, samples SD100:0 (A, C), SD90:10 (B, D), SD75:25 (E) and SD69:31 (F). 217

Figure 6.12 DSC thermogram of spray dried microparticles with 10% (w/w) CEL, samples SD100:0 (A), SD90:10 (B), SD75:25 (C) and SD69:31 (D). 219

..... 219

Figure 6.13 Representative XRPD profiles (B) of CEL-loaded microparticles with 10% (w/w) CEL, samples SD100:0, SD90:10, SD75:25 and SD69:31. 219

Figure 6.14 Drug release profile of spray dried microparticles prepared with different solvent ratios at 5% solute conc. and 10% drug loading, in phosphate buffer (pH 6.8) + 1.5% SLS, measured over 20 hours. Error bars indicate standard deviation (n=3-4).. 222

Figure 6.15 SEM images of spray dried microparticles after drug release in phosphate buffer + 1.5% SLS, samples SD100:0 (A), SD90:10 (B), SD75:25 (C) and SD69:31 (D). 222

Figure 6.16 Drug release curves of electrosprayed and spray dried particles prepared with 5% solute concentration and 10% drug loading using ACN or ACE. 234

Figure 7.1 Caco-2 transwell plate (From Corning.com) (A) and sketch of components in a single well (B). 250

LIST OF ABBREVIATIONS

ACE	Acetone
ACN	Acetonitrile
AFM	Atomic force microscopy
API	Active pharmaceutical ingredient
$AUC_{0 \rightarrow \infty}$	Area under the concentration time curve
B_t	Cumulative drug released as a function of time t
BSA	Bovine serum albumin
c*	Chain overlap concentration
C_{max}	Maximum drug concentration
CEL	Celecoxib
Conc.	Concentration
COX-II	Cyclooxygenase-2
CD	Cyclodextrin
DC	Direct current
DCM	Dichloromethane
DMSO	Dimethyl sulphoxide
DSC	Differential scanning calorimetry
EDX	Energy Dispersive X-ray spectroscopy
EE	Entrapment efficiency
ELP	Elastine-like polypeptide
FDA	United States Food and Drug Administration
FIB/SEM	Focused ion beam / scanning electron microscopy
FTIR	Fourier-transform infrared spectroscopy
GI	Gastrointestinal
H-bond	Hydrogen bond
HPLC	High performance liquid chromatography
HPMC	Hydroxypropylmethylcellulose
HPMCAS	Hydroxypropylmethylcellulose acetate succinate
Hv	High voltage
Hz	Hertz
IR	Infrared
K_H	Higuchi release constant

K_m	Martin constant
kV	Kilovolt
mA	Milliampere
nA	Nanoampere
NaOH	Sodium hydroxide
NaH_2PO_4	Sodium-Di-Hydrogen-Phosphate
NIR	Near-infrared
NMR	Nuclear magnetic resonance
NSAID	Non-steroid anti-inflammatory drug
MW	Molecular weight
Pe	Peclet number
pA	Picoampere
PEG	Polyethylene glycol
PLGA	Poly(lactic-co-glycolic acid)
PVP	Polyvinyl pyrrolidone
QbD	Quality by Design
Q_R	Rayleigh limit
RP-HPLC	Reverse phase HPLC
RPM	Revolutions per minute
SIF	Simulated intestinal fluid
Std Dev	Standard deviation
SLS	Sodium lauryl sulphate
SEM	Scanning electron microscopy
SLN	Solid lipid nanoparticles
SEDDS	self-emulsifying drug delivery systems
T_g	Glass transition temperature
T_m	Melting (fusion) temperature
TEM	Transmission electron microscopy
TGA	Thermo gravimetric analysis
UV	Ultraviolet
v/v	Volume over volume
w/v	Weight over volume
w/o	Water-in-oil
XPS	X-ray photoelectron spectroscopy

XRPD	X-ray powder diffraction
ε_0	Liquid to vacuum permittivity ratio

LIST OF SYMBOLS

A	Surface area
C	Concentration
d	Diameter
D	Diffusion coefficient
G	Dissolution rate
h	Thickness of the surface boundary layer
i	Electrical current
P	Pressure
Q	Electric charge
r	Radius
S	Siemens
t	Time
T	Temperature
U	Electrical potential
v	Volume
w	Weight
Ø	Diameter of jet
γ	Surface tension
ε	Liquid permittivity
η	Dynamic viscosity
η_{sp}	Specific viscosity
$[\eta]$	Intrinsic viscosity
θ	Angle
π	Number pi
ρ	Density
σ	Electrical conductivity
τ	Porosity
ν	Kinematic viscosity
χ	Viscometer constant
ϕ	Volumetric flow rate
ω	Evaporation rate

Chapter 1

Introduction

This chapter introduces to the background of the project and the importance of the subject within the life sciences and engineering fields. The chapter also presents the aims and objectives of this PhD project and outlines the content of the different chapters in this thesis.

1.1 Background

Advances in health sciences have led to an ever increasing number of pharmaceutical treatments available to treat diseases and improve quality of life. However, pharmaceutical innovation is an expensive affair, and it has recently been estimated that the development and marketing of a new drug compound on average costs more than $1 billion [Adams and Brantner 2006, Adams and Brantner 2010]. On the other hand, developing new delivery methods for existing drug compounds typically costs substantially less and may result in both improved efficacy and bioavailability and a reduction in side effects. This strategy can maximize the economic potential of a new drug during its early stage and lead to an extension in patent life [Yang *et al.* 2000]. Yet, despite progress in technologies and several successful drug delivery product on the market, preparation of clinically effective drug delivery systems still represents a significant on-going challenge for many drug delivery applications [Allison 2012].

Oral drug administration is generally regarded the optimal route of administration as it is easy to perform, allows various types of dosage forms, avoids pain and is often inexpensive to manufacture. An oral dosage form can be categorized as being either

liquid or solid of which the solid dosages offer certain advantages compared with liquid dosages including their greater stability and lower manufacturing costs [Sastry *et al.* 2000, Vasconcelos *et al.* 2007]. Notwithstanding, the oral administration route is also challenging for drugs that have either low aqueous solubility or low permeability across the intestinal wall. Indeed, there is a broad consensus within the pharmaceutical community that poor water-soluble active pharmaceutical ingredients (API) have become more prevalent in the last decades with an estimated 70% of all new drugs classified as being poorly soluble. This is considered a great challenge which needs to be overcome due to the cost and inconvenience of systemic administration of these drugs via intravenous injection [Lipinski 2002]. New drug candidates for oral delivery are becoming increasingly insoluble due to their tendency to increase in molecular weight, number of H-bond acceptors and lipophilicity, all of which are parameters associated with poor solubility. This tendency is based on the increasing complexity of new drug compounds as well as a large fraction of new drug targets being in the lipid-based cell membrane [Lipinski 2000]. Many of these drugs, however, have an intestinal permeability ranging from reasonable to good and thus their main issue is their poor solubility [Saharan *et al.* 2009].

The poor solubility of drugs poses a significant problem for the therapeutic performance of these drugs since with oral delivery the drug must first dissolve in the gastrointestinal tract (GI tract) before it can pass across the intestinal membrane. A slow and incomplete dissolution often results in low and erratic drug absorption during the relatively short absorption window of the digestive system and the consequence is suboptimal clinical efficacy of these drugs [Panchagnula and Thomas 2000]. Yet, an increase in the bioavailability is often demonstrated by improving the solubility or dissolution rate of these drugs. Further, it is believed that by controlling the drug dissolution to take place over several hours one may enhance the pharmacokinetics and prevent high variability

in the plasma concentration. Such extended drug release combined with good drug solubility/dissolution would result in high bioavailability and therapeutically relevant drug concentrations over an extended time [Nyholm *et al.* 2003, Tanaka *et al.* 2006]. There have been many attempts to deal with the poor oral bioavailability of low solubility drugs, which is evident from the numerous strategies available, and while excellent *in vitro* results are often shown, the results typically cannot be reproduced clinically [Emami 2006].

Some of the factors determining the success of drug delivery systems are better control of size, morphology and surface characteristics of the delivery vehicles used. Micro- and nanoparticles are small and flexible and can have different functions useful for producing effective formulations and delivery vehicles [Chow *et al.* 2007, Liversidge and Cundy 1995]. The large surface area to volume ratio of these drug carrier particles may be used as an advantage as it allows a greater area for interaction with cells and tissue and further increases the drug dissolution rate [Kohane 2007]. However, as particles decrease in size, beyond a certain range, they may become more unstable and difficult to work with. Also, the maximal encapsulated payload per volume of particles decreases as the surface to volume ratio increases, limiting the drug loading capacity of particles. Thus, it is not necessarily desirable to have particles in the nanoscale unless it is crucial for their function or application, i.e. cell uptake of particles but rather have particles in the lower micro-range [Kohane 2007, Wendorf *et al.* 2008].

Microparticles are seen used in many type of dosage forms including powders and aerosols for nasal and pulmonary delivery, compressed tablets or capsules for oral delivery and liquid suspensions for systemic delivery [Vehring 2008]. Until recently, the microparticles were mainly seen as a carrier for protecting and releasing drugs without any additional functions and attributes. New strategies focus on carefully

engineering these microparticles for superior performance with enhanced functionality and with better biological interaction [Chew *et al.* 2005]. This includes the engineering of particle shape and surface characteristics as well as engineering of size, size distribution and inner structure of the particles. Several studies have indicated that a narrow particle size distribution gives better control of drug release and better therapeutic effect of the drug [Ding *et al.* 2005, Valo *et al.* 2009]. Techniques that allow production of microparticles of different size, morphology and surface characteristics with an inexpensive process could thus be suitable for developing oral formulations of poorly soluble drugs. Such techniques include spray drying and electrospraying (also known as electrohydrodynamic spraying) and they may be used to produce microparticles that can further enhance dissolution of the drugs. Spray drying is the most developed and commonly used of the mentioned techniques and it is used in many commercial processes including pharmaceutical applications. Spray drying has also been used to produce microparticles intended for oral formulations of low solubility drugs [Janssens *et al.* 2008, Mu and Feng 2001].

Electrospraying has mostly been used for processes such as coating and painting, and most notably it is used for ionization purposes in many mass spectrometer setups [Gorovoi *et al.* 1969, Takáts *et al.* 2004]. However, recently the electrospraying technique has attracted the attention of many researchers for biomedical applications and for development of drug delivery carriers. Electrospraying is a process based on the formation, control and breaking up of a liquid jet under the influence of a strong electrical field. It is an inexpensive, one-step process that is compatible with a broad range of liquids and materials. Compared with spray drying, electrospraying can produce more monodisperse particles which are also well dispersed, and the process can be performed under ambient conditions [Jaworek 2008, Peltonen *et al.* 2010].

The suitability of electrospraying for particle engineering purposes has be demonstrated by several researchers and it has been observed that by adjusting the process parameters some particle properties can be controlled. Although many aspects of the technique and its applications have been studied, there are still a number of aspects related to drug formulation, particle formation and influences on particle characteristics that have yet to be fully examined. Further, the drug release kinetics and cellular uptake of drug from microparticles prepared using electrosprayed have only been touched briefly and should be explored in more detail [Chang *et al.* 2010, Enayati *et al.* 2009, Xie *et al.* 2006b]. By gaining more insight into the particle formation process, control of particle characteristics and drug release behaviour, electrospraying may provide improved formulation of low solubility drugs and allow development of better treatments.

1.2 Aims and objectives of this research

1.2.1 General aims

The aim of this project is to investigate the preparation of drug-loaded microparticles that provides enhanced oral bioavailability of drugs that have low water solubility and hence poor oral bioavailability. This is done by investigating the two technologies, electrospraying and spray drying, for producing microparticle-based solid dispersions with the main focus on electrospraying, a novel method for producing solid dispersions. The processing parameters influencing particle formation and characteristics as well as drug release behaviour from the particles are studied for electrospraying to gain better understanding of the technique. Two different polymers are studied using the same model drug to examine differences in particles properties and drug release kinetics. Then the electrospraying system is investigated from a particle engineering view point by studying particle formation mechanisms specifically with focus on the solvent

system used. Then electrospraying is compared with spray drying with regards to their differences in particle formation process, particle characteristics and drug release.

1.2.2 Specific aims

- Evaluation and validation of electrospraying for preparing solid dispersions and drug loaded microparticles
- Assessment of the adjustable parameters with electrospraying and exploration of the influence of these parameters on particle characteristics and drug release and the control of these attributes.
- Investigation of the role of solvent systems on the particles formation and resulting characteristics including drug distribution using electrospraying
- Evaluation of spray drying for the preparation of solid dispersion microparticles and the influence of solvent mixtures on particle formation
- Comparison of spray drying and electrospraying and their resulting products

1.3 Outline of the report

This report describes research performed during the project by introducing to the basic concepts of the research done, explaining present scientific knowledge in the areas covered in a literature review, describing the experimental setup and the analytical methods applied and by going through and discussing the results obtained so far in the project.

Chapter 1 briefly introduces to the background of this research. The aims and objectives of the research are presented and the scope of this work is defined.

Chapter 2 is a literature review that covers and explains the different concepts necessary to understand the later sections of the report. This review will go through

pharmaceutical and technological aspects of the research as well as a combination of the two, and further bring the reader up to date with the current research and findings within the specific field of this project.

Chapter 3 explains the materials and methods used in the investigation carried out. The different materials and the experimental setup used for microparticle production are described, and the different analytical and characterization methods used are explained.

Chapter 4 presents and discusses the results from the studies concerning characterization of spraying solutions and assessment of the electrospraying equipment, initial studies on electrosprayed celecoxib-loaded PLGA microparticles and the results from studying different electrospraying processing parameters and their influence on particle characteristics and drug release are shown and discussed.

Chapter 5 presents and discusses the results and discussion on the study of different solvents systems for preparing particles using electrospraying with focus on particle formation, characteristics, drug distribution and drug release. A system composed from HPMCAS is also discussed in this chapter.

Chapter 6 presents and discusses the results and discussion from the studies on celecoxib-loaded PLGA microparticles prepared with spray drying using different solvent systems and further compares and discusses the data obtained with spray drying and electrospraying.

Chapter 7 summarises the report and outlines the main findings and conclusions presented in chapters 4, 5 and 6 and the project in general and gives insight on the future perspectives of this project.

Chapter 2

Literature Review

This chapter provides a detailed literature review on the scientific concepts and prior research findings important for the understanding of the subsequent chapters. Formulation strategies for poorly soluble drugs with particular focus on solid dispersions as well as the theory and application of techniques electrospraying and spray drying will be reviewed.

2.1 Strategies to improve oral formulations of poorly soluble drugs

2.1.1 Introduction to strategies

The bioavailability of a drug-carrier system describes the rate and extent at which the active pharmaceutical ingredient is absorbed by the body from the administered dosage and becomes available in the blood circulation. The oral bioavailability is mainly linked to the permeability and solubility of a drug. Formulation plays a crucial role on the bioavailability of poorly soluble drug compounds and it is often a challenging task to develop oral formulations for such drugs [Amidon *et al.* 1988]. This is primarily due to their low aqueous solubility and their poor capacity to dissolve in the gastrointestinal fluid within a relevant window of absorption. Thus, drug dissolution is considered the main limitation for these drugs and in order to obtain adequate bioavailability, it is necessary to understand the mechanisms of dissolution and how it can be improved for immediate release purposes [Amidon *et al.* 1988, Fahr and Liu 2007].

Although oral formulations mainly aim at obtaining a high dissolution rate, in order to achieve supersaturation and quick absorption of the drug, there are also certain

advantages with an extended release formulation. Extended release formulations not only consider the net bioavailability but are also designed to provide increased patient compliance by reducing the dosing frequency as well as reducing fluctuations in the drug plasma concentration. They must, however, still provide sufficient drug dissolution rate over an extended time interval via one of another strategy [Riis *et al.* 2007].

In the following, the concept of dissolution rate is initially explained and subsequently different strategies for increasing the dissolution rate, and thereby bioavailability, will be discussed.

2.1.2 Dissolution rate

Dissolution is the process in which one or several substances go from the solid state into solution. The rate at which this process takes place is referred to as the dissolution rate. There is a direct proportionality between the solubility and the dissolution rate of a substance in a specific solvent and this relationship is described by the Noyes-Whitney equation (see equation 2.1) [Noyes and Whitney 1897]:

$$\frac{dC}{dt} = \frac{D \times A \times (C_s - C_t)}{h \times v} \qquad \text{(Equation 2.1)}$$

where D is the diffusion coefficient, A is the surface area of drug exposed to the dissolution media, C_s is the saturation solubility of the drug, C_t is the drug concentration at time, t, h is the thickness of the surface boundary layer and v is the volume of the dissolution media. An increase in the drug dissolution rate in a given medium can therefore take place either by an increase in drug solubility, an increase in the surface area exposed to the medium or a reduction in the diffusion layer thickness, assuming a constant volume of the medium. Several properties of the drug and drug-carrier system are tied to the parameters influencing the dissolution, and the dissolution rate of the drug can be improved by altering these properties. Formulation and drug design

strategies have been developed to improve the dissolution rate of poorly soluble drugs using the principles of the Noyes-Whitney equation and are typically based on physical modifications, chemical modifications or formulation strategies. These different strategies are briefly explained in sections 2.1.3-2.1.5.

2.1.3 Physical strategies

There are many dissolution enhancing strategies that make use of physical approaches, here among approaches where the surface area available for dissolution is maximized, solubility is enhanced via modifications in the solid state form of the drug, and lipid based formulations.

Increase in surface area

The surface area available for dissolution is increased via reduction in the drug particle size and is a very common approach for improving the dissolution rate [Gursoy and Benita 2004]. This is done either with a top-down approach or a bottom-up approach.

Top-down approach:

This involves breaking down large drug crystals into smaller crystals and is typically done via a milling process, referred to as micronization or nanonization depending on the final crystal size obtained. Micronization is a simple way to reduce particle size using various types of mills. Yet it does not provide good control of particle characteristics and produces drug particles around 2-5 µm, which are not small enough to allow significant enhancement of the dissolution rate [Chaumeil 1998, Rasenack and Müller 2004]. With nanonization using for instance Elan's NanoCrystal technology [Elan 2006], a wet milling process or high pressure homogenization particle sizes can be reduced down to 100-250 nm resulting in a significant improvement in dissolution rate. However, post processing is typically necessary for these processes, using

stabilizing agents in order to avoid aggregation/agglomeration [Merisko-Liversidge and Liversidge 2011].

Bottom-up approach:

This involves generating drug nanocrystals from a liquid medium via a controlled precipitation/crystallization process. The drug is typically dissolved in a solvent and an anti-solvent is then added resulting in precipitation of the drug [Keck and Müller 2006]. As the crystals begin precipitating a suspension is obtained, which is stabilized using surfactants or polymers and used as a suspension, or later made into a solid dosage via granulation or pelletization. Nanocrystals below 100 nm have been produced using this approach leading to significant dissolution enhancement. A challenge with this technology is the large amount of organic solvent used in the process, which makes it costly and cumbersome for large scale production [Shegokar and Müller 2010].

Solid state modifications

Solid state modifications of the drug can also lead to improved dissolution. The amorphous state is a metastable state in which the material exhibits short-range order only over a few molecular dimensions and thus possesses different physical properties compared with its corresponding crystalline state. It is associated with higher internal energy and specific volume than the ordered crystalline state, which can be favourable for pharmaceutical purposes because of their enhanced solubility. The solubility of the amorphous form is in the order of 10 to 1600 fold higher than that of the most stable crystalline form thus resulting in higher dissolution rate of the drug [Hancock and Parks 2000]. A drug in the amorphous form allows increased dissolution in a supersaturated solution, where it over time precipitates as the drug relaxes into a crystalline form. [Müllertz *et al.* 2010]. Amorphous drugs can be achieved in many ways including quench-cooling of a melt, rapid drying of a solution and condensation from vapour

state, where quench-cooling and spray drying are some of the more common methods. The amorphous state is, however, a non-equilibrium state and the drug has a strong tendency to crystallize over time to form a more stable crystalline polymorph. Different stabilizers have been used for amorphous formulations acting in order to prevent recrystallization characterized by Ostwald's step rule but stability still presents an issue with these formulations [Lindfors *et al.* 2007]. Recently, there has been some interest in the use of co-amorphous systems, where essentially two poorly soluble drug compounds are melted together and subsequently forms a co-amorphous system, one compound with good glass forming ability and one with poor glass forming ability. Such co-amorphous systems have been shown to enhance both dissolution rate and stabilization of the amorphous form [Löbmann *et al.* 2011].

2.1.4 Chemical strategies

Depending on the drug's ability to ionize different chemical approaches have also been developed to overcome the low dissolution rates of poorly soluble drugs. Ionisable drugs have been employed using salt formation while synthesis of prodrugs is another popular approach for different classes of drugs.

The solubility of basic and acidic drugs can often be improved by forming salts of the drug. This approach is commonly used for liquid parenteral dosage forms, but it has also been shown to increase the dissolution rate of solid dosage forms for oral use. Salts are formed using salt-forming agents which are typically acids for basic drugs and bases for acidic drugs. Salt formation is useful for some drugs, notably those which are basic or acidic, but for many drug compounds this method is not practical due to their physicochemical properties. Also, with some drugs salt formation does not improve dissolution rate and hence bioavailability [Serajuddin 2007, Sweetana and Akers 1996].

Soluble produgs have also been used for oral delivery by forming a reversible chemical derivative of an active drug. The prodrug approach aims at increasing the solubility of the drug by reducing the intermolecular hydrogen bonding. Reconversion into the original drug structure may take place at the intestinal mucosa via enzymatic cleavage and has good permeability across the intestinal wall. In addition to solubility enhancement, prodrugs may also provide some organ or tissue specific targeting. Typical progroups used to enhance the solubility of poorly soluble drugs include esters such as phosphate esters, amino acid esters choline esters, or carbonyls and acetates [Rautio *et al.* 2008, Testa 2009].

Multi-component crystalline systems are another approach where the dissolution rate of drugs in some cases can be improved with crystal pseudo-polymorphs such as solvates. Solvates are crystal structures where the unit cell consists of host drug molecules accompanied by guest liquid molecules. In the special case where the guest molecule is water, they are referred to as hydrates. Solvates occur by crystallization from a solution and occasionally have the potential to enhance the drug dissolution rate, as shown for some drugs [Rodríguez-Spong *et al.* 2004]. It has previously been reported, that the solubility of solvates can be about four times higher than the solubility of the drug in the most stable crystalline state [Hancock and Parks 2000]. Hydrates are the most common solvate and many drugs are capable of forming hydrates due to their small size and the multidirectional bonding capability of water molecules [Aaltonen *et al.* 2009]. Solvent levels in solvates using organic solvents may be at concentrations that are above the tolerated levels with toxicological consequences. Such solvates are thus typically avoided for pharmaceutical applications [Blagden *et al.* 2007].

2.1.5 Formulation strategies

Solubilizing agents

Cyclodextrins:

Cyclodextrins are a class of molecules that form inclusion complexes with other molecules such as small drug molecules. Inclusion of drugs in different cyclodextrin channels may take place through milling or non-covalent interactions. Cyclodextrins have different functions such as acting as stabilizers, solubility enhancement and taste and odour masking. They typically have a low absorption across the intestinal membrane. However, they may have a negative impact on membrane integrity at higher doses. Further, they can be difficult to scale up [Del Valle 2003].

Wetting agents:

Wettability is referred to as the ability of a liquid to maintain in contact with a solid surface via interactions. An increase in the wettability of the drug leads to an increase in dissolution rate, as it allows more interaction with the surrounding medium and thus enables more penetration into and around the solid surface. The wettability of a drug in a given medium can be determined either by the structure of the drug or by the contact angle at the liquid/solid interface. A low contact angle indicates that wetting is favourable, and hence that the solid drug is wettable. Poorly soluble drugs typically have poor wettability due to their high free surface energy from their inherent hydrophobicity. A non-wetting material can be made more wettable using surfactants, which lower the excess free energy at the solid surface, decreasing the surface tension and increasing wettability. Yet, surfactants result in alterations in the barrier functions of the intestinal epithelial.

Lipid formulations

Lipid-based formulations comprise a large group of approaches which share similar characteristics, mainly the lipophilic nature of the formulations. These formulations include oils, self-emulsifying formulations, emulsions and liposomes each with their specific advantages and limitations. However, in most cases they involve incorporating a lipophilic drug into an inert lipid-based vehicle. Currently, the most popular of the lipid formulations for oral delivery are the self-emulsifying drug delivery systems (SEDDS), which are essentially mixtures of oils, surfactants and/or solvents. SEDDS form emulsions or microemulsions loaded with lipophilic drug upon agitation and are considered good candidates for oral delivery [Gershanik and Benita 2000, Pouton 2000].

Lipid-based formulations enhance oral bioavailability by reducing particle size and thus increasing dissolution rate, decreasing gastric emptying rate, increasing solubility in the intestinal fluid and promoting absorption via intrinsic lipid pathways. [Saharan *et al.* 2009]. However, most lipid-based formulations are used in the liquid form, except for a few that are solid at room temperature such as solid lipid nanoparticles (SLN). These are lipid "nanoparticles" in the size range of 50-1000 nm and combine the advantages of conventional lipid formulations with that of nanoparticles. They have further been shown to improve oral bioavailability. SLNs are prepared via high pressure homogenization, microemulsion techniques, nanopellets or solvent evaporation precipitation. These formulations are, however, often influenced by food intake due to their lipophilic properties [Hu *et al.* 2004, Müller *et al.* 2000]. Although some lipophilic nanoparticles have been demonstrated to penetrate the intestinal mucosa without releasing their payload, it is not known whether they travel into to the bloodstream undigested. Lipid-based formulations seem to be a useful strategy, yet they are mainly

limited to highly lipophilic drugs and thus exclude many drugs [Gershanik and Benita 2000].

2.1.6 Solid dispersions

Solid dispersions are a different strategy for modifying the dissolution rate of low solubility drugs which combines the effect of several parameters in the Noyes-Whitney equation (see section 2.1.2). Solid dispersions are defined as solid dosages composed of a minimum of two components, the drug compound and a matrix material, which keeps the drug dispersed in a solid form as the name suggests. Solid dispersions were first described by Sekiguchi and Obi in 1961 [Sekiguchi 1964]. They showed that by forming a eutectic mixture consisting of a poorly soluble drug and urea, a water soluble carrier material, the drug dissolution rate was improved hence improving the drug bioavailability. An improvement in dissolution rate was found to essentially result from the small drug particle size and the increased wettability of the system [Chiou and Riegelman 1971].

There are many methods for reducing the drug particle size, as described in the previous sections, hence improving the dissolution rate. Yet, with solid dispersions, given the fine dispersion of drug in the carrier matrix, the drug particle size is arguably reduced to the molecular level, the smallest building blocks, and thus provides the largest possible surface area available for dissolution. Therefore, the release of drug would take place in the molecular form and dissolution would be quicker relative to its crystalline counterpart, forming a supersaturated solution [Leuner and Dressman 2000]. The drug is therefore considered to be amorphous due to the molecular dispersion within the carrier matrix and its lack of long-range order and provides similar solubility enhancement as the amorphous systems discussed in section 2.1.3.

Solid dispersions also provide improvement in wettability which in turn results in further increase of dissolution rate. Wettability is carrier dependent, and the highest wettability is observed for carriers or additives with high surface energy such as surfactants. Yet, an increase in wettability is also observed for materials without high surface activity, through close contact between drug and carrier and by decrease in crystallinity [Juppo *et al.* 2003].

2.2 Preparation of solid dispersions

2.2.1 Introduction to solid dispersions

In the beginning, solid dispersions were prepared with crystalline carrier materials such as sugars in which the drug was dispersed [Kanig 1964]. Solid dispersions formed from crystalline carriers have high thermodynamic stability, yet, their resulting drug dissolution rate is relatively low compared with that of other carrier materials used for preparing solid dispersions [Vippagunta *et al.* 2007]. A shift was then made towards using amorphous polymeric carriers, currently the most commonly used carriers for preparing solid dispersions. The most frequently reported amorphous polymeric carriers include cellulose-derived polymers such as hydroxypropyl methyl cellulose (HPMC), polymethacrylates, starch-derivatives, polyethylene glycols (PEG) and polyvinyl pyrrolidone (PVP) [Serajuddin 1999, Vasconcelos *et al.* 2007]. These carriers lead to drug dispersions either in the form of amorphous or crystalline clusters (solid suspension) or as molecular dispersions (glass solution) or a combination of the two [Van Drooge *et al.* 2006].

Solid suspensions typically form for drugs with a high melting point and a low solubility in the polymer phase while glass solutions typically arise when the drug is soluble or fully miscible in the polymer phase. Amorphous solid suspensions can be difficult to distinguish from glass solutions, but the suspensions tend to exhibit two

glass transition temperatures, T_g, one for the amorphous drug phase and one for the polymer phase. The glass solutions on the other hand only show one T_g, somewhere in between the T_g values of the drug and the polymer [Leuner and Dressman 2000]. Although amorphous polymeric carriers provide good enhancement in dissolution rate on their own, they are also often been used together with solubility enhancers such as surfactants in order to achieve further improvements in bioavailability [Müllertz *et al.* 2010, Wong *et al.* 2006]. These solubility enhancers including gelucire and poloxamer have also been used alone, together with the drug, to prepare solid dispersion formulations [Majerik *et al.* 2007, Yüksel *et al.* 2003].

2.2.2 Extended release solid dispersions

Set aside from the dissolution-based improvements in bioavailability, there has in the recent years also been a substantial amount of research directed towards solid dispersions for extended release applications. Despite not being as well explored as conventional immediate release applications such extended or sustained release solid dispersions seem to have a lot to offer. Extended release solid dispersions provide drug release after administration over a period of several hours at a pre-defined rate. They have several advantages over immediate release formulations including the fewer doses required each day, higher efficacy of each dose, and smaller variations in the drug plasma levels and fewer side effects experienced [Cui *et al.* 2003]. Yet, they have previously been associated with the risk of dose dumping, a premature and rapid release of drug in a short period of time, in the case of failure in the release system. Further, extended release formulations have also been associated with low *in vivo* predictability due to their complexity and dependence on environmental factors [Huang and Brazel 2001].

Extended release can be achieved in a variety of ways, but for solid dispersions they are generally prepared using a carrier material that has controlled disintegration or degradation properties and include materials such as cellulose-derived polymers, biodegradable polymers and waxes etc. The properties of the carriers as well as the preparation method determine the release mechanism of the drug from the solid dispersion. Currently however, there are different challenges to be overcome for optimizing the performance of extended release solid dispersions including finding a desirable method for producing the formulations with specific physicochemical characteristics with high reproducibility and ultimately at a commercial scale. Further the stability of the formulations is a matter of concern and may make it challenging to use solid dispersion as a method for preparing extended release dosages [Ohara *et al.* 2005, Tanaka *et al.* 2006].

2.2.3 Methods for preparing solid dispersions

Solid dispersions can be prepared using a number of different techniques and these are typically divided into *melting* methods and *solvent evaporation* methods. Melting methods include extrusion methods such as hot-stage extrusion and melt extrusion as well as melt agglomeration, while the common solvent evaporation methods are supercritical fluids technology, spray drying and freeze drying. Some of the main preparation methods will be explained briefly and the methods, spray drying and electrospraying, will be discussed in further details.

Melt extrusion:

Melt extrusion is widely used to prepare solid dispersions and is a useful technique as it produces solid dispersions in a single step process, without the need for any solvents, and therefore does not require lengthy drying times. This process consists of three parts, a conveyer system that moves the material through the die, which is typically either a

turning screw or a moving ram, a dye that forms the required shape and a cooling device to cool down the melt [Crowley *et al.* 2007]. The drug and carrier are initially mixed and are then heated by the extruder until it softens, and the conveyer system then pushes the mixture out through the die. The melt is then cooled down to obtain a solid product, in which the drug is dispersed within the carrier matrix, and can then be milled to reduce their size. Typically, granules or pellets are prepared from the process and can then be further processes into tablets or other dosages. The materials used for melt extrusion must have good thermal stability since the process takes place at high temperatures [Breitenbach 2002, Crowley *et al.* 2007].

Supercritical fluids technology:

Supercritical fluids are liquids and gases at temperatures and pressures above their critical point, a phase area in the liquid:gas pressure curve. These fluids have lower viscosities and higher diffusivities of solutes than liquids [York 1999]. The drug compound is filled into a vessel together with the carrier material and a gas is then added into the vessel. The gas is pressurized via a compressor before entering the vessel and becomes a supercritical fluid, which dissolves the drug and carrier within the vessel. Particles are then formed from the dissolved mixtures and are collected on a filter, at the outlet of the vessel, until the system is de-pressurized and the powder can be collected. With supercritical fluids technology non-volatile solvents can also be dissolved and carbon dioxide (CO_2) is the most widely used supercritical fluid, due to its low critical temperature and pressure ($T_{critical}$ = 31.1 ºC, $P_{critical}$ = 73.8 bar) [Sethia and Squillante 2004]. CO_2 is further inexpensive, non-toxic and non-flammable compared with organic solvent and is hence suitable for pharmaceutical processing. Supercritical fluids technology results in particles that are relatively small (0.5-10µm) and has been used as an alternative to milling [Van Nijlen *et al.* 2003].

Spray freeze-drying:

Spray freeze-drying is another solvent-based method where a solvent is removed to form a solid dispersion and is a combination of spray drying and freeze drying. In freeze-drying, the drug and carrier are dissolved and the solution is first frozen and the solvent is then removed through sublimation by applying a vacuum. This process would result in solid dispersion powders formed of porous particles with approximately the original size of droplets formed by the atomizing nozzle. With spray freeze drying the solution containing drug and carrier is atomized from a nozzle into a stream of cold air (around -60 ºC) at atmospheric pressure. The small droplets produced quickly freeze and then their solvent sublimates in the cold air stream resulting in dry particles in the collection chamber [Leuenberger 2002].

Spray drying

Spray drying is a widely used liquid atomization process that evaporates the solvent off a solution or suspension to produce a dry powder in one rapid step. It produces particles in the micro-scale while at the same time it can be used to prepare solid dispersions. Rapid drying takes place as a result of the small droplets formed with high surface to volume ratio. Spray drying is one of the most commonly used techniques for producing microparticles as well as for preparing solid dispersions and the process takes place as follows: Briefly, the liquid is fed into a nozzle and atomized, the droplets are mixed with the drying gas, the solvent of the droplets is evaporated and finally the particles are separated from the drying gas. Most of the components in a spray drying setup are similar from setup to setup, although different types of atomizers exist and make use of different atomization forces. Commonly used atomizers starting with the most common include, pneumatic nozzles, rotary atomizers, pressure nozzles and ultrasonic nozzles.

For more details on the construction and components of a spray dryer please refer to the excellent review by Cal and Sollohub [Cal and Sollohub 2010].

Electro-spray/electro-spinning

Electrospraying and electrospinning both belong to the class of electrohydrodynamic atomization techniques and are essentially based on the same physical principles. Both techniques make use of a strong electrical potential to drive the atomization of a liquid into either small droplets or fibres respectively. The droplets and fibres produced then solidify as the solvent evaporates, typically without the use of an active drying process, and result in products of size ranging between nano- and micro scale. The electrospraying and electrospinning setups are relatively simple and can be assembled in a laboratory setting using custom parts and the two techniques can practically be performed on the same device. The main distinction between the two processes is the range in viscosity of the polymer feed solution that is atomized. The principles and theories for each of these techniques will be explained to some detail in the following section. However, the detailed physical theories and governing equations of electrospraying and electrospinning are explained in more depth in other reviews [Cloupeau and Prunet-Foch 1989, Jaworek and Sobczyk 2008, Luo *et al.* 2012, Reneker and Chun 1996].

2.2.4 Particulate solid dispersions and particle engineering

Many of the preparation methods for solid dispersions described in Section 2.2.3 produce microparticle-based formulations, where each microparticle is composed of a carrier matrix with the drug dispersed. This applies for both the solvent based atomization techniques, where the solid dispersion precipitates from the atomized solution, and the melting techniques, where larger structures are formed but can subsequently be milled into microparticles. Microparticulate solid dispersions provide

quicker drug release compared with more bulky products, due to shorter diffusion distances, but this is less significant for systems composed of water soluble carriers. Further, microparticles may be better suited for processing or filling into tablets or capsules and are likely to provide better re-dispersion or disintegration upon wetting. The latter can be an important factor for achieving a desirable dissolution profile. Particle-based solid dispersions could also be useful in controlling specific qualitative features of solid dispersions including stability, by optimizing the spatial distribution of drug molecules in the matrix or by preventing phase separation between the drug and carrier. Progress in development of solid dispersion formulations have mainly focused on using different carrier materials and additives and a combination of these to achieve better bioavailability via dissolution enhancement [Van Eerdenbrugh and Taylor 2010]. Yet, with the conventional approaches to preparing and developing solid dispersions, there has been little or no attention on the particle aspect of formulations and its influence on the product performance [Vasconcelos *et al.* 2007, Yu *et al.* 2009].

Recent progress in nanotechnology as well as particle engineering have introduced new tools for preparation of particles providing better control of their attributes and thus allowing the design of particles with desirable characteristics. Although still in development, advanced nano processing techniques such as lithographical techniques and nano impregnation may allow precise control of particle size, shape and drug dose with triggered drug release [Guan *et al.* 2006, Lu and Chen 2004]. However, these techniques are typically expensive to operate and must be conducted in a clean room environment using several processing steps. Cheaper and less advanced technology such as atomization techniques seems to provide a more viable option at the present and still allow substantial control of particle characteristics. For example, the size, surface morphology and porosity can be controlled to some degree, thus the total surface area can be increased by preparing particles with a rough surface and a porous inner structure

[Iskandar *et al.* 2003, Yao *et al.* 2008]. Control of these and other particle characteristics can be used to optimize current drug formulations and seems be very promising. For this purpose, the techniques spray drying and electrospraying have proven interesting and suitable, since they allow inexpensive production of microparticles which can be done in a simple one-step process. Further, certain particle characteristics can be modified to improve their *in vivo* drug delivery performance.

Solid dispersions composed mainly from water-soluble carriers may not necessarily benefit from such a particle engineering approach, as they mainly rely on rapid dissolution. Even for bulky solid dispersions the drug release typically takes place very fast due to rapid dissolution of the matrix. There could, however, be a stability related benefit for these formulations, although this has not yet been demonstrated. For solid dispersions composed from non-water-soluble carriers intended for extended or sustained release it is important to be able to control the drug release profile. It is first of all desirable to have small particles where drug can be released within a relevant time span, due to the short diffusional distances for the drug molecules. Further, the particles may be tailored to provide better release kinetics and less agglomeration.

2.3 Spray drying

2.3.1 Principles of the spray drying process

Spray drying is a commercial manufacturing process capable of producing a solid product from a liquid in the form of a solution or a suspension, and has been used for a wide variety of applications ranging from manufacturing of foods to pharmaceutical products. The first spray dryer is considered to have been invented in 1872 with the registration of the first patent [Percy 1872]. Since then significant improvement have been made on the technology *per se,* concerning the process as well as hardware which is compatible with industrial level applications. Set aside its widespread use, there has

recently been an interest in gaining further understanding on the underlying mechanisms of particle formation using spray drying in order to better control the resulting particle characteristics.

The general spray drying process consists of three major subprocesses; atomization of the liquid feed, drying of the atomized droplets into solid particles and separation of particle from the drying gas with subsequent collection into a container. Each of these subprocesses have an impact on the resulting characteristics of the end product and are important to understand and control [Masters 2002]. A spray dryer consists of the following major components, sketched in Figure 2.1: A pump that drives the liquid feed (1) into the atomization nozzle at a constant flow rate, an atomizer which uses a certain driving force (2) to disrupt the liquid into small filaments at the nozzle tip (3), a drying chamber (4) where the droplets are exposed to a heated gas, a cyclone (5) which separates the dried particles from the drying gas and a collection vial which is used to collect the spray dried product (6) [Cal and Sollohub 2010].

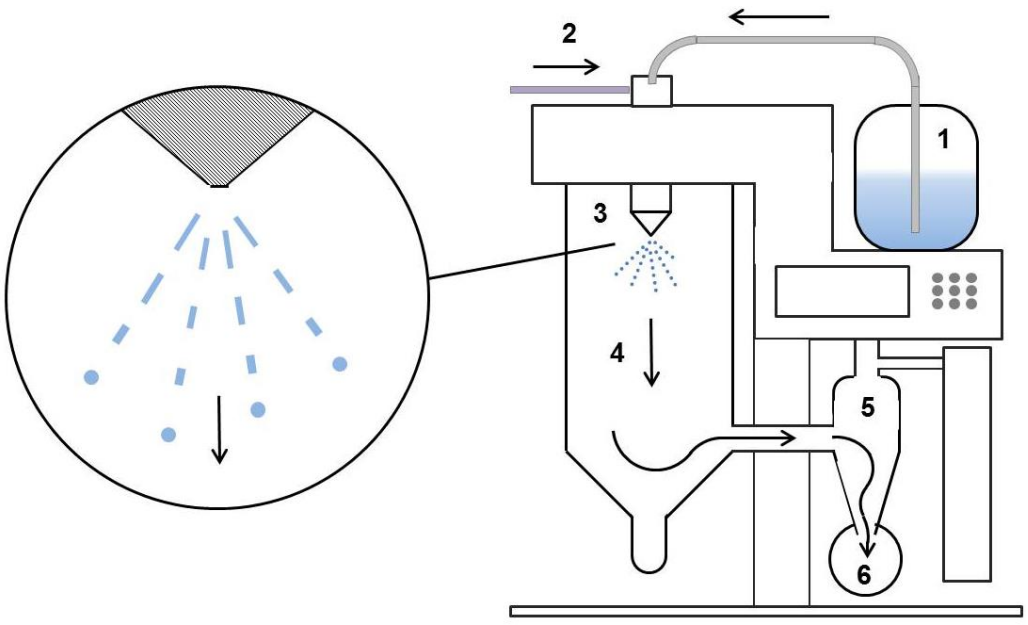

Figure 2.1 General spray drying setup and jetting process.

Interest in better control of particle characteristics has led to several reports discussing how to control different characteristics using principles from particle formation theory and models. In the following sections the different models describing the particle formation process and mechanisms in spray drying, the properties of the molecular dispersion obtained and their advantages for spray drying will be discussed.

2.3.2 Particle formation models for the spray drying process

Much effort has been put into investigating the particle formation process with spray drying, and several types of models have been developed to explain the separate steps involved in the process. Further, there has specifically been focus on the evaporation stage, which is a critical stage where most of the droplet mass is evaporated to form dry particles. The models include both theoretical and experimental models, yet most of these models are simplifications, since there are many intervariate parameters that complicate the process from being fully simulated.

Experimental methods that have been used to increase the knowledge on particle formation include methods in which the solutes of a solution are analysed during evaporation of the solvent and methods in which droplets are observed in their transition from droplets to particles. For example, Lin and Gentry monitored the morphological characteristics of a single droplet hanging from a capillary filament using a device they built [Lin and Gentry 2003]. In this study, the steady state drying of the droplet was monitored, although taking place at a larger geometric scale, and similar methods have been used by others to understand the solidification process [Walton and Mumford 1999]. Aerodynamic levitators, acoustic levitators as well as concave hot plates have been used to hold a droplet in the air while observing the process with a CCD camera or a high speed camera. The two types of methods used to study the evaporation of a single droplet differ since the levitation methods allow free rotational motion of the droplet,

resulting in better approximation of the heat and mass transfer taking place [Adhikari *et al.* 2000, Schiffter and Lee 2007, Tsapis *et al.* 2005]. Levitation techniques have also been coupled with spectroscopic methods such as infrared spectroscopy to continuously measure precipitation during drying of the droplet [Biedasek *et al.* 2007, Santesson *et al.* 2003, Tuckermann *et al.* 2009].

The main limitation with these methods is that they are based on droplets larger than 170 μm that solidify over much longer time and under different conditions than in the spray drying process [Vehring *et al.* 2007]. They therefore are not fully representative of the actual process.

Another more common strategy to explain the particle formation process is to analyse the prepared particles and retrospectively elucidate the particle formation mechanisms using the observations. This approach has been performed by correlating properties such as particle size, porosity and morphology with mechanisms in the particle formation [I Ré 1998, Iskandar *et al.* 2003].

Purely numerical approaches to describe the droplet evaporation process for spray drying also exist. The constant rate model is one of such models and is based on Fick's second low of diffusion under a set of assumptions [Feng *et al.* 2011, Vehring *et al.* 2007]. The evaporation rate, κ is then defined as:

$$d^2(t) = d_0^2 - \omega t \qquad \text{(Equation 2.2)}$$

where d is the droplet diameter, d_0 is the initial droplet diameter and t is time.

Further, the Peclet number, a dimensionless number, describes the radial distribution of solutes in the drying droplet. It has been used to describe particle formation and to predict particle characteristics for given formulation and processing conditions. A simplified version of the Peclet number is given as:

$$Pe_i = \frac{\omega}{8D_i} \qquad \text{(Equation 2.3)}$$

where Pe_i is the Peclet number and D_i is the diffusion constant of a solute i in the liquid phase of the droplet. Further, various models have been developed to simulate particle formation using Monte Carlo simulations to rank different parameters used in spray drying, thus identifying the factors playing the greatest role in particle formation [Ivey and Vehring 2010]. These and other numerical models are mainly based on the drying kinetics of droplets containing solids in still air and are not fully representative of the droplet drying process in spray drying, yet they can be used to make predictions on the characteristics of the resulting particles, given a set of parameters.

2.3.3 Particle formation in spray drying

The spray drying process starts with the atomization of droplets and is then followed by droplet evaporation until solid particles are formed (see Figure 2.1). Initially, the feed solution (1) and the atomization gas (2) are fed into separate inputs of an atomization device (rotary, pneumatic, hydraulic or ultrasonic) and the liquid stream is atomized at the tip of the nozzle (3) resulting in liquid filaments which develop into fine droplets. The droplets in the drying chamber then come in contact with a drying gas of a certain temperature and the solvent component of the droplets evaporates until a solid product is formed (4). Finally, the dried particles are separated from the drying gas in a cyclone (5) and collected in a receiving container (6) [Cal and Sollohub 2010, Dravid *et al.* 2006].

The sub-processes in spray drying all have an influence on the product yield and different relevant particle characteristics, but the droplet drying stage is considered the most essential sub-process. In this stage the transition from droplet to dry particles takes place and determines a large part of the particle characteristics. This transition is a

coupled heat and mass transfer phenomenon, which is driven by the difference between the partial pressure of the gas phase and the vapour pressure of the solvent and is often described by the solvent evaporation and solute diffusion processes [Masters 2002, Vehring *et al.* 2007]. Depending on the number of solvents and solutes used the process becomes more complex to analyse and control, and the simplest system with a solute and one solvent is thus often used to study the process mechanisms.

The evaporation of a droplet to form a dry particle can be divided into three main stages which are not only specific to spray drying but also take place in other solvent evaporation processes. First, the heating of the droplet initiates shrinking due to evaporation of solvent from the droplet surface. Simultaneously, the solutes become more concentrated around the surface of the droplet and resulting in a concentration gradient of solutes radially in the droplet. The solutes thus move along this concentration gradient from the surface towards the centre of the droplet in order to balance out the gradient. This unidirectional movement of molecules can be explained by Fick's first law and the diffusion is dependent on the molecular mobility of the solutes or the viscosity, molecular size and temperature as explained in the Stokes-Einstein equation. Often the diffusion of solutes cannot follow with the radial shrinking as a result of solvent evaporation and the solute molecules start depositing and eventually cover the droplet surface like a shell trapping the remaining liquid inside.

From the point where a shell is formed, the particles volume stays fixed and solvent continues to evaporate at the surface until it is more or less dry. Then the evaporation continues, but now from inside the shell where solutes are still dissolved [Chen and Xie 1997, Farid 2003]. The shell thickens as solvent evaporates from the interior and increases the resistance to mass transfer of solvent across the shell, resulting in a reduction in the evaporation rate. This resistance prevents heat transfer across the shell

and instead promotes a rise in temperature inside the shell, resulting in increased internal pressure. The pressure accumulates until it is finally released together with the remaining solvent by inflation, cracking or explosion, depending on the strength/thickness and permeability of the shell at this stage [Nešić and Vodnik 1991]. Figure 2.2, modified from [Farid 2003], indicates the different stages in the transition from droplet to particle.

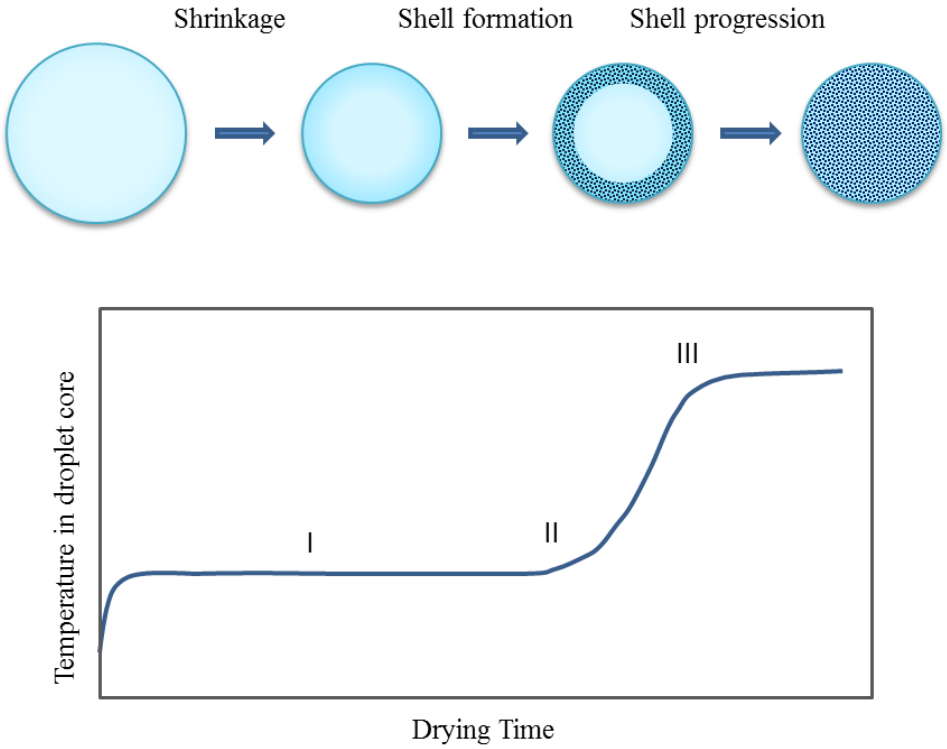

Figure 2.2 The drying stages of a liquid droplet with single solute and single solvent.

The drying process of droplets and later the characteristics of particles is dependent on the solvent as well as the solute used, which influence the evaporation rate of the droplet, molecular mobility of the solute and precipitation of the solutes. Several studies have looked into the relationship between evaporation rate and diffusional motion of solutes during the particle formation process for systems of a single solvent with a single solute, typically a polymer [Okuyama *et al.* 2006, Weiler *et al.* 2010]. Here the relationship between evaporation rate and solute diffusion is described using the *Peclet*

number (*Pe*) (see equation 2.3). When $Pe_i < 1$ the diffusional motion of the solute is faster than the recession rate of the droplet surface due to evaporation, and diffusion can thus keep up with droplet shrinkage. In this case, precipitation of the solute takes place homogenously, late in the drying process, and results in solid particles without a pronounced shell/core structure. When $Pe_i > 1$ the diffusional motion of the solute is slower than the recession rate at the droplet surface and thus the solutes cannot keep up with droplet shrinkage, which results in earlier precipitation at the droplet surface and hence shell formation. In this case, there will be a density gradient within the particles, and depending on the *Pe* number there may be voids inside the particles resulting from low, local solute concentration during particle formation. The *Pe* number thus gives an indication of the radial concentration profile of the particles prepared [Vehring 2008, Vehring *et al.* 2007].

In the case where more than one solute is used, the differences in molecular mobility between the solutes as well as differences in solubility in the solvent will influence the drying process and the final distribution of the two solute components within the particles. The same applies for systems with two or more solvents, where differences in evaporation rate and solvent power may result in an inhomogeneous distribution among solutes or result in other events [Iskandar *et al.* 2003, Okuyama *et al.* 2006]. In both cases the dimensionless number *Pe* can be applied but it would be necessary to expand the model with a time dependent function for the varying evaporation rates of the solvent mixture and the varying diffusion constants of the solutes using differential equations. Further, interactions between the solutes as well as differences in solubility and mobility of the solutes may need to be considered in order to determine the distribution of solutes.

2.3.4 Parameters influencing particle properties in the spray drying process

In the spray drying process a range of processing parameters can be adjusted to control the drying process and the final particle characteristics. The most important parameters include inlet and outlet temperature (T_{inlet} and T_{outlet}), the atomising gas flow rate (atomising pressure), the liquid flow rate, the viscosity of the liquid and finally the properties of the materials in the liquid [Masters 2002]. T_{inlet} and T_{outlet} are important parameters for functional monitoring of the process and it has been stated by several researchers that the ratio between T_{inlet} and T_{outlet} influences the particle characteristics as well as the system yield [Baldinger *et al.* 2012]. Further, the drying gas flow does not seem to have any direct effect on the particle characteristics, but it is recommended to keep it at the maximum as it has an influence on T_{inlet} and T_{outlet} [Cal and Sollohub 2010]. The effect of both the formulation and operation conditions on particle properties have been elucidated by Maa *et al* as well as Cal and Sollohub, who have performed a large study on these effects [Cal and Sollohub 2010, Maa *et al.* 1997]. In their review article, Cal and Sollohub present a table of the spray drying process parameters that influence the resulting particle properties. However, they do not discuss the influence of process and formulation parameters on the density and shape of particles and on the surface and molecular distribution of drug in particles prepared with spray drying.

2.4 Electrospraying

2.4.1 Principles of the electrospraying process

Electrohydrodynamic spraying (or simply electrospraying) is a technology for producing particles in the nano- and micro scale which has been used in a variety of application, also recently including pharmaceutical applications [Chakraborty *et al.* 2009, Pareta and Edirisinghe 2006, Xie *et al.* 2006b]. Electrospraying is based on the phenomenon where a liquid is passed through a concentric nozzle, at a controlled flow

rate, to which a strong electric potential of several kilovolts is applied. As the liquid passing through is exposed to this electric potential the surface tension of the liquid is reduced at the tip of the needle and small, charged droplets form (see Figure 2.3). The basis of this technology has been known since 1879, when Lord Rayleigh discovered that a sufficiently strong electric force could cancel out the surface tension and create instability of a drop at the tip of a nozzle [Rayleigh 1882]. The electric charge limit at which a droplet exposed to an electric force is no longer stable is called the Rayleigh limit and is given as:

$$Q_R = 2\pi(16\gamma\varepsilon_0 r^3)^{1/2} \qquad \text{(Equation 2.4)}$$

where Q_R is electric charge, is γ the surface tension at the liquid-gas interface, ε_0 is the liquid to vacuum permittivity ratio and r is the radius of the drop. Some years later, Zeleny carried out experimental studies with electrospraying based on findings made by Rayleigh and discovered several different modes in which spraying could be performed, which he also quantitatively described [Zeleny 1917]. Since then, the electrospraying process has been employed and described by many either via numerical descriptions or experimentally [Cloupeau and Prunet-Foch 1989, Taylor 1964]. However, there are still areas of electrospraying that remain relatively unexplored, including the detailed particle formation process from droplet to particle, the use of electrosprayed particles for pharmaceutical applications and the commercialization of electrospraying.

2.4.2 Cone-jet and spraying modes

There are various modes by which the jet can form from the nozzle tip in electrospraying. These modes are typically defined by the geometrical form of the liquid at the nozzle tip and the behaviour and disintegration of the jet into droplets (see Figure 2.3). These different modes are of interest because each of these modes has different stability and gives rise to droplets of different size, size distribution and shape

[Cloupeau and Prunet-Foch 1990]. Based on these definitions the spraying modes can be divided into two major groups; those in which small fragments of the liquid are ejected from the nozzle and those that produce a long continuous jet, which disintegrates further downstream of the jet [Jaworek and Krupa 1999]. The first group includes micro-dripping, spindles and ramified-meniscus modes and the latter includes cone-jet, multi-jet, oscillating-jet, ramified-jet and precession mode (see Figure 2.3). Additionally, a corona discharge may also be present and can also affect the jetting behaviour and the resulting particles. These modes of atomization are obtained by adjusting the operation parameters such as flow rate and applied voltage or by changing the liquid composition or the electric field distribution [Cloupeau and Prunet-Foch 1994].

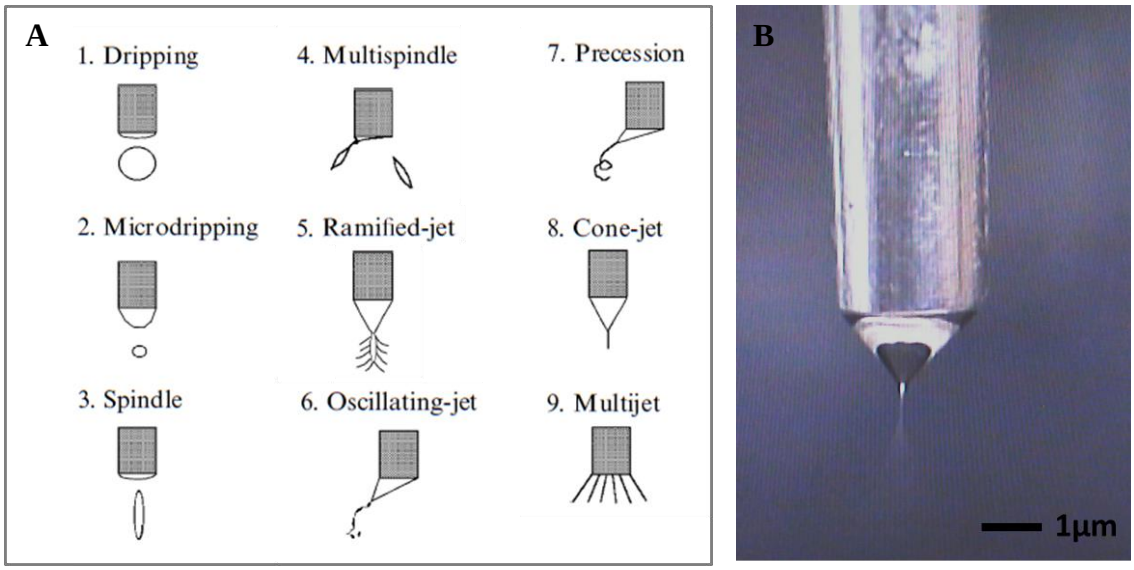

Figure 2.3 Overview of electrospraying atomization modes (A) adapted from [Jaworek and Krupa 1999] and illustration of cone-jet mode captured with CCTV camera (B).

Of all the different jetting modes the cone-jet mode is the one of particular interest to most people using electrospraying. In this mode the liquid meniscus takes the form of a cone leading on to a thin, long jet, which eventually breaks up into small, charged droplets (see Figure 2.4). The cone-jet mode was first discovered by Zeleny, but has

since been described and used by many others [Zeleny 1915]. Studies done by Taylor demonstrated that the diameter of the jet achieved in the cone-jet mode could be very small compared with the capillary diameter. He also showed theoretically that a cone-like interface between two liquids can exist in equilibrium in an electric field when the angle at the apex of the cone is 49.3º. The critical voltage applied to transform a spherical drop to a cone-shape at the tip of a concentric nozzle was predicted based on the angle of 49.3°. This was also demonstrated experimentally where angles during a stable cone-jet were very close to 49.3º. The cone-jet formed at this angle is known as the Taylor cone-jet and has also been shown to be a material-dependent value [Taylor 1964].

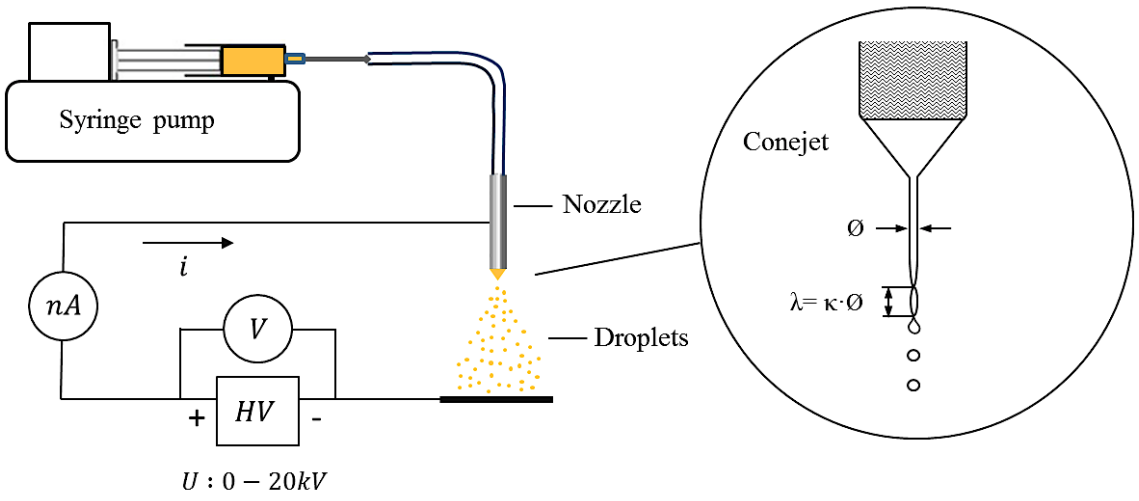

Figure 2.4 General electrospraying setup with droplet formation, where *i* indicates the direction of the electric current, which is in the *nA* range, and *HV* is the high voltage power source with an electric potential, *U*, of several kV.

The cone-jet forms a jet at its tip and as long as the jet does not have too high a charge, the jet will break up into droplets. This break-up takes place into a number of main, primary droplets and secondary droplets. The distance between the breaks in the jet, λ,

(see Figure 2.4) is likely to be the diameter of the jet, Ø, multiplied with a constant, κ, which is influenced by the solution viscosity [Cloupeau and Prunet-Foch 1994, Gomez and Tang 1994]. The cone-jet mode is attractive because it is stable and can produce small particles down to the nano-scale, and it is able to produce near-monodisperse droplets. The monodispersity is, however, considered superior in the dripping and microdripping modes but these modes result in much larger droplets [Jaworek and Krupa 1999].

2.4.3 Electrospraying setup

Electrospraying equipment is generally customized and can vary a lot from one setup to another, depending on the applications it is used for, with some setups being more advanced than others. In general, an electrospraying setup consists of a syringe pump that feeds the liquid into the atomization nozzle(s) at low but constant flow rates (< 6 mL/h per nozzle for the cone-jet mode), a flat-ended capillary nozzle for uniform drop formation and a high voltage power source to drive the atomization process. As with spray drying it provides several operation parameters that can be adjusted to control the process and the output. Some of the essential parameters include the voltage, the flow rate of the liquid feed, humidity and temperature, the collection conditions and the properties of the liquid. Of these the most commonly described parameters used to monitor and manipulate the process are the applied voltage and liquid flow rate.

The particles produced are also highly influenced by the method of collection, and since most electrospraying setups are custom built or assembled the particle collection method especially varies. It is important that the method for collection results in a good yield, due to a low output from a single nozzle in the cone-jet mode. It is most common to collect the particles directly onto a substrate, for instance onto a glass plate/container or onto a filter [Valo *et al.* 2009]. A ground electrode can be used to facilitate this

process by changing the geometry of the electric field present between the nozzle and the ground electrode. This would focus the deposition of particles onto a given substrate [Pareta and Edirisinghe 2006]. Some have collected particles in a liquid either by dispersing the droplets in the gaseous phase above the liquid or collected directly into a continuous liquid phase [Jaworek 2008] or around its surface. Particles collected into liquid are subsequently washed, filtered or centrifuged, and dried to obtain a dry powder or otherwise simply used as a liquid suspension [Xu and Hanna 2006]. However, when collected into a liquid it is most likely that the drug that is on or near the particle surface is released in the liquid and thus results in a reduced drug load and a change in release kinetics compared with particles collected on a dry surface [Bock *et al.* 2011].

2.4.4 Particle formation models for the electrospraying process

Although electrospraying is considered a suitable technique for obtaining particles with a near-monodisperse size distribution, it is neither easy to operate the process nor to control the particle characteristics, and the conditions may differ for each set of materials used. Compared with spray drying, it is necessary with electrospraying to also consider the electrical properties of the spraying feed, the electrical field architecture and its influence on particle attributes. In order to produce particles with better control of characteristics it is important to gain further understanding on the particle formation as well as find clearer definitions of the effect of inter-dependent parameters through multivariate analysis. In section 2.6.3 a brief overview of the efforts in this area is described.

Compared with spray drying there are not many reports on experimental models describing the particle formation process with electrospraying. This is believed to be partly because the drying process with electrospraying is a passive process in most experimental setups and therefore not easy to control and influence by the external

environment. Also, the drop models used for spray drying cannot be used to model particle formation with electrospraying, since the effect of the electric charge is not taken into account and does not correlate to particles at the micro level.

There are, however, several numerical models that have been developed to explain the particle formation process. These include theoretical models that determine the size and frequency of electrosprayed droplets from parameters such as viscosity, electrical conductivity, voltage applied to nozzle, jet diameter etc. [Jaworek 2007]. A frequently used model is the expression for droplet size developed by Gañan-Calvo (see Equation 2.5), which has been experimentally confirmed by several others:

$$d = \alpha \left(\frac{\varphi^3 \varepsilon_0 \rho_1}{\pi^4 \sigma_1 \gamma_1} \right)^{1/6} \qquad \text{(Equation 2.5)}$$

Where α is a constant, φ is the liquid flow rate, ε is the liquid permittivity, ρ is the liquid density, σ is the electrical conductivity and γ is the surface tension [Gañán-Calvo 1999]. The charge on each droplet has been calculated and the relationship between charge and droplet size was studied by [Chen *et al.* 1995]. There are also several models and simulations concerning the break-up of the jet into droplets but not many mathematical models explain the mechanisms taking place from droplet to dry particle [Gañan-Calvo 1997, Lastow and Balachandran 2006, López-Jerrera and Gañan-Calvo 2004].

2.4.5 Particle formation mechanisms with electrospraying

There are three continuous processes involved in the particle formation using the cone-jet mode of electrospraying. First a jet is formed from the liquid meniscus at the nozzle tip, then the jet becomes unstable and breaks up into droplets and finally the droplets dry out into particles.

1: Jet acceleration: The cone-jet forms when the outward stress of the liquid meniscus resulting from the applied electric field balances the inward stress from the surface tension of the liquid. This corresponds to outbalancing the surface tension of the liquid to air interface so that a narrow jet can be formed (see Figure 2.5A). The electric force imposed on the liquid cone results in free charge in the liquid and due to the direction of the electric field the ions in the liquid are accelerated towards the apex of the cone. The ions help forming a thin jet by accelerating the surrounding liquid at the apex of the cone [Hartman *et al.* 1999b, Hartman *et al.* 2000].

2: *Jet break-up*: When a liquid is ejected from the cone it stays a thin, straight jet for some length, typically until surface instabilities occur. At this point, the jet breaks up into small, charged droplets as a result of axisymmetric instabilities (see Figure 2.5B). Lateral instabilities (see Figure 2.5C) may also occur when the surface charge of the jet increases and would result in a broader size distribution of the particles, an often undesirable property [Cloupeau and Prunet-Foch 1989].

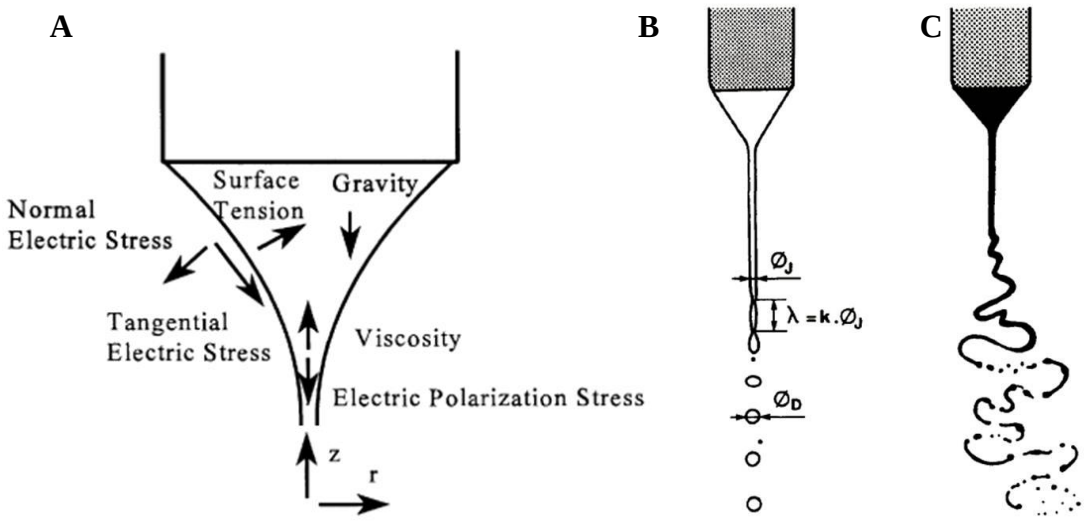

Figure 2.5 Schematic representation of forces in the liquid cone (A) (adapted from [Hartman *et al.* 1999b]) and axisymmetric (B) and lateral (C) instabilities of the liquid jet (adapted from [Cloupeau and Prunet-Foch 1994]).

3: *Particle formation from charged droplets*: Similar to spray drying, the particle formation from droplets in electrospraying takes place through different stages of solvent evaporation (see Figure 2.6). Generally, particle formation with electrospraying can be divided into the following steps.

I) The liquid jet is broken up into small electrically charged droplets that repel each other and disperse. Solvent evaporation takes place at the droplet surface as the droplets are gravitated down in the electric field and the droplet shrinks [Yao *et al.* 2008].

II) The net electric charge of the individual droplet remains constant during droplet shrinkage and hence the charge becomes more concentrated, until it reaches the Rayleigh limit. At this point the droplet cannot hold further charge due to the balance between electric stress and surface tension and undergo a so-called Coulomb fission to form smaller droplets and may then continue to shrink again [Smith *et al.* 2002].

III) The shrinking of the droplet results in a gradual increase in the concentration of solutes until the point where the solutes begin to dry out or precipitate on the droplet surface. Eventually, the entire surface dries out, a shell is formed just as with spray drying, and the particle volume remains constant from this point onwards [Okuzono *et al.* 2006].

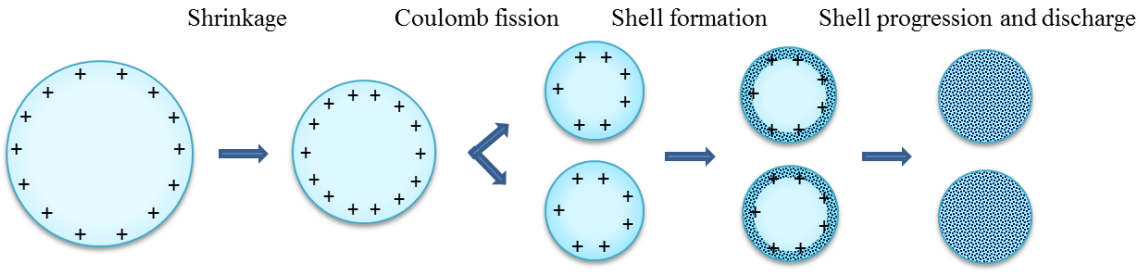

Figure 2.6 Particle formation stages of droplets composed of a single solute and a single solvent, during electrospraying.

IV) Solvent evaporation continues from inside the shell until the particle is dry. Diffusion of solutes within the droplet takes place continuously during solvent evaporation and depending on the balance between evaporation rate and polymer diffusion rate different particle characteristics will be obtained [Xue *et al.* 2010]. Further, there is likelihood that the electric field as well as the electric charge carried by the droplets has an influence on the particle formation process and on the distribution solutes in the particle although this has not yet been elucidated.

2.4.6 Parameters influencing jet stability and particle properties

The electrospraying process is governed by numerous process parameters, which have varying degree of influence on the final particle characteristics. The extent of variables that can be altered and the interdependent effect of different parameters make it very difficult to predict the particle outcome without experimental testing. Generally, these parameters can be categorized as being either process operation parameters or liquid formulation parameters. Some of the main parameters for jet stability and particle characteristics will be discussed in the following.

Nozzle dimensions

One can argue that the atomization nozzle is the main component of the electrospraying setup and that the geometry and dimension of the nozzle will have influence on its output. There are mixed opinions on the role and importance of the nozzle dimensions, where some claim that it largely influences the spraying jet, while other say that it has no influence on the particle formed but only on the stability of the jet [Jaworek and Sobczyk 2008]. Most studies on nozzle dimensions discuss the role of the nozzle diameter of a concentric nozzle. Cloupeau and Prunet-Foch studied different aspects of the electrospraying setup and mechanisms and noted that the liquid flow rate varies as the nozzle diameter changes [Cloupeau and Prunet-Foch 1990]. Tang and Gomez also

studied the role of nozzle diameter but reported that it had no influence on the particles. They found that the stable region of flow rate and voltage was reduced and shifted downwards [Tang and Gomez 1996].

The needle thickness, commonly expressed as the needle gauge, is different for each setup and can vary to a large extent, typically ranging between 0.33-2.38 mm in outer diameter and 0.18-1.77 mm in inner diameter [Cloupeau and Prunet-Foch 1990, Xie *et al.* 2006a]. Generally the needles are flat at the droplet end but there are also angled tips and narrowing tips. The needle dimensions do not seem to have a primary role on the particle characteristics, although some authors have claimed that particle size distribution and jet stability change with needle gauge [Tang and Gomez 1996].

Nozzle configurations

There are also different nozzle configurations that have been used in electrospraying where the most simple is the single nozzle setup. With the single nozzle setup generally a single liquid containing one or several substances is atomized into particles consisting of a mixture of the substances that are sprayed. Another common configuration is the co-axial nozzle setup where two nozzles are arranged co-axially with the purpose to fully encapsulate one material inside another one as a core-shell structure (see Figure 2.7 A) [Loscertales et al. 2002]. If the inner material is a gas, hollow particles can be prepared using the co-axial setup [Chang et al. 2010]. The same co-axial principle can also be used with more than two co-axially arranged nozzles where a similar encapsulation effect has been observed [Ahmad et al. 2008].

Further, another method is to have two capillaries with different liquids merge into one nozzle and form a bi-phasic jet, which can result in Janus particles (see Figure 2.7 B) [Roh et al. 2005]. Examples of particles formed using the mentioned configurations are shown in Figure 2.7 C. Other configurations exist but are not mentioned here. The

single nozzle setup is the most apparent and simple setup for producing solid dispersions because the drug and carrier are mixed together in the spraying feed.

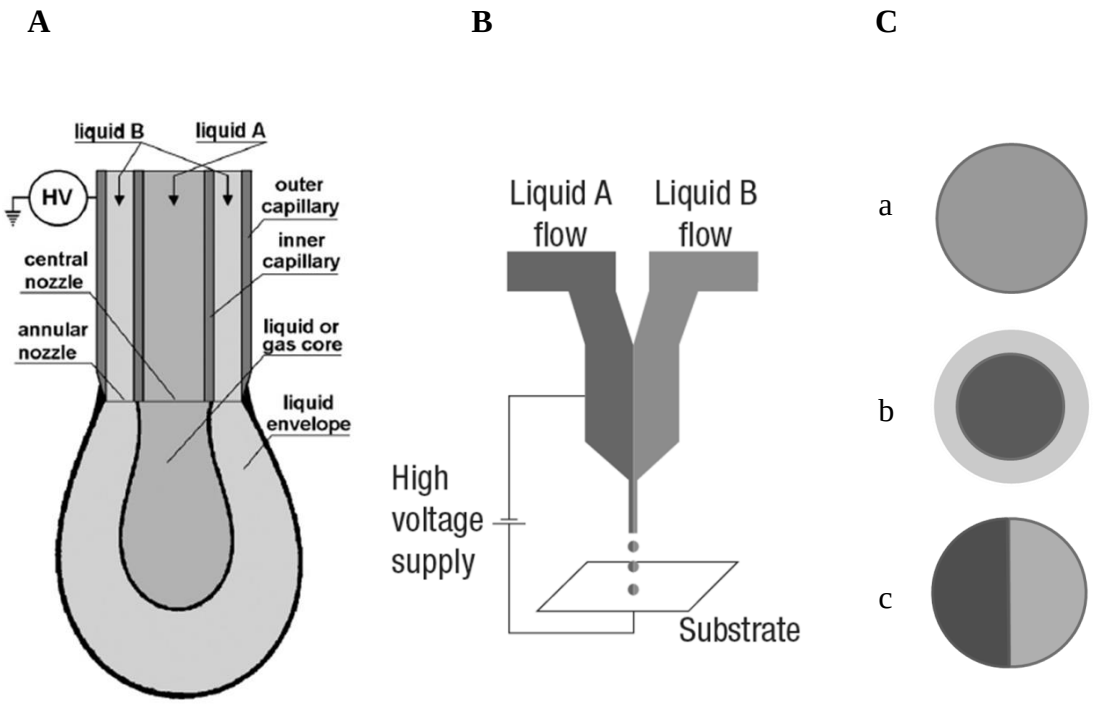

Figure 2.7 Encapsulation via Co-axial spraying (A) (adapted from [Jaworek 2008]), biphasic jetting via dual capillary (B) (adapted from [Roh *et al.* 2005]) and sketch of particles ideally formed by single (a), co-axial (b) and bi-phasic jet (c).

Applied voltage

The strength of the electric field between the capillary and a ground electrode placed at the collection site is mainly controlled by adjusting the applied voltage. The atomization process in electrospraying takes place because electrical forces counteract the surface tension at the liquid–air boundary. An increase in the applied voltage results in an increase in the field strength and hence a stronger atomization effect on the liquid. The cone-jet mode is only obtained in a narrow voltage range, where the meniscus of liquid is conical and stationary. Below this range the meniscus may be conical but will be

unstable and pulsate together with the jet. Above the cone-jet range an unstable multi-jet or another type of unstable jet is formed [Ganan-Calvo *et al.* 1997]. This voltage is thus a key variable in establishing a stable cone-jet. Yet, it is important to know that the voltage range depends on other factors such as the liquid flow rate.

Another influence of the applied voltage within the cone-jet region is its influence on droplet size and hence particle size. It has been demonstrated that droplet size decreases when the voltage is increased within the stable cone-jet range [Jayasinghe and Edirisinghe 2004]. However, when highly conductive liquids and highly viscous liquid were used the effect of applied voltage on droplet size was shown to be minimal [Ku and Kim 2002].

Liquid flow rate

The liquid flow rate is one of the main operation parameters of any liquid atomization technique and this is also the case with electrospraying. This flow rate can be controlled in a broad range using a high precision syringe pump but a stable cone-jet is only established in a certain range. The width and position of this range is dependent on the properties of the liquid as well as other factors. At the minimum flow rate necessary to establish a cone-jet for a given liquid, the jet break-up happens due to varicose instabilities and results in a very narrow particle size distribution. At higher flow rates the surface charge on the jet increases and kink instabilities become more influential on the jet break-up. This results in a broader particle size distribution when the flow rate is increased [Hartman et al. 2000; Jayasinghe and Edirisinghe 2004].

Another effect of the flow rate which has been observed by several groups is its influence on the mean particle size. When increasing the flow rate within the stable cone-jet range an increase in particle size was also observed [Enayati et al. 2009].

Viscosity of liquid

The viscosity of a spraying liquid plays an important role in the electrohydrodynamic process and distinguishes whether the liquid is sprayed into particles or spun into fibres. With electrospraying, the viscosity also has great influence on the break-up of the jet and the size of the droplets produced. It has been demonstrated by Jayasinghe and Edirisinghe (2002) that an increase in viscosity over three orders of magnitudes leads to a dramatic increase in particle size. This observation has also been confirmed by several others [Jayasinghe and Edirisinghe 2002].

Surface tension

The surface tension of a spraying liquid may be important for the stability of the cone-jet and must be overcome by the electrical stresses. A liquid with a high surface tension needs equally high electric field strength to overcome its surface tension so that small droplets can be formed. However, there is a certain limit at which the electric field necessary to outbalance the surface tension is so large that a stable jet cannot be formed because it results in a breakdown of the gas surrounding the cone. This is typically seen as the presence of sparking and results in polydisperse particles or no particles output. An example of a liquid with a high surface tension is water, which can only be sprayed by lowering its surface tension or by changing the gas surrounding the jet into a gas with higher electrical breakdown strength. The surface tension can for instance be lowered by adding surfactants to the liquid and an example of a gas with higher electrical breakdown strength than atmospheric air is CO_2 [Smith 1986; Tang and Gomez 1995].

Electrical conductivity

The electrical conductivity of the spraying liquid is also among the important parameters when staying in the cone-jet mode, both for establishing a stable cone-jet

and also for controlling the size of the droplets produced. Liquids that either have too high or too low conductivity cannot reach a stable cone-jet and thereby cannot carry out their desired function. The conductivity range, which allows the formation of a stable cone-jet, has been reported by Jones and Thong, and Mutoh *et al* to be between 10^{-5} and 10^{-3} S/m [Jones and 1971; Mutoh et al. 1979]. If the electrical conductivity is higher than this range, cone-jet cannot be established due to electrical discharge. When the electrical conductivity is lower than the given range, a stable cone-jet cannot be established due to the insufficient charge building up in the liquid and hence a lack of tangential stress. Yet, in this case the liquid can still potentially be used by increasing the conductivity via addition of salts or other conductivity enhancers [Cloupeau and Prunet-Foch 1989; Hartman et al. 1999b].

Moreover, the value of electrical conductivity within the stable cone-jet window also influences the properties of the droplets generated, most notably their size. A spraying solution with a high electrical conductivity has been demonstrated to give rise to smaller particles than a solution with low electrical conductivity [Ganan-Calvo et al. 1997; Lopez-Herrera et al. 2003].

Particle size is one of the most studied particle characteristics and is closely linked to the size of the droplets formed and the Peclet number of the feed solution. Equation 2.5 which describes the droplet size indicates the parameters influencing particle size such as flow rate, viscosity, surface tension and electric conductivity. Also, the Peclet number (see section 2.3.2) is linked to the particle diameter as the ratio between the evaporation rate and solute diffusion determines when the solutes begin to precipite. Studies have shown that a decrease in evaporation rate allows longer diffusion time for the solutes and leads to smaller particles. However, this may also be associated with a

higher solubility of solutes in the solvent resulting in higher polymer mobility [Park and Lee 2009].

The applied voltage may be adjusted to influence particle size but typically also alters the stability and shape of the jet. Increasing the voltage imposes more electric charge on the droplets and is seen to alter the shape of the particles, leading to more elongated particles and even fibres given the right solution conditions [Enayati *et al.* 2009]. The mode of particle collection obviously has an influence on evaporation time and the resulting particle characteristics and the distance of collection can be controlled to give optimal conditions as sufficient drying is necessary to obtain non-collapsed particles. The particles prepared with electrospraying are very sensitive to changes in the liquid properties but also to temperature, humidity and other external factors.

2.4.7 Advantages and disadvantages of electrospraying

Although electrospraying is currently not as developed as some conventional techniques such as spray drying and freeze drying there are definitely some advantages with electrospraying. The most apparent advantages of electrospraying when compared with other atomization technologies are:

1. Due to the exposure to an electrical potential the droplets produced are electrically charged, repelling each other and are thus self-dispersing. This acts to prevent aggregation of particles [Jaworek 2007].

2. Smaller droplets can be produced with atomization using electrospraying, partly due to the lowering of surface tension and the electrical charge-related droplet fission process. Small droplets will naturally result in small particles [Peltonen *et al.* 2010].

3. Due to the fragmentation mechanism of liquid filaments from the jet during cone-jet mode, a very homogenous distribution of particles can be achieved without post-

processing such as filtering. Good stability of the jet (e.g. cone-jet mode) results in near-monodisperse particles [Chen *et al.* 1995].

4. The deposition of particles onto a substrate can be controlled by modifying the electric field limiting particle loss and narrowing the deposition area to a specific region [Jaworek and Sobczyk 2008].

The main disadvantage of particle production with electrospraying is its low throughput, which is typically a fraction of a gram of dry weight per hour for a single nozzle setup. This is much lower compared with the throughput of a laboratory scale spray dryer and is far from sufficient for production in accordance with good manufacturing practice (GMP) guidelines. However, efforts have been made in upscaling electrospraying devices by using multiple nozzles placed in one plane [Almekinders and Jones 1999, Regele *et al.* 2002] or by spraying through uniform holes in a plate [Bocanegra *et al.* 2005, Deng *et al.* 2009] (see section 2.6.5).

2.5 Challenges in formulating solid dispersions

2.5.1 Stability of solid dispersion

Although solid dispersions provide great improvements in drug dissolution rate and other favourable properties, they suffer from both physical and chemical instability. In solid dispersions the drug is amorphous or partially amorphous within the polymer matrix and is thus not stable from a thermodynamical point of view, eventually resulting in devitrification, the process in which an amorphous phase converts into crystalline phases. However, such devitrification ideally does not happen for several years if careful considerations are made during formulation [Van den Mooter *et al.* 2001]. Nonetheless, due to the properties and characteristics of solid dispersion instability of

the solid dispersions may occur during processing as well as during storage, most notably leading to crystallization of the drug.

The stability of solid dispersions can be evaluated using different analytical tools including X-ray powder diffraction and differential scanning calorimetry, which are often used in combination to determine the physical state of a material, including the percentage of crystallinity present [Leuner and Dressman 2000]. Recently, the advance of process analytical technology (PAT) has shifted the direction more towards fast, non-destructive methods in particular vibrational spectroscopy such as Raman, Near infra-red and Fourier Transformed infra-red spectroscopy in combination with chemometrics to identify the solid-phase of these dosage forms [Qian *et al.* 2010, Strachan *et al.* 2007].

Molecular mobility and drug-polymer interactions

Molecular mobility is considered one of the key determinants governing the physical stability of amorphous phases such as the case with solid dispersions. The molecular mobility is related to the number of collisions of the molecules per unit time and is representative to some degree of how fast recrystallization takes place. The molecular mobility of a material undergoes a remarkable change as the temperature is increased above the T_g, and the T_g is known to give an indication of the degree of molecular mobility of the system [Zhou *et al.* 2007]. Molecular mobility in solid dispersions can be reduced by selecting a polymer with a high glass transition temperature (T_g), which thereby increases the T_g of the whole amorphous system and implies a reduction in molecular mobility. This reduces the crystallization at given storage conditions [Hancock *et al.* 1995]. Although mobility is reduced and storage is performed under the T_g of the systems, there may still be enough mobility for recrystallization to take place over pharmaceutically relevant time scale. However, molecular mobility was reported to

become insignificant when the storage takes place 50 K below the T_g. Amorphous drugs with a low T_g also benefit from the a high T_g of the polymer, which can lead to an antiplasticising effect [Gunawan *et al.* 2006]. Also, the molecular mobility not only depends on the properties of the drug and carrier used but also on the processing method used to prepare the solid dispersion.

The physical stability also depends on the miscibility of the drug in the polymer and is ideally molecularly miscible in the polymer. It has been demonstrated that the drug has a lower chemical potential when mixed with a polymer, from a thermodynamics viewpoint, and thus a reduction in crystallization process is experienced. Further, such miscibility will also be influenced by the degree of interaction between the drug and the polymer. Several types of such interactions may form and those frequently observed include intermolecular hydrogen bonds, van der Waals, and electrostatic interactions.

A majority of poorly water soluble drugs contain hydrogen bonding sites and by formation of bonds between the drug and the polymer hydrogen bonding otherwise characteristic to the crystal structure is disrupted, thus promoting stability [Qian *et al.* 2010, Taylor and Zografi 1997]. The strength of the molecular interactions formed between the polymer and the drug is of high importance for the physicochemical properties and physical stability of the system. Some polymers exhibit stronger hydrogen bonds to a specific drug than other polymers and for instance PVP has been observed to form stronger hydrogen bonds than PEG does, with their interaction energies estimated at 30-36kJ/mol and 19-21 kJ/mol for PEG and PVP respectively for this specific system [Teberekidis and Sigalas 2007].

The polymers can act as either intermolecular hydrogen bond donors or acceptors and some polymers such as HPMC have both hydrogen bond donating and accepting groups, which from a stability stand point could be advantageous for interactions with

both a drug and a excipient with hydrogen bonding properties [Bee 2010]. It is, however, important to match the properties of the carrier with the drug in order to achieve enhanced interaction between them and restrict molecular mobility and thus obtain better stability. In addition to hydrogen bonding other types of bonds may also enhance stability. It has for instance been shown that Eudragit E100 can stabilize the amorphous drug by forming ionic interactions. Such interactions are stronger than intermolecular hydrogen bonding and thus may provide further advantage in the physical stability compared with systems where hydrogen bonds are formed [Moustafine *et al.* 2005]. Ideally, a combination of these stabilizing strategies would be desirable to obtain optimal hindrance of recrystallization.

A study by Ke *et al.* has further shown that the physical stability of solid dispersions is process dependent and by testing three processes, spray drying, melt quenching and ball milling to prepare solid dispersions, it was found that ball milled dispersions were the least stable while surface relaxation time was highest for spray dried samples and molecular mobility was lowest for melt quenched samples [Ke *et al.* 2012].

Storage considerations

The formulation, processing method and material selection have all been reported to have an influence on the physical stability of solid dispersions. Yet, the storage conditions of samples also has a significant impact on the stability and shelf life of the samples, and can be optimized to compensate for tendencies of instability from the formulation and improvement of already stable formulations. It is in particular the temperature and humidity during storage that seems to have a considerable effect on physical stability. Studies have been performed on different polymers and humidity conditions to observe the influence on stability of amorphous solid dispersions.

Comparing PVP, HPMC and HPMCAS at 5-95% relative humidity at 10% intervals it was found that all polymers absorbed more water relative to the drug thereby increasing the moisture content of the systems. Yet, the crystallinity tendencies were limited although in particular PVP was more prone to recrystallization, probably due to the hygroscopicity of PVP [Rumondor *et al.* 2009]. However, it is also seen that moisture may lead to phase separation, crystal growth and transformation of polymorphs, all of which would lead to a decrease in dissolution rate and thus a critical diversion from the intended effect [Van den Mooter *et al.* 2006].

It seems clear that solid dispersions often have a vulnerability to storage conditions, partly due to the hygroscopicity of many hydrophilic polymers. Thus, it is important to thoroughly test the influence of storage conditions on each formulation and develop a set of guidelines for packaging, handling and storage of these products, both in order to optimize the shelf life and the performance of the products.

2.5.2 Dissolution and *in vivo* correlation of solid dispersions

Although solid dispersions have proven effective in increasing the bioavailability of poorly soluble drugs the mechanisms governing the dissolution are still not completely understood. There are many parameters dictating the dissolution mechanisms of the drug and this also largely depends on the carriers materials used in the formulation. The release of drug has been suggested either being controlled via disintegration of the polymer or via drug diffusion [Craig 2002]. For solid dispersions composed of a water-soluble polymer the dissolution mechanism of the system and dissolution rate of the drug has been shown to be dependent on the drug loading. At high drug loadings the polymer dissolved quicker than the drug leaving behind a drug rich phase, possibly in an amorphous form, which regulated the dissolution rate of the remaining solid. At low drug loadings the drug dissolution rate was higher and the polymer and drug essentially

dissolved simultaneously making the drug dissolution dependent on polymer disintegration [Simonelli *et al.* 1969]. Drug dissolution has in such drug loading dependent manner been suggested described via the following equation [Alonzo *et al.* 2011]:

$$G_D = \frac{G_C \times C_D}{C_C} \qquad \text{(Equation 2.6)}$$

where G_D is the dissolution rate of the drug, G_C is the dissolution rate of the carrier, C_D is the component concentration of drug and C_C is the component concentration of the carrier. Further studies have shown that the physical stability and the crystallization behaviour upon contact with dissolution media and the precipitation kinetics of the supersaturated drug are both important factors for the drug concentration profile [Alonzo *et al.* 2010]. Often studies on dissolution mechanism have focused on the drug-carrier interactions and the composition of the solid dispersions and less on the supersaturation properties. Yet, much indicates that the ability of the drug to remain supersaturated for longer times under non-sink conditions via properties of the drug or precipitation inhibition properties of the carriers may provide considerable improvements in the *in vivo* performance of the formulation [Curatolo *et al.* 2009].

Solid dispersions have traditionally been thought to increase the release of poorly soluble drugs *in vitro* and *in vivo*, compared with conventional dosage forms, resulting in enhanced bioavailability. Although enhanced *in vitro* dissolution rates and enhanced absorption rates have been demonstrated and in many studies there is often not a straightforward correlation between the *in vitro* and *in vivo* data [Craig 2002]. Different studies are used to try to predict the *in vivo* performance of these solid dispersions but this can often be a challenging task given the complexity of the GI tract biology and the variation between species and even among humans. By examining the *in vitro / in vivo*

correlation of a formulation it is observed whether dissolution of the drug is the rate limiting step and hence the formulation may be optimized to allow more precise dosing or a better pharmacokinetic profile. In order to assess the *in vitro / in vivo* correlation of drug formulations the C_{max} (or $AUC_{0 \rightarrow infinity}$) and the drug dissolution (% dissolved) values are typically plotted in an XY-plot and a linear regression is performed. In this case a linear relationship between the pharmacokinetic parameters and the dissolution profile represents a good correlation [Zerrouk *et al.* 2001].

Emara *et al* [Emara *et al.* 2002] prepared solid dispersions of PEG6000 and Nifedipine using the fusion method, solvent evaporation and freeze drying and compared the *in vitro* and *in vivo* behaviour obtained with these three preparation methods. They found that the samples prepared with solvent evaporation and freeze drying had faster dissolution compared with those prepared with fusion method. However, the *in vivo* data was contradictory to the dissolution data indicating higher bioavailability for the samples prepared with the fusion method despite a good correlation generally between the dissolved and absorbed amount of drug. Good in vitro / in vivo correlation was observed for extended release formulations in dogs by Tanaka *et al [Tanaka et al. 2006]*

One of the major considerations for oral formulations is the effect of the gastro-intestinal environment on the drug release, due to varying milieus such as pH and variations due to food intake. These factors and often have a major impact on the drug dissolution demonstrated by the divergence in the *in vitro / in vivo* correlation [Dokoumetzidis and Macheras 2006]. Variation between the subjects studied also lead to significant divergence. Better understanding on the mechanisms of the GI tract as well as its influence on drug is believed to provide better prediction of the *in vivo* performance of drug formulations.

2.5.3 Molecular dispersions, homogeneity and drug distribution

As previously mentioned solid dispersions in which the drug is molecularly dispersed in the carrier matrix generally provide the best barrier against crystallization and are thus desirable to obtain. In addition to the form of dispersion it is also important to have some knowledge on the homogeneity of the dispersion and whether there are some areas or local phases with a higher drug concentration. Finally, it is important to know more about the spatial distribution of drug in cases where the drug is not present as a homogeneous, molecular distribution as this would most likely influence the release kinetics and the physical stability [Urbanetz and Lippold 2005].

There are several analytical methods to determine the characteristics of the drug dispersion and these are often used in combination to describe the molecular properties of the solid dispersion.

Nuclear magnetic resonance (NMR) has been used to study polymer mobility and drug migration in solid dispersion formulations. Both 2D and 3D images can be obtained with NMR, yet with the current spatial resolution available the technique seems more suitable for looking at the microstructure of tablets [Dahlberg *et al.* 2010]. Dahlberg *et al*, however, used the technique to study the drug diffusion process from solid dispersions.

X-ray photoelectron spectroscopy (XPS) has been used in several studies to examine the chemical composition of the outer surface layer (~5 nm) of solid dispersions and can give an estimate of the concentration of drug in the measured area. XPS has been used to study the surface drug concentration in order to examine the possible tendency for drug molecules to migrate towards the surface of spray dried powders [Dahlberg *et al.* 2008].

Time-of-flight secondary ion mass spectroscopy (ToF-SIMS) has also been used to investigate the surface chemical composition of solid dispersions but with this method a thickness of approximately 1-2nm is examined [Scoutaris *et al.* 2012]. Scoutaris *et al* used this technique to study the chemical composition of solid dispersion particle surfaces and prepared 2D images by generating a chemical map from the ToF-SIMS data. In this way it was demonstrated that the drug was homogeneously distributed on the particle surface.

Confocal Raman spectroscopy has been used to determine the physical state of the drug in a solid dispersion and it has in some cases also been used to examine the homogeneity of the drug distribution [Breitenbach *et al.* 1999]. In a study by Breitenbach *et al.* an area of 45 × 25 μm^2 was studied via 200 measurements in the area using Confocal Raman spectroscopy. They demonstrated that the homogeneity of the sample could be mapped relatively well with a resolution of 2 μm^3 using a scale for drug concentration obtained by setting up a correlation with HPLC measurements [Breitenbach *et al.* 1999]. Although this may be useful for detecting the presence of larger drug aggregates or to determine the general homogeneity of melt extrudates or other larger samples, the resolution is not sufficient to look at the drug distribution in small microparticles prepared with spray drying and electrospraying.

Fourier Transformed Infrared (FTIR) imaging uses an array of infrared detectors to gain information on spatial differences in the concentration of compounds and interactions between them. FTIR imaging has also been used to examine the distribution of drugs in solid dispersions [Chan and Kazarian 2004]. In a study by Chan and Kazarian a detector setup with a pixel size of around 60 µm was used to study a Nifidipine/PEG formulation with 5-20% drug loading as the formulation came into contact with water. They observed a relatively homogeneous drug distribution before

dissolution and could locate the formation of drug crystals in the matrix as the PEG progressively dissolved, and this observation was more prominent for higher drug loading.

Phase separation between the drug and carrier material is an event that could occur in solid dispersions. Such phase separation has been studied using methods including *micro-thermal analysis* (μ-TA), which is essentially an AFM technique where the cantilever is substituted with a Wollaston wire thermistor. With this technique the thermal conductivity in different areas of the sample is mapped in the microscopic scale [Six *et al.* 2003]. In solid dispersion extrudate samples it was demonstrated that phase separation took place between the drug, Itraconazole, and polymer, Eudragit. When studying phase separation it is interesting to investigate the influence of different solvent systems on the drug distribution in the polymer matrix. For binary solvent systems phase separation may occur when the solutes have different degrees of solubility in the two solvent phases.

It seems that by combining two or more techniques it is possible to gain some understanding of the drug distribution and possible phase separations and crystallization processes in amorphous solid dispersions. Currently, one of the better methods to obtain information on the radial drug distribution in amorphous solid dispersions would be XPS or ToF-SIMS where the exact drug concentration within a specific surface area can be determined. There does not seem to be any methods for specifically measuring the drug concentration or molecular drug distribution in the deeper areas of particles. It should, however, be possible to make cross sections through particles using FIB/SEM and subsequently use Energy Dispersive X-ray (EDX) spectroscopy to obtain a spectrum of the elements present in the uncovered area of the particle, which may be quantified using Monte Carlo simulations. Yet, also simpler or less time consuming

methods may appear in the near future. Techniques such as Confocal Raman spectroscopy and FTIR imaging may become more useful for studying the general homogeneity of solid dispersion samples and for visually detecting phase separation and presence of crystals in the samples. NMR may also be used for such purposes and can additionally provide 3D images of the samples, but it seems that the spatial resolution is currently still too low for this type of application.

It is well known for liquid atomization processes that solvent selection has an influence on the particle characteristics and it has further been reported that the properties of the solvent have an influence on the drug distribution in the prepared particles [Vehring *et al.* 2007]. Based on a binary solid dispersion system of drug and polymer the characteristics and drug release kinetics of solid dispersions prepared with spray drying have previously been correlated to solvents and mixture of solvents used to prepare the solid dispersions [Rizi 2011]. The drug and polymer component of a solid dispersion can be very different in both size and solubility in a given solvent and may thus result in a non-homogenous dispersion and even phase separation during solvent evaporation and solute diffusion.

Properties of the solvent that may influence the drug distribution include in particular volatility and solvent power for dissolving the solute components as these properties govern the mobility of the solutes in the solvent and the time in which diffusion of solutes is allowed. Further, by using a mixture of solvents the solute components may have different solubility in each solvent resulting in additional differences in the architecture of the dispersion. There have even been cases where an improvement in *in vitro* performance was observed for solid dispersions prepared with a solvent mixture compared with single solvents [Paudel and Van den Mooter 2012]. Although, there is evidence for the importance of solvents and solvent mixtures on the solid state

properties of solid dispersions, there is still no detailed account on the exact impact of solvent chemistry on the phase behaviour and resulting drug release kinetics of solid dispersions.

2.6 Applications of spray drying and electrospraying

Spray drying has been widely applied for preparing solid dispersions and remains one of the main methods for preparing solid dispersions. A wide range of drugs and carriers may be used with spray drying due to the relatively mild processing conditions, including thermolabile materials and polymers with a high melting point. Also with electrospraying a wide range of drugs and carriers can be used, although the technique is much less explored compared with spray drying, especially for solid dispersions purposes. In the following, different formulation strategies currently used for solid dispersions are introduced and examples of applications, where solid dispersions are produced using spray drying and electrospraying, are provided. The formulation approaches for spray drying are relatively similar to those that can be used for electrospraying applications.

2.6.1 Formulation strategies for solid dispersions

A variety of carrier–drug combinations has been studied using spray drying. The carriers have mainly been polymeric and generally have been selected based on their physicochemical properties, including their T_g, solubility properties, ionization constant, hydrogen bond forming profile as well as suitability with a specific drug compound [Janssens and Van den Mooter 2009]. Most polymers used are hydrophilic, increase the drug dissolution rate and act as crystallization inhibitors, due to their anti-plasticing effect.

In order to spray dry a solid dispersion both the drug and the carrier must be soluble in the common solvent used. Since poorly soluble drugs do not readily dissolve in water at useful concentrations, an organic solvent or a mixture of solvents are typically used for solvent based spray dried solid dispersions [Bee 2010]. There are however applications where a melt is spray dried to form a dry solid dispersion powder without the use of solvents such as with spray cooling/spray congealing [Serajuddin 1999]. In any case it is important that the drug and carrier components are dissolved or very well mixed since suspensions tend to give rise to phase separation and instability of the formulation. Binary solid dispersions are still commonly used, yet ternary or higher degree mixtures combining solubilizers, fillers, binders, stabilizers or disintegrants are also becoming more common as they often provide further improvement of the dissolution rate and better stability.

Polyvinylpyrrolidone (PVP) is one of the most studied polymers for solid dispersions and continues to be popular for binary and multi-component systems. Some grades of PVP have a high T_g above 120 ºC and thus act as a good anti-plasticizers lowering molecular mobility. PVP is soluble in water as well as several organic solvents including ethanol and acetone which makes it is easy to use for spray drying and possibly electrospraying applications [Rowe 2009]. A notable concern of using PVP is the relatively high hygroscopicity, which lowers the physical stability of the formulations at elevated humidity conditions, although appropriate storage conditions may help prevent drug re-crystallization [Patterson *et al.* 2007].

Polyethylene glycol (PEG) is a widely studied polymer for pharmaceutical applications in general but also for solid dispersions. These polymers range from being liquid to solid at room temperature depending on their molecular weight. PEG is typically semicrystalline with a relatively low T_g 58-63 º C for 3400-20000 MW [Craig 1995]. It

is soluble in water as well as many organic solvents which makes it simple to prepare solid dispersions using spray drying and possibly electrospraying [Fouad *et al.* 2011]. Solid dispersions formed with PEG generally have the drug molecules dispersed in the polymer in an amorphous form or partly crystalline state within the amorphous and crystalline sections of the polymer [Weuts *et al.* 2005, Zhu *et al.* 2012]. Although, PEG-based solid dispersions result in an increase in dissolution rate, unless combined with other excipients they typically have poor physical stability and result in recrystallization of the drug at elevated temperature or humidity [Weuts *et al.* 2005].

Polymethacrylates are synthetic polymers mainly marketed by Evonik under the name Eudragit® and come in a variety grades and monomer ratios. These polymers can show pH dependent solubility and are thus often used as enteric coating materials for tablets and other dosage forms. They are soluble in several organic solvents making them suitable for processing via spray drying and possibly also electrospraying [Six *et al.* 2004]. Polymethacrylates carry hydrogen bond accepting groups and are therefore suitable for drugs with hydrogen bond donating drugs. In addition to hydrogen bonds cationic methacrylates provide ionic interactions which are believed to further improve the physical stability of the solid dispersions [Bee 2010].

Cellulose derivatives include hydroxypropyl methyl cellulose (HPMC), hydroxypropyl cellulose (HPC), HPMC-phthalate (HPMC-P) and HPMC-acetyl-succinate (HPMC-AS). This group of polymers has become the most used polymers for preparing solid dispersions. HPMC is a water-soluble polymer and is insoluble in most commonly used organic solvents and necessitates hydroalcoholic solvents or a mixture of methanol and DCM depending on the polymer grade [Bee 2010]. It has a high T_g above 170º C but its hygroscopicity makes the solid dispersions sensitive to humidity [Rowe 2009].

However, it has been reported to provide improvement in dissolution rate resulting from increased wettability and its anti-plasticizing effect [Boghra *et al.* 2011].

HPMCP and HPMC-AS are both polymers with pH dependent solubility and are typically used as enteric coating materials for tablets and granules because they are insoluble in gastric fluid but dissolve in the intestine at a pH above 5-6.5 depending on the polymer grade [Bee 2010]. HPMC-AS is soluble in several organic solvents, which makes it suitable for spray drying while HPMCP is mainly soluble in mixture of solvents such as DCM and acetone and are thus slightly more difficult to use for spray drying applications. Both polymers have a high T_g above 120 ºC and are relatively stable during storage [Rowe 2009]. In a study by Friesen et al solid dispersions of HPMC-AS were prepared with 9 different poorly soluble drug compounds using spray drying and it was observed that the drugs remained amorphous during a storage time of more than two years [Friesen *et al.* 2008].

In addition to their dissolution enhancing and stabilizing properties, the cellulose derivates and in particular HPMC and HPMC-AS are known as effective precipitation inhibitors prolonging the supersaturation of drugs for many hours after dissolution (see Figure 2.8). The pronounced effect observed with HPMC-AS is explained by the formation of a reservoir of nanosized amorphous drug-polymer aggregates resulting from ionized state and from hydrophobic interactions [Curatolo *et al.* 2009]. These nanosized aggregates result in a drug precipitation process resembling a parachute landing where the drug molecules precipitate slowly from the supersaturated state. In comparison, the conventional solid dispersion systems using water-soluble polymers typically result in a drug precipitation process resembling the behaviour of a spring with the drug molecules rapidly precipitating from the supersaturated state (see Figure 2.8).

For more information on precipitation inhibition the reader is referred to the review by Warren *et al* [Warren *et al.* 2010].

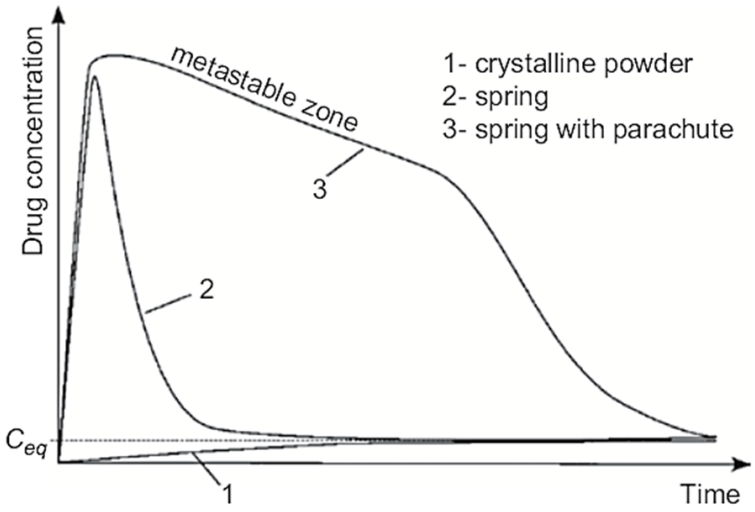

Figure 2.8 Representation of supersaturation in different systems, aqueous drug concentration versus time profile. 1: dissolution of pure crystalline drug, 2: dissolution of amorphous solid dispersion and 3: dissolution of amorphous solid dispersion under presence of precipitation inhibitor(s) (from [Warren et al. 2010]**)**.

The combination of more than two excipients is also widely applied for preparing solid dispersions in order to improve the stability, dissolution rate, powder properties etc. of the dispersions [Saharan *et al.* 2009]. Surfactants are commonly added to increase wettability and solubility of the formulation and include poloxamer, a co-polymer of poly(ethylene oxide) and poly(propylene oxide), sodium lauryl sulphate and poly vinyl alcohol. Acids such as maleic, citric acid and tartaric acid have been used for pH modification of the systems and to allow better solubility [Paudel *et al.*]. Yet, the addition of excipients other than the main carrier material may in turn make the formulation more complex and result in destabilization of the dispersion or result in unexpected dissolution results.

2.6.2 Particle-based solid dispersions using spray drying

There are many examples of applications where spray drying has been used to prepare particle-based solid dispersions using a poorly soluble drug together with one or another combination of the carrier materials described above. Generally, a powder of microparticles is formed and for hydrophilic carriers the results show increased dissolution rate of the drug compared with the spray dried drug alone and physical mixture of the drug and carrier. For extended release application diffusion controlled release of the drug is observed.

Griseofulvin was spray dried with Poloxamer 407 using a laboratory scale spray drier. It was demonstrated that both solubility and bioavailability increased compared with a control formulation of griseofulvin alone [Wong *et al.* 2006]. Solid dispersions with ibuprofen, HPMC and poloxamer were prepared and resulted in increased dissolution rate and bioavailability compared with crystalline ibuprofen [Park *et al.* 2009]. PVP has been co-spraydried with many different API's to form solid dispersion and generally results in good dissolution and bioavailability. PVP is typically present in an amorphous form in the solid dispersion and reduces the mobility of API in the polymer matrix reducing crystallization of drug post drying [Paradkar *et al.* 2004].

A comparative study by Qian *et al* of solid dispersions of polyvinylpyrrolidone-vinyl acetate (PVP-VA, a PVP variant with less moisture absorption) and a poorly soluble API with solid dispersions of HPMC-AS and the same API showed significantly greater bioavailability with HPMC-AS than with PVP-VA. HPMC-AS showed slow dissolution with long supersaturation of the drug while the fast dissolution with PVP-VA resulted in drug recrystallization before dissolution was completed thus affecting *in vivo* performance [Qian *et al.* 2012]. Friesen et al have prepared solid dispersions of HPMC-AS with various poorly soluble drugs and have reported high dissolution rates compared

with the crystalline form of the drug and high concentrations of the drug were observed for long time periods due to the precipitation inhibiting effect of HPMC-AS. Further, significant enhancement in oral absorption and hence enhanced bioavailability of the drugs was observed and good stability was obtained with shelf lives of more than 2 years [Friesen *et al.* 2008]. Examples of spray dried particles are shown in Figure 2.9.

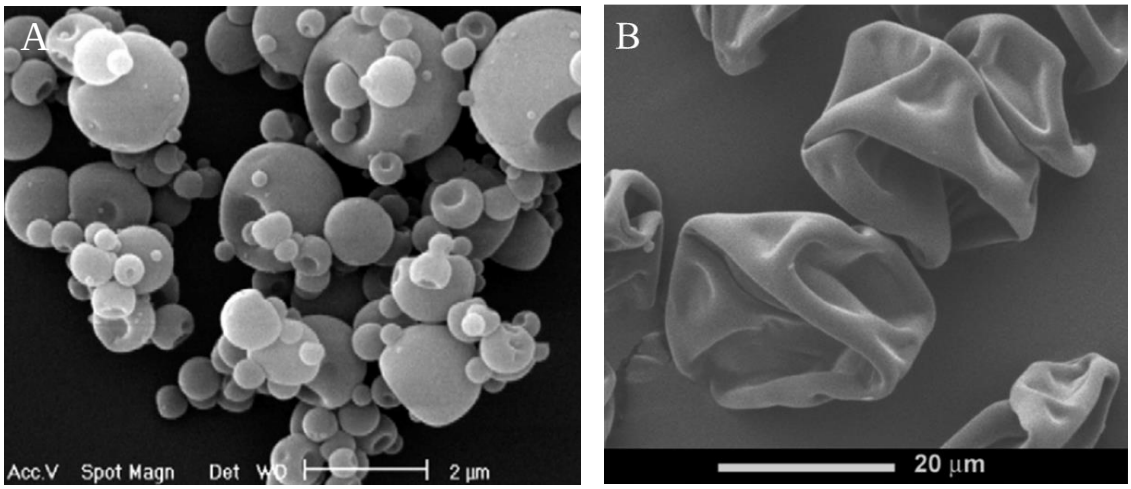

Figure 2.9 Example of spray dried particulate solid dispersions prepared using Netilmicin sulphate (A) [Vehring *et al.* 2007] and HPMC-AS with AMG 517 (B) [Kennedy *et al.* 2008].

Further, the influence of process parameters on the prepared solid dispersions and their solubility and physical stability have also been studied by a few researchers. Kojima *et al* used a Büchi B-290 laboratory scale spray drier to prepare solid dispersions from HPMC together with the drugs nilvadipine and nifedilipine at a constant drug:polymer ratio while altering the nitrogen flow rate, feed rate and solute concentration [Kojima *et al.*]. They showed that the dissolution profiles as well as the glass transition temperature of the systems changed as a function of these parameters and their results indicated that although the particles were similar in size and morphology, microstructural phase separation could occur.

The effect of the process parameters are, however, not easy to isolate and use for controlling particle characteristics and dissolution behaviour due to the numerous interactions between the parameters and their dependence on the individual formulations parameters. In such a scenario it may be more advantageous to utilize multivariate data analysis to evaluate the influence of a collective set of parameters on specific characteristics. With such strategies one could gain more comprehensive understanding on the interaction between process parameters and for instance how to better control and optimize particle and formulation characteristics for better performance [Baldinger *et al.* 2012, Dobry *et al.* 2009]. High throughput screening studies can also help set up a more generalized model for influence of process variables and control of characteristics [Gibson *et al.* 2011].

2.6.3 Control of particle characteristics with spray drying

There are numerous reports on the application of spray drying for producing solid dispersions but only few reports focus on the resulting particle characteristics and even less focus on controlling particle characteristics to improve formulation properties. Yet, spray drying is not only a suitable process for industrial scale production of solid dispersion formulations but also for tailoring microparticles with desirable attributes. Studies on such particle engineering approach is in its early phase but has demonstrated its importance in several studies [Chow *et al.* 2007, Kennedy *et al.* 2008].

The control of particle morphology using spray drying has been studied by different researchers and several different morphologies have been demonstrated and presented in the following reviews [Nandiyanto and Okuyama 2011, Vehring 2008]. Generally spherical morphologies are obtained as they are energetically most favourable during drying of the droplet and have maximum structural stability. The distinction of producing solid or hollow spherical particles depends on the mass and heat transfer

mechanisms during drying. It is a balance between solute diffusion and evaporation rate and can be controlled using these parameters [Okuyama *et al.* 2006]. Also, different particle shapes such as doughnut shape and disc shape have been obtained via controlled collapsing of the particles during formation and may be tailored further through understanding of their structural stability [Iskandar *et al.* 2003].

Particles can also be made from precursor nanoparticles where these are assembled during the spray drying process to form relatively complex microstructures with the nanoparticles as their building blocks [Tsapis *et al.* 2002]. The porosity of such structures has been controlled by preparing composite particles consisting of different phases or materials and by later removing one of the materials to obtain a controlled pore size [Nandiyanto and Okuyama 2011].

Studies have demonstrated the control of several fundamental characteristics such as particle size, to some part morphology, surface topology and porosity. Currently, much of this is based on processing of a single material or at the most two materials. When two or more materials are spray dried together the interactions and mechanisms become more complex. For solid dispersions in which there are at least two components it is important to understand the phase structure and drug distribution within the matrix. There are currently no studies explaining in detail the influence of process variables on drug distribution within the matrix, however, some studied have reported varying degrees of drug deposition onto the particle surface [Dahlberg *et al.* 2008].

2.6.4 Electrosprayed solid dispersions

Electrospraying is still a relatively novel method for pharmaceutical applications and currently not many reports exist on the preparation of solid dispersions using these methods. The few existing reports are presented and discussed in the following.

In a majority of electrospraying studies organic solvents are used due to their often faster evaporation rate and lower surface tension compared with aqueous solvents. Also, many studies make use of particle collection in an aqueous phase or another liquid phase thus necessitating solidification before collection. Due to such considerations materials used for electrospraying have typically been non-water soluble polymers such as PLGA, poly-lactic acid (PLA), polycaprolactone (PCL), although there are some examples where water soluble polymers have been used. Natural polymers such as elastine-like peptide (ELP) [Wu *et al.* 2008] and chitosan [Arya *et al.* 2009] have been used. The existing electrosprayed solid dispersions have not necessarily been prepared with considerations towards enhancing the physical stability and dissolution rate, but instead the studies have mainly focused on the release behaviour and particle characteristics.

The solvents used for electrospraying are mainly organic solvents with acetone [Xu and Hanna 2006], dichloromethane [Ranganath *et al.* 2009], ethanol [Valo *et al.* 2009], chloroform [Hong *et al.* 2008], N,N-dimethylformamide, dimethyl acetamide [Enayati *et al.* 2010] and methanol [Enayati *et al.* 2012] being most frequently reported in literature. Important consideration for selecting the appropriate solvent include sufficient volatility for drying of droplets as well as their electric conductivity, surface tension and viscosity being important in allowing formation of a cone-jet and suitable resulting characteristics of the particles.

Pure drug particles have been prepared without excipients using the drugs beclomethasone dipropionate and methylparahydroxybenzoate, and led to particles with a narrow size distribution, but stability was not tested although they are presumably not stable [Ijsebaert *et al.* 2001]. For solid dispersions Arya *et al* [Arya *et al.* 2009] used electrospraying to prepare chitosan particles loaded with ampicillin and obtained

particles around 520 nm that released most of their payload within 20 hours in phosphate buffer (pH 7.4). Hong *et al* [Hong *et al.* 2008] prepared solid dispersions of PLGA with rifampicin and produced particles around 3-7 µm and further showed 40 % drug release in phosphate buffer after 10 days, a relatively slow release rate.

In a study by Yu *et al* [Yu *et al.* 2011] solid dispersions were prepared with tristearin, a lipophilic excipient and the drug naproxen and resulted in particles with a mean size of 376 nm and a narrow size distribution. A sustained release was achieved here, lasting over 24 hours. PLGA has also been used to prepare particles loaded with the drugs doxorubicin [Almería *et al.* 2011] and paclitaxel (see Figure 2.10) resulting in 65-73 % drug release over 50 hours and 60 % drug release in 30 days, respectively, when dissolution studies were performed in phosphate buffer [Kumar Naraharisetti *et al.* 2007]. Xie *et al* studied PLA/PLGA and PLA for preparing particles loaded with cisplatin and particles around 5µm were obtained. In this study a burst release as high as 40-70 % was observed in the first 15min. Further, a surface drug loading of < 25 % of drug was measured on the particle surface [Xie *et al.* 2008]. Solid dispersions of budesonide with polycaprolactone were prepared and resulted in small particles around 100-200 nm and a drug release taking place within 10 days [Midhun 2011]. Another study using polycaprolactone with paclitaxel resulted in particles of 4-32 µm and a drug release over several days in phosphate buffer [Ding *et al.* 2005]. Moreover, poly(amidoamines)-cholesterol particles were prepared with Tamoxifen and indicated that the drug was amorphous and resulted in 26 % release in 6 hours in phosphate buffer [Cavalli *et al.* 2011]. Currently, there is very little *in vivo* data available in literature using electrospraying even for applications other than solid dispersions and possible improvements in bioavailability from electrosprayed solid dispersions have not been investigated.

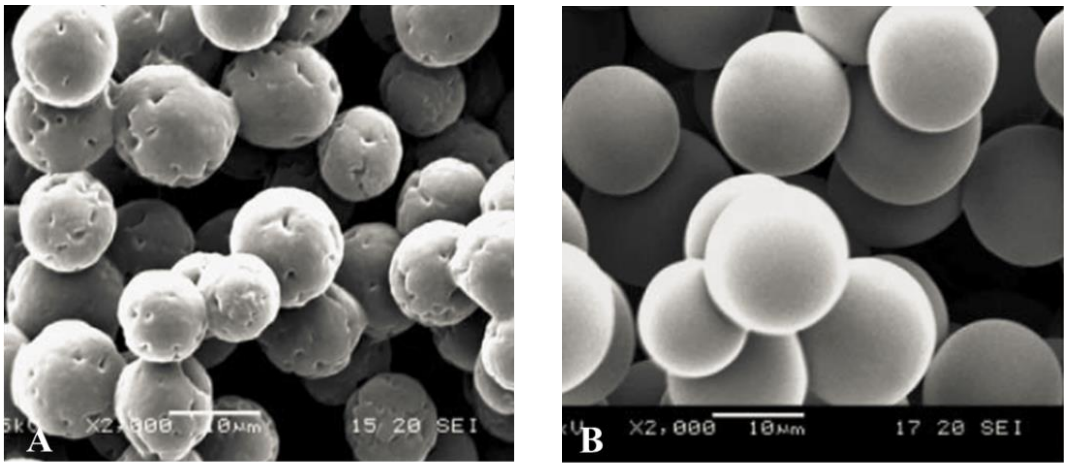

Figure 2.10 Electrosprayed particles prepared with PCL (A) and PLGA (B) loaded with paclitaxel indicating different morphology [Xie *et al.* 2006b].

Application with electrospinning

There have also been some studies where polymers were electrospun with poorly soluble drugs to form solid dispersions with the purpose of achieving immediate release. Verreck *et al* [Verreck *et al.* 2003] prepared electrospun fibres containing the poorly soluble drug itraconazole in HPMC 2910. The electrospun fibre mesh was milled subsequently to obtain fibre fragments of approx. 27 µm and with a diameter of 0.5-3 µm and these fibres were compared with Melt Extruded samples prepared using a co-rotating screw extruder. Dissolution studies performed in 0.1N HCl showed complete drug release after 240 min of dissolution. The study further demonstrated using thermal analysis that itraconazole was amorphous with some residual crystallinity possibly resulting from the milling process. Studies by Yu *et al* reported the preparation of electrospun solid dispersions from PVP K30 with the drugs ibuprofen [Yu *et al.* 2009], ketoprofen [Yu *et al.* 2010a], ferulic acid [Yu *et al.* 2010c] as well as PVP K90 with acetaminophen [Yu *et al.* 2010b] in ethanol (see Figure 2.11). The studies using ibuprofen indicated that the drug was in an amorphous form, observed via DSC and XRPD. Further, FTIR data suggested interaction between the polymer and the drug

through intermolecular hydrogen bonding. Dissolution studies performed in water showed that all drug was dissolved in less than 1 min.

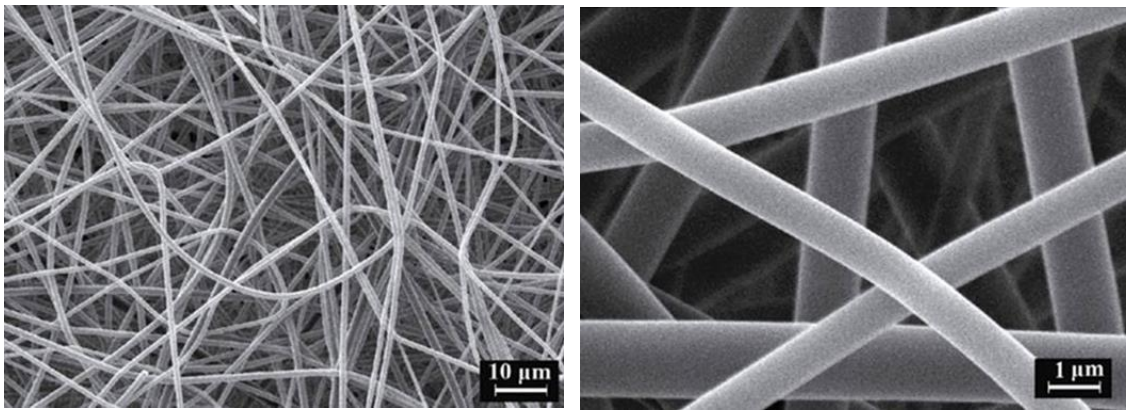

Figure 2.11 High and low magnification SEM images of electrospun solid dispersion fibres composed from PVP K30 and ibuprofen (from [Yu *et al.* 2009].

Electrospinning requires less solvent per gram dry weight of fibre/particle produced compared with both electrospraying and spray drying, which makes the technique more cost-effective, especially when using organic solvents. However, electrospraying provides more possibility for tailoring the characteristics of the product, which may be of special interest for particle engineering purposes and for optimizing the drug release behaviour for sustained release purposes.

2.6.5 Preparation of the final dosage form

Particle-based solid dispersion formulations are attractive as they may provide enhanced performance, but they may be difficult to process into a useful dosage forms. Downstream post processing may disrupt or destroy the beneficial characteristics of the particles via mechanical or thermal stress. This could prevent the re-dispersion of the particles and thus alter both the release kinetics of the drug and the physical stability of the formulation making it less desirable than otherwise expected.

Compression and tableting

The development of dosage forms from solid dispersion systems has not been widely studied but nevertheless is an important aspect of bringing more solid dispersion formulations onto the market. Processing steps that take place after formation of the actual solid dispersion may have an influence on several properties of the formulation, including the structure of the dispersion, physical stability and the dissolution kinetics.

There are many ways in which solid dosage forms can be produced from particle-based solid dispersions including granulation or compression and later tableting or capsule filling. However, for particle-based solid dispersions such as those prepared with spray drying or electrospraying it is desirable to retain the engineered particle attributes which may be damaged during compression or granulation and compaction which are necessary for making tablets. Thus, these particles are more suitable for gentle methods such as capsule filling, where the particles would be exposed to mechanical stresses.

Several studies have reported on the tableting behaviour of the spray dried powders, yet such studies seem to be conducted more in industry and results are thus not as widely available. Moretti *et al* showed that microparticles in the size range of 5-10 µm formed with HPMCP, cellulose acetate butyrate and Ketoprofen using spray drying could be loaded into hard gelatin capsules or compressed into tablets via direct compression together with maltose or HPMC. They did not report any significant changes to the particle morphology as a consequence of tablet compression or capsule filling [Moretti *et al.* 2001]. It has also been reported in other studies that microparticles could be compressed into tablets and remain intact without merging with each other or rupturing [Soppimath *et al.* 2001, Xu *et al.* 2008]. Although the morphology of the particles may not have changed significantly the compression process could still have an influence on the properties of the solid dispersion and the physical form of the drug dispersed.

Compression of the particle could for instance lead to polymer-drug de-mixing at the microscopic level, making subsequent relaxation processes more probable [Ayenew *et al* 2012].

For now it appears that the compression of particles can be performed to produce tablets from the particle formulations without severe concerns. Yet, for particles engineered with fine surface attributes this may different. The post-processing of particle powders should be studied more carefully, to make sure that particles can be re-dispersed into their original form with and without the use of dispersing agents. It is especially important that such re-dispersion can take place *in vivo* to provide the intended purposes of the particles.

One method of making tableting available for these particle-based solid dispersions techniques is to combine the atomization process with a fluidized bed coating system in which the solid dispersion is directly sprayed onto the granular surface of excipients such as sugars so that the formulation is immediately ready for tableting immediately after, and hence even less damage may be caused on the particles [Beten *et al.* 1995]. This has both been done with organic solvents and without organic solvent where a hot melt process was used [Kennedy and Niebergall 1996].

A recent study by Leane *et al* 2012 [Leane *et al.*] has looked into the effect of tableting and coating processes and subsequent storage of solid dispersions prepared from PVP K-30, SLS and ibipinabant using spray drying. Tablets were prepared using either microcrystalline cellulose or mannitol. The study demonstrated that the physical stability and release profile are dependent on the filler and coating materials used.

Scale-up of the system

Often processing techniques are not feasible for commercial scale production and may thus fail in their translation into industrial application. Indeed there are numerous cases where a technology could not be further developed due to too high costs associated with production. Spray drying has long been known as a commercially viable technology and is used to produce pharmaceuticals as well as other products in an industrial scale [Cal and Sollohub 2010]. Thus, it is generally not of concern to scale-up the particle-based solid dispersions with spray drying.

The situation is different with electrospraying which is still mainly used on an experimental level with custom built setups being most common. The most well-known application of the electrospraying principle is as a sub-process for mass spectroscopy, where it is used to ionize fragments of molecules [Takáts *et al.* 2004]. There are only few examples of commercial applications using electrospraying for particle production, which are presented on the websites of companies offering such devices (e.g. yflow.com), however not on a commercial scale. There have been plenty of efforts in scaling-up the electrospraying process, which has become somewhat notorious for its low output, by spraying concurrently from multiple closely aligned nozzles or holes/slits [Bocanegra *et al.* 2005, Deng *et al.* 2006]. Multiple configurations have been developed for such scale-up attempts (see Figure 2.12), and it has been shown that neighbouring jets have an electrical shielding effect, where the electrical potential required to stabilize the jet increases as the distance between the jets is reduced [Regele *et al.* 2002]. It is not clear yet to which extent the output can be improved with such multijet models and whether such setups provide stable, continuous jetting and particle production.

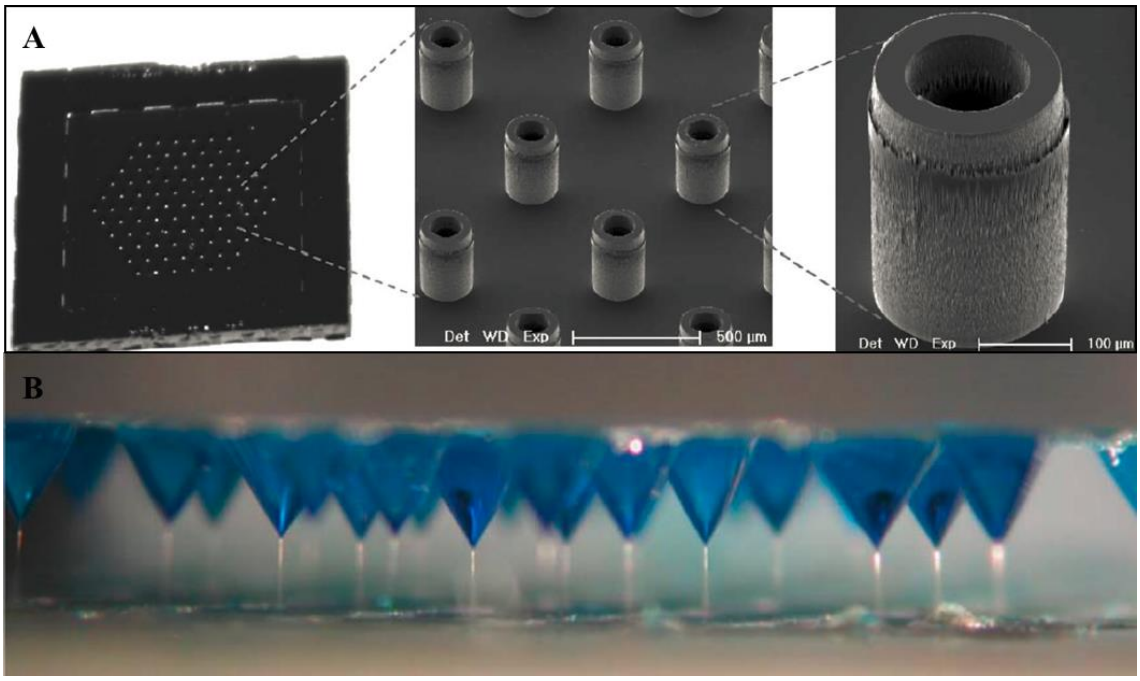

Figure 2.12 Multiple jet electrospraying setup built using a nozzle array system (A) (adapted from [Deng *et al.* 2006]) and a multi-hole injector (B) (adapted from [Bocanegra *et al.* 2005]).

2.7 Drug release models

Drug release is a process which involves drug molecules leaving a carrier system and can be described in many ways including the time and mode in which the release takes place. Drug release studies are recognized as an important element in drug development and assessment of formulation performance [Washington 1990]. Several models have been developed to describe the drug dissolution from immediate and extended release formulations as well as other types of release such as modified, delayed and pulsatile release [Edlund and Albertsson 2002]. Most of these are based on dissolution of drug as a function of time and the curves obtained from such drug release is quantitatively assessed via mathematical interpretation. Here the dissolution curves are mathematically translated as a function of different pharmaceutical parameters or equations that are obtained from theoretical interpretation of the process. The drug release models are

often simple and are typically used to obtain approximate curves used for curve fitting of experimental data [Costa and Sousa Lobo 2001].

The simplest release model is for the zero order release which is based under the assumptions that drug release takes place slowly from a non-disintegrating structure with no change in area and without drug release achieving en equilibrium. There would then be a linear relationship between the amount of drug released and the time taken. Such zero order release can be used to describe several pharmaceutical systems such as matrix based delivery systems and transdermal release devices and this is often a desirable behaviour since there is a release at a constant rate [Ranade 1991].

Drug release from matrix-based systems

Drug release from a delivery system comprised of a matrix may take place via different mechanisms including diffusion and erosion depending on the solubility of the drug and the matrix material in the release medium. Drug release from systems were the external geometry or matrix structure remains unchanged during drug release would take place via diffusion [Washington 1990]. This is the case for non-disintegrating tablets as well as solid dispersions prepared with a non water-soluble matrix materials. The models are mainly been based on the principles of dissolution and specifically the dissolution at the solid-liquid interface of the drug-carrier system and the release medium [Edlund and Albertsson 2002]. For non-water soluble matrix systems the most applied drug release model is the Higuchi model and was developed by Higuchi *et al* as the first model to mathematically describe the release of drug from an insoluble matrix based on Fick's law of diffusion [Higuchi 1963]. Higuchi *et al* showed in several reports that diffusion mediated release from spherical pellets could simply be modelled as a function of the square root of time (see Equation 2.7),

$$Q_t = [2DC_D\tau(C_m - 0.5C_D\tau)]^{0.5} * t^{0.5} \quad \text{(Equation 2.7)}$$

where Q_t is the cumulative drug released as a function of time t, D is the diffusion coefficient, C_D is the solubility of the drug in the release medium τ is the porosity and C_m is the content of drug per unit of volume of matrix.

$$Q_t = k_H * t^{0.5} \quad \text{(Equation 2.8)}$$

A simplified model of the Higuchi model is presented in Equation 2.8. Again here Q_t is the cumulative drug released as a function of time t and k_H is the Higuchi release constant. A plot of a release curve using the Higuchi model has the percentage of drug released in the y-axis and the square room of time in the x-axis. When the drug release profile of a drug-carrier sample follows the Higuchi model the release profile should indicate a linear curve on the plot. In this case the Higuchi release constant represents the slope of a plotted curve and is tied to the parameters presented in Equation 2.7 [Simonelli *et al.* 1969]. It is most common to use a linear regression to fit the release curve to the drug release model. Yet, the use of non-linear regression such as a polynomial function is also seen used to perform curve fitting between the empirical data and the model. The coefficient of determination, R^2, is typically used to assess the fit of the model or modified model [Lemaire *et al.* 2003].

The release of drug from drug-carrier systems often involve several mechanisms and multiple steps influenced by different physicochemical characteristics and it is therefore difficult to obtain a mathematical model that accurately describes the release mechanism [Costa and Sousa Lobo 2001]. The Higuchi model is often suitable for describing matrix-based polymer-drug systems while the zero order model can be useful for describing coated formulations. Further there are other models to describe other types of release or more specific release mechanisms [Costa and Sousa Lobo 2001].

Chapter 3

Experimental Details

This chapter introduces and describes the materials and experimental procedures used to obtain the results in this thesis. For each of the materials and procedures details of the supplier and product are given and the methods are explained. The first section comprises an overview of the materials used and explains some of the properties and common applications of the materials. Further, the selection criteria are explained for the drug compounds and polymers used. The following sections introduce and explain the methodology used for all preparative and analytical work. A brief theoretical background is also provided for most of the analytical methods used. In some cases similar methodology has been used with different equipment or with slight differences in the methods and this will be further specified in the results chapters.

3.1 Materials

The main materials used in this project are the polymers, drug compounds and solvents used to prepare the drug-loaded particles. Secondary materials such as buffer solutions and certain chemicals are also mentioned in this section.

3.1.1 Polymers

Poly(Lactic-Co-Glycolic acid) (PLGA)

Biodegradable polymers are a class of polymers designed to degrade into non-toxic by-products at a predetermined rate, thereby releasing their therapeutic payload for prolonged and even site-specific delivery. Poly(lactide-co-glycolide) (PLGA) is the most commonly used biodegradable polymer for drug delivery application. It is

aliphatic polyester (see Figure 3.1A) and is approved by the food and drug administration for implants and for oral and pulmonary applications. The by-products of PLGA, glycolic acid and lactic acid are a favourable attribute of PLGA as both of these acids are naturally occurring substrates in the Krebs cycle. PLGA is easy to work with, although only soluble in harsh solvents such as acetone and dimethyl formamide, and is amorphous when consisting of 25-70% glycolide:lactide ratio [Edlund and Albertsson 2002a]. Its degradation takes place via hydrolysis and the degradation rate depends on the composition and properties of the PLGA, most notably the glycolide:lactide ratio and the molecular weight of the PLGA. The PLGA used in this study was acquired from Boehringer Ingelheim (Now Evonik) (Boehringer Ingelheim, Germany) (Evonik, Germany) and Purac (Purac Biochem, Netherlands). More specifically the following PLGA products were used:

1: Resomer RG 503H from Boehringer Ingelheim was used, with a molecular weight of 24,000-38,000 g/mol depending on the given batch (three different batches were used during the project due to availability) and a lactide and glycolide ratio of 50:50 (molar ratio) and a T_g of 44-48 ºC.

2: Purac PLGA was used in some studies with a molecular weight of around 18,000 g/mol.

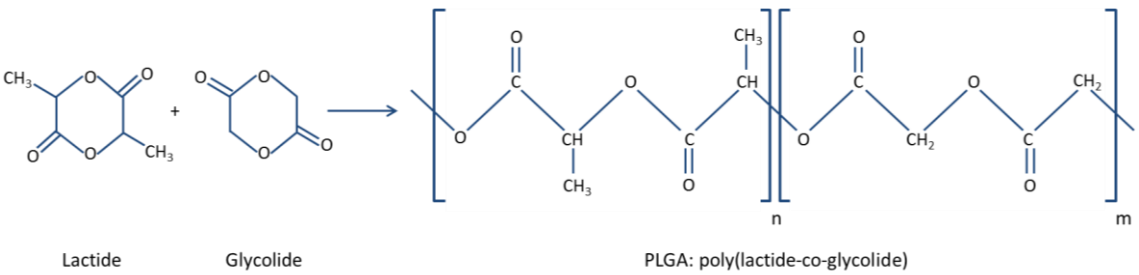

Figure 3.1 Chemical structures of PLGA and its building blocks.

Hypromellose Acetyl Succinate (HPMC AS)

HPMCAS is in the family of cellulose derived polymers, a commonly used group of polymers for preparing solid dispersions. HPMCAS is also used for enteric coating of tablets, due to its pH dependent solubility in aqueous solvents. It is insoluble at low pH below 5.5-6.5 (depending on the polymer grade) and is thus used to prevent dissolution in the gastric fluid while dissolving in values of pH above 5.5-6.5, hence also in intestinal fluids. Moreover, HPMCAS has a special property that they act as effective precipitation inhibitors prolonging the supersaturation of drugs for many hours after dissolution (see section 2.6.1). Much indicates that this ability of the polymer to keep the drug in a supersaturated state under non-sink conditions by preventing precipitation may provide considerable improvements in the *in vivo* performance of formulations.

The HPMCAS used in this study was acquired from Shin Etsu (Shin Etsu, Japan) and more specifically AQOAT HPMCAS-LF was used, which is a micronized low molecular weight grade in the HPMCAS series. HPMCAS-LF is partly soluble at a pH above 5.5 and has a molecular weight of approximately 18,000 g/mol [Fukasawa *et al.* 2004].

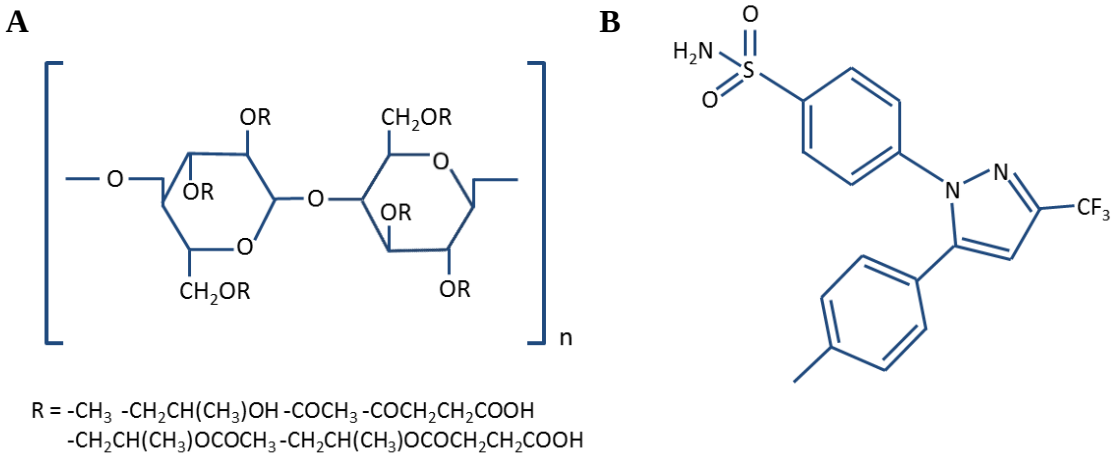

Figure 3.2 Chemical structure of HPMCAS (A) and chemical structure of CEL (B).

3.1.2 Drug

Celecoxib (CEL) was the active pharmaceutical ingredient (API) used in the following studies and was used as a model poorly water-soluble drug. CEL is a non-steroidal, anti-inflammatory drug (NSAID) (see Figure 3.2B) or, more specifically, an inhibitor of the enzyme, selective cyclooxygenase-2 (COX-II), responsible for inflammations and pain. CEL is widely used for the treatment of osteoarthritis, rheumatoid arthritis and acute pain [Thakkar *et al.* 2004]. It has a very low aqueous solubility (2-7 µg/mL), is weakly acidic with a pKa of 11 and is generally acquired as a crystalline powder [Chawla and Bansal 2007].

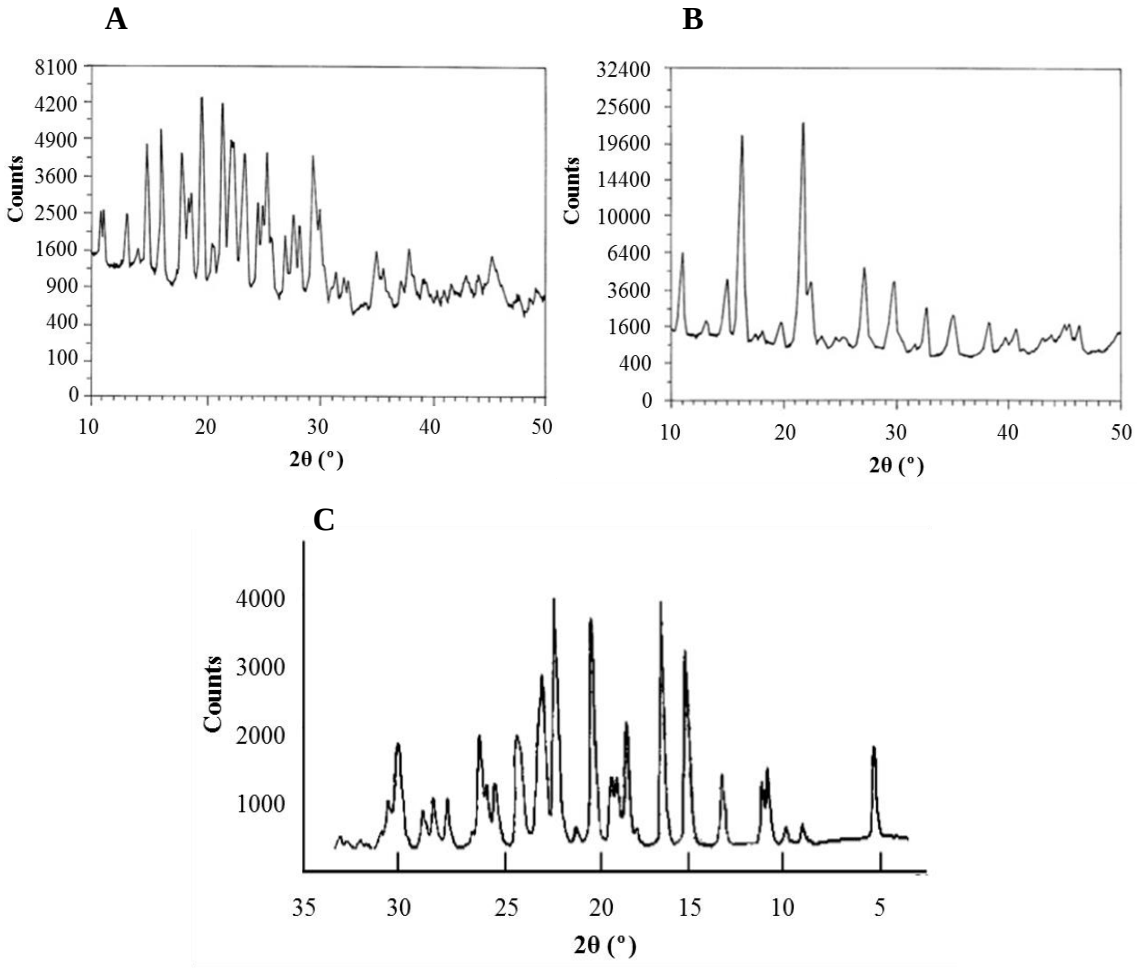

Figure 3.3 XRD diffractogram of CEL crystal form I (A), II (B) and III (C). From [Chawla *et al.* 2003, Lu *et al.* 2006]

There are more than four known CEL crystalline polymorphs of which type III with its characteristic needle-shaped crystals is the thermodynamically stable form at ambient conditions. CEL is further associated with undesirable properties such as low compressibility and cohesiveness, and it is found that increasing the dissolution rate of CEL improves its oral bioavailability [Chawla *et al.* 2003; Dolenc *et al.* 2009; Paulson *et al.* 2001]. CEL crystalline powder was acquired from Dr. Reddy (Hyderabad, India) with a purity of 99.9% and with a molecular weight of 381.38 g/mol.

3.1.3 Solvents

Acetone

HPLC grade acetone ($[CH_3]_2CO$, Sigma Aldrich, Poole, UK) was used in this work. Acetone was used as a solvent component in some electrospraying and spray drying feed solutions as well as for cleaning of nozzles and glassware.

Acetonitrile

HPLC grade acetonitrile (CH_3CN, Sigma Aldrich, Poole, UK) was used in this work. Acetonitrile was used as a solvent component in some electrospraying and spray drying feed solutions as well as a component of the mobile phase for HPLC measurements.

Methanol

HPLC grade methanol (CH_3OH, Sigma Aldrich, Poole, UK) was used in this work. Methanol was used as a solvent component in some electrospraying and spray drying feed solutions.

Ethanol

General purpose research grade ethanol (C_2H_5OH 99.9%, Sigma Aldrich, Poole, UK) was used in this work. Ethanol was used as a solvent component in some

electrospraying and spray drying feed solutions, used for calibration of measuring apparatuses and for the cleaning purposes.

Dimethyl Sulphoxide (DMSO)

Research grade DMSO (($[CH_3]_2SO$, Sigma Aldrich, Poole, UK) was used in this work. DMSO was used in Caco2 drug transport studies to increase the drug solubility in the HBSS-based release medium.

Ultrapure water

Ultrapure water was produced using a Millipore Filtration device (Millipore, USA) and was used to prepare buffers and release medias, used as a solvent component in some electrospraying and spray drying feed solutions and for cleaning purposes.

Properties of solvents used for atomization

Some of the main properties of the solvents used are presented in Table 3.1.

Table 3.1 Properties of solvents used for atomization of solutions. Values obtained from [Smallwood 1996].

	Density ($kg \cdot m^{-3}$)	**Boiling point (°C)**	**Dielectric constant (20 °C)**	**Electrical conductivity (S/m)**	**Viscosity (mPa·s) (at 25 °C)**	**Surface tension ($mN \cdot m^{-1}$)**
Acetone	790	56	20.6	5E-9	0.33	23.3
Acetonitrile	782	82	37.5	6E-9	0.38	29.1
Ethanol	789	78	22.4	1.4E-9	1.08	22.3
Methanol	792	64	32.6	1.5E-9	0.6	22.6
Water	998	100	79.7	5.5E-6	0.89	72.8

3.1.4 Miscellaneous materials

Phosphate buffer solution (pH 6.8)

Phosphate buffer was prepared from $NaHPO_4$ (Sigma Aldrich, Pool, UK) and NaOH pellets (Sigma Aldrich, Pool, UK) and used as a release medium for drug release studies

Sodium Lauryl Sulphate (SLS)

SLS powder was acquired from Fagron (Fagron, Waregem, Belgium). SLS was used as surfactant in the release medium mixed in phosphate buffer to provide sink conditions during drug release.

3.2. Preparation and characterization of solutions

Some properties of the solvents and solution used were measured using the following methods while other properties were found in literature (see section 3.1.3).

3.2.1 Electrical conductivity:

Values for electrical conductivity of solvents and spraying solutions were measured using a multimeter (InLab, Mettler Toledo). The electrical conductivity of the suspension/solution was measured using the conductivity probe. The measuring range of the conductivity meter used was 0.001 to 500 μS/cm (according to Mettler Toledo). The conductivity measurements were performed at ambient temperature (~ 25 °C) and the electrode probe was always cleaned with 99.9% ethanol, which has a very low conductivity around 0.0014 μS/cm. The electrical conductivity measurements were done by using ~20 mL of solvent/solution in a cylindrical glass container. The electrode was immersed in the liquid up to the specified mark for a few seconds, air bubbles residing in the suspension were removed by shaking the suspension gently, and the reading was recorded. Five consecutive readings were taken and averaged for all measurements.

3.2.2 Surface tension measurements

The pendent drop method was used to find values for surface tension in the liquid to air interface and a Krüss DSA 100 Drop Shape Analysis System (Krüss, Germany) was used. A syringe was filled with the given solvent/solution and connected to a flat-ended needle. The liquid was dispensed slowly from the needle tip until a drop was hanging from the needle tip. A camera was used to monitor the drop and determine the surface tension based on the geometry of the drop. The measurements were performed at 25 °C and readings were performed every 2 seconds until the values had stabilized, and a mean value was determined.

3.2.3 Viscosity

The viscosity of solvents and spraying solutions were determined using an Ubbelohde viscometer (Cannon instruments, USA) in a size 50 with a calibration constant of 0.0036 mPa and measurements were done at 25 ºC in a heated water bath. Viscosity was measured for pure solvents and solutions with different concentrations of PLGA. The kinematic viscosity (ν) was calculated using the viscometer constant (χ) and the measured time (t) for the liquid head to pass the two indicators,

$$\nu = \chi \cdot t \qquad \text{(Equation 3.1)}$$

The dynamic viscosity (η) was calculated from the kinematic viscosity and the solution density (ρ),

$$\eta = \nu \cdot \rho \qquad \text{(Equation 3.2)}$$

The viscosity results are based on a mean value of two or three readings.

3.2.4 Properties associated with viscosity

The specific viscosity (η_{sp}) divided by the concentration (c_x) was found for each of the

different polymer concentrations (x=1-7%) using equation 3.3,

$$\frac{\eta_{sp}}{c_x} = \frac{\eta_x}{\eta_{solvent}} - 1 \quad \text{(Equation 3.3)}$$

The intrinsic viscosity ([η]) of PLGA in the different solvents was determined by extrapolation of values for the specific viscosity η_{sp} as the polymer concentration went to zero using equation 3.4. The intrinsic viscosity refers to the capability of a specific polymer to enhance the viscosity of the solvent in which it is dissolved. This depends partly on the molecular weight of the polymer and the polymer-solvent compatibility [Jen Tsi 1962].

$$[\eta] = \lim_{c\to 0}\left(\frac{\eta_{sp}}{c}\right) \quad \text{(Equation 3.4)}$$

Further, the Martin constant (K_m) was calculated for solutions with 5% polymer concentration by using equation 3.5, the Martin equation [Son *et al.* 2004]. The Martin constant (Km) is similarly used to indicate the interactions between solutes and between solute and solvent, with a higher value indicating more polymer-polymer interaction.

$$\frac{\eta_{sp}}{[\eta]c} = exp(K_m[\eta]c) \quad \text{(Equation 3.5)}$$

3.2.5 Evaporation rate

The evaporation of solvents and solutions used were measured using thermo gravimetric analysis (TGA) and the evaporation rate was also found. Briefly, approximately 20 μL solvent or solution was transferred into a platinum crucible and placed on the sample holder and enclosed inside the temperature-controlled furnace (25 °C, to mimic typical ambient conditions in which electrospraying experiments also are performed) continuously purged with nitrogen gas at 20 mL/min flow rate. The change of weight as a function of time was recorded until stabilizing around 0 for solvents and at the initial

solute weight for solutions containing both polymer and drug. Each measurement condition was repeated three times to limit the uncertainty of the measurements.

3.2.6 Solubility studies

Solubility of polymers and drugs in solvents and solvent mixtures were measured by adding the given solute(s) little by little into a container with 5 mL or 10 mL of solvent while continuously stirring until the solution reached the cloud point was reached or the solute(s) began precipitating out. The solutions were occasionally heated slightly using a hot plate or placed in an ultrasound bath to aid the dissolution process.

3.3 Particle preparation using electrospraying

Particles were fabricated using a single-nozzle electrospraying setup (see Figure 3.4). The same spraying nozzle was used in all experiments and was custom built by Stanley Engineering (Birmingham, UK). The nozzle was made of stainless steel with an inner and outer diameter of 1.77 mm and 2.34 mm respectively and a length of 40 mm. All of the electrospraying experiments were carried out using a nozzle connected to a programmable syringe pump (PHD 4400, Harvard Apparatus, Edenbridge, UK). A syringe (made from glass or plastic) with the capacity of 5 mL was mounted onto the pump and liquid was infused into the nozzle via plastic tubing (Tygon tubing, Sigma, UK). The nozzle and a ground electrode were connected to a high voltage DC power supply unit (FC30 P4 12w, Glassman Europe Limited, Bramley, UK) using a high voltage power cable. The output voltage range of the unit was 0-30 kV and the output current range was 0-4 mA. A high speed video camera with an in-built magnifying lens (Leica S6D JVC-colour) was used to monitor the jet at the nozzle tip during particle generation. Such a high speed camera is necessary to ensure a stable jet as small fluctuations or instability in the jet may result in a different particle output. A fibre optic light source was also used when the lighting was not sufficient to visualize the jet.

All solutions were electrosprayed with an applied electric potential difference of between 7-13 kV, depending on the feed solution used, and a direct current of 1.0mA, with the positive electrode attached to the tip of the nozzle and the ground electrode attached to the collector (see Figure 3.4 A). A continuous flow rate between 10-50 µL/min was used to obtain a stable cone-jet while adjusting the electrical potential. The particles produced were collected at a distance of 70 mm from the nozzle either onto a microscopy glass slide, onto a sheet of aluminium foil or into a beaker with deionized water. The particle samples were left to dry completely in a desiccator under vacuum. All particle samples were prepared in the stable-cone-jet mode to get a narrow particle size distribution.

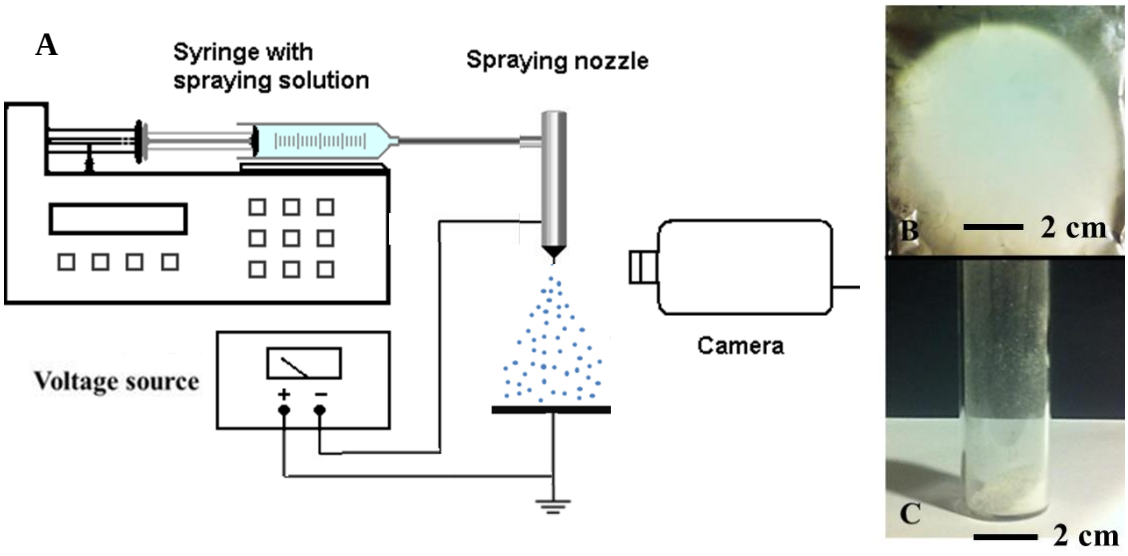

Figure 3.4 Schematic diagram of electrospraying setup (A), photographs of samples collected on aluminium foil (B) and in a glass vial (C).

3.4 Particle preparation using spray drying

Particle preparation with spray drying was performed using a Büchi Mini Spray Dryer B-290 (Büchi Labortechnik AG, Flawil, Switzerland)(see Figure 3.5 A). A sketch of the mechanisms in the setup is shown in Figure 3.5 B. A 0.7 mm two fluid nozzle was used

for all of the spray drying experiments and spraying solutions were sprayed in a co-current flow with gas for drying. Due to the use of an organic solvent base and the risk of explosion at high temperatures an additional device, an Inert Loop B-295 (see Figure 3.6), which provides a closed loop of inert gas, was used with nitrogen gas instead of atmospheric air. The spray dryer was operated at 90% (22500 L/h) aspiration rate and the remaining adjustable operating parameters were set as follows for all spray drying experiments: Liquid feed rate ~ 3 mL/min, inlet temperature 45 ℃, outlet temperature 30 ℃ and atomizing air flow rate 742 L/h. The spray drier was flushed using pure solvent in the feed before and after spraying the particles.

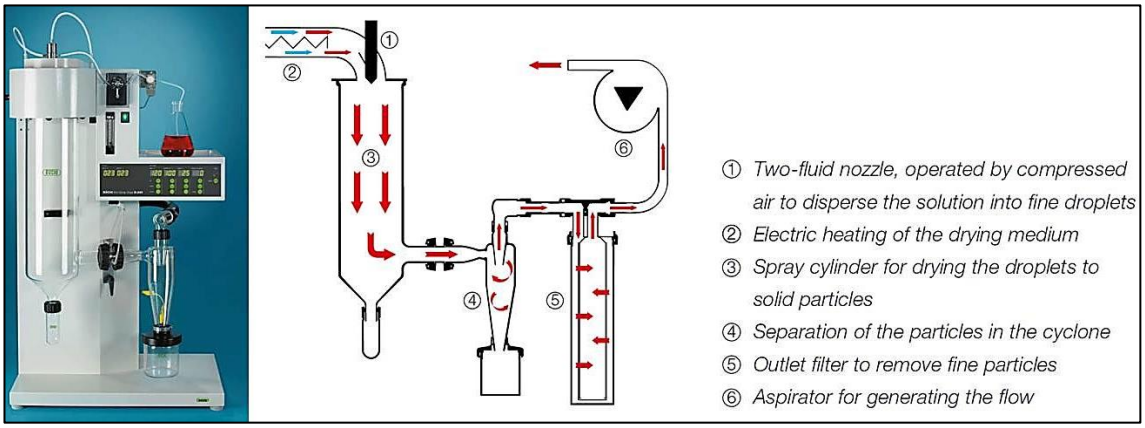

Figure 3.5 Picture of Buchi spray dryer (A) and schematic image of spray drying mechanism (B) (adapted from Buchi B-290 catalogue).

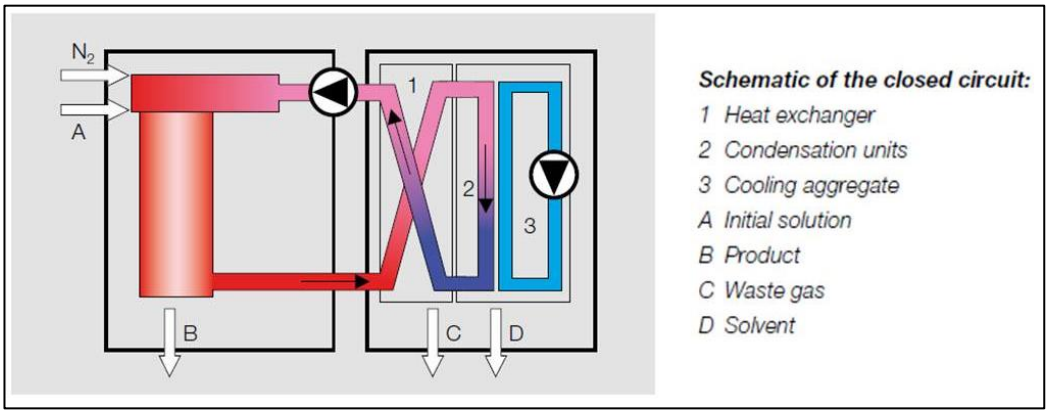

Figure 3.6 Schematic view of inert loop closed circuit

Spray-dried powders were separated from the cyclone and collected in a vial. The produced powder was scraped off the inside of the glass vial, inserted into capped glass vials and stored in a desiccator at ambient temperature. The drying chamber, cyclone and collection vial were cleaned between spraying of each sample.

3.5 Micronization and preparation of physical blend

3.5.1 Ball milling

Micronized drug samples were prepared using a two chamber oscillatory ball mill (Mixer Mill MM301, Retch GmbH & Co., Haan, Germany. Approximately 500 mg of crystalline drug was placed into each of the two milling chambers with three 9 mm stainless steel balls and milled at 30 Hz oscillation for 30 min. The ball mill was placed in a cold room (+4 °C). The micronized samples were scraped of the walls of the ball mill chamber after milling, collected in a capped glass vial and stored at ambient temperature in a desiccator.

3.5.2 Physical blend

Physical blends of polymer and drug were prepared to set up comparisons with the drug-loaded particles. Drug and polymer were weighed at the specified ratio and were then mixed using a mortar and pestle for 1 min.

3.6 Characterization of particle size and morphology

3.6.1 Size and morphology

Particle morphology and size were characterized and measured using SEM. Optical microscopy was also used to visualise particles immediately after preparation, but was mainly used for screening of samples before performing SEM.

Optical microscopy

An optical microscope uses light in the visible wavelengths to magnify images of small samples using a system of lenses with different predetermined magnifications. Samples are most commonly observed via images from transmitted light but it is also common to use reflected light, typically employed for analysis of surface morphology of samples. The resolution limit for optical microscopes with conventional lenses is around 200 nm.

Particles were collected on glass slides either directly onto the glass or covered with a film of water, and their general structural appearance was examined using an optical microscope (Nikon Eclipse ME 600, Nikon, Japan). Scale-bars and particle size measurements were done using 'Acquis' digital imaging software (Synoptics Ltd., Cambridge, UK).

Scanning Electron Microscopy

An SEM microscope scans the sample surface with a high-energy beam of electrons to obtain an image in the micro- to nano-scale. The signal received in a SEM contains information such as surface topography and the composition of the sample. Particle morphology and size were characterized in detail using different SEM setups (JEOL JSM-6301F, Hitachi VP-SEM S-3400N and Quanta 200 ESEM FEG) depending on availability and location. The prepared samples, consisting of a thin layer of particles on glass slides, were sputter-coated with gold, mounted on metallic studs with double-sided carbon tape and viewed at an accelerating voltage of 3 kV (for JEOL JSM-6301F and Quanta 200 ESEM FEG) or 10 kV (for Hitachi VP-SEM S-3400N). Images representative of the whole sample were taken at different orders of magnification for each of the samples, where possible. If unusual structures were observed there were also captured and saved. The images obtained were used to calculate the mean diameter and

size distribution for the different particle samples. For each sample 200-300 particles were measured from different sites of the sample, using the software ImageJ. The sizes were calculated as the Feret's diameter based on the circumference of the particles, and their diameters were calculated using the image scale bars.

The particle size distribution of samples was determined by calculating the polydispersivity index, a measure indicating how polydisperse a sample is. The polydispersivity index is found from the mean diameter and standard deviation of the sample and is given as:

Polydispersivity index = Standard deviation / Mean diameter * 100

3.7 Inner structure and porosity of particles

Cross-sectional images of the drug loaded microparticles were prepared using a combined dual beam focused ion beam (FIB) – SEM instrument. A FIB/SEM instrument contains both an FIB and an SEM source and uses SEM to visualize the sample while using FIB both for visualization and ablation of the sample. FIB functions by using a focused beam of ions generated from an ion source, which can be focused directly onto a small area of the sample with a spot size of only a few nm. This beam can then be used for milling (removal of material) a section of the sample to reveal the inner morphology of a given particle. The milling process is typically monitored using the SEM source.

A Zeiss XB 1540 Cross Beam SEM equipped with a Gemini SEM column and Orsay Physics Canion 31 FIB column was used to prepare FIB/SEM images shown in the results sections. Particle samples were sputter-coated with gold and mounted on metallic studs with double-sided carbon tape. FIB milling of samples was done with a Ga^+ ion beam at an accelerating voltage of 30 kV. Layer by layer milling of the

microparticles was done at a beam current of 30-100 pA, with the final thinning being in the lower current range. Secondary electrons formed during the milling process enabled simultaneous imaging of the sample. Reducing the beam current generally helped to reduce specimen damage during scanning with the ion beam.

3.8 Crystallinity and physical form of particles

3.8.1 Differential Scanning Calorimetry

DSC is a thermal analysis technique used for a broad range of applications for both crystalline and amorphous materials. A DSC is typically used to heat or cool small samples (a few milligrams) at a predetermined rate inside a closed furnace and then measure the difference in heat flow required to increase or decrease the temperature of the sample and reference. This heat flux is plotted as a function of time or temperature and the curve obtained is used to determine thermal events such as glass transition and melting. The glass transition temperature is observed as a change in heat capacity and can be used to determine the presence of amorphous material, the miscibility of materials and some interactions between materials. The melting peak can be used to detect crystallinity and determine polymorphism, and the amount of crystallinity can in some cases also be quantified.

DSC was used in this project to gain information on the physical state of the drug and polymer components of the particles and any interaction between the two. The DSC analyses were performed using three different DSC instruments, a Netzsch STA 449 C Jupiter (Netzsch, USA) instrument together with software, Proteus, a Perkin Elmer Diamond with autosampler (Perkin Elmer, Norwalk, CT) and software, Pyris, a Mettler Toledo DSC 1 (Mettler Toledo, Columbus, OH) with software, STAR-e depending on availability and location performed. For the Netzsch instrument dry particle samples

(~10 mg) were prepared in open aluminium pans and were analysed under a helium purge (50 mL/min). TGA was performed simultaneously with these DSC measurement to verify low residual solvent and hence a relatively constant mass over the measurement. For the Perkin Elmer instrument dry particle samples (3-4mg) were prepared in closed aluminium pans and were analysed under a nitrogen purge (10mL/min). Lastly, for the Mettler Toledo instrument dry particle samples (2-3 mg) were prepared in 40 µL aluminium pans with pinned lids and were analysed under a nitrogen purge (10 ml/min). The samples were all heated from 10 °C to 200 °C or 20 °C to 200 °C at a rate of 10 °C / min.

3.8.2 X-Ray Powder Diffraction

XRPD is a versatile technique and one of the main analytical techniques for pharmaceutical solid state characterization. XRPD uses an X-ray beam and the scattering hereof to determine the distance between the planes in a crystal lattice structure. A detector scans the intensity of the reflections over a given angle (2θ) and some interference will occur between the reflected beams. The intensity of this scattered radiation is then related to the angle of the incident X-ray hitting the crystal using Bragg's law (equation 3.6), which is used to calculate the phase information.

$$n\lambda = 2d \sin\theta \qquad \text{(Equation 3.6)}$$

XRPD is typically used to detect crystallinity and to identify polymorphism and solvates. XRPD is often regarded as the gold standard when it comes to identifying whether a sample is amorphous or crystalline. Different crystal structures will result is different diffractograms and this also applied for crystalline polymorphs, which would also show different peaks in the X-ray diffractograms. An XRPD diffractogram of an amorphous product results in a featureless "halo". The detection limit of crystallinity

with XRPD is typically around 0.5% and small nanocrystals may also be overlooked by an XRPD measurement.

X-ray powder diffraction pattern of samples were analysed at ambient conditions using a PANalytical X'Pert PRO MPD system (PW3040/60, Philips, The Netherlands) equipped with a PIXcel detector. The particle powder samples were placed on flat aluminium sample holders and measured in reflection mode in the 2θ range of 2-40º using a Cu K_α radiation (λ = 1.542 Å). Samples were scanned at an operating voltage and current of 45 kV and 40 mA, respectively, and each diffractogram was recorded at a scanning speed of 4º min-1 with a step size of 0.02. The diffraction patterns were generated using the software, X'Pert High Score, version 2.2.0 (Philips, The Netherlands). Sample spinning was used during the measurements in order to avoid effects from preferred orientation.

3.8.3 Polarized light microscopy

Polarized light microscopy works similarly to conventional bright-field light microscopy but has a pair of polarizers, one between the light source and the specimen, and one between the specimen and the observational tubes. The polarizer between the light source and the specimen is adjusted to control the transmission of light and usually to obtain plane-polarized light. The presence of an anisotropic specimen, a highly refractive specimen such as most crystalline materials divides the light rays into orthogonal components, which become out of phase but are recombined in the second polarizer with constructive and destructive interference. Having the polariser oriented at 90 degrees means all directly transmitted light can be blocked, so only the contrast from the anisotropic specimen is seen. This is used to observe the presence of crystallinity in a sample, which would be highly visible and would "light up" while amorphous, isotropic material would be dark.

A polarized light microscope (Axiolab, Carl Zeiss, Göttingen, Germany) was used for detecting crystallinity in the microparticles samples together with XRPD and DSC. A thin coating or layer of the particle samples was placed on microscopy glass slides and visualized using the microscope at 5x, 10x or 20x magnification. The polarizing filter was oriented at 90º to block transmission of direct light and observe the presence of crystalline material. A digital camera (Deltapix, Maaloev, Denmark) was used with an image resolution of 1024 x 1280 and together with the software, Deltapix, to capture images of potential crystallinity in the samples.

3.9 Drug physical stability

Physical stability was studied by placing samples prepared using spray drying and electrospraying into a desiccator at ambient temperature for several months and then examining them using XRPD and DSC to observe changes in their physical form. Some samples were placed in an oven for 2-3 weeks at 50 °C and ambient humidity to observe if changes would take place at elevated temperature.

3.10 Surface chemical analysis and drug distribution

Surface chemical analysis using XPS was mentioned in section 2.5.3 as a technique to determine the ratio between drug and polymer on the surface of the particles. The measurements would give some information of the distribution of drug in the particles and can be used to explain parts of the particle formation process for a specific system.

The surface chemistry of particle samples was analysed by XPS using a K-Alpha spectrometer (Thermo Scientific, Denmark) equipped with a monochromated AlKalpha X-ray source. Wide energy survey scans (0-1350 eV binding energy) were made with a pass energy of 200 eV and a step size of 1.0 eV. An angle of 90° was used between sample surface and analyser (take-off angle). An X-ray spot size of 200 µm was used

for the particle samples to take possible inhomogeneity of the sample into account. The surface drug content of the microparticles was determined by calculating the ratio of the detected amount of fluorine in the samples to the amount of fluorine in pure CEL thereby determining the concentration of CEL (in wt %) on the surface of the particles. The atomic concentration (in %) of elements C, O, F, N and S (H was not measured) used for pure CEL were 65.38%, 7.69%, 11.54%, 11.54% and 3.85%, respectively. Similarly, the relative concentration (in %) of elements C and O used for PLGA were 55.56% and 44.44%, respectively.

3.11 Drug detection

3.11.1 Drug detection using UV-Vis spectroscopy and HPLC

UV-Vis spectrophotometry is commonly used for detection of drugs and other molecules that absorb UV and visible light. A UV-Vis spectrophotometer measures the intensity of light transmitted through a sample as a function of light with wavelengths in the UV and visible range. This absorbance of light is then determined and can be correlated to the concentration of the material measured using the Beer-Lambert law. Molecules that absorb light in the UV-Vis range can thus be detected and quantitated over a certain concentration range where a linear relationship exists between the absorbance and the concentration of the molecules of interest.

When there are several different molecules in the sample that absorb UV-Vis light it can be difficult to distinguish these molecules using a conventional UV-VIS spectrophotometer. In this case chromatography, and in particular High Performance Liquid Chromatography (HPLC), is used to separate the molecules so they can be detected and, if necessary quantitated, separately using a UV spectrophotometer or mass spectrometer connected to the HPLC chromatograph. Due to the separation of the

molecules and the design of modern, automated HPLC instrumentation more sensitive and precise measurements can be obtained compared with a conventional stand-alone UV-Vis spectrophotometer.

3.11.2 Drug entrapment efficiency

Drug entrapment efficiency (EE) was measured by evaluating the total amount of drug in the collected samples. Samples with 10-20 mg microparticles were accurately weighed, dissolved in acetonitrile (10 mL) and agitated for 1 hour. This solution was then diluted 1:10 in acetonitrile:water (20:80 v/v) and centrifuged at 3000 rpm for 10 min. The drug content in the supernatant was analysed using a HPLC unit with Pump P680 and ASI 100 sample injector and UVD340U (Dionex, Germany) equipped with Kromasil 126 column (Kromasil, Sweden). A mobile phase of acetonitrile:water (60:40 v/v) was used at a flow rate of 0.5 mL min^{-1} and the injection volume of 10 μL was detected at wavelength 230 nm and a run time of approximately 15 min. A calibration curve was obtained from reference CEL solutions between 0.5 μg/mL and 50 μg/mL and a good linear correlation was achieved in the entire range. The drug entrapment efficiency was then determined using following equation:

EE % = 100 · Mass of drug loaded in particles / Mass of drug processed

3.12 Drug release studies

Drug release studies from particles were performed using two different methods: A method used for initial drug release studies involved release of CEL from particles, in 30 ml water/ethanol media, while later studies were more in line with official compendial methods used to test oral dosage forms, using a paddle dissolution apparatus and release media recommended by the United States Pharmacopeia (USP).

3.12.1 Initial release study

A UV-Vis spectrophotometer (Lambda 35, Perkin-Elmer, UK) was used to measure the released amount of CEL from the particles at different time points. A suitable UV absorption peak of CEL was found at 250 nm where a good linear response was observed over the target concentration range. Appropriate calibration and blanking procedures were done before the measurements. Release studies were performed by dispersing weighed, dry particle samples (~6 mg) in glass vials containing 30 mL release medium. The studies were all performed under ambient temperature and under continuous magnetic stirring at approximately 250 rpm. A 50:50 volume ratio mixture of ethanol and water was used as release medium. At discrete time intervals 3 mL was removed from the samples and centrifuged at 4000 rpm for 20 min. The supernatant was removed and diluted in methanol to reach the measurable concentration range of CEL for UV absorption.

Four measurements were performed for each particle sample at each sample time and the mean absorbance value was found. The measurements were done over a period of 10 days.

3.12.2 Paddle drug release study

Drug-loaded particle powder samples were weighed (10-20 mg) and placed in a release media of 500 mL phosphate buffer (0.01M, pH=6.8) + 1.5% w/v sodium lauryl sulphate (SLS). Drug release studies were performed on a Sotax AT7 dissolution station (Sotax, Switzerland) equipped with a USP II (paddle) apparatus and 1000 mL glass vessels (see Figure 3.7). Release samples were drawn from a location on the paddle shaft and up through 2.7 μm glass microfiber filters (Whatman Ltd, England) using an autosampler, Biolab/Gilson GX-271 (Biolab, UK). During release studies the paddles were run at a rotation of 50 rpm and the release medium was kept at 37 ºC with a temperature bath.

Samples of 5 ml were taken at 17 time points over 24 hours and later filled into HPLC vials. HPLC analysis was conducted as previously described for drug entrapment efficiency in 3.9. A minimum of 4 experiments was performed for each sample condition and the results were averaged to construct drug release profiles. The drug entrapment efficiency was taken into consideration when analysing the drug release data and the release data was corrected by linear scaling of data point. The software Chromeleon, version 6.8 was used to manage and calculate drug release results.

Figure 3.7 Sotax dissolution tester with 6 vessels.

Chapter 4

Electrospraying of solid dispersions: The influence of process parameters and control of particle characteristics and drug release

This chapter describes the investigation of electrospraying for preparing solid dispersion microparticles using the poorly soluble drug, Celecoxib (CEL). PLGA microparticles containing CEL were prepared with the objective of producing near-monodisperse microparticles with the drug in an amorphous form. Further, the influence of different process parameters on particle characteristics as well as on drug release profile was examined to understand how to control these properties. It was found that microparticles loaded with CEL could be formed and that these particles could be prepared with a near-monodisperse distribution. By adjusting the different parameters it was observed that particle characteristics such as size, morphology, shape and porosity could be controlled with a good correlation between process parameters and the resulting characteristics. Further, the release profiles of the particles could also be controlled via these process parameters indicating a link between the release kinetics and the characteristics of the particles. Curve fitting of the release curves indicated diffusion mediated release from the particles over an extended time. This study forms the foundation for studies on electrosprayed solid dispersions described in Chapter 5.

4.1 Selection and characterization of drug and carrier

A model drug and a few polymeric carrier materials were investigated for preparing solid dispersions using electrospraying and spray drying. These materials and their properties were first characterized.

4.1.1 Selection and characterization of model drug

CEL was selected as a model drug due to its very low water solubility and its physical characteristics including its relatively high molecular weight (381.38 g/mol) which makes it difficult to formulate. CEL is a class II compound under the Biopharmaceutics Classification System, thus being poorly soluble but having high intestinal permeability [Chawla *et al.* 2003]. It was also selected due to its commercial interest as a blockbuster drug without any salt formulations available, which makes it necessary to deal with its inherently low solubility by other means, for use via oral administration.

Although some of the characteristics of CEL were explained in section 3.1.2 studies were performed to examine the characteristics of the specific batch of CEL used in the experiments throughout this PhD project.

Appearance of CEL crystalline powder:

The unprocessed CEL powders consisted of crystals of variable size and mostly of rod-shaped appearance (see Figure 4.1). The CEL powder had a fluffy texture and was very electrostatic.

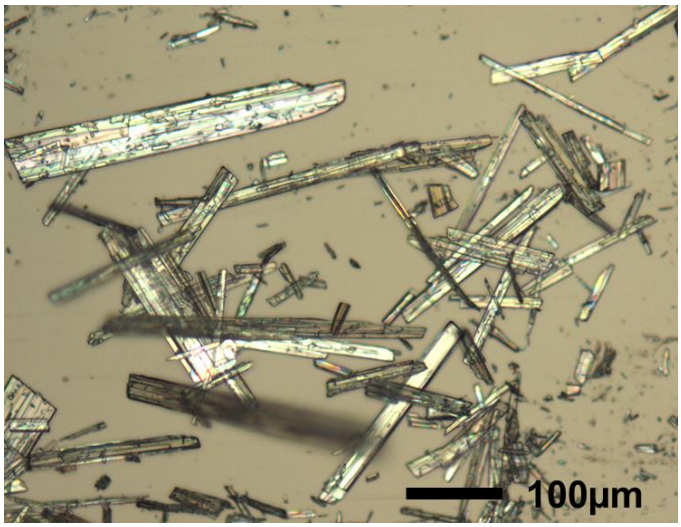

Figure 4.1 Optical micrograph of crystalline CEL

Physical state and thermal properties of CEL:

DSC measurement of CEL showed a sharp endotherm peak at 162 °C indicating the melting point of CEL crystals (see Figure 4.2).

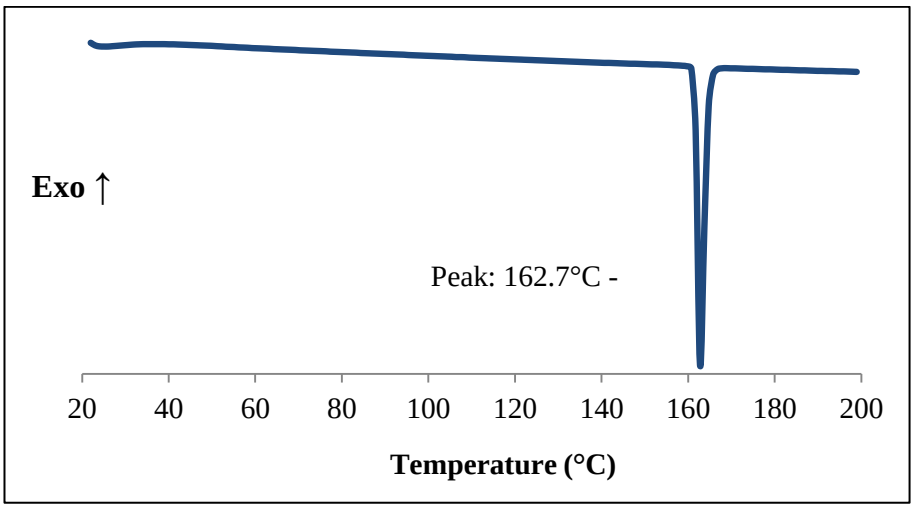

Figure 4.2 DSC thermogram of CEL indicating melting endotherm.

The XRPD diffractogram on Figure 4.3 again demonstrates that the CEL powder used is crystalline and that the crystalline peaks correspond to the peaks from Figure 3.3 B, the crystalline polymorph form II.

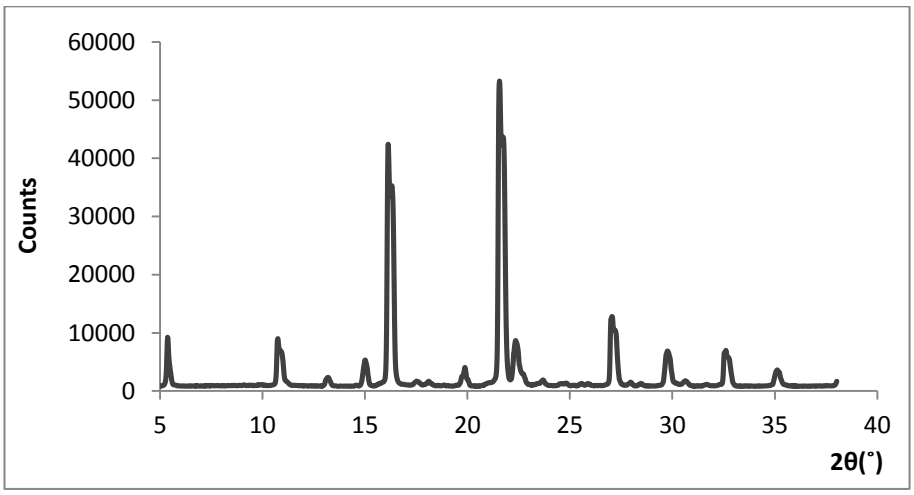

Figure 4.3 XRPD spectrogram showing profile of crystalline CEL.

4.1.2 Selection and characterization of polymer

There are many different polymers used in drug delivery applications each with their individual properties and functions and each with their advantages and disadvantages. In this study, PLGA was selected as the main polymer, partly because it is FDA approved and widely recognized, but also because of its prior use and successful application with electrospraying [Almeria *et al.* 2010, Enayati *et al.* 2010].

Two other polymers, chitosan and poly-ethylene glycol (PEG, MW= 6000 g/mol) were also initially studied but proved difficult to electrospray in the cone-jet mode. These polymers were initially sprayed in aqueous solutions, which have a high surface tension due to the high surface tension of water. This makes it difficult to form a stable jet without the addition of surfactants. Further, water has a relatively high boiling point which makes it more difficult to boil off the solvent to obtain dry particles at collection. Chitosan also makes the solution very viscous, even at low concentrations, making it difficult to atomize a solution at concentrations above 1-2% w/v. PEG was later electrosprayed in acetone where a cone-jet could easily be obtained. However, due to the preferred crystalline state of PEG, it did not seem to mix well with CEL, resulting in rapid crystal growth from the prepared particles. Chitosan and PEG were thus not ideal carrier materials for preparing electrosprayed solid dispersions.

Characteristics of PLGA

Appearance of PLGA granules:

Microscopy images PLGA granules showed an indistinguishable appearance (not shown here) and the powder was fluffy with low density.

Physical state and thermal properties of PLGA

DSC measurement of PLGA powder showed an endothermal event at 54 °C indicating the glass transition of PLGA (see Figure 4.4).

A

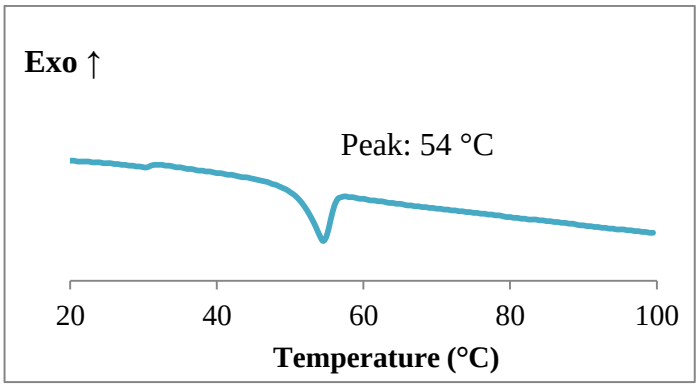

B

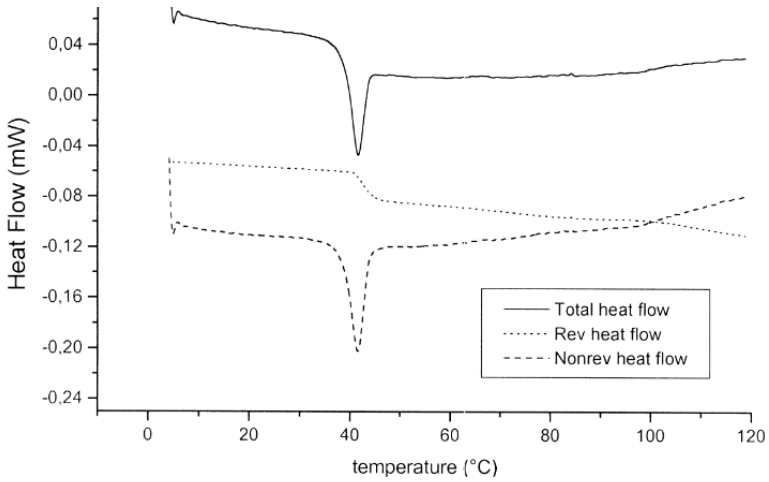

Figure 4.4 DSC thermograms of pure PLGA powder indicating glass transition event (A) and PLGA microspheres measured by [Passerini and Craig 2001] using modulated DSC (B).

It is seen in Figure 4.4A that the glass transition event of PLGA does not have the appearance of the typical T_g and instead shows a strong signal with a distinct peak unlike the typical T_g events. This may be explained by the graphs presented by Passerini and Craig (see Figure 4.4B) where a modulated DSC was used to separate the heat flow signal into the reversing and non-reversing heat flow signals thereby facilitating the detection of a T_g. The T_g event observed for the non-reversing heat flow signals resembles that of the DSC curves for PLGA and CEL-loaded microparticles shown in this thesis and could be due to the separation of heat signals [Passerini and Craig 2001].

XRPD of PLGA on Figure 4.5 shows a halo indicating amorphous PLGA.

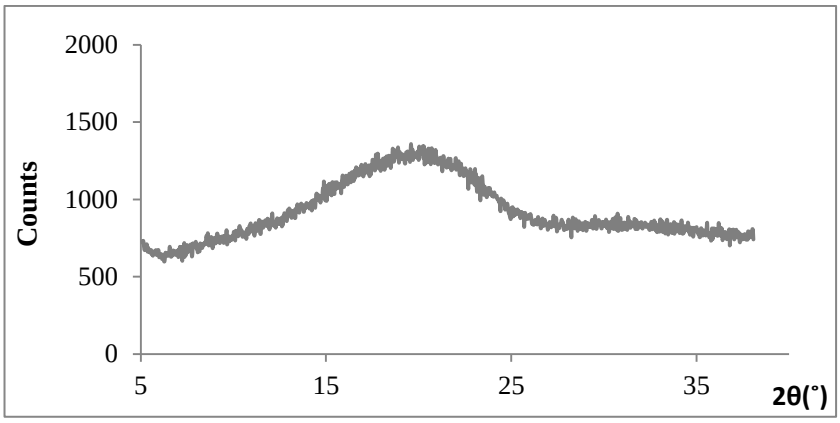

Figure 4.5 XRPD spectrogram of PLGA.

4.1.3 Physical mixture of CEL and PLGA

Physical mixtures were prepared from CEL and PLGA at 1:4 weight ratio and 1:1 weight ratio. DSC measurements of the physical mixtures showed an endothermal event at around 55 °C and a small endothermal event at 162 °C, which could indicate that CEL was partly amorphous and partly crystalline (see Figure 4.6). However, it is also possible that most of the crystalline CEL dissolved in PLGA above the glass transition of PLGA and thus did not melt.

XRPD diffractograms of physical mixtures of PLGA and CEL indicate the presence of both an amorphous and a crystalline phase (see Figure 4.7). When the CEL:PLGA ratio is increased the crystalline peaks become more dominant.

4.2.1 Selection of solvent and preparation of solutions

Solvents for particle preparation were initially selected based on the criteria that both CEL and PLGA need to be readily soluble in the solvent. Further, it was decided that the solutions formed need to have an electrical conductivity (see section 2.5-2.6) and a surface tension in a window that allows the cone-jet to be formed without addition of salts or surfactants. On the basis of these criteria, four solvents (acetone, acetonitrile, dimethylformamide (DMF) and dimethylacetamide (DMAc)) were selected for testing.

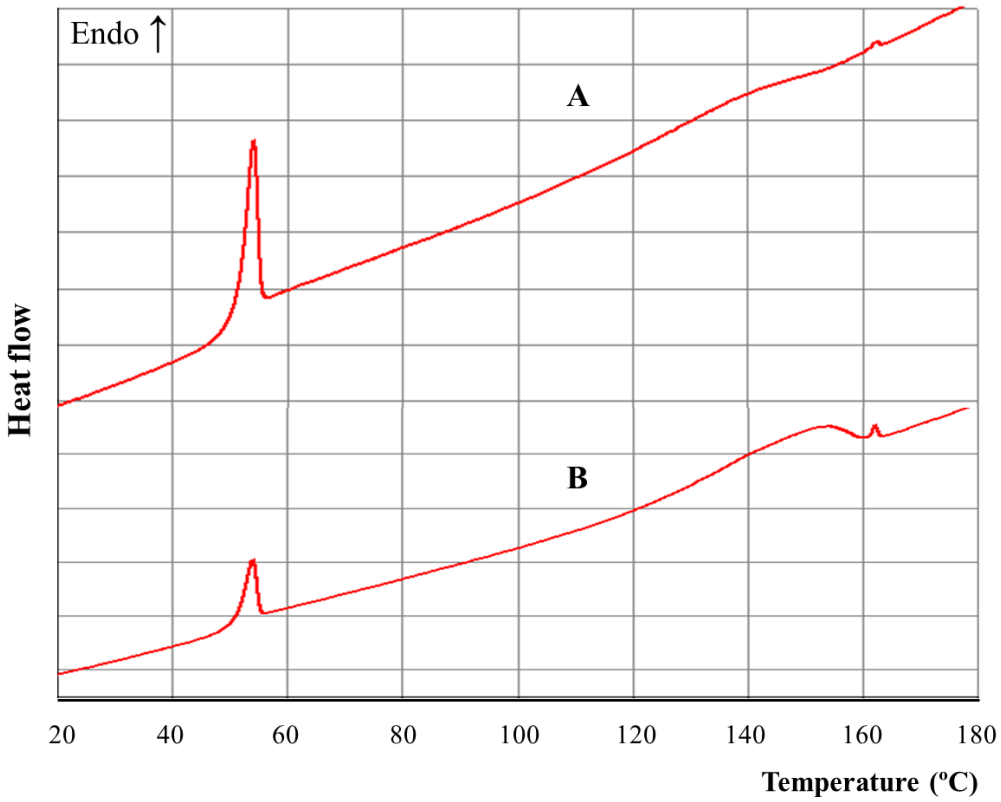

Figure 4.6 DSC thermogram of PLGA and CEL physical mixtures at 1:4 ratio (A) and 1:1 ratio (B) indicating melting endotherm.

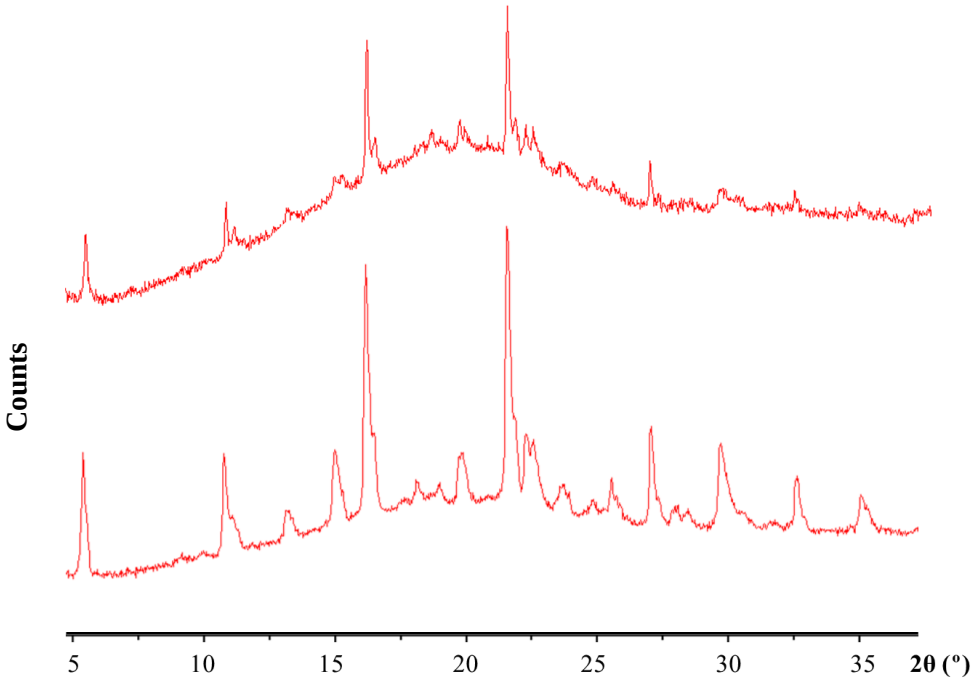

Figure 4.7 XRPD diffractogram of PLGA and CEL physical mixture.

4.2 Preparation and characterization of spraying solutions

Following preparation of PLGA particles using DMF or DMAc, it was observed that a cone-jet was obtained and some droplets were formed and collected on glass slides. Yet, the solvent had only partly evaporated at collection and the many wet particles collected would re-dissolve on the glass slide, where they later dried to form a film. DMF and DMAc have a boiling point of 153 ºC and 165 ºC, respectively, and are thus not volatile enough to form dry particles at collection without an active drying mechanism [Smallwood 1996]. These solvents were therefore not used any further with this experimental setup which makes use of a passive drying process.

The studies were instead continued with the solvents acetonitrile (ACN) and acetone (ACE), both of which are more volatile than DMF and DMAc with a boiling point of 82 ºC and 56 ºC respectively. ACN and ACE have similar density and surface tension while ACN has a slightly higher viscosity and electrical conductivity compared with ACE (see Table 4.1).

Table 4.1 Physical properties of solvents used to fabricate microparticles [Smallwood 1996]. * Relative to the evaporation rate of Butyl Acetate.

Property	**Acetone**	**Acetonitrile**
Viscosity (mPa·s) at 25 °C	0.33	0.38
Boiling point (°C)	56	82
Evaporation rate (BuAc=1)*	5.6	2.0
Dielectric constant	20.6	37.5
Electrical conductivity (µS/cm)	0.06	0.23

4.2.2 Solubility of CEL and PLGA

Solubility was measured visually by observation of the onset of a cloud point or precipitation of the solute (see Table 4.2). All values are approximations and were mainly used to evaluate the solvent power of the different solvents used. For values of solubility higher the 50% w/v the solubility could not be clearly determined and instead minimum solubility values were given. Table 4.2 indicates that acetone and acetonitrile are both good solvents for CEL and PLGA, while methanol and ethanol dissolve CEL to some extent but not PLGA. Both CEL and PLGA are practically insoluble in water.

Table 4.2 Solubility of CEL and PLGA in solvents used in the study.

Solvent	Solubility of CEL (mg/mL)	Solubility of PLGA (mg/mL)
Water (deionized)	~ $2 \cdot 10^{-3}$	Insoluble
Ethanol	~ 50	Insoluble
Methanol	~ 100	Insoluble
Acetone	600-700	500-600
Acetonitrile	500-600	400-500

4.2.3 Characterization of spraying solutions

Electrical conductivity and Viscosity

Measurements of electrical conductivity showed that ACE was less conductive than ACN (see Table 4.2). The addition of 5% PLGA to the solvents did not contribute notably to the electrical conductivity whereas the addition of 5% CEL resulted in a significant increase in the electrical conductivity, which indicates that CEL carries more electric charge than PLGA. With electrospraying the electrical conductivity is known to influence the properties of the particles obtained most notably with an increase in conductivity resulting in a decrease of particle size, according to the scaling laws

[Gañan-Calvo *et al.* 1997].

Measurements of viscosity showed that ACE is less viscous than ACN and that the addition of PLGA has a great influence on the viscosity of the solution while the addition of CEL does not seem to have noticeable influence on the viscosity of the solution. The greater influence of PLGA on the viscosity is explained by much higher molecular weight and hydrodynamic volume of PLGA compared with CEL. It was also observed that the solution with PLGA in ACE is more viscous than the solution with PLGA in ACN, although ACE is less viscous than ACN by itself, indicating that ACE is a better solvent for PLGA. In a good solvent the polymer chains are extended and interaction between the chains and entanglement of the chains begin taking place at a lower concentration than for a not so good solvent, hence resulting in higher viscosity [Ayal *et al.* 1993]. With both electrospraying and spray drying the viscosity of a solution is known to influence the properties of the particles obtained most notably with an increase in viscosity resulting in an increase in particle size [Jayasinghe and Edirisinghe 2002].

Table 4.3 Properties of solvents and solutions containing CEL or PLGA.

Solvent/solution	**Electrical conductivity** (μS/cm)	**Dynamic Viscosity** (mPa·s), at 25 °C	**Surface tension** (mN/m), at 25 °C
ACE	0.11	0.30	25
ACN	0.28	0.35	30
CEL in ACE (5% w/v)	1.01	0.37	25
CEL in ACN (5% w/v)	1.06	0.41	30
PLGA in ACE (5% w/v)	0.23	1.13	25
PLGA in ACN (5% w/v)	0.40	1.08	29

Measurements of surface tension showed that ACN has a higher surface tension than ACE and that the addition of CEL or PLGA to the solvents does not have a noticeable influence on the surface tension of the liquid. The surface tension of organic solvents is generally low and does not seem to be influenced by the addition of solutes used in this study. A relatively low surface tension is necessary in order to obtain a stable cone-jet with electrospraying. The values obtained here are much lower than the surface tension of water (72 mN/m, at 25 °C) and are thus assumed to be in an acceptable range.

Viscosity and polymer configuration

The polymer conformational structure, solubility and behaviour of PLGA molecules in ACE and ACN were studied by determining the intrinsic viscosity, overlap concentration and Martin constant in these two solvents. Since CEL does not contribute much to viscosity compared with PLGA, and since only PLGA is relevant in the context of polymer entanglement, only PLGA solutions without CEL were studied. The intrinsic viscosity relates to the capability of a polymer to enhance the viscosity of the solution it is in, and gives an indication of the molecular weight of the polymer as well as the solubility of the polymer in the given solvent. The intrinsic viscosity was determined as the y-intercept of the specific viscosity / PLGA concentration curve as described in section 3.4.

The intrinsic viscosity of PLGA in ACE and ACN were 0.276 dL/g and 0.216 dL/g respectively (see Figure 4.8). ACE resulted in a higher intrinsic viscosity than ACN, which suggests more extended chains, more polymerization and better solubility of PLGA in ACE. The overlap concentration, c*, refers to the cross over from the dilute regime to the semi-dilute regime of a polymer in solution. This value represents the concentration at which polymer chains begin to entangle with each other and was found from the intrinsic viscosity values. The c* for PLGA in ACE and ACN were 3.6% and

4.6% respectively. This indicates that polymer chain entanglement begins at a later point for PLGA in ACN. The Martin (K_m) constant is used to gain information on the interactions between solutes, with a higher value indicating more interaction between the PLGA molecules. In this case ACN showed a higher value than ACE indicating weaker interactions between PLGA molecules in ACE than ACN.

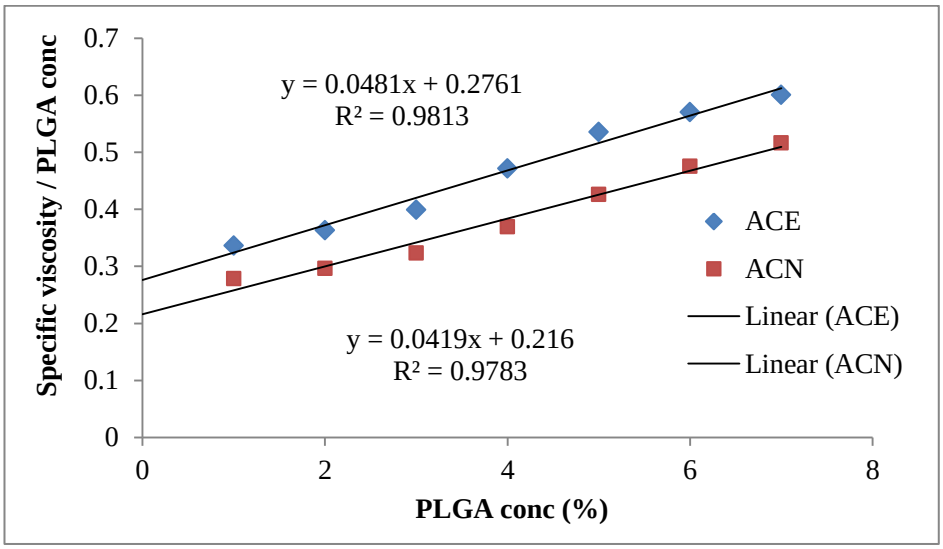

Figure 4.8 Specific viscosity of ACE and ACN solutions as a function of PLGA concentration, including intrinsic viscosity (intercept with y-axis).

Table 4.4 Intrinsic viscosity and Martin constant of PLGA solutions.

Solvent	**ACE**	**ACN**
Intrinsic viscosity (dL/g)	0.28	0.22
Martin constant (K_m)	0.48	0.63

Evaporation profile

The evaporation profile of an ACE solution and ACN solution both containing 5%wt solutes (90% PLGA and 10% CEL) were studied using TGA at 25 °C (see section 3.2.5) and the evaporation curves are shown in Figure 4.9 A. It is observed that both curves flatten out around 7% where there is no longer any measurable change in the mass of

the sample. The ACE solution reaches this point four times quicker than the ACN solution indicating that ACE evaporates much quicker than ACN at this temperature. Figure 4.9 B shows the first derivative of the evaporation curve which is essentially the evaporation rate as a function of time. The curves show that the evaporation rate is not constant but decreases with time as the solutes become more and more concentrated until a critical point where it essentially decreases down to zero.

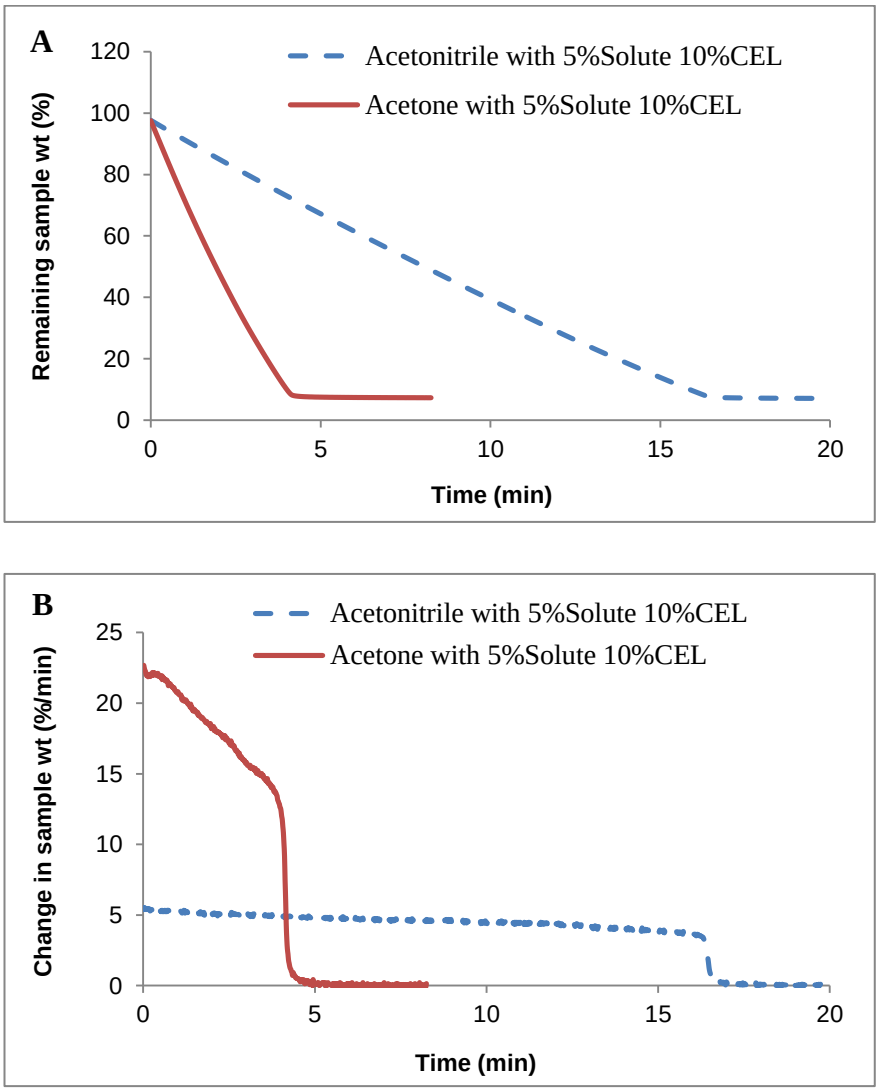

Figure 4.9 Evaporation of solutions at 25 ºC (A) and first derivative of evaporation curve (B).

4.3 Electrospraying of poorly water-soluble drugs

4.3.1 Sprayability and particle collection

The prepared solutions were all sprayed using the single nozzle setup shown in Figure 3.4 and it was demonstrated that a cone-jet can be obtained (see Figure 4.10 A) and that particles are formed from the resulting jet (see Figure 4.10 B). Samples of CEL microparticles and CEL-loaded PLGA microparticles could be successfully prepared in an ACE solution at different operating conditions and their characteristics were studied using various techniques.

By varying the collection distance different levels of dryness of the samples were observed via optical microscopy, going from still being wet (~ 1 cm) to being more or less dry (~ 5-10 cm). Although a short collection distance results in wet particles, a long collection distance spreads out the particles too much and decreases the collection yield (see Figure 4.10C), and hence a distance of 7cm was chosen. In this study, it was thus assumed that a majority of the solvent had evaporated by the time the particles reached the collection surface.

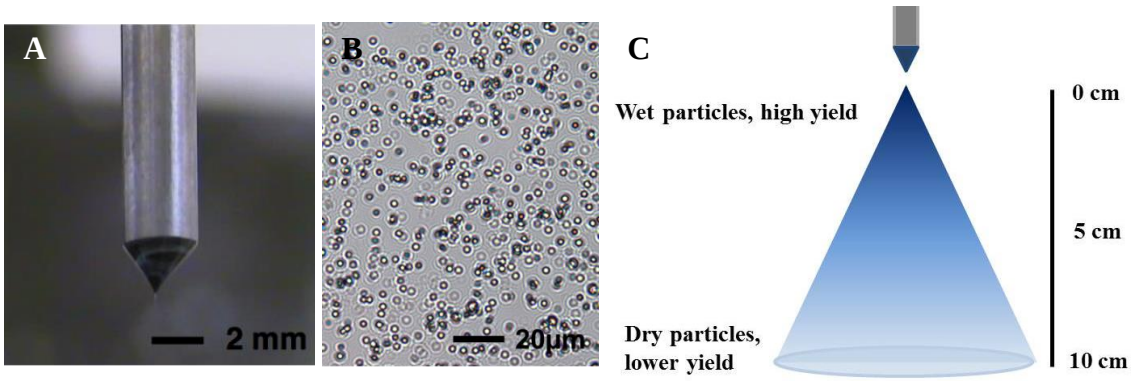

Figure 4.10 Video camera image of stable cone-jet (A), microscopy image of PLGA particles on a glass slide (B) and particle drying and yield as a function of collection distance (C).

4.3.2 Particle appearance and crystallization

Particles of pure CEL were prepared by electrospraying a solution of ACE containing 5%wt CEL and collecting them on different substrates at a distance of 7 cm from the jet. SEM images of collected CEL particles are shown in Figure 4.11 and demonstrate that it is possible to obtain spherical microparticles without the addition of support materials such a polymer. Figures 4.11 A and B show that when collected directly on glass, spherical particles are formed and in some areas together with rod like relics connecting the spheres, presumably drug crystals. Such crystals would grow as a function of time and results in larger crystalline structures which makes them more stable. When collected on a glass slide with a film of water needle-shaped crystals begin forming (see Figure 4.11 A) immediately after collection and no spherical particles were observed. Water induces rapid crystallization of CEL microparticles by allowing more interaction between the hygroscopic CEL molecules. The rapid crystallization of CEL even in absence of water necessitates mixing it with a carrier material such as a polymer in order to stabilize the spherical particle structure and get prepare drug in a stable amorphous form.

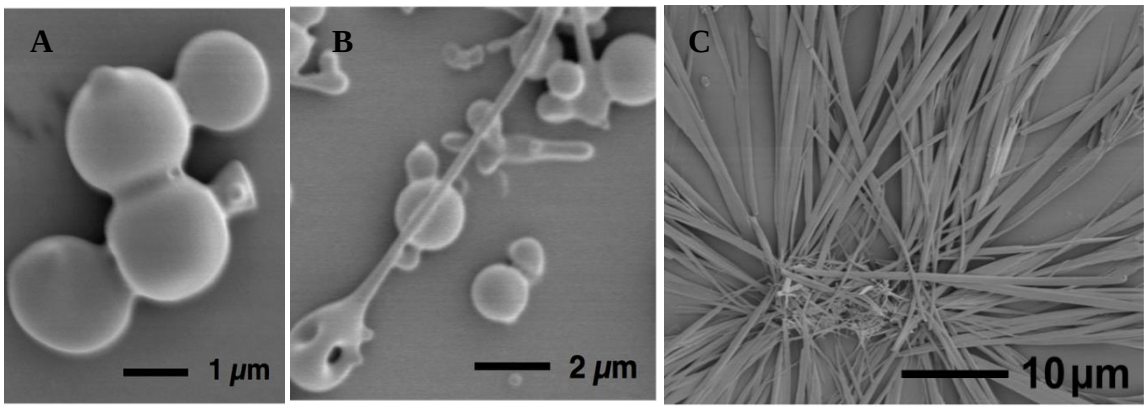

Figure 4.11 SEM images of CEL particles collected on glass slides without water (A and B) and with a thin layer of water (C).

CEL-loaded PLGA particles were then prepared in the same way as for the CEL particles at different ratios of PLGA and CEL. SEM images of the prepared particles are shown in Figure 4.12 and it is seen that the particles all seem to be spherical with no characteristic needle-shaped CEL crystals protruding from the particles at the studied CEL loading (10%, 20% and 50%). This indicates that PLGA and CEL are mixed well within the particles and prevents CEL molecules from going together to form large crystal structures. It has also been demonstrated that PLGA can form interactions with drug molecules, and in this case hydrophobic interactions are likely between CEL molecules and hydrophobic segments of PLGA [Jeon *et al.* 2000].

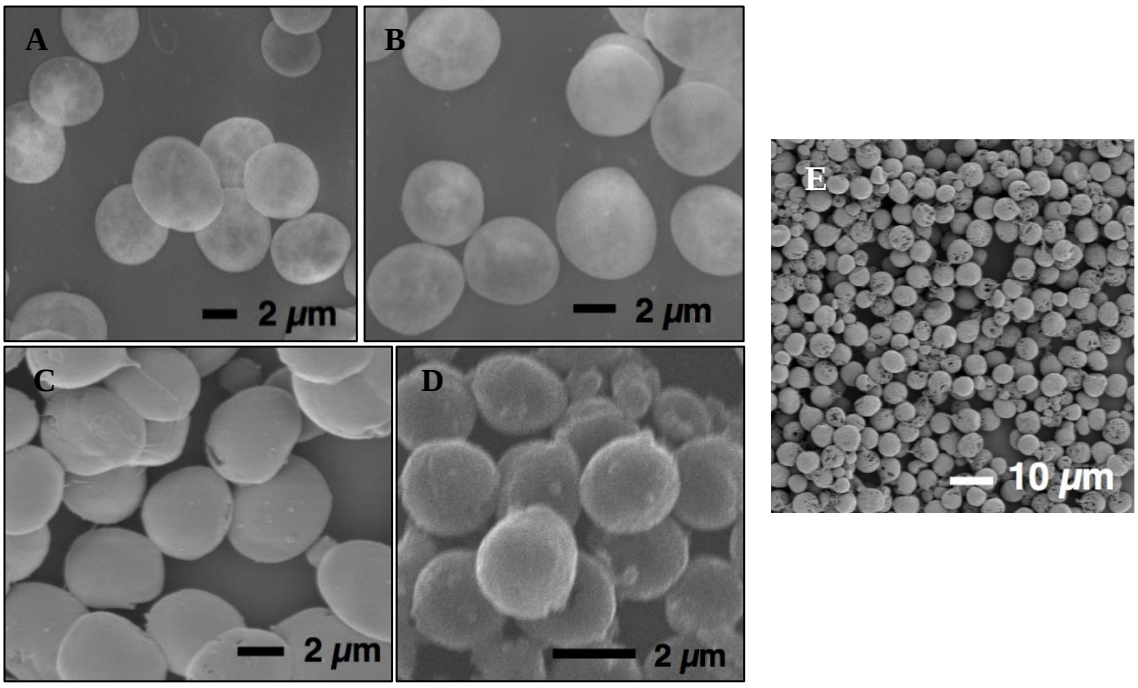

Figure 4.12 SEM images of CEL-loaded PLGA particles prepared in ACE with varying drug loading. 0% CEL (A), 10% CEL (B), 20% CEL (C), 50% CEL (D) and SEM images of electrosprayed PLGA particles taken with low magnification (E).

The size of the particles were generally around 2-5 μm with the particle size decreasing as the drug loading was increased. The size distribution was generally narrow as it is observed in Figure 4.12 E and 4.13 and all particle samples were found to have a

polydispersivity index below 10%, except for the particles prepared with 50% drug loading which were less homogenous. The particles seem to follow a Gaussian distribution indicating that particles size is influenced by several factors. The influence of different process parameters on particle size, morphology and porosity will be discussed in section 4.4.

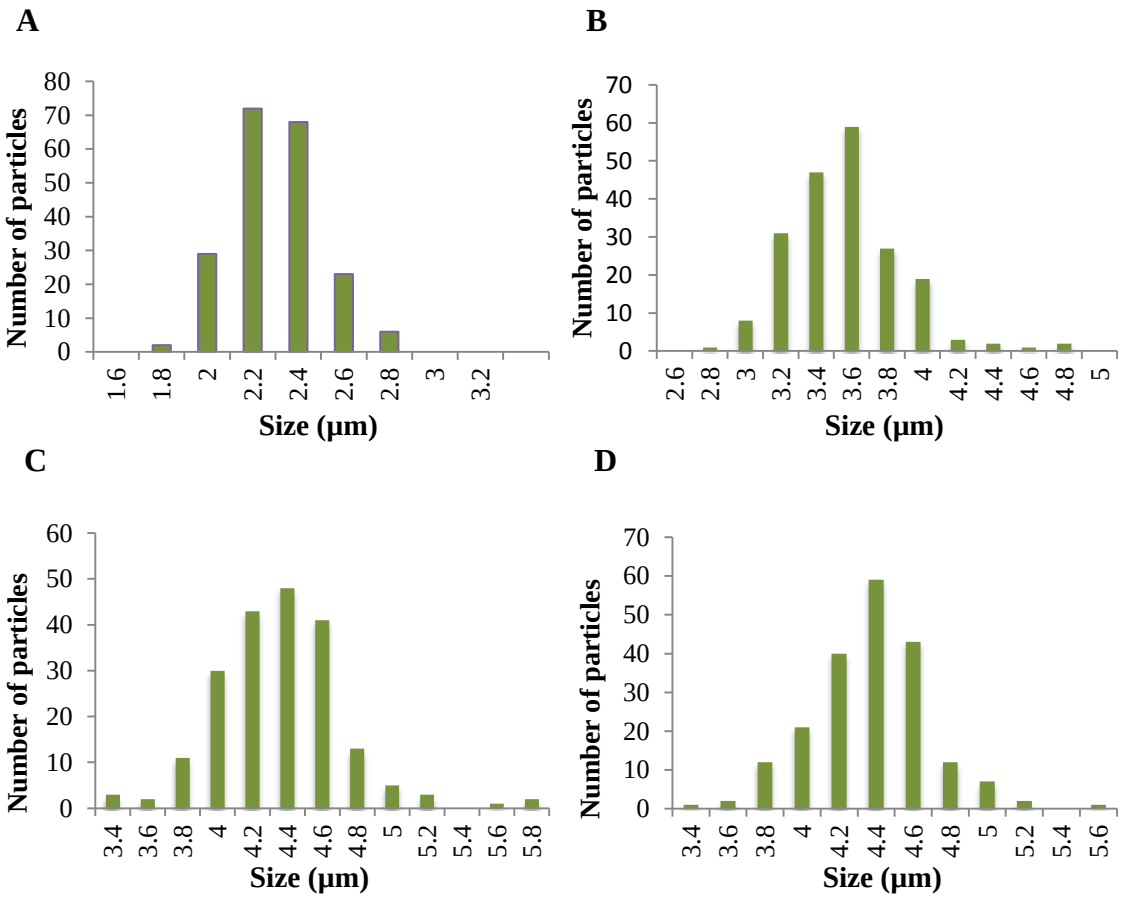

Figure 4.13 Size distribution of electrosprayed PLGA microparticles prepared with 50% (A), 20% (B), 10% (C) and 0% drug loading (D).

4.3.3 Physical form of CEL-loaded particles

The physical form of the CEL microparticles and CEL-loaded PLGA microparticles was analysed using DSC and measured between 10 and 200 ºC at a heating rate of 10 ºC/min. Figure 4.14 shows DSC thermograms for unprocessed CEL powder (A) and

electrosprayed CEL microparticles (B), measured within an hour after particle preparation. The unprocessed CEL powder shows a characteristic melting endotherm at 162 ºC indicating that CEL is in a crystalline form. The electrosprayed CEL microparticles show both a similar endotherm peak at 162 ºC and an exotherm peak at 90 ºC, and further no clear T_g event was observed around 58 ºC, the characteristic T_g of CEL [Gupta et al. 2005]. However, the exotherm peak observed could indicate the recrystallization of partly amorphous CEL in the microparticles. In this case, it seems that the glass transition signal may have been too weak to detect. A similar curve was also observed for unprocessed CEL powder which was quench-cooled using DSC to obtain amorphous CEL, suggesting that the electrosprayed CEL was also partly amorphous.

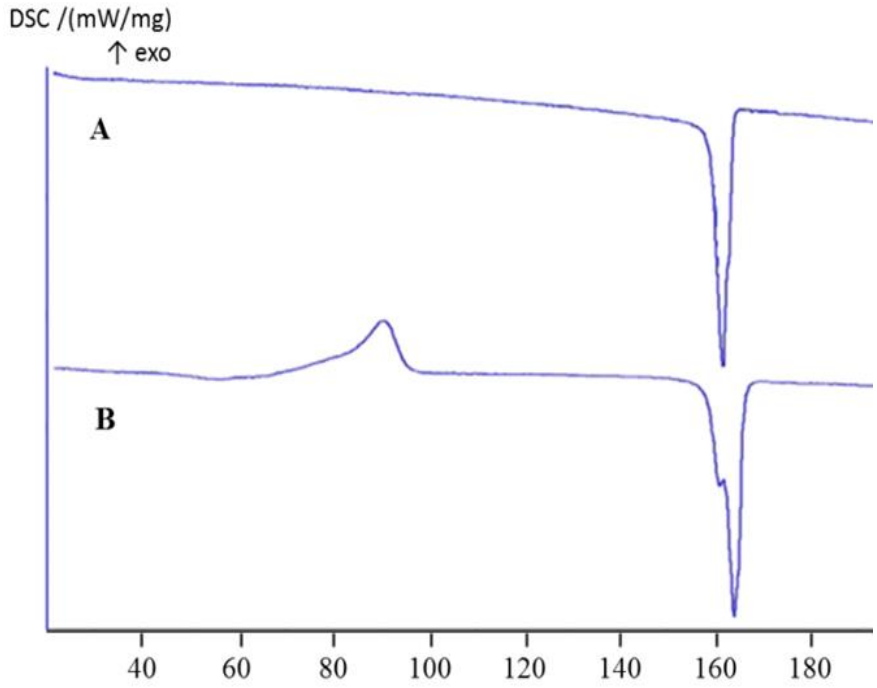

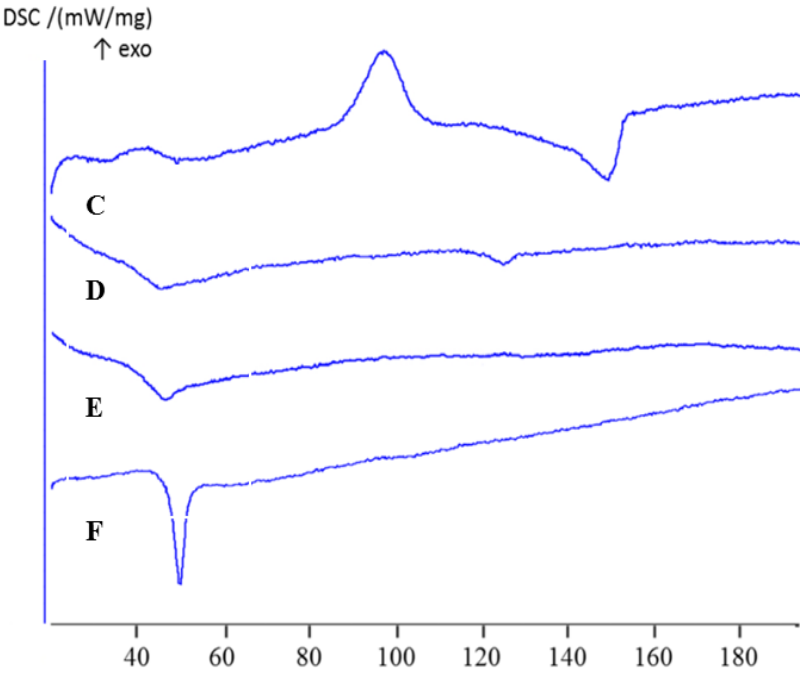

Figure 4.14 DSC thermograms of unprocessed CEL powder (A), electrosprayed CEL microparticles (B), CEL-loaded PLGA microparticles prepared in ACE with 50% (C), 20% (D), 10% (E) and 0% (F) CEL-loading.

DSC curves of CEL-loaded PLGA microparticles are also presented in Figure 4.14. Microparticles with 50% CEL (C) showed an exotherm peak at 97 ºC and an endotherm peak at 149 ºC indicating recrystallization and melting of CEL, respectively. The melting point may have been shifted downwards here by the presence of PLGA. No distinct glass transition event was observed although it seems likely that there would have been a glass transition for CEL, PLGA or both. Particles with 20% CEL (D) showed an endotherm event around 47 ºC, which is likely to be a glass transition and they further showed another event at 126 ºC, which could again indicate a shifted melting peak of CEL. Particles with 10% CEL (E) also showed an endotherm event around 47 ºC, which is likely to be a glass transition, but no melting endotherm was observed. Particles composed exclusively from PLGA (F) showed a glass transition around 51 ºC.

Generally, small downward shifts in the T_g were observed for particles with 20% CEL and 10% CEL compared with the T_g of pure PLGA particles. Only a single glass transition event was observed for particles with 20% CEL and 10% CEL although containing both CEL and PLGA. The single glass transition events observed could thus represent the glass transition of both PLGA and CEL, a common observation for solid dispersions where the drug is well dispersed in the polymeric matrix. It was also reported by [Dubernet 1995] that a reduction in the polymer T_g and an absence of drug melting peak may take place when a drug is in a solid solution inside a polymer matrix. The melting endotherms for CEL in CEL-loaded microparticles were shifted downwards or disappeared. All in all the observations indicate that CEL is in an amorphous form in the CEL-loaded PLGA particles and that interactions are present between PLGA and CEL.

4.3.4 Comparison with micronized drug

CEL microparticles were also prepared using ball milling for comparing with electrosprayed CEL particles. SEM images of ball milled CEL powder are shown in Figure 4.15 A and indicate elongated structures a few microns in their long axis. The XRPD diffractogram of ball milled CEL shown in Figure 4.15 B demonstrates that these micronized particles are partly amorphous and partly crystalline, based on the halo shape and crystalline peaks observed.

Compared with the electrosprayed particles, these ball milled particles were fractioned from larger structures and are thus different in their shape, retaining the rod-like shape from the CEL crystals. The ball milled particles also seem more likely to stay in a crystalline state observed from their X-ray pattern.

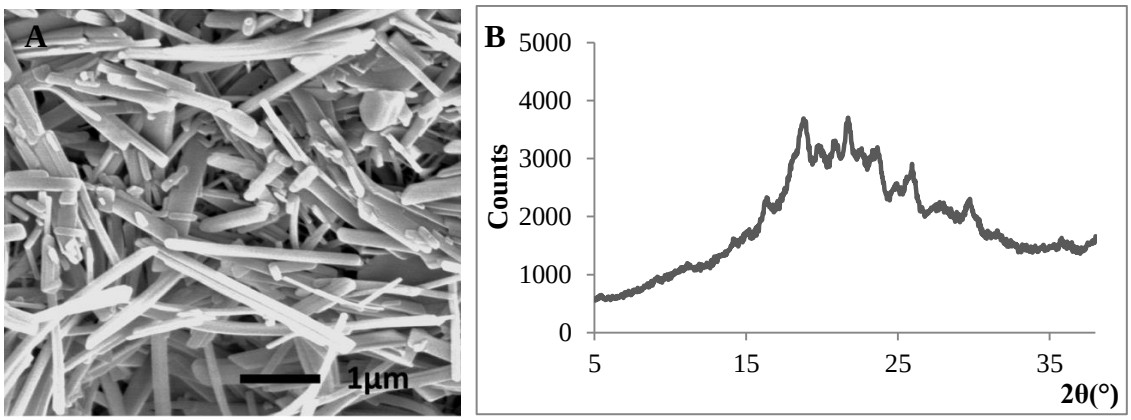

Figure 4.15 SEM image of ball milled CEL (A) and XRPD of ball milled CEL (B).

4.3.5 Drug release from drug-loaded PLGA particles

Initially, drug release studies were performed using glass vials with 30 mL release medium where samples were taken at different time intervals, as explained in section 3.12.1. The release medium consisted of a 50:50 v/v mixture of EtOH and H_2O and was selected after studying several different solvent mixtures. CEL is poorly soluble in aqueous solvents and it was thus necessary to ensure that CEL could be fully dissolved in the release medium in order to study the drug release from the particles. The EtOH:H_2O mixture was selected partly because it provides sink conditions for CEL. Also, PLGA is insoluble in EtOH:H_2O and allows a diffusion driven release from the particles. Sink condition refers to the condition at which the drug is placed in a volume of medium which is greater than 3 times its saturation point. In the case where sink conditions is not maintained the drug release cannot be consistently measured because the medium approaches the saturation point.

The UV absorbance measurements of the microparticles showed similar absorbance as for pure CEL and PLGA and indicates that CEL molecules remain chemically intact after being dissolved and exposed to a high voltage in the electrospraying process. UV absorbance was measured at 250 nm and showed a linear correlation between the

concentration of CEL and the absorbance measured. Drug entrapment measurements of the CEL-loaded microparticles showed that the amount of drug in the samples could deviate ± 10% from the originally added amount, which is possibly a result of measuring uncertainties.

The drug release curves in Figure 4.16 show that the majority of CEL in the particle was released during the measurement for all three samples. A high burst release between 39-54% was observed for all three samples indicating that a large amount of CEL was located near the surface of the particles. Particles with 50% drug loading had the highest drug release rate and were quickest to reach a plateau level in the release curve after 4 days. The release rate decreased as the drug loading was reduced and particles with 10% drug loading showed the lowest release rate of the three curves. The drug release from particles could thus be modified by changing the drug loading of the particles. A similar observation was made by Piñon-Segundo *et al.*, who demonstrated for polymer matrix microparticles that an increase in drug release rate results from an increase in porosity created in the polymer matrix as well as a reduction in the distance within the matrix a drug must diffuse through [Pinon-Segundo *et al.* 2005]. This may also well be the case here where the drug release rate increased when the drug loading was increased.

Further control of the microparticle characteristics may also result in better control of the release profile, for instance a more constant release over a shorter time. The measured drug release profiles are not indicative of the release of CEL *in vivo* due to the much different conditions. It is believed that the biodegradable property of PLGA may provide increased drug release rates *in vivo* due to the presence of different enzymes and pH environments. The continuous renewal of release medium, *in vivo,* may also provide enhanced dissolution of CEL from the microparticles. Better resemblance to *in vivo*

conditions could be obtained by studying drug release in biorelevant media which contain relevant enzymes and solubilisers.

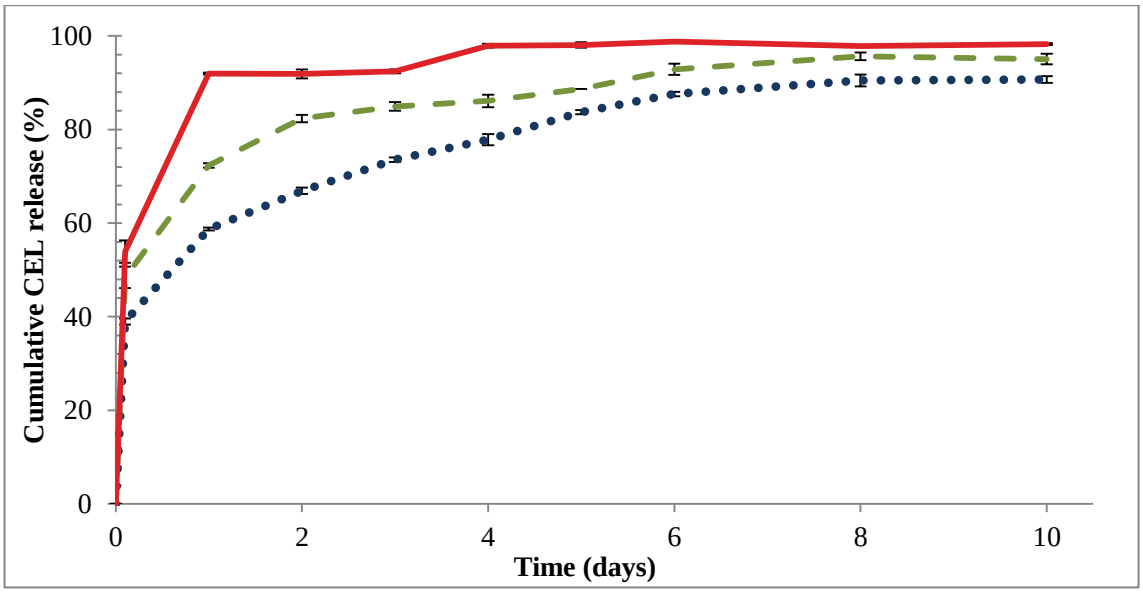

Figure 4.16 Release of CEL from particles with 50% (solid line), 20% (dashed line) and 10% (dotted line) drug loading. Error bars indicate standard deviation from UV measurements.

4.4 Parametric Study – Design and setup

4.4.1 Design of study

As a continuation of section 4.3, the fabrication of microparticles composed of CEL and PLGA were further studied by examining the influence of different formulation and operating conditions on the particle characteristics and drug release behaviour. The influence of four different parameters, flow rate, solute concentration, drug loading and type of solvent were investigated by selecting two or more data points for each parameter. For these studies ACE was again used as one of the solvents for dissolving and atomizing the solutes and acetonitrile (ACN) was used as the second solvent. ACN showed good sprayability, resulting in formation of a stable cone-jet, and is less volatile than ACE as clearly observed in Figure 4.10 with the lower evaporation rate of ACN.

In section 4.2.3 the intrinsic viscosity of PLGA in both ACE and ACN were found and shown in Figure 4.8 and Table 4.4. The intrinsic viscosity gives an indication of the solvent power of the solvent to dissolve the specific polymer and the degree of interaction between the polymer and the solvent. Moreover, the intrinsic viscosity can be used to find the overlap concentration of a polymer:solvent system. The overlap concentration, c*, is given as:

$$c^* = \frac{1}{[\eta]} \qquad \text{(Equation 4.1)}$$

and indicates the transition concentration of polymer in a solvent at which the intermolecular interactions become important and transient networks are formed. In other words, this is the concentration at which the intra and inter-polymer chain entanglements begin to form [Baldursdóttir *et al.* 2003]. From the intrinsic viscosities of PLGA in ACE, 0.276 dL/g, and PLGA in ACN, 0.216 dL/g, the c* of the two systems were found to be 3.62% w/v and 4.63% w/v respectively. These values were considered for designing the experimental setup in order to also investigate the role of polymer chain entanglements in the spraying solutions on the electrospraying process. Three values for solute concentration were thus selected for each solvent system, one near the c* value for the polymer-solvent system, one below the c* value and one above the c* value. Thereby, the influence of c* and polymer conformational state on the particle attributes could be investigated.

The values for drug loading were selected based on earlier observation from section 4.3. For this study a more incremental difference in the drug loading was examined. As for the flow rate, initial observations were made from applying high and low values for the flow rate, to see whether a stable jet could be maintained and if dry particles could be prepared. Based on these observations a suitable range was determined, 10-50 μL/min.

Other important parameters for the electrospraying process such as the applied voltage, current and sample collection distance were not studied in detail but optimized to achieve a stable cone-jet and uniform particles, and otherwise kept constant during the study (see Table 4.5).

Table 4.5 List of microparticle samples prepared.

Sample	Solvent	Solute conc. (%)	Polymer conc. (%)	Drug loading (%)	Flow rate (µL/min)
N1	ACN	7	6.3	10	10
N2	ACN	7	6.3	10	30
N3	ACN	7	6.3	10	50
N4	ACN	7	4.9	30	30
N5	ACN	5	4.5	10	30
N6	ACN	3	2.7	10	30
N7	ACN	3	2.1	30	30
N8	ACN	3	2.7	10	10
N9	ACN	3	2.7	10	50
A1	ACE	7	6.3	10	10
A2	ACE	7	6.3	10	30
A3	ACE	7	6.3	10	50
A4	ACE	7	4.9	30	30
A5	ACE	5	4.5	10	30
A6	ACE	3	2.7	10	30
A7	ACE	3	2.1	30	30
A8	ACE	3	2.7	10	10
A9	ACE	3	2.7	10	50
A10	ACE	7	7.0	0	30

4.5 Parametric Study – Particle characteristics

Particle characteristics were studied by examining the particle morphology, size, porosity and inner structure using methodology described in the experimental section. The results for particles prepared with ACN are presented first and the results for particle prepared with ACE are presented subsequently for each section in order to divide the results for clarity.

4.5.1 Particle morphology

Particle size and morphology were studied using SEM, and representative SEM images of each sample produced are shown in Figure 4.17. Generally, the particles fabricated were spherical and some had visible pores on their surface while others appeared to have a smooth surface. The very small particles observed in some of the images are most likely offspring particles arising from Coulomb fission of the evaporating droplet [López-Jerrera and Gañan-Calvo 2004].

Particles from samples N3, N6 and N7 all appeared to have small pores on their surfaces and particularly those from sample 3 were covered with homogenously distributed pores around 100 nm in size (see Figure 4.17J). In all cases the small surface pores were formed for droplets with a low surface area to volume ratio relative to their polymer concentration, for N3 due to their large volume and for N6 and N7 due to their low polymer concentration. The presence of such small pores on the surface could be explained by a pressure developing inside the particles during particles formation. Assuming that the particle shell was initially formed and was rigid enough to prevent it from collapsing, small pores may have formed to release some of the pressure accumulated inside [Park and Lee 2009].

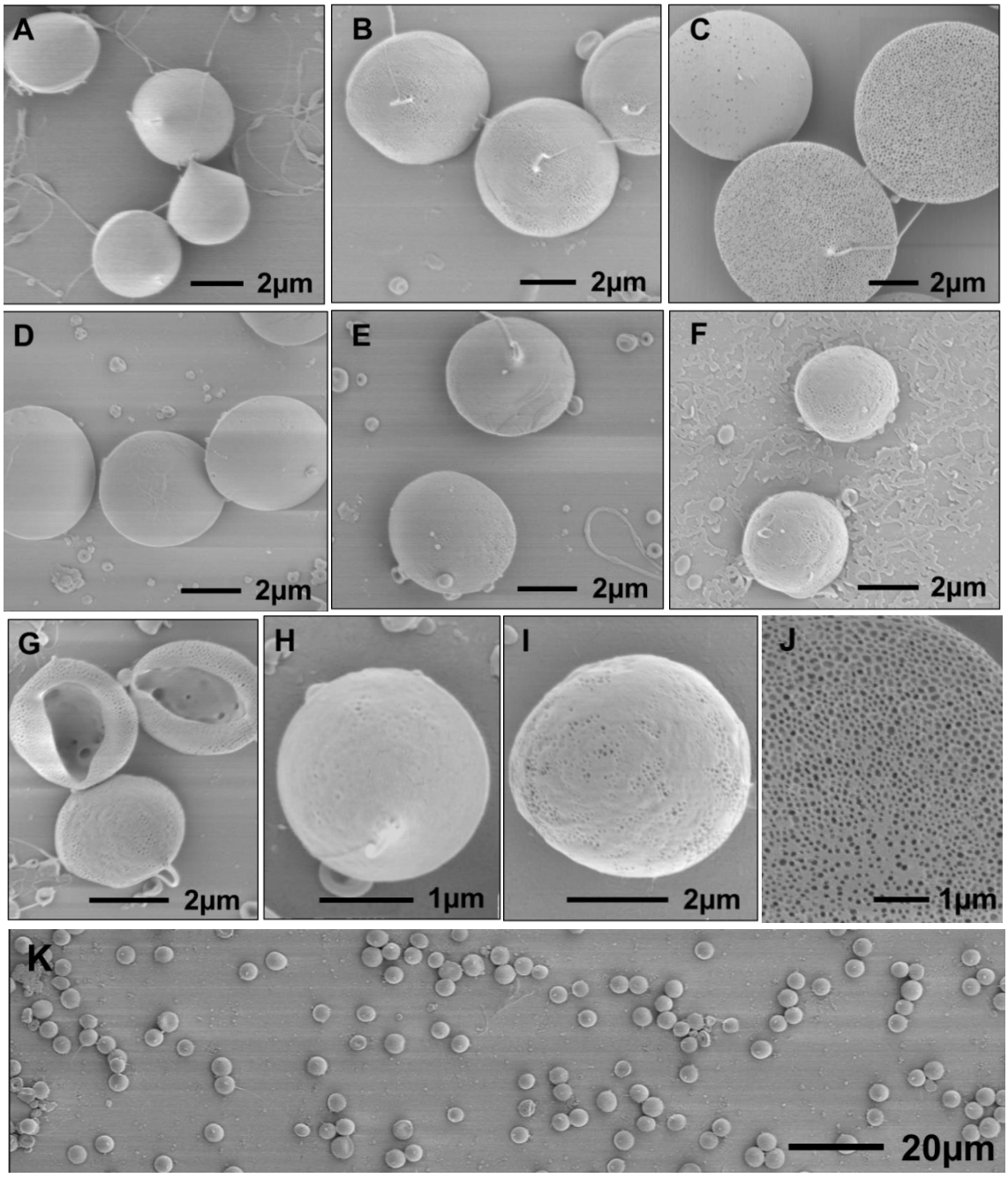

Figure 4.17 Representative SEM images of different microparticle samples prepared in ACN: Samples N1(A), N2(B), N3(C), N4(D), N5(E), N6(F), N7(G), N8(H), N9(I), close-up of sample N3(J) and overview of sample N5(K).

Particles from sample N7 were collapsed with a visible opening on one side, resulting in a cuplike morphology and revealing the inner particle structure. The collapse of these particles is explained by the low polymer concentration in the processed solution (≈

2%). When the polymer concentration is low (relative to the c* of the system) it can result in the particle shell not being strong enough and collapsing due to lack of structural support, during solvent evaporation [Bittner and Kissel 1999].

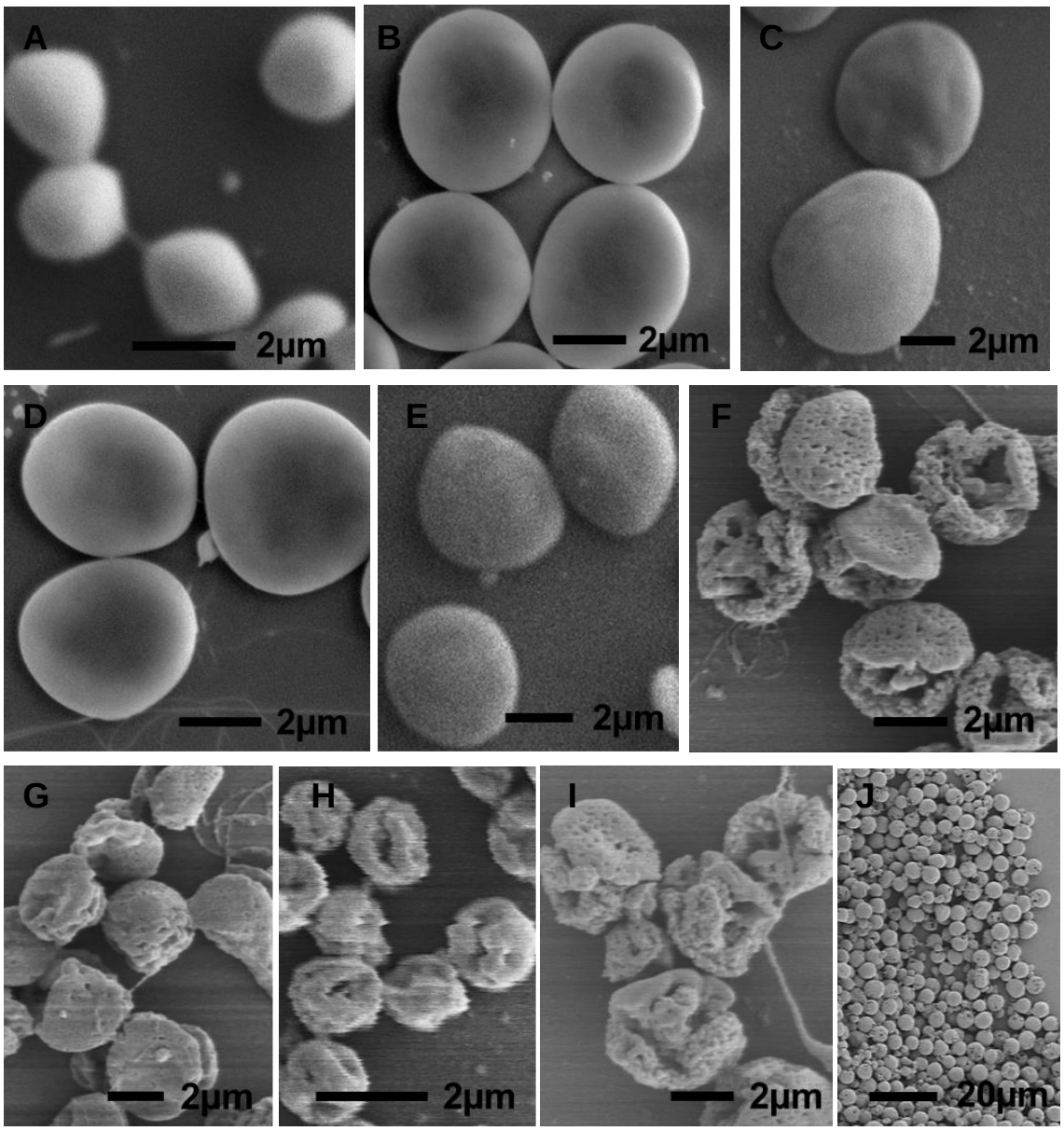

Figure 4.18 Representative SEM images of different microparticle samples prepared in ACE: Samples A1(A), A2(B), A3(C), A4(D), A5(E), A6(F), A7(G), A8(H), A9(I), overview of sample A5(J).

Representative SEM images of microparticle samples prepared with ACE are shown in Figure 4.18. The SEM images show that most of the generated microparticles had a

spherical-like geometry with either smooth or corrugated surfaces. Particles from samples A6-A9, prepared with 3% solute concentration (Figure 4.18 F-I), showed visible pores on their surface as observed with some of the samples prepared with ACN. This observation may be explained by the higher amount of solvent that needs to escape the electrosprayed droplets during solvent evaporation for 3% solute concentration, which could result in channels forming through the particle shell as the solvent escapes. A study by Megelski *et al.* also reported that the presence of humidity during particle formation can result in pores on the particle surface due to condensation of air surrounding the droplet, from the evaporative cooling of the droplet, resulting in water droplets which leave an imprint on the particle surface [Megelski *et al.* 2002, Srinivasarao *et al.* 2001]. A similar event may have taken place in the present study.

Further, while particles from samples 4.18 A-E had smooth surfaces particle from samples 4.18 F-I showed corrugated raisin-like morphology. This type of morphology could have resulted from a collapse of the particles in the late stages of particle formation. Compared with the samples prepared with ACN more samples prepared with ACE have a rough morphology, indicating that at similar solute concentrations particles prepared with ACE are more prone to collapsing. The morphological differences between particles from Figure 4.17 G and 4.18 F-I could indicate that the former collapsed by exploding while the latter collapsed by letting out the remaining solvent from small pores on their surface. A similar event has been described by Farid *et al*. [Farid 2003]. The collapse of particles from sample N7 indicates that the solvent did not fully managing to evaporate before the particles were being collected. The impact of the particle at collection may then have resulted in its collapse due to a thin shell.

In similar studies, using ultrasonic atomization combined with spray drying for preparing drug-loaded microparticles, it was also reported that particle morphology may

depend both on solute concentration and on drug loading. With low solute concentrations it was observed that spherical particles could not form and that particles tended to collapse or shrink to give a "raisin-like" morphology [Bittner and Kissel 1999]. In a study using electrospraying it was observed that particles became more spherical and less concave as the polymer concentration was increased towards the maximum value, at which a stable jet could be achieved [Xue *et al.* 2010]. These findings support the observations made from Figures 4.17 and 4.18, where particles with both raisin-like appearance and collapsed particles were observed at low solute concentrations, whereas higher concentrations gave rise to spherical particles, although not elongated particles.

The particle morphologies observed could be explained by the c* of PLGA in the two solvents. Of the particle samples prepared with ACN, samples N5-N9 had a PLGA concentration below the calculated c* of the system (4.63% w/v) while for samples prepared with ACE, samples A6-A9, had a PLGA concentration below the c* of the system (3.62% w/v). This indicates that polymer entanglement had not yet initiated at the time of atomization. Polymer chain entanglement took longer time for particles from these samples and some of the samples thus may not have managed to become spherical and smooth. The differences in morphology seen between particles from sample N7 and A7 prepared using ACN and ACE, respectively, could be explained by the higher solubility of PLGA in ACE and hence a greater ability to retain the particle shell through polymer diffusion during drying. They may thereby manage to avoid collapsing and instead shrink. Xie *et al* observed in a similar study using electrospraying, that a faster evaporation rate of the droplets resulted in a smoother particle surface [Xie *et al.* 2006b].

Images of particles acquired using AFM (tapping mode) (see Figure 4.19) indicates that the particle surface was not smooth but had small pores (A) for particles prepared with ACN and a dotted pattern (B) for particles prepared using ACE. The morphology observed using AFM could be more representative of the actual surface morphology of the particles since the samples were not sputter coated and because the image depth contrast seems to be better with AFM compared with SEM. The particles were flattened before scanning with AFM, in order to provide a smaller curvature range for the cantilever and for better visualization of the surface morphology.

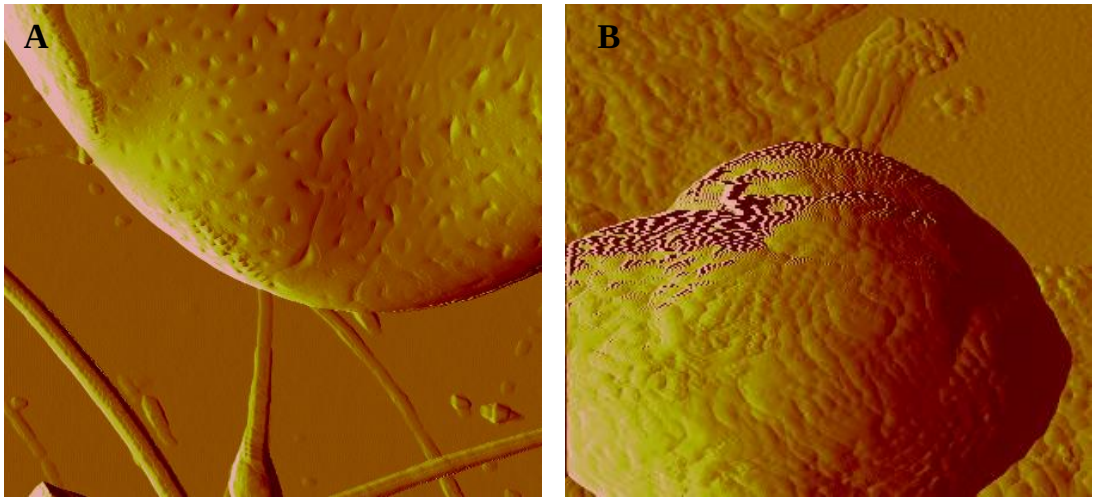

Figure 4.19 Atomic Force Microscopy images of samples N2 (A) and A2 (B).

4.5.2 Particle size

The particles prepared ranged between 2-8 µm in diameter depending on the sample conditions and all samples had a relatively narrow size distribution with a polydispersivity index between 6.0% and 16.1% (see Table 4.6). Figure 4.20 demonstrates that the particle size was dependent on a combination of processing parameters. Flow rate had the greatest influence on particle size with as much as a three-fold increase in size resulting from an increase in flow rate from 10 µl/min to 50 µl/min (see Figure 4.20 A+B). This was the case for 3% and 7% solute concentration

and samples prepared with both ACN and ACE. The results are further consistent with previous studies [Chang *et al.* 2010; Jaworek and Sobczyk 2008] where a similar relationship was observed.

The solute concentration also showed a clear trend with the particle size increasing as the solute concentration was increased (Figure 4.20 C). The solute concentration is proportional to the viscosity of the solution and the results obtained were consistent with similar reports on the influence of viscosity on particle size [Jaworek and Sobczyk 2008; Rohner *et al.* 2004].

Table 4.6 Characteristics of particle samples.

Sample	Yield (%)	Entrapment eff. (%)	Particle size (μm)	Polydispersivity index
N1	85	94 +/- 3	2.5 +/- 0.2	9.3
N2	87	88 +/- 1	4.9 +/- 0.4	8.3
N3	86	92 +/- 2	7.2 +/- 0.9	12.3
N4	93	98 +/- 1	4.1 +/- 0.4	9.9
N5	81	89 +/- 1	4.2 +/- 0.3	6.0
N6	91	99 +/- 1	3.4 +/- 0.3	8.7
N7	85	90 +/- 1	3.0 +/- 0.3	8.3
N8	89	97 +/- 2	2.0 +/- 0.2	7.3
N9	86	95 +/- 1	4.5 +/- 0.4	8.1
A1	90	94 +/- 3	2.6 +/- 0.3	10.8
A2	89	97 +/- 2	5.6 +/- 0.9	16.1
A3	95	101 +/- 2	7.6 +/- 1.0	13.1
A4	92	98 +/- 3	4.4 +/- 0.5	11.4
A5	90	99 +/- 1	4.3 +/- 0.4	9.3
A6	88	93 +/- 3	3.6 +/- 0.4	10.6
A7	92	97 +/- 2	3.3 +/- 0.4	11.8
A8	90	99 +/- 2	1.6 +/- 0.2	9.4
A9	N/A	N/A	N/A	N/A

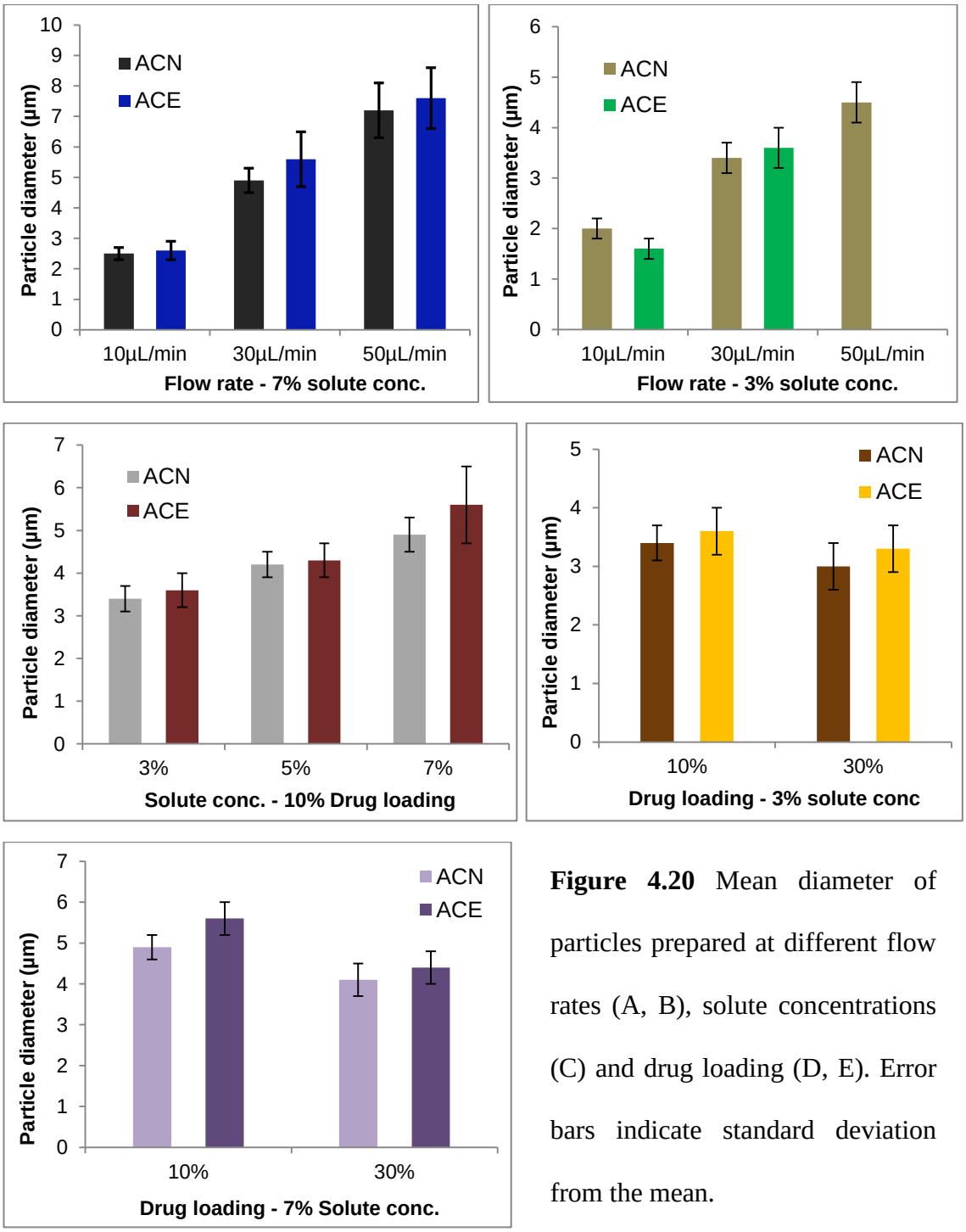

Figure 4.20 Mean diameter of particles prepared at different flow rates (A, B), solute concentrations (C) and drug loading (D, E). Error bars indicate standard deviation from the mean.

Finally, the drug loading also had an influence on the particle size with the particle size decreasing as the drug loading was increased (Figure 4.20 D+E). Moreover, the effect observed was correlated with the solute concentration and a greater effect was seen between samples N2 and N4 (7% solute conc.) than between N6 and N7 (3% solute conc.). The influence of drug loading on particle size can be partly explained by the less

significant contribution of the drug compared with the polymer on the viscosity of the solution. The drug loading is further related to the electrical conductivity of the solution as shown in Table 4.3.

The particle sizes measured were similar for particles prepared using ACE and ACN following the same trends as a function of flow rate, solute conc. and drug loading. Yet, the particles prepared with ACE were slightly larger than those prepared with ACN, for all sample pairs except those prepared with 3% solute conc. and 10 μL/min.

Several studies have demonstrated that an increase in solute concentration and hence viscosity results in larger particles due to the larger diameter of the atomizing jet and the higher polymer density of the droplets formed [Jayasinghe and Edirisinghe 2002]. In the present study good proportionality was demonstrated between the solute concentration and particle size with good control of the particle size in a narrow range. An increase in flow rate had a similar increasing effect on particle size due to the larger droplets formed at high flow rates. In this case, larger droplets were formed with increasing flow rate, but since the droplets are unchanged in concentration, a larger volume of solvent must evaporate per unit surface area for the larger droplets to dry. Again proportionality was shown between the flow rate and particle size with good control of particle size. The drug loading mainly influences polymer concentration and hence solution viscosity but also has a significant effect on the electrical conductivity of the solution as seen in Table 4.3. An increase in the electrical conductivity reduces the particle size by increasing the tendency for the droplets to undergo Coulomb fission [Hartman *et al.* 1999b]. A decrease in particle size was observed in all cases where the drug loading was increased thus supporting the explanation.

The influence of the type of solvent on the particle size appeared to mainly be driven by the differences in electrical conductivity. The electrical conductivity of ACE is the

lower of the two solvents used and would therefore result in the larger particles as was the case in the study. Similar effect of the type of solvent on particle size was observed by Xie *et al*. [Xie *et al.* 2006b]. Further, the viscosities of ACE and ACN were similar and if anything they showed contradictory effects. Also, the lower evaporation rate of ACN (see Figure 4.9) could have resulted in more pronounced droplet shrinking and was further enhanced by the later polymer chain entanglement with ACN (explained from Figure 4.8). This effect of solvent evaporation rate on particle size can only be speculated upon in the work, as information on particle density is necessary to assess whether more porous particles were produced with ACN due to the balance between polymer diffusion and solvent evaporation.

4.5.3 System yield and entrapment efficiency

The collection yield of particles was measured to be between 81 and 95 wt% of the actual solute mass that was electrosprayed (see Table 4.6). Microparticle samples were collected onto electrically grounded sheets of aluminium foil and most of the particles were attracted onto the sheets. Yet due to the wide angle of the atomized jet some of the particles, possibly including small satellite droplets in the peripheries of the jet [Hartman *et al.* 1999a], were lost during flight, dispersed out in the surroundings or attracted onto other nearby surfaces. A part of the spraying solution may have also precipitated out on the outer surface of the nozzle wall during spraying.

The collection yield could possibly be optimized by coating the surface of the nozzle with a non-conductive, hydrophobic material, by shielding all conductive surfaces in the vicinity of the jet and by increasing the area of the collection surface. In an actual manufacturing process the particles would most likely be atomized into a closed-loop chamber, similar to setups used for both laboratory-scale and commercial-scale spray dryers, and loss of material would be limited when producing large batches. Further, by

implementing a continuous manufacturing approach the material loss could be further reduced as the concept of batches would no longer be of same relevance. In this study there was no obvious correlation between the measured yield and the sample preparation conditions. However, the yield values in wt% obtained here are comparable or slightly higher than values reported with other liquid atomization techniques such as spray drying and ultrasonic atomization [Bittner and Kissel 1999, Maa *et al.* 1998, Sollohub and Cal 2010].

The drug entrapment efficiency ranged between 88-101% without any specific correlation between the parametric condition of the samples and the entrapment values observed. Using an Energy-dispersive X-ray spectroscopy (EDX) function built within the SEM apparatus used, the elements present in the particles were measured. This was done to examine whether the CEL molecules were actually entrapped within the particle observed in the SEM images to support the data from the drug entrapment efficiency (see Figure 4.21).

EDX was performed on a single particle by marking the visible surface of the particle (Figure 4.21 A). The measurements indicated the presence of the elements sulphur (S) and fluorine (F), which are elements specific for CEL in this system. The gold (Au) and carbon (C) peaks derive from the gold sputter coating and carbon tape, respectively, both of which are present on the whole sample surface. An EDX measurement was also done in an empty area right beside the particle (Figure 4.21 B) as a negative control and showed that there was no measurable sulphur or fluorine. This suggests that CEL is at least partially present inside or on the surface of the microparticles.

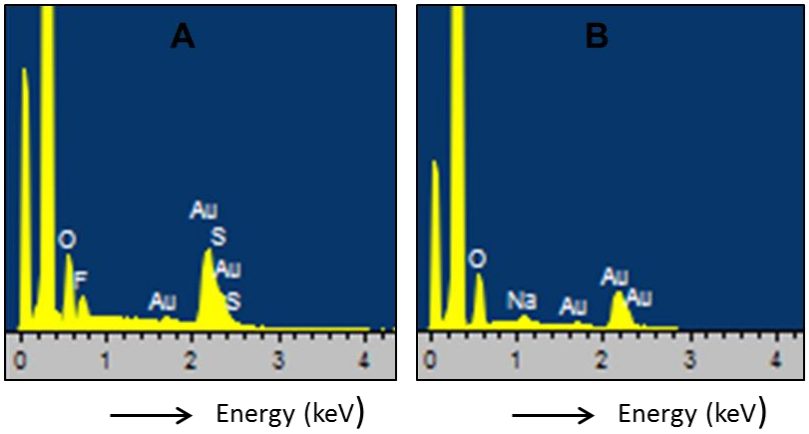

Figure 4.21 EDX spectra of a single CEL-loaded PLGA microparticle (A) and a blank area of same size beside the particle (B). Carbon peaks were cropped due to their height.

4.5.4 Porosity and inner architecture

The porosity and internal structure of the microparticles was studied by making cross sections of the particles using FIB/SEM, and images from selected particle samples are shown in Figure 4.22. The images indicate that it was possible to section the particles using a weak FIB beam while preventing the particle from melting or collapsing. The images in Figure 4.22 A-J were captured using an SEM beam while the images in Figure 4.22 K+L were captured using a FIB beam. The latter are only shown to give an idea of the image resolution with FIB and the sectioning process.

It was not possible to see different phases of CEL or PLGA which would indicate the presence of aggregates, and the images support that CEL molecules are dispersed within the PLGA matrix. Figure 4.22 indicates that all particle samples prepared using ACN (Figure 4.22 A-F) as well as A5 (Figure 4.22 G) had a porous interior while samples A2 and A10 had a solid interior. Sample N6 was the most porous of the four samples prepared using ACN with large holes dominating its interior. Figures 4.22 C-E indicate that the porosity decreased as a function of solute concentration with sample N2 being the least porous. Further, the samples prepared with ACE were generally less porous than those prepared with ACN.

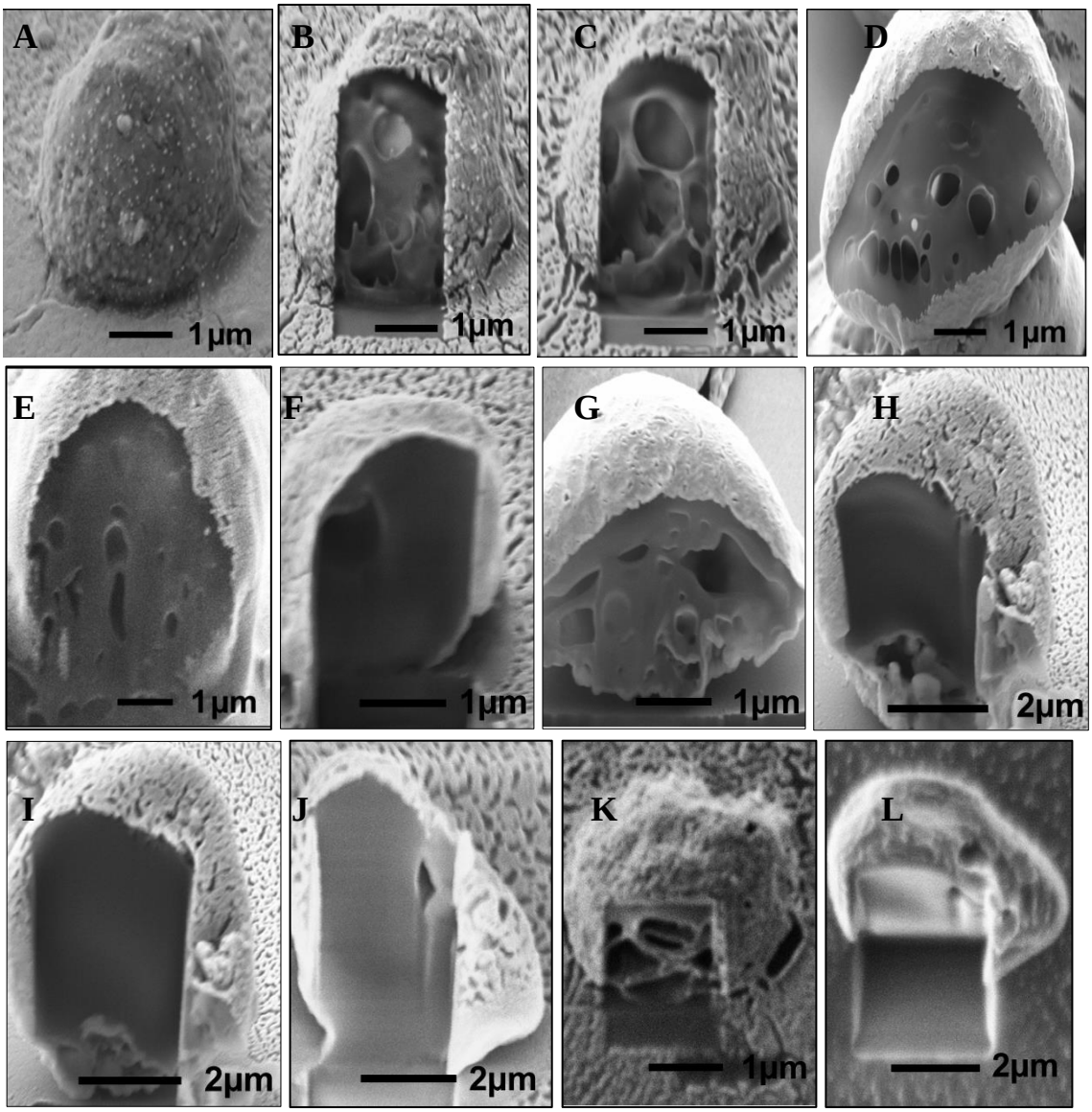

Figure 4.22 FIB/SEM images of microparticles showing the cross-sectional structure of sample N6 before (A) and after (B, C) milling, sample N5 (D), sample N2 (E), sample N1 (F), sample A5 (G) and sample A2 (H, I), sample A10 (J), and FIB beam images of samples N6 (K) and A10 (L).

The formation of pores in the particles could be explained by several mechanisms that influence the formation of particles. During particle formation solvent evaporation takes place at the surface and a shell is typically formed entrapping solvent in the particle core [Yao *et al.* 2008]. As the remaining solvent evaporates across the shell it may leave behind pores and result in visible pores on the surface of particles as was observed. In a

study by Park and Lee it was reported that the solvent used influenced the porosity of the particles prepared with electrospraying, and with volatility solvents resulting in more porous particles than low volatility solvents [Park and Lee 2009].

In this study, ACN had a lower evaporation rate than ACE but the particles prepared using ACN were more porous than those prepared using ACE. Thus the opposite relationship between solvent volatility and particle porosity was observed. The contradicting results could be explained by differences in properties of the solvents used, in addition to evaporation rate, such as the solubility of polymer in the solvent or a combination of different properties.

The lower solvent power and lower evaporation rate of ACN could have led to earlier PLGA precipitation and shell formation, and resulted in larger amount of solvent trapped within the solidifying particles compared with particle formation using ACE. The larger amount of solvent entrapped inside the shell is likely to result in higher pore volume as was observed. A higher degree of porosity was observed for particles prepared at 3% solute conc. compared with particles prepared at 5% and 7% solute conc. This is again explained by the larger volume of solvent that had to escape the particle core and the lower polymer concentration available to maintain the inner particle structure. The drug loading is likely to have had similar but smaller effect on particle porosity by altering the polymer concentration of the solution but was not examined. Flow rate was demonstrated to have the greatest influence on droplet size and hence particle size, with more solvent likely to be entrapped within their large particle shell. Particles prepared at high flow rates are thus believed to be more porous than particles prepared at low flow rates. This is also indicated by the porous surfaces of particles prepared at 50 µl/min (see Figure 4.17 J). However, flow rate is believed to have less influence on porosity at high solute concentration since the polymer

concentration is unchanged and could maintain the internal structure during solvent evaporation.

4.5.5 Solid state form of CEL

The solid state form of CEL within the particles was studied using XRPD and selected diffractograms are shown in Figure 4.23. It was observed from Figures 4.3 and 4.7 that CEL was crystalline both in its pure form and when physically mixed with PLGA, by the characteristic peaks observed.

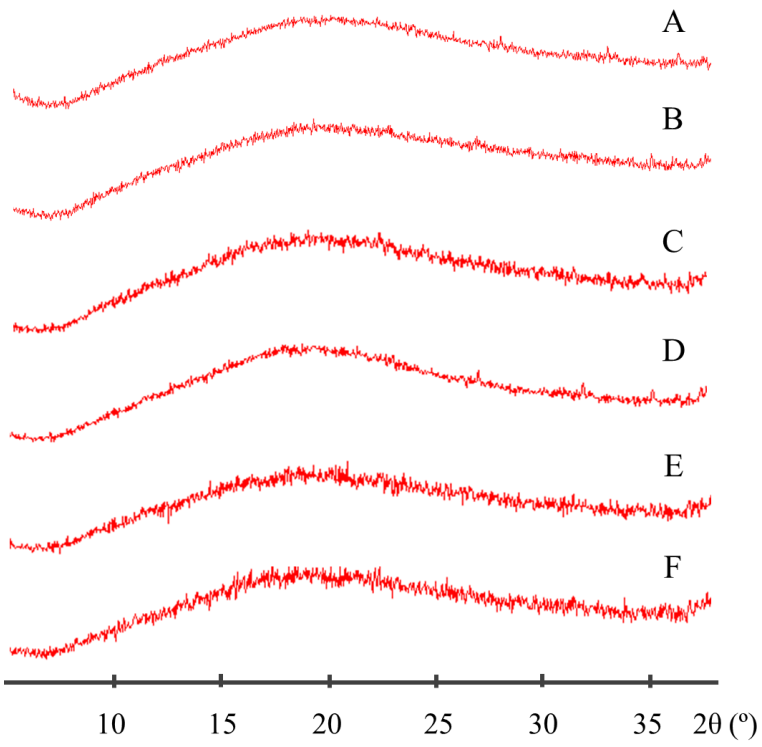

Figure 4.23 XRPD diffractograms of particle samples prepared using electrospraying at different parametric conditions. Samples N1 (A), N2 (B), N4 (C), N5 (D), N6 (E), N7 (F).

4.5.6 Physical stability

Selected CEL-loaded microparticles were stored in a climate chamber at a temperature of 20 ºC and a humidity of 60% at all times after particle preparation to determine the physical stability on the solid dispersions prepared. A well-known disadvantage of solid

dispersions and amorphous drugs is their possible instability under storage [Kaushal *et al.* 2004]. The solid-state stability of the microparticles was therefore studied for a period of 8 months using XRPD analysis to detect possible changes in crystallinity. Figure 4.24 shows XRPD diffractograms of microparticles from sample N2 taken with two months gaps. No visible changes were observed during the 8 months in storage, which indicates good physical stability. To further support these findings, SEM images of samples were taken after 8 months of storage and it was observed that the particles still maintained their shape and size, indicating no crystalline growth or agglomeration.

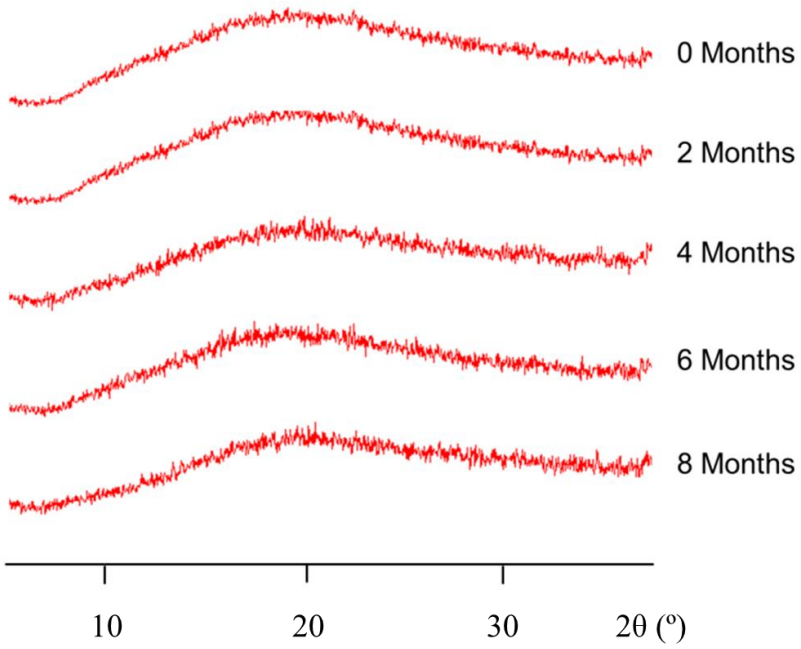

Figure 4.24 XRPD diffractograms of microparticles taken during 8 months of storage.

4.6 Parametric Study – Drug release

4.6.1 Solubility measurements

In this study the drug release was studied using a paddle dissolution apparatus described in section 3.12.2. Initially, the solubility of CEL in phosphate buffer added Sodium Lauryl Sulphate (SLS) was determined in order to ensure sink conditions.

1.2 mg CEL was added to 100 mL of Phosphate buffer with and without SLS and stirred for 3 hours at slightly elevated temperatures, and subsequently the amount of CEL dissolved was measured using HPLC. The maximum concentration of CEL used in the release studies was 6 mg in 500 mL of release medium and thus 1.2 mg CEL was added to 100 mL medium. The percentage of CEL dissolved in phosphate buffer with different SLS concentrations is shown in Table 4.7 and indicates that 0.3% SLS is required to fully dissolve the given concentration of CEL. In the subsequent drug release studies phosphate buffer with 1.5% SLS was used to ensure sink conditions for all samples.

Table 4.7 Solubility of CEL in phosphate buffer containing different conc. of SLS.

Drug release medium	**% CEL dissolved**
H_2O	4.8
Phosphate buffer + 0% SLS	3.2
Phosphate buffer + 0.05 %wt. SLS	13.9
Phosphate buffer + 0.1 %wt. SLS	66.6
Phosphate buffer + 0.2 %wt. SLS	72.2
Phosphate buffer + 0.3 %wt. SLS	103.7
Phosphate buffer + 0.4 %wt. SLS	104.3
Phosphate buffer + 0.8 %wt. SLS	104.8
Phosphate buffer + 1.5 %wt. SLS	102.2

Further, drug release studies performed for electrosprayed microparticles in release media consisting of phosphate buffer with and without SLS showed that the addition of SLS had a significant influence on the amount of CEL released from the particles (see Figure 4.25).

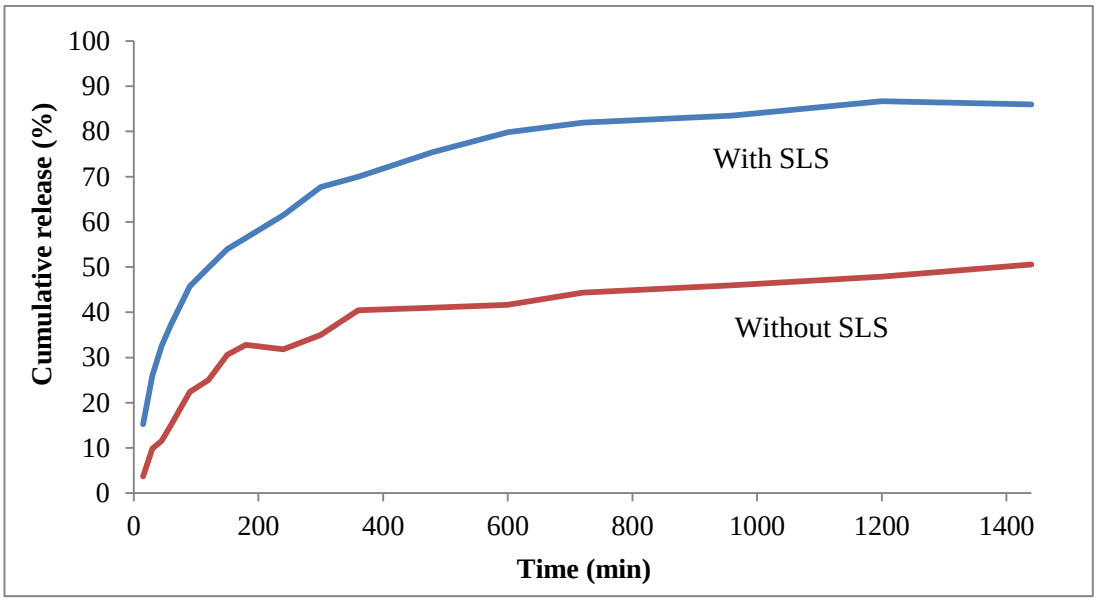

Figure 4.25 Drug release profile of microparticles prepared with 5% solute concentrations, with 20% drug loading using ACE, measured over 24 hours in release medium with and without SLS.

4.6.2 Drug release profiles

CEL release profiles from the microparticles are shown in Figures 4.26-4.30. Drug release from the microparticles took place at a time-varying rate, with an initial burst release followed by a diffusion driven release. The burst release in the first 15 min was between 5 and 50% of the cumulative release, depending on the particle sample. All microparticle samples released between 84 and 98% of their drug content within 20 hours of exposure to the dissolution medium under sink conditions. Figure 4.26 shows that pure CEL dissolved almost instantaneously and stayed dissolved in the dissolution medium. Many of the samples did not reach above 90% release during the 24 hours of measurement, indicating that there was still drug entrapped within the polymer matrix. Degradation of PLGA typically does not take place within this time span and this could explain the residual drug trapped within the polymer network [Klose *et al.* 2008].

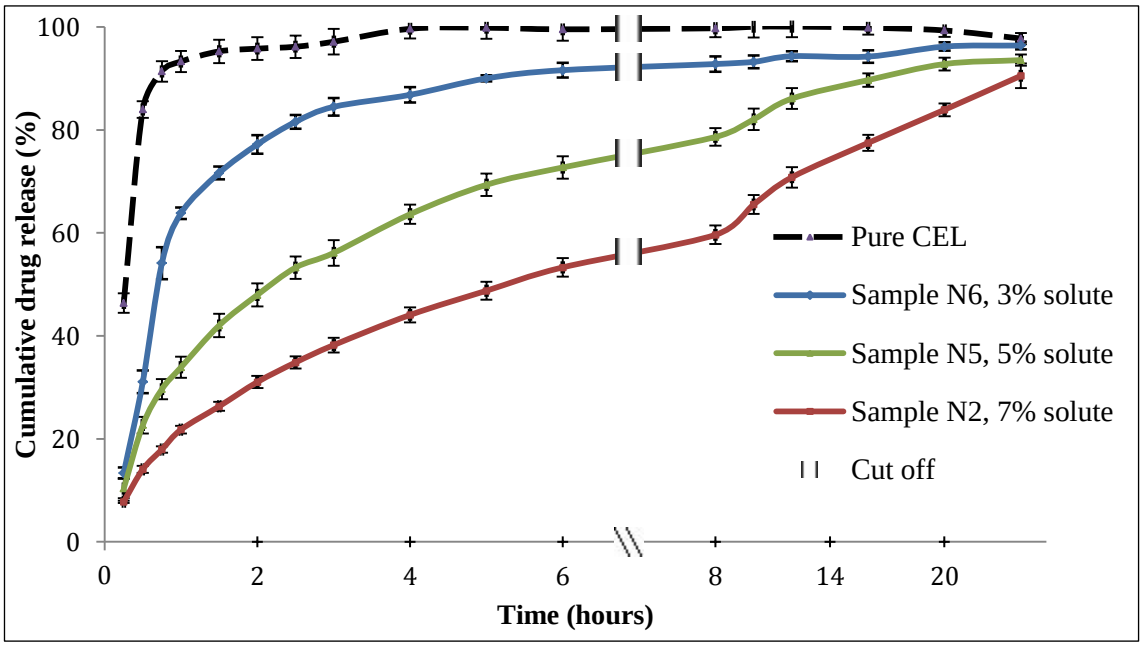

Figure 4.26 Drug release profile of microparticles prepared with different solute concentrations, with 10% drug loading and at a flow rate of 30 µl/min, measured over 24 hours. Error bars indicate standard deviation.

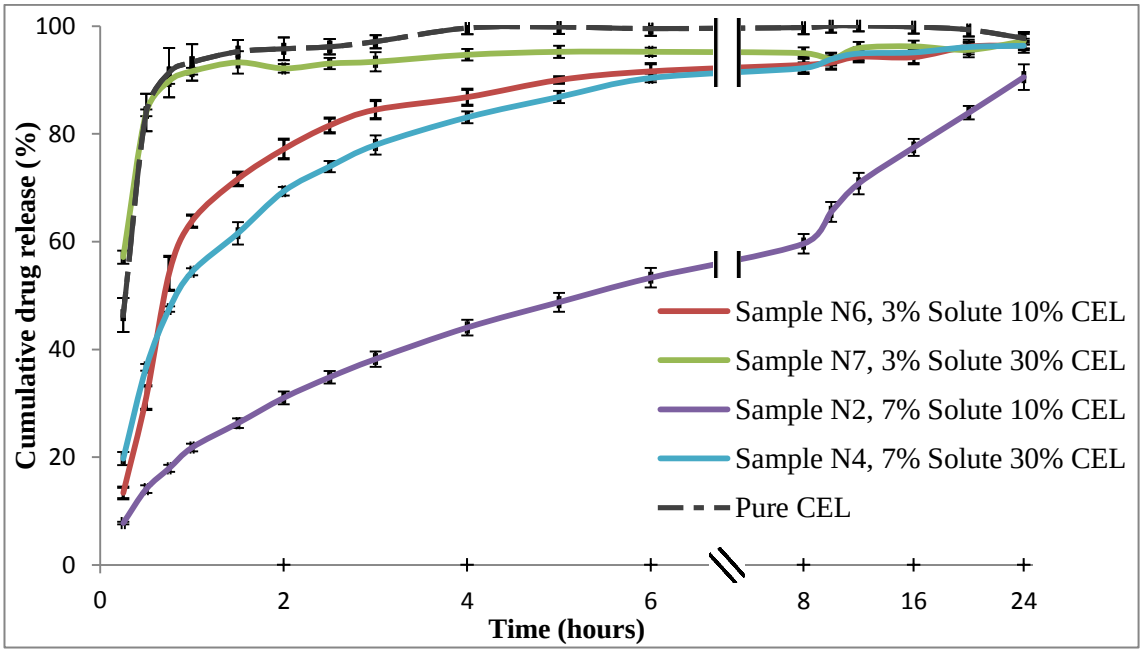

Figure 4.27 Drug release profile of microparticles prepared with different drug loading at a flow rate of 30 µL/min, measured over 24 hours.

It was observed that the drug release rates increased as the solute concentration was reduced, both for ACE and ACN (see Figure 4.26 and 4.30), and samples A2 and N2 with the highest solute concentration had the release curve closest to a linear curve. The drug release curves of samples prepared with different drug loading (see Figure 4.27) showed that an increase in drug loading resulted in a significant increase in drug release rates, both for 3% and 7% solute concentration. Comparison of drug release from particles prepared at different flow rates (see Figure 4.28) did not show a clear trend. Samples A1 and A3 both release their drug quicker than sample A2.

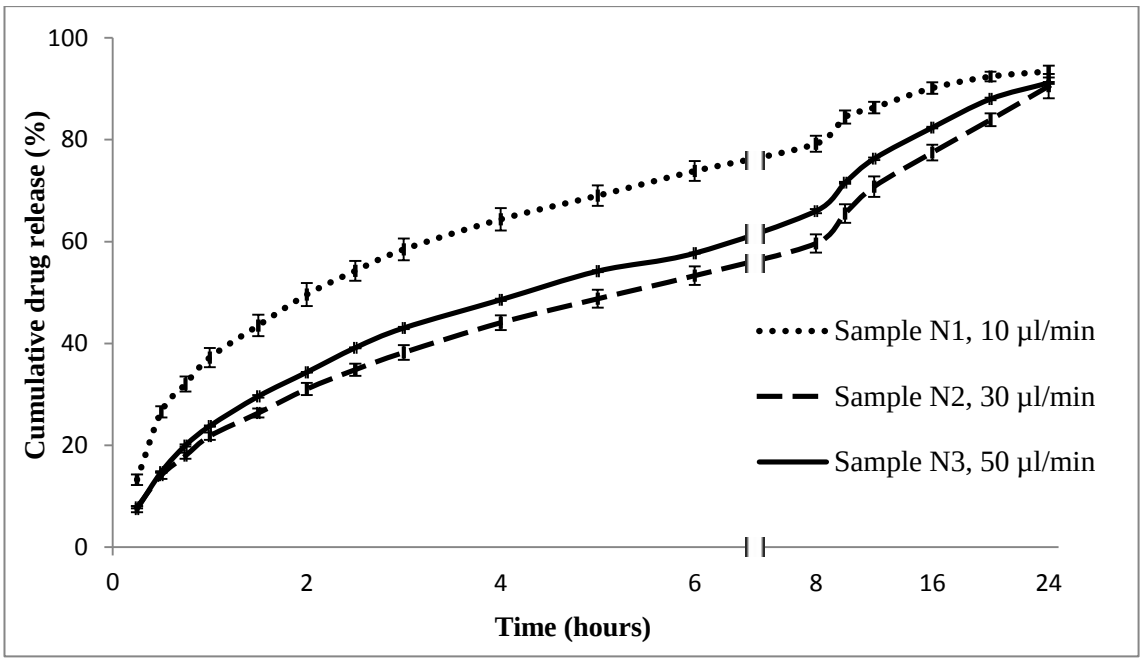

Figure 4.28 Drug release profile of microparticles prepared with ACN and with 7% solute concentration and 10% CEL at different flow rates measured over 24 hours.

Figures 4.26-4.28 indicate that solute concentration, drug loading and flow rate all had an influence on the measured drug release profiles. Translating to the observed particle properties particle size, morphology, porosity and drug density all influenced the drug release from the particle. A reduction in particle size resulted in an increase in the drug release rate. This can be explained by the increase in the surface area to volume ratio of

the particles as the size was reduced, resulting in an increase in the dissolution rate according to the Noyes-Whitney equation, and therefore not surprising. Although the flow rate had the greatest influence on particle size the correlation between surface area and release rate was not clear in Figure 4.28. This could be due to a high degree of surface porosity in the particles from sample N3.

The degree of porosity observed from the cross section images (Figure 4.22) was inversely proportional to the size of the particles (Figure 4.20) and also seemed to influence the release rate. Drug release rate increased with increasing porosity which is partly explained by the differences in particle size but can also be due to an increase in the surface area to volume ratio as a result of porosity. Access of release medium through pores into the core of the particles would most likely result in an increase in drug release rate. However, it is difficult to distinguish between the effect of particle size and porosity on the release rate based on the data from this study.

The influence of drug loading on drug release is consistent with observations from other studies [Berkland *et al.* 2002; Pinon-Segundo *et al.* 2005] and could have two explanations:

1) that the increase in drug density reduces the relative amount of polymer matrix acting as a diffusional barrier.
2) that a partial phase separation occurs between the drug and polymer molecules resulting in increased release rate due to pores created by the drug phase.

Both of these explanations may account for the increased release rate observed.

Comparisons of drug release from samples prepared using ACE and ACN (Figure 4.31 and 4.32) show that particles prepared with ACN release slightly quicker than those prepared in ACE in most cases, except for samples A2 and N2 where A2 released

quicker. Moreover, a large difference is observed between the release rates of A4 and N4. The higher release rates from particles prepare with ACN could be explained by the smaller particles produced with ACN which thereby release their drug load quicker. Further, particles prepared using ACN were slightly more porous on their surface (Figure 4.18). Also, inside the particles cross section images for instance showed porosity for sample N2 whereas the particle from sample A2 was solid (Figure 4.23) explained by less polymer entanglement and slower drying with ACN. Even a modest presence of pores is believed to have a visible effect on the drug release rate from the particles given the larger surface area they result in. Particles that were collapsed (Figure 4.18 and 4.19) exposed more surface area and are therefore also expected to have quicker release. Finally, the more extended and interactive polymer conformation of PLGA in ACE could mean that can incorporate more drug molecules within its matrix compared with PLGA in ACN.

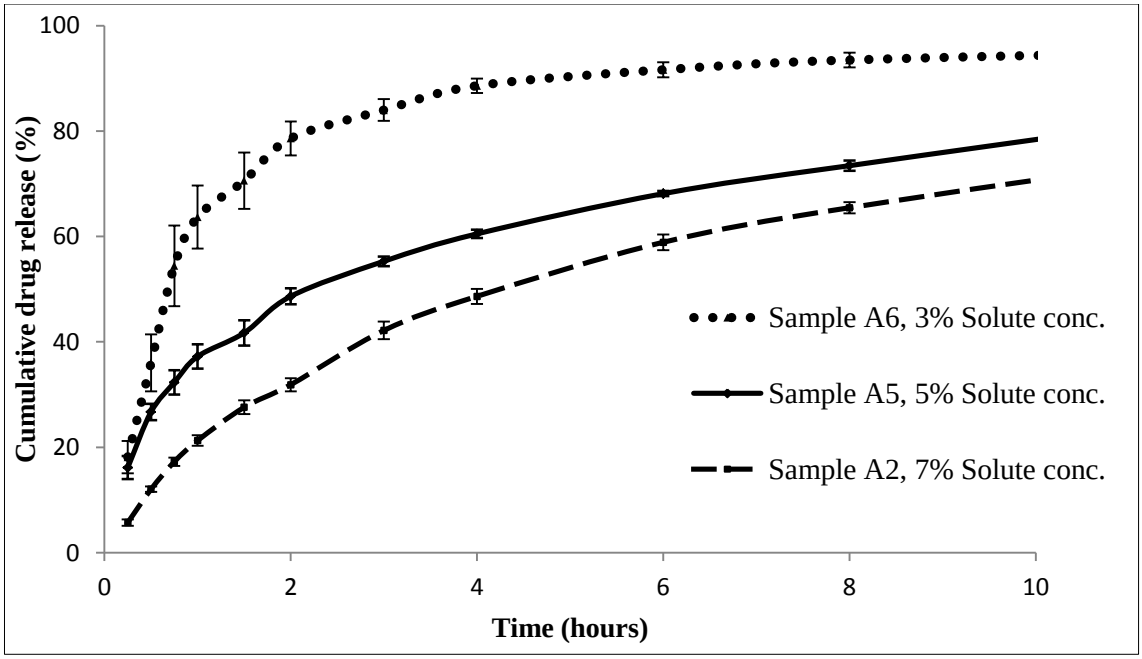

Figure 4.29 Drug release profile of microparticles prepared with ACE at different solute conc. at a flow rate of 30 µL/min and 10% CEL.

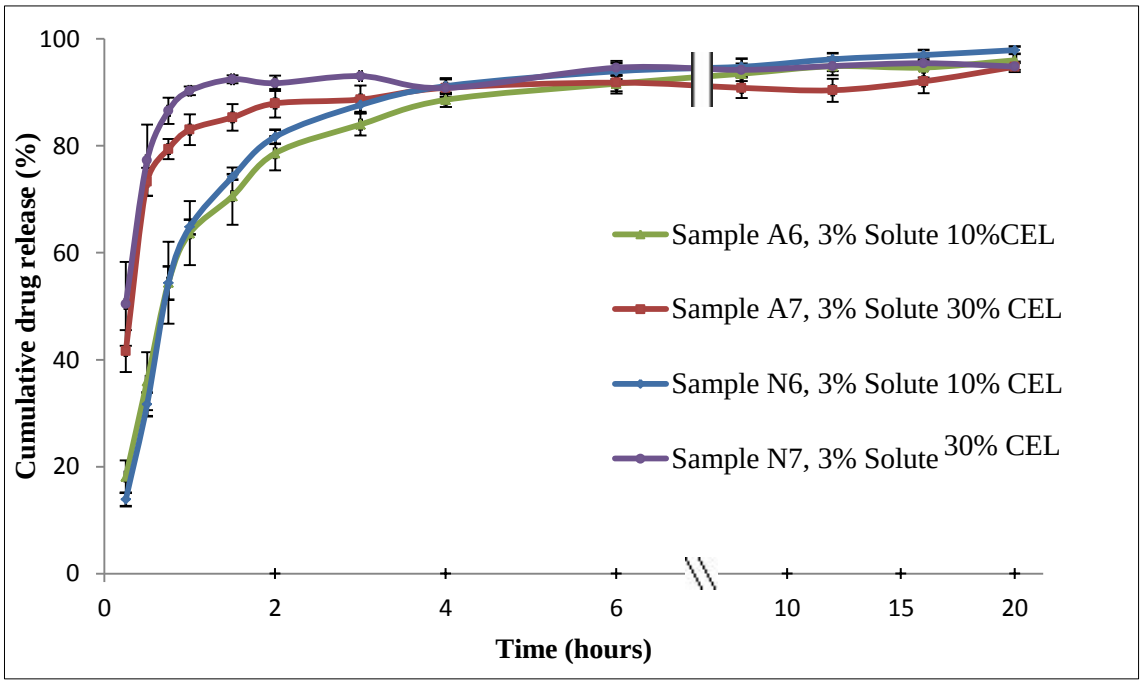

Figure 4.30 Drug release profile of microparticles prepared with ACN or ACE at 3% solute conc. and 10% or 30% CEL measured over 20 hours.

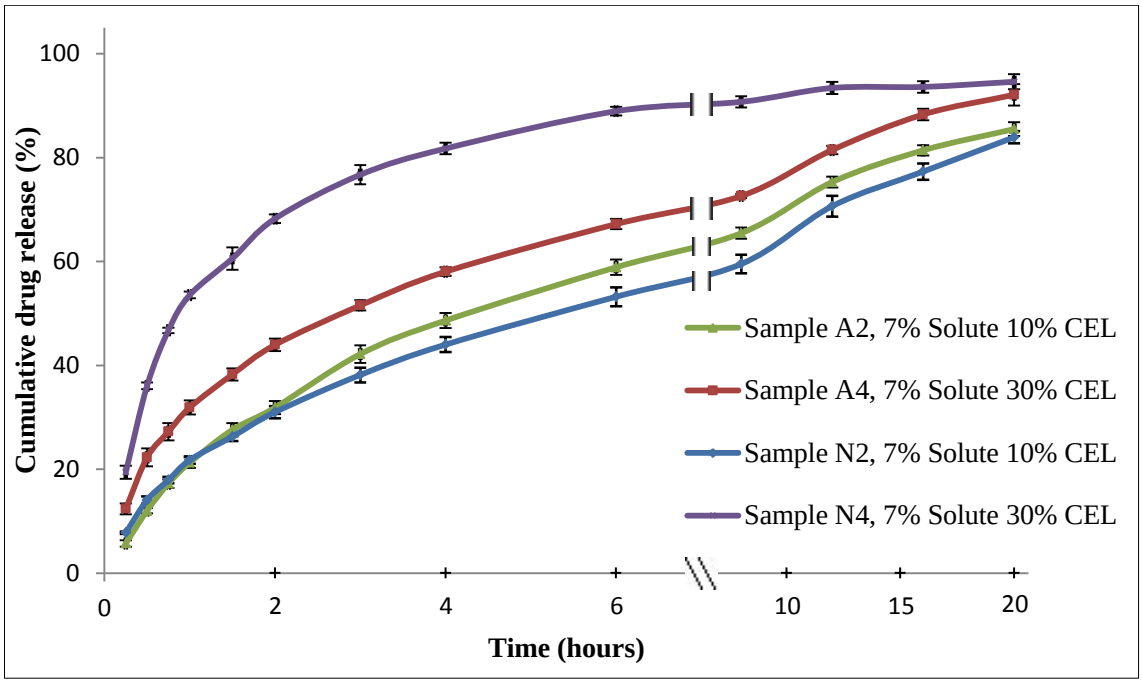

Figure 4.31 Drug release profile of microparticles prepared with ACN or ACE at 3% solute concentration and 10% or 30% CEL measured over 20 hours.

4.6.3 Drug release models

Curve fitting

Drug release from the electrosprayed microparticles mainly took place via diffusion mediated release and this was demonstrated by fitting the selected release curves with the Higuchi model. In the Higuchi model, release of drug is based under the assumptions that the drug molecules are dispersed within a solid matrix and are released through diffusion from the surface, mediated by the surrounding solvent. According to the Higuchi model, drug is released linearly as a function of the square root of time [Higuchi 1963]. Figure 4.32 shows drug release curves of microparticles prepared with ACN at 7% solute concentration and 10% CEL loading as a function of the square root of time. All three curves were fitted with linear regression in the first 6 hours of release and gave the R^2 values 0.976, 0.995 and 0.998 and dissolution constants 27, 22 and 24 % release / $s^{1/2}$ for samples N1, N2 and N3, respectively.

It is observed that the curves all follow their trend line very well with only minor deviation in the first 6 hours of drug release as seen in the figure. After the first 6 hours, drug release decelerates and begins deviating from the model in the remaining 18 hours. The good accuracy of the curve fitting indicates that the Higuchi model fits well for a major part of the drug release data points and thus indicates that the drug release from the electrosprayed particle samples is controlled by diffusion driven release. However, the Higuchi model did not apply well on the drug release from microparticles prepared with less than 5% solute concentration as well as samples with a drug loading of 30%. The fitted release curves for these samples are therefore not shown here. It is believed that the model did not fit on these samples due to their higher degree of porosity inside the particles and because of the lower diffusion barrier provided by PLGA with increasing drug loading (the latter is mentioned in section 4.3.5).

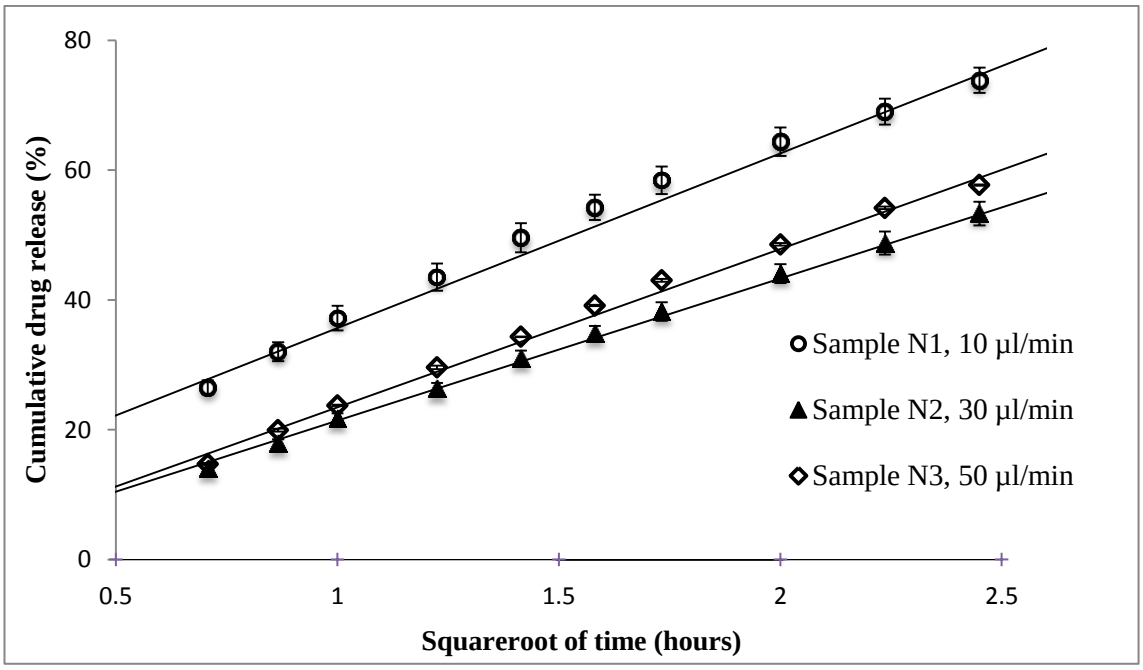

Figure 4.32 Selected drug release curves fitted to the Higuchi model.

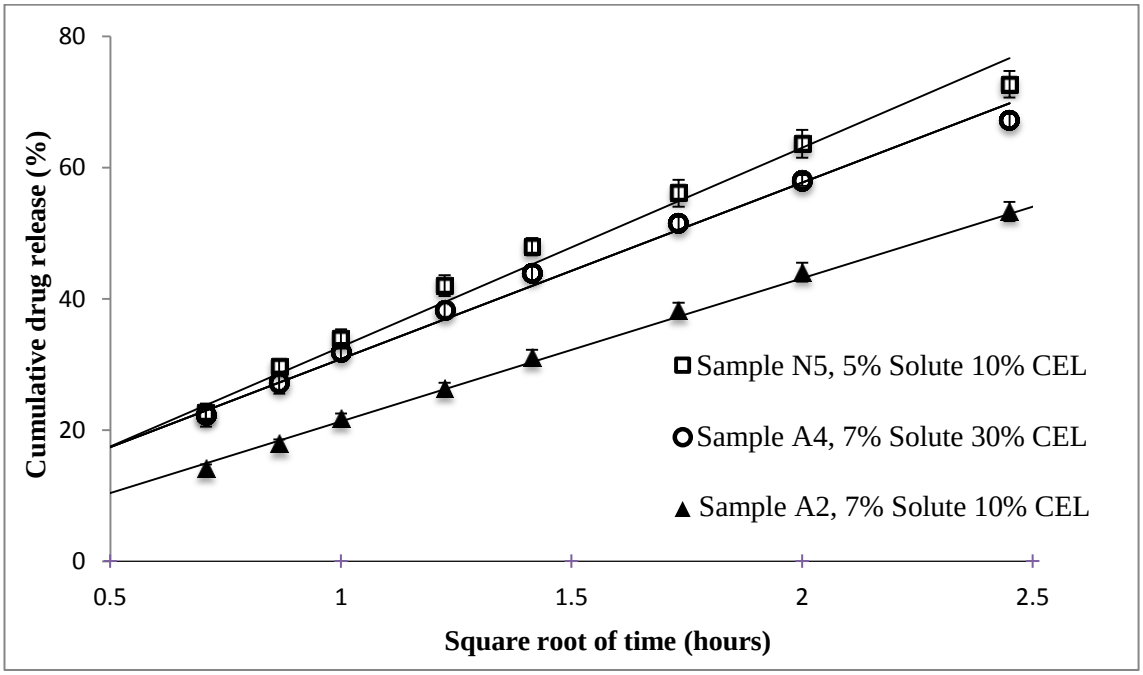

Figure 4.33 Selected drug release curves fitted to the Higuchi model.

Drug release from selected samples prepared with ACE and ACN are shown in Figure 4.33 as a function of the square root of time. The three curves shown were again fitted with linear regression in the first 6 hours of release and gave the R^2 values 0.984, 0.992

and 0.995 for samples N5, A4 and A2, respectively. It is again observed that the curves follow their trend line very well with only minor deviation in the first 6 hours of drug release indicating good fitting with the Higuchi model. Thus, the drug release from these particles samples can be said to take place by diffusion mediated release, at least in the first 6 hours of release.

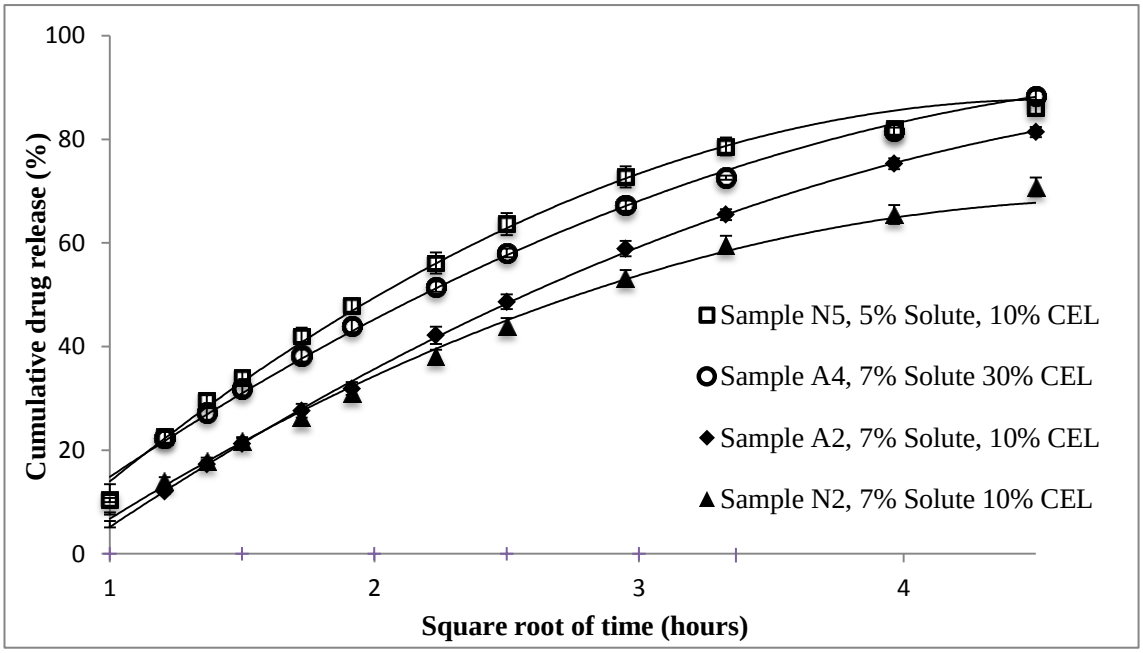

Figure 4.34 Selected drug release curves fitted to the modified Higuchi model.

Figure 4.34 shows selected drug release curves fitted with a modified version of the Higuchi model as a function of the square root of time. Here the curves were fitted with a level 2 polynomial regression instead of a linear regression and gave the R^2- values 0.997, 0.998, 0.999, 0.995 for the samples N5, A4, A2 and N2, respectively. All of the curves fitted very well with their trend line for a period of 20 hours. Although the linear regression on Figure 4.32 gave lower R^2 values than the polynomial regression these curves only followed the trend lines in the first six hours of drug release. In comparison, with the polynomial regression the curves followed the trend lines for the whole 20 hours, indicating a better fit of the polynomial regression. Again, the modified Higuchi

diffusion model was not compatible with the release profile of some particle samples as they released their drug load at a quicker rate.

Curve fitting of selected drug release curves for samples with low release rates (see Figures 4.32-4.34) supports the hypothesis of a diffusion driven release mechanism according to the Higuchi release model [Higuchi 1963]. However, the Higuchi model was modified by using a level 2 polynomial regression due to improved correlation over a straight line. The drug release rate from the CEL-loaded PLGA particles was observed to fall off with time (after 6 hours of release) compared with a conventional linear Higuchi model. This could be explained by an inhomogeneous radial distribution of CEL in the particles, a reduced diffusion rate due to the distance travelled or a lack of sink condition. Also, samples with quicker release rates did not fit well with the Higuchi model, indicating either high porosity in the particles, an uneven drug distribution towards the surface of the particles or clustering of drug molecules due to lack of interaction with the polymer chains.

Other researchers have reported similar trends in the release profile with an initial burst followed by a diffusion-mediated release [Mu and Feng 2001, Wang and Wang 2002, Xu and Hanna 2006] from drug-loaded, biodegradable microparticles prepared with electrospraying and other particle preparation techniques. In many of these studies drug release took place over longer time, from several days to weeks, including partial release through erosion of the polymer, although the particles were of similar size. The quicker release observed in this study could be explained partly from the porosity of the particles, the sink conditions provided in the present study and the relatively small size of the drug (Mw=381.38 g/mol), which has been shown to increase drug mobility and enable quicker release [Freiberg and Zhu 2004, Huang and Brazel 2001, Klose *et al.* 2006].

4.7 Particle elongation

It has been shown in several studies that the shape of particles has an influence on the mechanisms of drug delivery as well as on the interactions with cells. It affects the drug release kinetics from the particles and can be tailored to obtain controlled release profiles [Abebe 2002, Klose *et al.* 2008]. A large surface to volume ratio of the particles results in both quicker release as well as better attachment to cells for targeting purposes [Fugh-Berman 2000]. Also, it has been demonstrated that the vascular clearance rate of particles by phagocytes is dependent on the geometry of the particles, with elongated particles being phagocytised much slower than spherical particles [Champion and Mitragotri 2006].

With electrospraying it is known that spraying of high viscosity solutions may result in fibre-like appearance of the resulting particles, typically with thin fibres connecting individual particles, like beads on a string [Shenoy *et al.* 2005b]. Also, in section 2.4.5 it was mentioned that droplets produced with electrospraying undergo Coulomb fission due to accumulation of charge on the droplet surface as the droplet shrinks from solvent evaporation. Further, it was predicted by Rayleigh that at a threshold, known as the Rayleigh limit, Coulomb instabilities would result in a temporary elongation of the droplet and emission of thin jets from the droplets [Rayleigh 1882]. This was experimentally confirmed by Duft *et al.* who captured microscopy images of the elongation and jet emission of a droplet using single droplet levitation (see Figure 4.35) [Duft *et al.* 2003]. It was observed that droplet became more and more elongated until it emitted lateral jets, and then gradually returned to its spherical shape. Also, Li *et al.* have demonstrated that elongated particles can be produced by solidifying droplets during Coulomb instability using a sol-gel reaction (see Figure 4.36). This indicates that if solidified at the right moment, particles of different geometry can be formed with the

electrospraying process. However, the mechanism is believed to be very difficult to control given the short intervals noted in Figure 4.35.

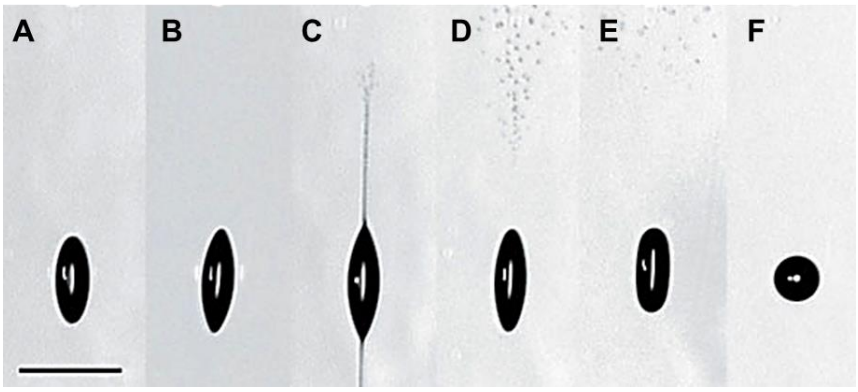

Figure 4.35 A droplet (radius, 24 µm) during Coulomb instability elongates and fires lateral jets and returns to its original spherical shape. Images taken at time (in µs) 140 (A), 150 (B), 155 (C), 160 (D), 180 (E) and 210 (F) [Duft *et al.* 2003].

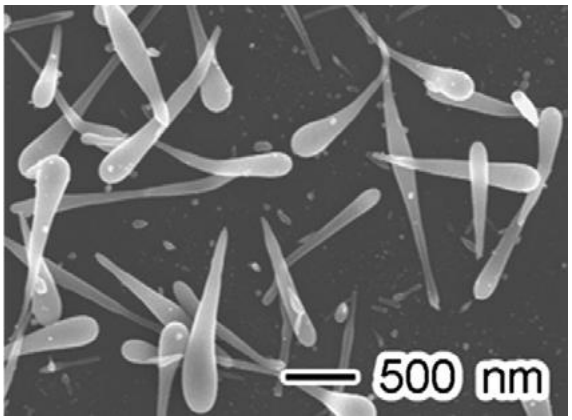

Figure 4.36 Elongated particles produced from Titanium oxides using sol-gel reaction to capture shape during Coulomb instability [Adams and Brantner 2010].

In the present study CEL/PLGA solution were electrosprayed at high solute concentration (> 10% w/v) to study the effect on particle shape. Particles were prepared using 10% and 11% solute concentration, with 20% drug loading and sprayed at a flow rate of 25 µL/min. A different PLGA product (from Purac) was used for this study, with a lower molecular weight, than the PLGA (from Evonik) used in the previous studies (see section 3.1.1). A stable cone-jet was obtained and particle samples were collected

on glass slides for the two samples. SEM images of the particle samples collected indicated mainly two types of particle shapes, tadpole-shaped particles (Figure 4.37 A, B) in samples prepared at 10% solute concentration and elongated, rod-shaped particles (Figure 4.37 C, D, E) in samples prepared at 11% solute concentration. Although some elongated particles were observed at 10% solute concentration and some tadpole-shaped particles were observed at 11% solute concentration the particle samples were surprisingly homogeneous. The results observed could be explained by the Coulombic elongation phenomenon described earlier in this section. The particles may have solidified during the droplet elongation phase, by chance, due to the high solute concentrations used. Yet the results have been reproduced several times demonstrating that such structures can be produced and perhaps controlled.

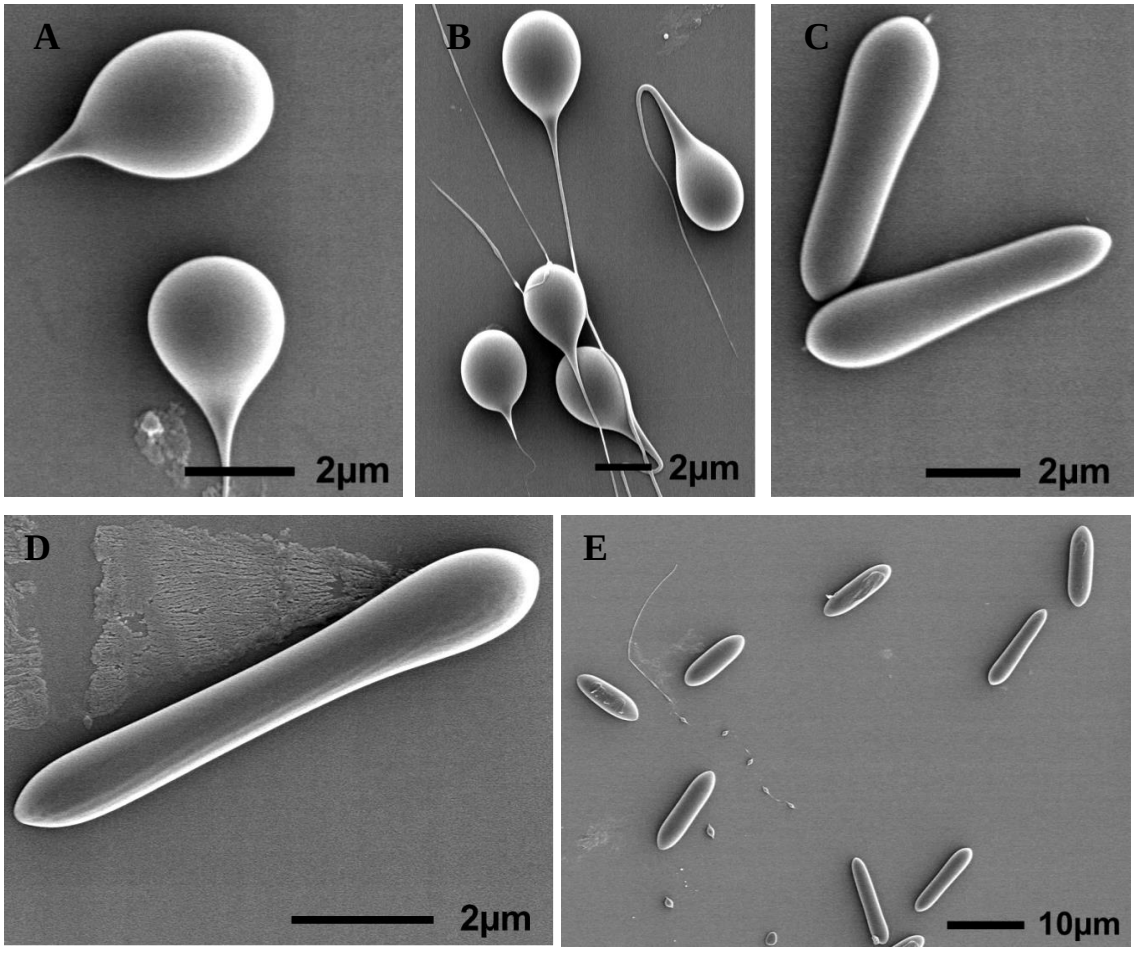

Figure 4.37 SEM images of particles prepared at 9% solute concentration (A, B) and particles prepared at 10% solute concentration (C, D, E).

4.8 Summary

PLGA microparticles containing CEL, a low solubility drug, were prepared using electrospraying with the objective of producing near-monodisperse microparticles with the drug in an amorphous form. It was found that near-monodisperse CEL-loaded PLGA microparticles could be produced at different polymer:drug ratios. Thermal analysis and XRPD measurements further indicated that CEL was present in an amorphous form inside the microparticles. Drug release studies showed diffusion driven release with an initial burst release and indicated drug release kinetics dependent on particle characteristics.

Parametric studies on particle characteristics demonstrated that electrospraying is a precise and controllable technique for producing drug-loaded microparticles with pharmaceutically useful physicochemical properties. The size and morphology of CEL-loaded, electrosprayed PLGA microparticles particles could be controlled by adjusting the flow rate, solute concentration and drug loading, with flow rate having the greatest influence. The porous inner structure of the particles was explained by an early shell formation and subsequent evaporation of ACN during particle formation. Particle porosity was dependent on solvent concentration but remains to be investigated in detail. Although, CEL was presumably in an amorphous state, XRPD analysis demonstrated that the CEL dispersion in the PLGA particles were physically stable for more than 8 months.

The release of CEL from the particles could be controlled to provide a rapid release over a few hours or a sustained release over 24 hours. Particle size, porosity and drug loading had the greatest influence on the release rate and some of the release profiles could be fitted to the Higuchi diffusion release model. Particles prepared at 5 or 7% solute concentration with a drug loading of 10% and at a flow rate of 10 or 30 µl/min

thus seem the most suitable of the samples from this study and depending on the desired release rate these parameters can be chosen accordingly. Careful control of the drug distribution within particles would greatly impact the drug release mechanism, possibly resulting in more useful extended release behaviour with improved bioavailability and therapeutic efficacy.

Chapter 5

Electrospraying of solid dispersions: The influence of mixed solvent systems on particle formation, particle characteristics and controlled drug release

This chapter describes the further investigation of electrospraying for preparing solid dispersion microparticles using the poorly soluble drug Celecoxib (CEL) as a model drug. Microparticles from poly(lactic-co-glycolic acid) (PLGA) as well as hypromellose acetyl succinate (HPMCAS) containing CEL were prepared with the objective of producing microparticles with controlled particle characteristics and drug release profile. Particles were prepared with solvent mixtures at different ratios to investigate the influence of solvent composition on the resulting particle morphology, porosity, drug distribution and drug release profile as well as the particle formation process. For CEL-loaded PLGA particles it was found that microparticles were highly influenced by the presence of an anti-solvent, methanol, to PLGA, and the particle size, morphology, drug distribution and drug release changed gradually with increasing amounts of anti-solvent. CEL-loaded HPMCAS particles were also influenced by variations in the solvent composition, especially with respect to their particle morphology. However the drug distribution in the HPMCAS microparticles and their drug release profiles did not seem to be greatly influenced, compared with the PLGA particles.

5.1 Mixed solvent study – Characterization of solvents and solutions

As a continuation of the parametric study described in sections 4.4-4.6 the same model polymer, PLGA, and drug molecule, Celecoxib, were used to study particle formation

and performance with the focus shifted towards the solvent compositions used in preparation of the particles. The study was performed with a specific interest in studying the resulting particle morphology, the distribution of drug within the particles and the drug release profile.

5.1.1 Selection of solvents

The solvents and solutions for particle preparation were again selected based on some conditions that allow consistent preparation of near-monodisperse particles and differentiation in particle attributes and performance. For this study a binary solvent system was used with the two solvents having markedly different evaporation and solubilisation properties, in order to influence the resulting particle properties. It was established in the previous chapter that solvent properties such as their evaporation rate and solvent power have an important influence on particle formation. Other studies have also reported, both with electrospraying and with other liquid atomization techniques, that the interplay between evaporation rate of solvents and solubility and migration of solutes within droplets has an important role in the formation of polymeric particles [Tsapis *et al.* 2002, Vehring *et al.* 2007, Yao *et al.* 2008].

Table 5.1 Physical properties of the solvents used to fabricate microparticles. Values in italic are adapted from [Smallwood 1996].

Property	**Acetone**	**Methanol**
Viscosity (mPa ·s) at 25 °C	0.30	0.57
Boiling point (°C)	*56.0*	*64.0*
Evaporation rate (BuAc=1)*	*5.6*	*4.1*
Dielectric constant	*20.6*	*32.6*
Electrical conductivity (μS/m)	6	50

Acetone was again selected as one of the solvents due to its good ability to dissolve PLGA and its high evaporation rate, allowing dry particles to be formed at collection. Methanol was selected as the other solvent due to its poor ability to dissolve PLGA but intermediate capacity to dissolve CEL. The difference in the solubility of the solutes, i.e. CEL and PLGA in MeOH is thought to have an influence on the solidification process during particle formation. Further, MeOH has a lower evaporation rate than ACE and thus the concentration of MeOH would increase as the solvents evaporate and result in a greater effect on the solidification process.

5.1.2 Design of study – solutions and samples

The solubility of CEL and PLGA in ACE and MeOH were measured and shown in Table 5.2. Four different ratios of the solvent compositions of ACE and MeOH, i.e. 100:0, 90:10, 75:25, 69:31, all indicated in molar ratio, were selected to dissolve CEL and PLGA. These values were selected to have a few ratios between pure ACE and a ACE:MeOH ratio close to the saturation point for PLGA (ACE:MeOH - 65:35) for a solute concentration of 5%, at which PLGA is precipitated out to form a suspension. A solute concentration of 5% was chosen due to the successful previous preparation of microparticles at 5% solute concentration and in order to set up comparisons with spray drying at similar concentrations. Samples were prepared at a constant flow rate using 10% or 20% drug loading to examine differences in particle characteristics and release upon different values of drug loading.

5.1.3 Characterization of spraying solutions

Electrical conductivity

Measurements of electrical conductivity of the CEL and PLGA solutions showed that solutions containing CEL were much more electrically conductive compared with solution containing PLGA (see Table 5.3), which indicates that CEL carries more

electric charge relative to PLGA. Further, the electrical conductivity increased as the MeOH concentration was increased both in solutions containing CEL and PLGA, indicating that MeOH is more conductive than ACE. As observed in the previous chapter, the electrical conductivity of solutions influences the properties of particles prepared with electrospraying, most notably with an increase in conductivity resulting in a decrease in particle size [Gañan-Calvo *et al.* 1997].

Table 5.2 List of microparticle samples prepared.

Sample	ACE:MeOH molar ratio	Solute conc. (%)	Polymer conc. (%)	Drug loading (%)	Flow rate (μL/min)
10D100:0	100:0	5	4.5	10	30
10D90:10	90:10	5	4.5	10	30
10D75:25	75:25	5	4.5	10	30
10D69:31	69:31	5	4.5	10	30
20D100:0	100:0	5	4.0	20	30
20D90:10	90:10	5	4.0	20	30
20D75:25	75:25	5	4.0	20	30
20D69:31	69:31	5	4.0	20	30

Table 5.3 Electrical conductivity of solutions containing CEL or PLGA.

Solution	Electrical conductivity (μS/m)
5% CEL in ACE:MeOH (100:0)	101
5% CEL in ACE:MeOH (90:10)	105
5% CEL in ACE:MeOH (75:25)	109
5% CEL in ACE:MeOH (69:31)	111
5% PLGA in ACE:MeOH (100:0)	23
5% PLGA in ACE:MeOH (90:10)	26
5% PLGA in ACE:MeOH (75:25)	32
5% PLGA in ACE:MeOH (69:31)	37

Viscosity and polymer configuration

Rheological measurements of the spraying solutions showed that the viscosity decreases as a function of the MeOH concentration of the solution (Table 5.4). Yet, it was observed from Table 5.1 that ACE is less viscous than MeOH, which seems contradictory with the dynamic viscosity values observed in Table 5.4. This can be explained by the better solvent power of ACE compared with MeOH which allows the polymer chains to extend out and possibly interact with each other, resulting in a steeper increase in viscosity as a function of polymer concentration. The addition of CEL did not have a noticeable influence on the viscosity of the solutions compared with PLGA and was thus left out in the measurements to simplify the study on polymer conformation. The greater influence of PLGA on the viscosity is explained by the much higher molecular weight and hydrodynamic volume of PLGA compared with CEL.

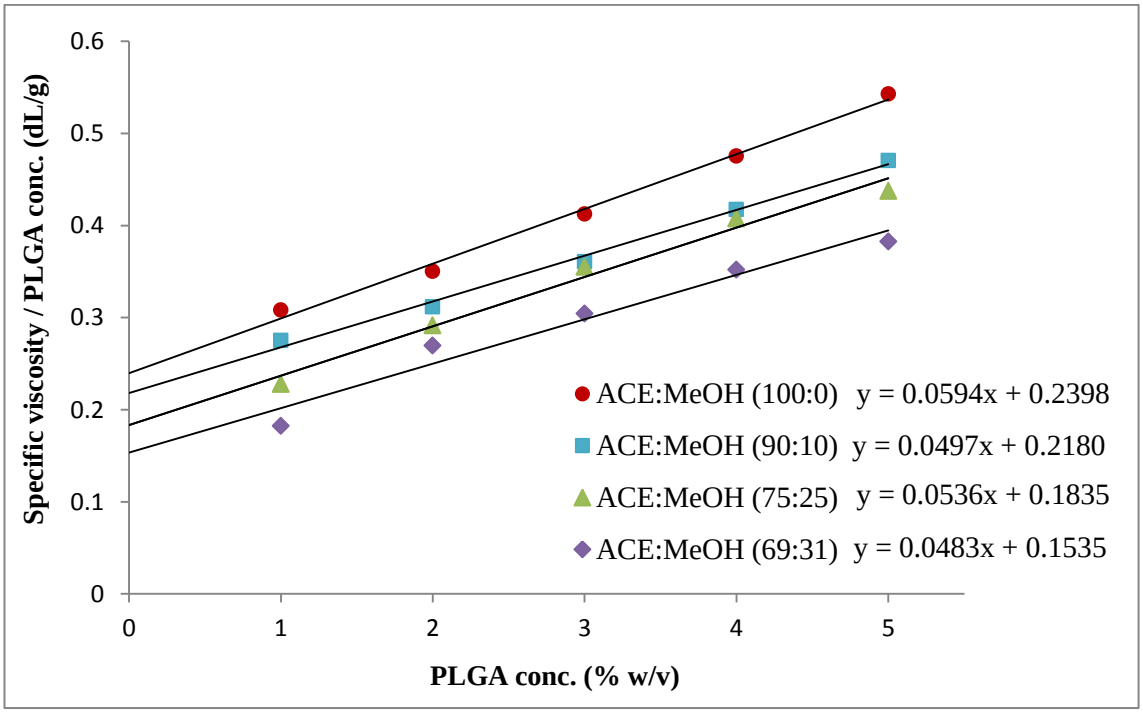

Figure 5.1 Specific viscosity / PLGA concentration of spraying solutions plotted as a function of PLGA concentration.

The conformational structure and solubility of PLGA in ACE:MeOH feed solutions were studied by determining the intrinsic viscosity, Martin constant and overlap concentration. The intrinsic viscosity was determined as the y-intercept of the specific viscosity / PLGA concentration curve (see Figure 5.1) as described in the methods section (see section 3.2.4). The Martin constant and overlap concentration were then found using equations 3.5 and 4.1. The intrinsic viscosity of PLGA in the feed solutions ranged between 0.15 and 0.24 dL/g and decreased as the MeOH content was increased. The observed trend indicates that solubility of PLGA is highest in pure ACE with more extended chains and gradually decreases as MeOH is added, until PLGA begins to precipitate at 65:35 ACE:MeOH molar ratio. The Martin constant calculated at 5% PLGA concentration increased as a function of MeOH concentration and indicated more interaction between PLGA molecules and between PLGA and solvent, as the MeOH concentration was increased. The overlap concentration, c*, ranged between 4.23 and 6.49 and increased as a function of MeOH concentration. This indicates that the cross over concentration at which polymer chains begin to entangle with each other becomes higher as the MeOH content is increased.

Table 5.4 Viscosity related properties of PLGA solutions with different solvent ratios.

Solution	**Dynamic viscosity** (mPa·s) at 25 °C	**Intrinsic viscosity** (dL/g)	**Martin constant** (5% PLGA)	**Overlap conc. (c*)**
PLGA in ACE:MeOH (100:0)	1.13	0.24	0.71	4.23
PLGA in ACE:MeOH (90:10)	1.04	0.22	0.82	4.90
PLGA in ACE:MeOH (75:25)	1.03	0.18	0.88	5.45
PLGA in ACE:MeOH (69:31)	0.95	0.15	1.19	6.49

Evaporation profile

The evaporation profiles of the solvent mixtures and the feed solutions are shown in Figure 5.2 A-D. Figures 5.2 A and 5.2 C show that evaporation of solvent from the solvents and feed solutions took place at a steady rate until the solvent had fully evaporated (A) or until a lower limit was reached corresponding to the solid components (C). The time scale of the evaporation process was similar for all the samples but with evaporation taking place at a slightly lower rate with increasing MeOH concentration. Figures 5.2 B and 5.2 D show the evaporation rate of the solvent mixtures (B) and the feed solutions (D) as a function of time and indicate that the evaporation rate decreased continuously for all samples. Initially, a high evaporation rate was observed, which decreased gradually and then more sharply, followed by another slow decrease. The evaporation time was generally shorter for the solvent mixtures than for the feed solutions. Figures 5.2B and 5.2D also indicate that the evaporation rate became slightly lower with increasing MeOH concentration.

Although the evaporation rate was here measured by mimicking the drying process with electrospraying it may be quite different from the actual drying process. Under the current setting it was not possible to directly measure droplet drying rates during the actual electrospraying or spray drying process due to the small size and short evaporation times of the atomized droplets. Therefore, model systems are typically used to study the drying kinetics such as the single droplet models described in section 2.3.2. Here, we studied the drying kinetics of different solvent systems by measuring the evaporation rates of the solvents and the feed solutions as a function of time, by monitoring the weight loss of a drop using TGA under fixed temperature, surface area and nitrogen flow. Although the drop that was studied here is many times larger than

the small droplets produced from the atomizing nozzle the same heat and mass transfer processes were assumed to apply during drying of the larger drop.

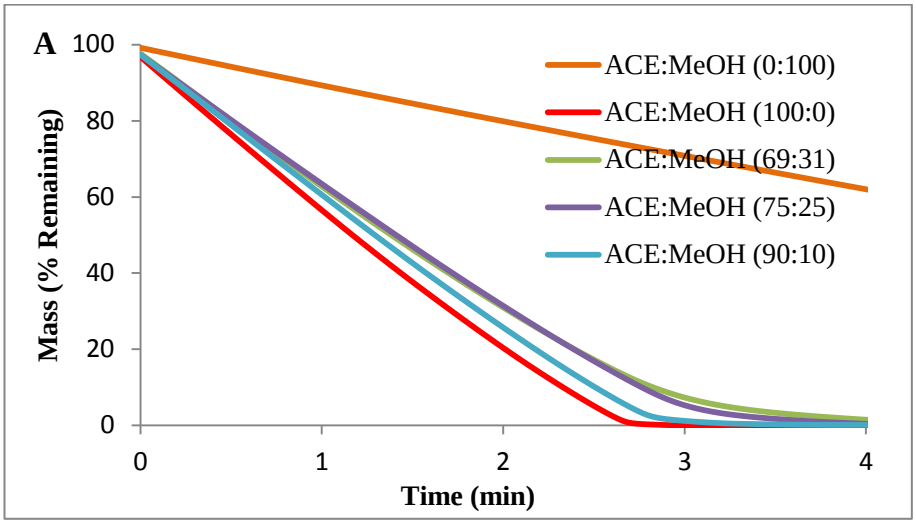

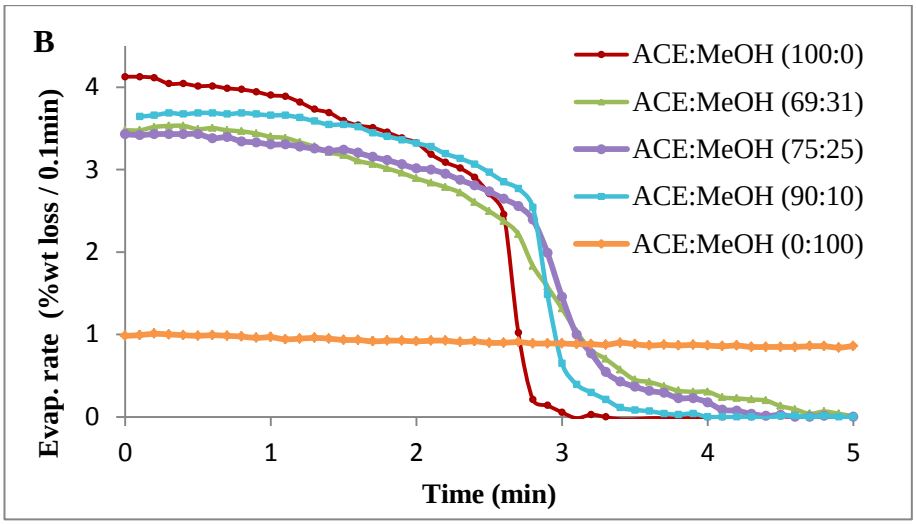

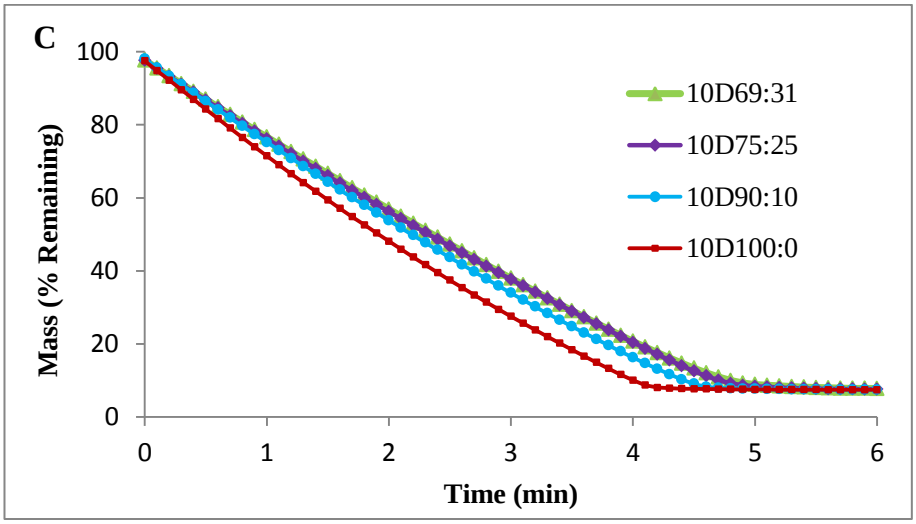

(Figure continued on next page)

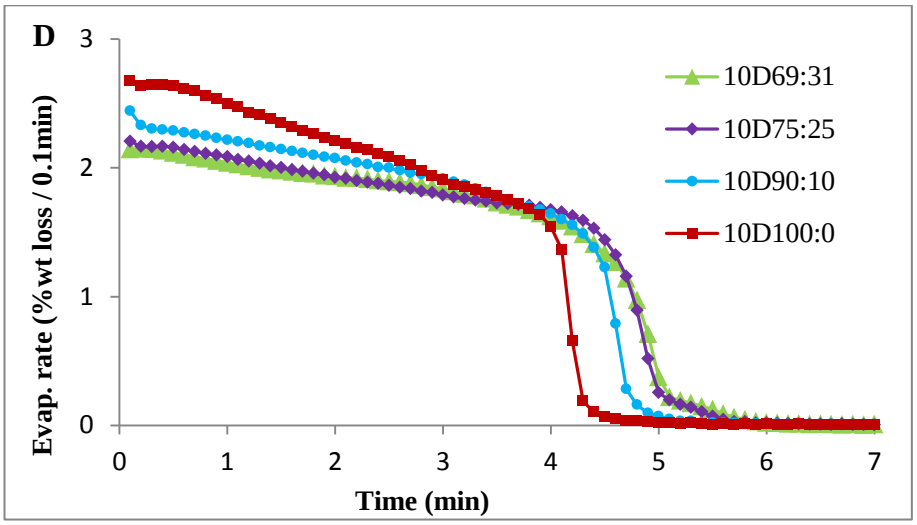

Figure 5.2 Evaporation of solvent mixtures (A) and solutions (B) at 25 ºC and the first derivative of the evaporation curve for solvents (C) and solutions (D).

5.2 Mixed solvent study – Particle formation

Particle engineering relies largely on understanding the underlying particle formation mechanisms. Electrospraying (production of particles) and electrospinning (production of fibres) are essentially two sub-techniques based on similar physical principles with solutions of higher viscosity being used for electrospinning. It has been reported that the formation of chain entanglement of the polymer in the solution has an important effect on the progression in fibre formation with electrospinning [Shenoy *et al.* 2005b, Zhang *et al.* 2012]. It is equally important that the absence or limited progression of such chain entanglement leads to the formation of particles instead of fibres at a given critical limit with some overlap between the two resulting types of products [Almeria *et al.* 2010]. The overlap concentration is an indicator for degree of inter-chain entanglement in a given polymer/solvent combination. Further, polymer entanglement levels cannot be very high before Coulomb fissions have occurred as the particles would otherwise become elongated or fibre-like at fission due to early precipitation of the polymer. Entanglement and precipitation occur at different concentrations depending on the

solvent system but whereas polymer chain entanglement would take place at a lower concentration in a good solvent compared with a poor solvent, precipitation would take place at a lower concentration in a poor solvent compared with a good solvent.

As solvent evaporates from the surface of the droplets, which it does relatively quickly given the high surface to volume ratio of the droplets, and the solutes will naturally begin to deposit at the droplet surface. This process is, however, counteracted by the inwards diffusion of solutes towards the centre of the droplet where the solutes are less concentrated. The ratio between the solvent evaporation and the solute diffusion rates is crucial for the particle formation process and the resulting characteristics of the particles depend thereon. This ratio is referred to as the Peclet number (see section 2.3.2), a dimensionless quantity that has been studied by several groups in order to understand particle formation from droplets [Tsapis *et al.* 2002, Vehring 2008].

The evaporation kinetics of solvents in a passive drying process is determined by the vapour pressure of the solvent and the temperature and humidity of the environment. In this study the evaporation measurements were performed at 25 °C and it may be seen from Figure 5.2 A that the evaporative weight loss took place almost linearly in the first four minutes, and an increase of the MeOH concentration reduced the evaporation rate. Figures 5.2 B and 5.2 C, however, show that the evaporation rate of the solvents decreased in the presence of PLGA indicating that there were interactions between PLGA and the solvent molecules, which influenced the evaporation rate.

The solubility of the solutes in the solvent is another important factor for consideration for any liquid atomization process. In the present study two different solutes, i.e. CEL and PLGA, were used with binary mixtures of two solvents. In this case both the solubility of the polymer and the drug in the two solvents is of importance as it can result in separation of the solutes into two solute phases. Both PLGA and CEL are

soluble in ACE while only CEL is soluble in MeOH. The boiling point of ACE is lower than that of MeOH resulting in a decrease in the ACE:MeOH ratio as solvent evaporation progresses leading to less favourable conditions for PLGA dissolution. In a "good" solvent the individual polymer chain is extended thus taking up the maximum amount of space. When the solubility of a polymer in the solvent decreases, the polymer chains begin to coil up or crumple and take up less space in the solution until a point where the polymer begins to precipitate out. In a good solvent the polymer chains interact well with the solvent and mainly form polymer-solvent interactions while in a poor solvent the interaction mainly takes place between polymer chains [Grosberg *et al.* 1997].

The particle formation process is dependent on the solution properties such as evaporation rate, electrical conductivity and viscosity as well as the polymer conformation in the solutions, both before and after droplet formation. In Table 5.4 it is seen that the intrinsic viscosity is highest for PLGA in 100% ACE and decreases with the proportion of MeOH added. This indicates that the polymer chains interact well with solvent molecules in 100% ACE whereas the interaction between polymer chains becomes predominant in the ACE-MeOH solvent mixtures.

Polymer solutions are typically electrosprayed in the concentration region close to the c* of the system [Park and Lee, 2009]. When the polymer concentrations are below the c* of the system polymer chain entanglements begin after the droplets have been formed thereby easing breakup of the liquid. In Table 5.4 it was observed that the overlap concentrations of the solutions increased as the MeOH content was increased. It can be seen that all feed solutions used had a PLGA concentration below the overlap concentration apart from 10D100:0, which had a PLGA concentration slightly above the c*. Thus for most of the solutions used chain entanglement would have taken place

between droplet formation and droplet drying while for 10D100:0 some chain entanglement would have existed before droplet formation.

In a solvent with high capacity to dissolve both solutes particle formation would mainly be controlled by solvent evaporation and solute diffusion, while in the presence of a poor solvent particle formation could also be influenced by the polymer precipitation process. ACE evaporates at a higher rate than MeOH, and thus the MeOH fraction of the solution increases over time and is likely to reach the limit at which PLGA precipitates. Once saturation is reached with the mixed solvent system the PLGA molecules would be expected to curl up and form compact precipitates while the solvent continues to evaporate.

5.3 Mixed solvent study – Particle characteristics

Particle characteristics were studied by examining the particle size, morphology, inner structure and physical form using methodology described in the experimental section.

5.3.1 Particle size

The size and size distribution of the particles prepared using different solvent ratios and drug loads are presented in Table 5.5. Particles ranged between 2-4 μm in diameter and had a relatively narrow size distribution with the exception of sample 20D69:31.

A correlation is observed between the ACE:MeOH ratio and particle size, with the particle size decreasing as the MeOH content is increased. This size dependency is partly explained by the increasing electrical conductivity as a function of the MeOH content, which is known to result in smaller droplets and hence smaller particles [Gañan-Calvo *et al.* 1997]. It can also be explained by the decrease in viscosity with increasing MeOH concentration (see Table 5.4), which would result in smaller droplets and particles such as observed here.

It was further observed that particles prepared with 20% drug loading were slightly smaller than those prepared with 10% drug loading for all sample pairs. This is explained by the lower polymer concentration and thereby lower viscosity of feed solutions with 20% drug loading resulting in smaller particles (see section 2.4.6). The higher electrical conductivity of solutions with 20% drug loading is also likely to have had a small influence on the resulting particle size (see section 4.5.2).

The difference in particles size between the different samples was quite subtle with the average size ranging from 2-4 μm. The polydispersivity indices of the samples indicated that the particle size distribution became wider as the MeOH ratio was increased.

Table 5.5 Particle samples prepared and their size, size distribution and drug entrapment efficiency.

Sample	Size (μm)	Polydispersivity index (%)	Drug entrapment efficiency (%)
10D100:0	3.83±0.37	9.53	97.4
10D90:10	2.73±0.30	10.93	102.9
10D75:25	2.61±0.35	13.40	100.4
10D69:31	2.62±0.42	15.88	99.6
20D100:0	3.06±0.31	10.19	100.2
20D90:10	2.47±0.34	13.92	96.3
20D75:25	2.28±0.34	14.84	97.4
20D69:31	2.10±0.51	24.38	99.8

5.3.2 Particle morphology and porosity

The morphology of the particles may be seen in Figures 5.4 and 5.5 which show SEM images from each of the microparticle samples at different magnifications. While the particles prepared with only ACE appeared to have a relatively smooth surface the

particles prepared with varying proportions of MeOH all had a rough, grain-like appearance with the roughness increasing as the MeOH ratio was increased. This is explained by the differences in the properties of the two solvents used and the differences in solubility of CEL and PLGA in the two solvents.

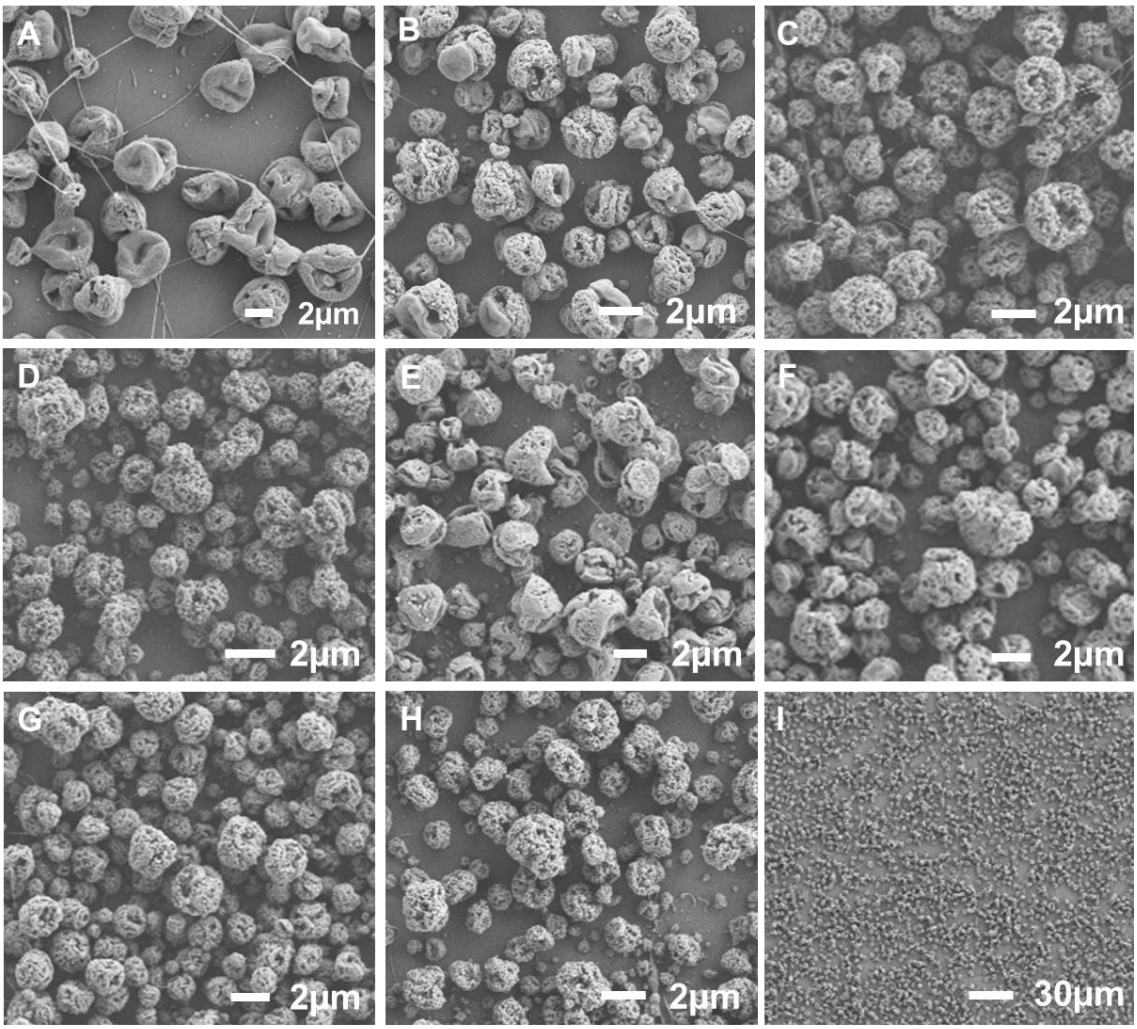

Figure 5.4 SEM images of microparticle samples, 10D100:0 (A), 10D90:10 (B), 10D75:25 (C), 10D69:31 (D), 20D100:0 (E), 20D90:10 (F), 20D75:25 (G), 20D69:31 (H) and overview of 10D100:0 (I).

Both ACE and MeOH would have evaporated rapidly from the surface of the droplets and hence the solutes, especially PLGA, would have become concentrated and in turn created localized regions of very high viscosity, from which the PLGA would have precipitated out to form a shell structure. The PLGA precipitation would have been

influenced by the solvent composition and thus would have influenced the particle formation process and surface morphology of the resulting particles. The particles produced with ACE were relatively smooth while those produced with ACE/MeOH all had a rough appearance with the level of surface roughness increasing with the MeOH content (see Figure 5.5). In a solvent mixture with high intrinsic viscosity the polymer chains would be stretched out but entangled with each other within the solution. They would thus precipitate out in a homogenous network, more likely to have a smooth appearance on the surface as seen in Figures 5.4 A and E. Meanwhile, if the solvent mixture has a low solubilisation capacity for the polymer, in this case by the addition of MeOH to ACE, the polymer chains would already be in a compact conformation in the solution, before atomization. As the solvent evaporates, the molecules would have adopted a more compact conformation and could have precipitated out as small clusters, producing a grainy morphology such as that seen in Figure 5.4 B, C, D, F, G and H.

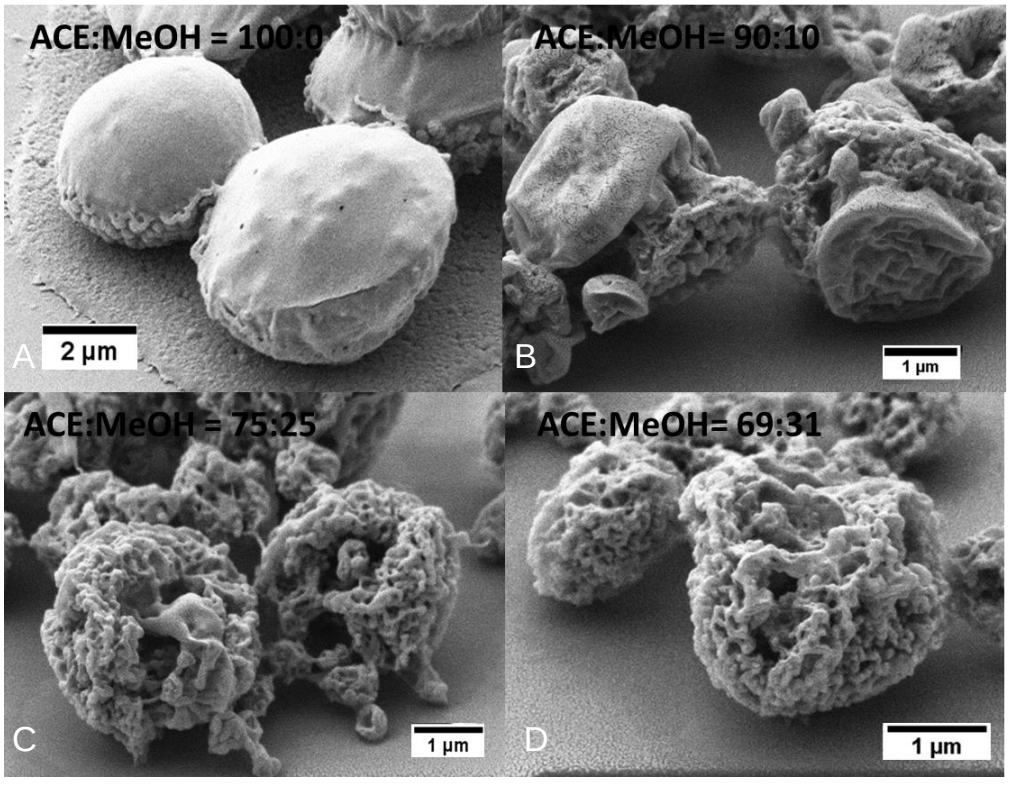

Figure 5.5 Close-up SEM images of microparticle samples, 10D100:0 (A), 10D90:10 (B), 10D75:25 (C) and 10D69:31 (D).

Similar observations were made by Roula *et al.* who showed that a poor solvent resulted in early polymer precipitation and wrinkled particle appearance [Raula *et al.* 2004]. Zhou et al also studied mixed solvent systems using spray drying and found that when applying low drying heat, hence low evaporation rate, nanoclusters were formed, whilst high drying heat gave rise to a highly porous honeycomb structure [Zhou *et al.* 2001].

5.3.3 Particles porosity

Cross sectional images of the particles taken using FIB/SEM show that the particles had varying degrees of porosity. It may be seen that particles from sample 10D100:0 were hollow while particles prepared with various MeOH contents in the solution had multiple pores inside (Figure 5.6). Although it appears that 10D90:10 was more porous than 10D75:25 and 10D69:31, which appeared to be denser, the degree of porosity was not further quantified.

At a fixed feed concentration the degree of porosity is mainly determined by two factors, the solvent evaporation rate and the average size of droplets formed as has been demonstrated in several studies [Bae *et al.* 2009, Kim *et al.* 2006]. Porosity typically stems from a non-uniform distribution of solutes in the solidifying droplet where some areas, most often at the droplet surface, become more concentrated than others [Wu and Clark 2007]. Pores can thus derive from the areas of lower concentration or localized phase separation within the droplets. When the concentration of solutes increases in the surface region during evaporation of solvent from the droplet surface, it is likely that a hollow structure forms if the diffusion of solutes towards the core cannot keep up with the evaporation of solvent. This effect is more pronounced if the droplets are initially larger, partly because the particles will dry more slowly due to their smaller surface area to volume ratio and the longer diffusion path for the solutes, which makes it difficult for the solutes on the surface to diffuse to the core of the particles.

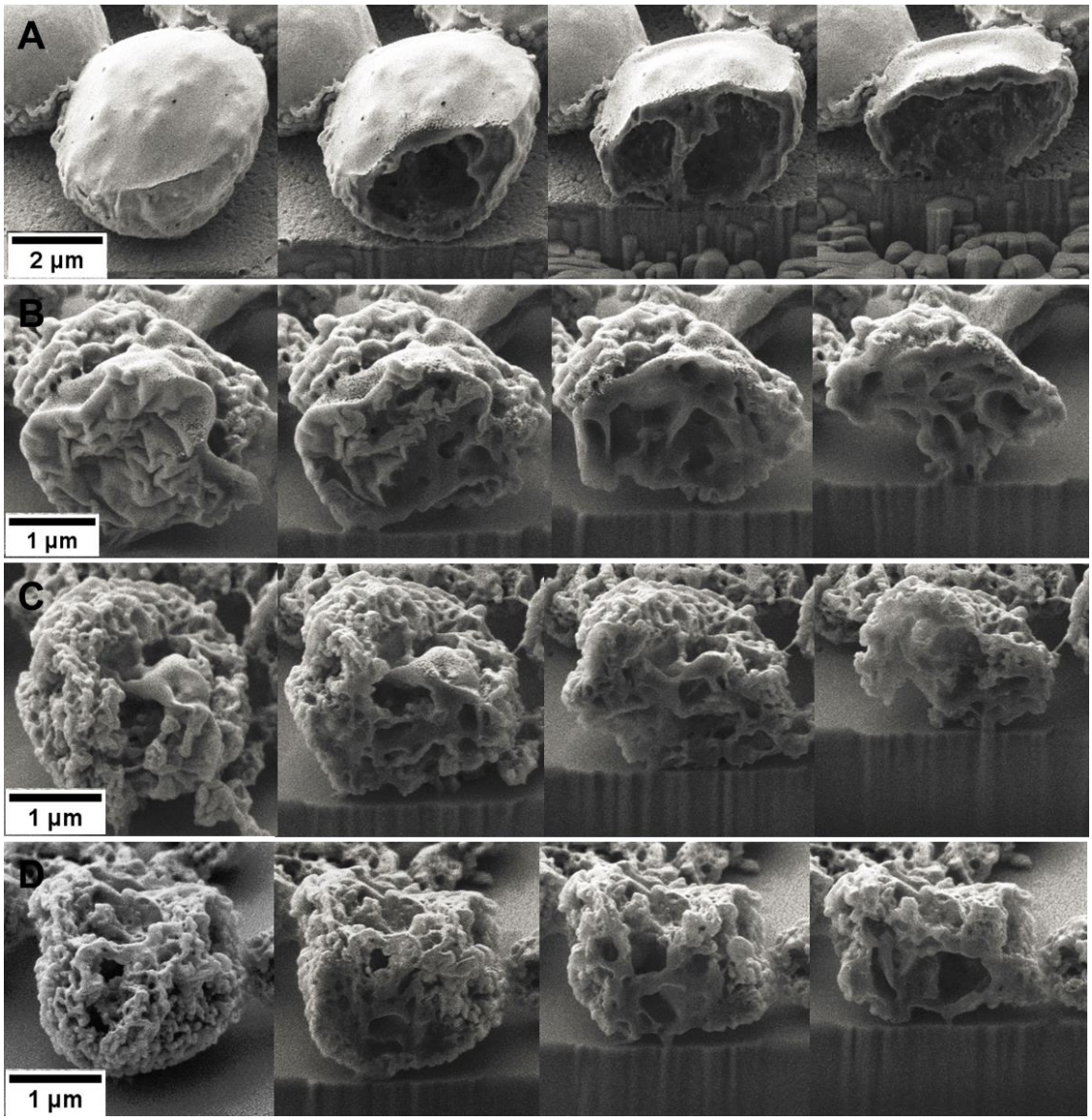

Figure 5.6 FIB/SEM images of microparticles at progressing sections, samples 10D100:0 (A), 10D90:10 (B), 10D75:25 (C) and 10D69:31 (D).

In the present study we showed that porosity is also influenced by adjusting the ratio between the solvents. The FIB/SEM images showed that particles prepared with ACE were nearly hollow and were larger than the particles prepared with ACE-MeOH mixtures. This indicates that larger droplets were formed and rapid evaporation resulted in pores inside the particles. The particles prepared with ACE-MeOH mixtures were also porous and the number of pores inside the particles was higher for the samples prepared with lower MeOH concentrations. This could be explained by the slightly

smaller droplets and particles produced with samples 10D75:25 and 20D75:25 compared with 10D90:10 and 20D90:10, respectively (see Table 5.5). Also, the more rapid precipitation of PLGA with increasing MeOH concentrations likely did not provide sufficient time for an extensive porous network to form.

5.3.4 Physical state of drug

The XRPD diffractograms in Figure 5.7A demonstrate that CEL is crystalline in its powder form and also when it is physically mixed with PLGA, indicated by the consistency of the characteristic peaks. PLGA is amorphous in its powder form. The diffractograms for the electrosprayed microparticles prepared using different solvent ratios shown in Figure 5.7B do not have any characteristic crystalline peaks and the particles are therefore all presumably in an amorphous state.

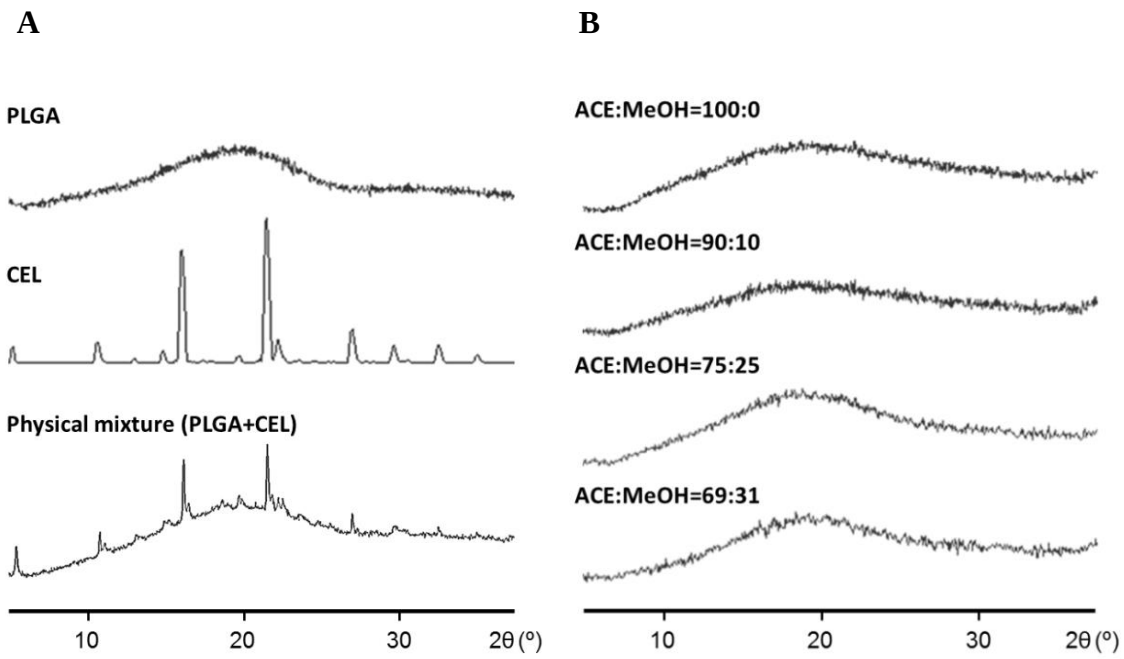

Figure 5.7 XRPD patterns of pure CEL, PLGA and the physical mixture of these (A) and CEL-loaded PLGA microparticles prepared with different solvent ratios at 10% drug loading (B).

Observations made with polarized light microscopy (data not shown) also indicated that no crystallinity was present at this microscopic scale in any of the particles samples, supporting the results from DSC and XRPD. Polarized light microscopy generally has high sensitivity to the presence of anisotropic crystals, even a few small microcrystals.

5.4 Mixed solvent study – Drug distribution and Drug release

5.4.1 Drug distribution in microparticles

As mentioned in section 2.5.3 it is important to have some knowledge of the homogeneity of the drug in the solid dispersion and whether there are some areas with a higher drug concentration or phase separation. Also, it is important to know more about the spatial distribution of drug in cases where the drug is not present as a homogeneous, molecular distribution as this would most likely influence the release kinetics and the physical stability [Urbanetz and Lippold 2005]. Several methods were mentioned for measuring the drug distribution in particles including X-ray photoelectron spectroscopy (XPS). XPS has previously been used to examine the chemical composition of the outer surface layer of solid dispersions and can give an estimate of the concentration of drug in the measured area. XPS has been used to study the surface drug concentration in order to examine the possible tendency for drug to migrate towards the surface of spray dried particles [Dahlberg *et al.* 2008].

The surface chemical compositions of the dry microparticle samples were examined here using XPS to give an estimate of the distribution and general homogeneity of CEL in the PLGA matrix. The relative theoretical atomic concentration (in %) of C, O, F, N and S (H was not measured) of pure CEL were 65.38%, 7.69%, 11.54%, 11.54% and 3.85%, respectively. Similarly, the relative theoretical atomic concentration (in %) of C and O for PLGA were 55.56% and 44.44%, respectively. The concentration of CEL could be estimated directly from the atomic concentration of F, N and S atoms. In order

to eliminate the errors, ratios of N/F, S/F and F/C were used to calculate the CEL concentration at the surface of the microparticles. The chemical structure of CEL and PLGA are shown on Figures 3.1 and 3.2B.

The surface concentration values of CEL as well as ratios of the three elements exclusive to CEL in these particles are shown in Table 5.6. The CEL concentration on the surface of the microparticles ranged between 20-57% depending on the sample. It was observed that the particles containing 20% CEL generally showed higher surface CEL concentration than those containing 10% CEL. Additionally, there was a clear trend for the surface drug concentration to increase when the MeOH concentration increased, both for samples containing 10% CEL and 20% CEL.

Table 5.6. Surface chemical composition of CEL-loaded PLGA microparticles prepared at different drug loadings and with different solvent ratios.

Sample	N/F	S/F	F/C	CEL concentration
10D100:0	0.92	0.33	0.053	20 ± 1%
10D90:10	0.94	0.33	0.071	31 ± 2%
10D75:25	0.84	0.28	0.077	38 ± 1%
10D69:31	0.96	0.26	0.096	41 ± 1%
20D100:0	0.95	0.32	0.074	32 ± 1%
20D90:10	0.82	0.31	0.099	43 ± 4%
20D75:25	0.80	0.28	0.114	46 ± 3%
20D69:31	0.79	0.29	0.125	57 ± 2%

All surfaces analysed contained more than the 10% and 20% CEL initially loaded, respectively, indicating a migration of drug towards the surface of the particles during

particle formation. This is explained by the early precipitation of PLGA and the significantly lower molecular weight of CEL. PLGA is insoluble in MeOH while CEL can be dissolved up to 100 mg/mL in MeOH. At 5% solute concentration, PLGA precipitates at around an ACE:MeOH molar ratio of 65:35. During evaporation of ACE from the surface of the droplet both PLGA and CEL move towards the core of the droplet following the diffusion gradient. Then, as the solute concentration reaches a critical level PLGA begins to precipitate while presumably CEL is still dissolved in the droplet and can move in and around the PLGA molecules. After a shell has formed, some ACE is still trapped within it. ACE then slowly escapes through the shell provided that the particle does not collapse.

In this process it is believed that the CEL molecules, small as they are, can diffuse out to the surface together with the ACE resulting in a slightly uneven drug distribution. When MeOH is added to the system the MeOH ratio increases during evaporation due to its lower boiling point compared with ACE and so PLGA begins to precipitate earlier while CEL is still in solution. CEL could thus have more time to diffuse towards the particle surface once the PLGA has precipitated and the compact conformation of PLGA, in presence of MeOH, may allow easier movement out to the surface.

The surface drug content reached up to 41% for particles prepared with 10% drug loading and the XRPD measurements showed that the drug was still in an amorphous state. This indicates that there was not an actual separation of the solutes into a crystal-rich CEL phase and an amorphous PLGA phase, but instead that CEL remained highly dispersed in the PLGA matrix. The polymer molecular conformation in the solvent mixture immediately before atomization into droplets is likely to have had a strong influence on the resulting matrix structure and on the polymer-polymer and polymer-drug interactions. However, detailed understanding of such interactions between solutes

and of the molecular distributions in solid dispersions is still lacking and is needed to achieve better control of the process. There have nevertheless been cases where an improvement in *in vitro* performance was observed for drug dispersions prepared with solvent mixtures [Paudel and Van den Mooter 2012].

5.4.2 Drug release from microparticles

The drug entrapment efficiencies of the microparticle samples were seen to be 96% or above, with no correlation to the solvents used (see Table 5.5). The particles were collected directly onto a dry surface and therefore no significant loss in total drug content was expected. Drug release studies were all performed using the paddle dissolution apparatus described in section 3.12.2 and using phosphate buffer (pH 6.8) + 1.5% SLS as the release medium. Drug release rate was measured for each of the particle samples and the drug release profiles are shown in Figures 5.8 and 5.9.

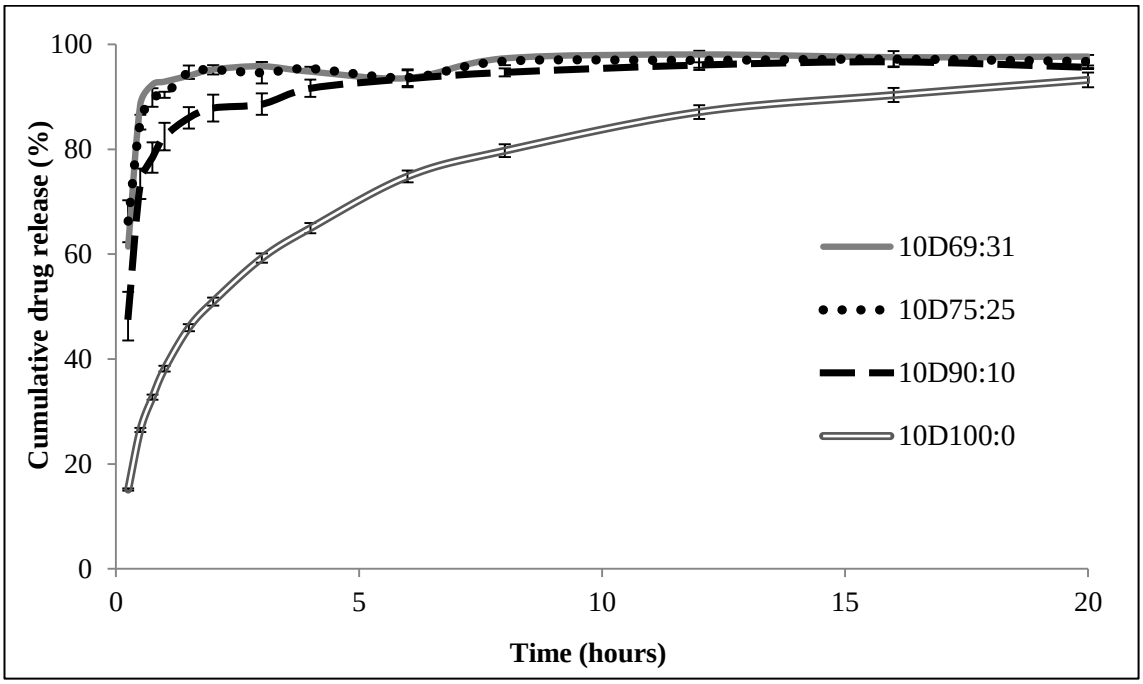

Figure 5.8 Drug release profile of microparticle samples 10D100:0, 10D90:10, 10D75:25, 10D69:31.

For all microparticle samples more than 90% of their drug content was released during the 20 hours of exposure to the dissolution medium. Generally, a large burst release was observed especially for particles prepared in solutions with high MeOH content. Further, the drug release rate also increased as a function of the MeOH content for the samples prepared with both 10% and 20% drug loading. The difference in release rate was most significant between particles prepared in ACE alone and those prepared from a mixture of MeOH and ACE. This indicates a clear relation between the addition of MeOH and the resulting near-instantaneous drug release.

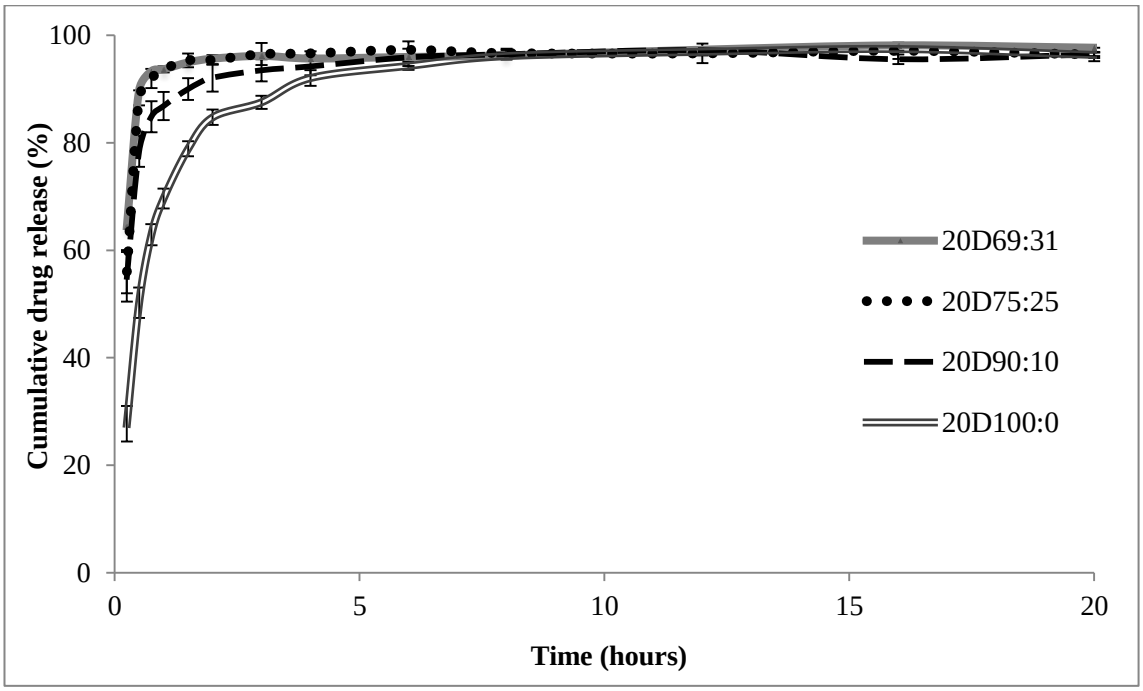

Figure 5.9 Drug release profile of microparticle samples 20D100:0, 20D90:10, 20D75:25, 20D69:31.

The drug release curves for particles prepared with 10% drug loading and 20% drug loading both demonstrate a high drug release rate for most of the particle samples considering that PLGA is insoluble in the dissolution medium and that the release of the drug thus took place via diffusion. There is a clear difference in the release profile of 10D100:0 compared with 10D90:10, 10D75:25 and 10D69:31 and a trend that the

release rate increases with increasing MeOH content. Drug release from samples 10D75:25 and 10D69:31 take place rapidly with most of their drug load released within 30 min. A similar trend was observed for samples with 20% drug loading, which had an even higher drug release rate. The results correlate well with the XPS results as well as the observations from the SEM images (see Figure 5.4). The samples which were shown to have a high surface drug content also exhibited rapid burst release as would be expected given the lower diffusion boundary to be overcome. The particles produced with high MeOH content were also smaller with a grainy surface and hence a higher surface area to volume ratio and shorter diffusion distances.

In the presence of MeOH, limited polymer chain entanglement takes place during solvent evaporation from the droplet and the polymer precipitates into compact clusters within the droplet. Drug molecules diffuse out towards the surface as the remaining solvent escapes. In ACE some polymer chain entanglement takes place at droplet formation and the chains form a network as the solvent evaporates. The dense polymer network at the surface results in the formation of a smooth shell which the remaining solvent escapes across, while some drug molecules also diffuse towards the surface.

Figure 5.10 shows SEM images of particles captured after being used for drug release studies. The images indicate that particles from sample 10D100:0 were still structurally intact, retaining their shape after losing 10% of their dry weight. In comparison, particles from samples 10D90:10, 10D75:25 and 10D69:31 showed no preservation of their shape and morphology. They seemed to have disintegrated during the drug release studies and agglomerated into an unrecognizable, bulky mass. This supports the morphological findings in Figure 5.5 where particles seemed to be formed from small grains and the rheological measurements, which indicated that the polymer chains were compact with less entanglement compared with particles prepared using ACE. The

disintegration into smaller fragments would result in an even higher surface to volume ratio for release and again shorter drug diffusion distances. This disintegration of the PLGA structures could be explained by the compact conformation of the polymer chains and the lack of interaction between polymer chains to maintain structural stability (see Figure 5.11).

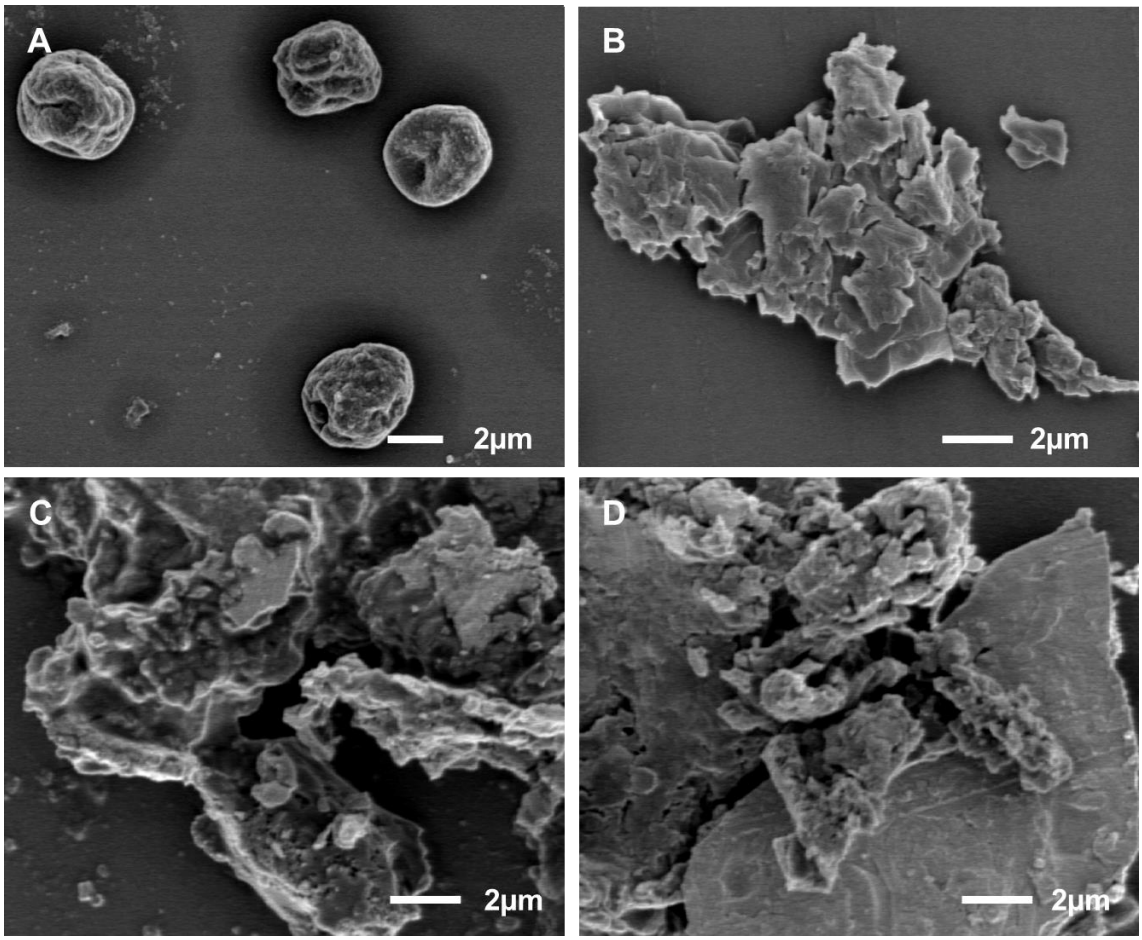

Figure 5.10 Representative SEM images of Electrosprayed microparticles loaded with 20% (w/w) CEL taken after drug release studies. Images represent samples 20D100:0 (A), 20D90:10 (B), 20D75:25 (C) and 20DD69:31 (D).

5.4.3 Summary of study with mixed solvent system

CEL-loaded PLGA microparticles were produced from a mixed solvent system at different solvent ratios using electrospraying to investigate the interactions of solvents

with the solutes and the influence of solvent compositions on the particle formation process. This study demonstrated that particle formation in the electrospraying process depended markedly on the solubility of the solutes, i.e. CEL and PLGA and also on the evaporation rate of the solvents. By using an anti-solvent (MeOH) for PLGA in the solvent mixtures the molecular conformation of PLGA became more compact and further resulted in early precipitation of PLGA during the formation of the particles.

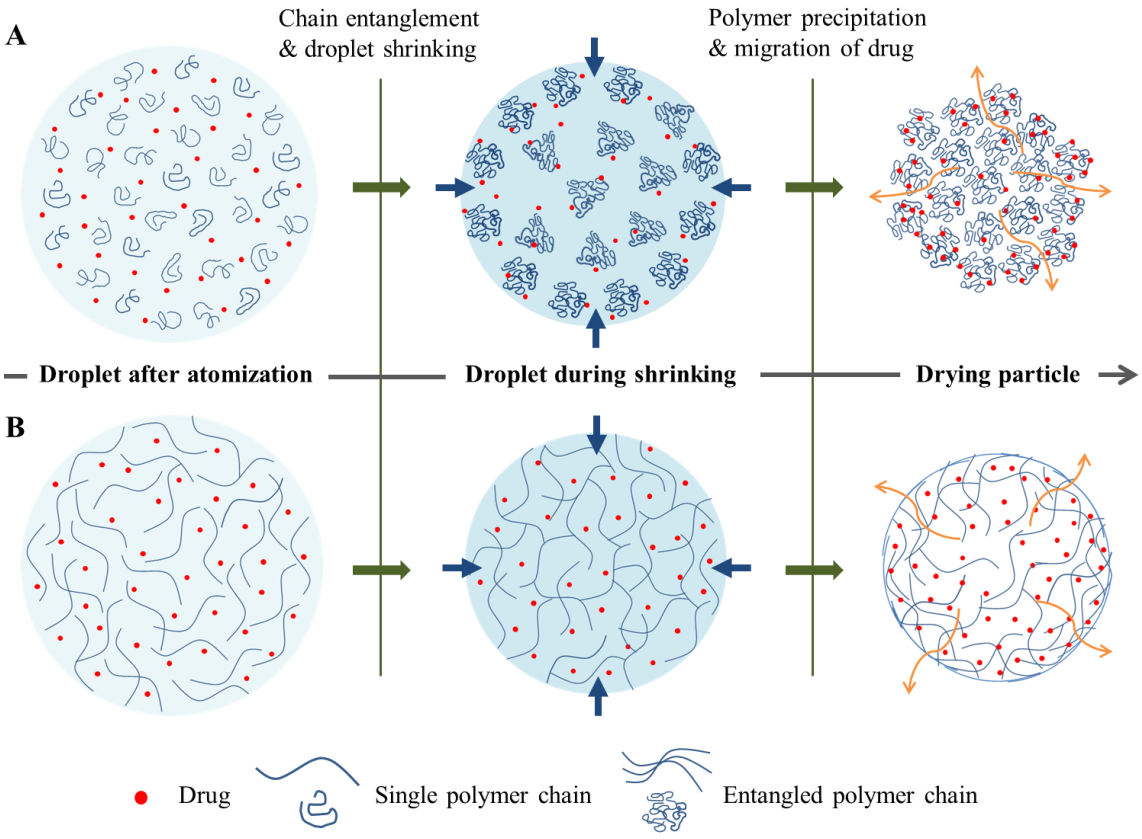

Figure 5.11 Particle formation process for solutions containing MeOH (A) and solution consisting of only ACE (B).

Depending on the amount of the anti-solvent (MeOH), different degrees of roughness were observed in the surface morphology as well as different accumulation of CEL at the particle surface. A clear correlation was observed between the concentration of the anti-solvent in the solvent mixture and the surface content of CEL, which was also evident from the release rates observed in the drug release studies. This shifting in the

drug distribution is likely to have taken place as a result of the better solubility of CEL in both solvents and its higher molecular mobility than PLGA. The mechanisms by which the different particle morphologies and drug distributions have formed with different solvent mixtures were related to the balance between precipitation of solutes and evaporation of solvents.

5.5 Water-soluble microparticles – Introduction and setup

5.5.1 Introduction to study

In extension of the mixed solvent study with electrosprayed CEL-loaded PLGA particles, another polymer and different solvent mixtures were studied to investigate the influence of solvents in more detail. Since all of the previous studies were performed using the water-insoluble polymer PLGA, in the present study a water-soluble polymer was chosen to look at that aspect of particle-based solid dispersions and also to observe the difference in release profiles compared with PLGA. Here the polymer HPMCAS was chosen due to its good solubility in water at a pH values above 5.5-6 (depending on the molecular weight of the polymer).

As mentioned in section 3.1.1, HPMCAS is used for enteric coatings due to its pH dependent solubility and further it has commonly been used to prepare solid dispersions. HPMCAS is also special due to its ability to interact with dissolved drug molecules and act as an effective precipitation inhibitor, whereby poorly soluble drug compounds can be kept in a supersaturated state for many hours after their release (see section 2.6). HPMCAS is soluble in several organic solvents including ACE and is further soluble in mixtures of solvents such as ACE and H_2O, H_2O and EtOH at certain ratios.

To follow up from the previous study using PLGA, different solvent mixtures were here investigated not only focusing on the solubility of the polymer but also on the solubility

of the drug. Four different combinations of solvents were selected based on solubility studies using HPMCAS and CEL. Based on the previous experience where high surface CEL concentrations were observed with an increase in anti-solvent for PLGA, in this study solvent mixtures with higher solubility for the polymer were examined.

5.5.2 Experimental design

In order to direct the focus of the study towards the solvent compositions, the solute concentration and drug loading were kept constant for the different sample conditions. Similar to the previous studies using PLGA a solute concentration of 5% was selected based on the higher viscosity of HPMCAS compared with PLGA since with PLGA the solute concentration was slightly in the low range resulting in hollow and porous particles. Further, a drug loading of 20% was selected in order to demonstrate a clearer correlation between the solvent compositions and the surface drug distribution measured using XPS.

Different solvent compositions were studied by testing the solubility of HPMCAS and CEL in the mixtures. Pure ACE was used as a reference solvent since it has previously been used for PLGA and was shown to be a good solvent for both HPMCAS and CEL. HPMCAS was soluble in ACE:H_2O mixtures with up to 70% H_2O v/v if it was first dissolved in ACE, and HPMCAS + CEL was soluble in ACE:H_2O up to 50% H_2O due to the poor solubility of CEL in H_2O. ACE:H_2O mixtures were studied because of the lower solubility of CEL compared with HPMCAS at increasing H_2O concentrations, and ACE:H_2O volume ratios 95:5, 85:15 and 65:35 v/v were selected based on the inability to electrospray solutions with higher H_2O concentrations. HPMCAS was found to be more soluble in EtOH:H_2O mixtures than in pure EtOH where it is insoluble. It was soluble in mixtures with >50% H2O, whereas CEL could only be dissolved in mixtures with up to 25% H_2O. Thus the EtOH:H_2O mixtures were studied at the ratios,

95:5 and 85:15 v/v. Both CEL and HPMCAS are soluble in ACE:EtOH mixtures at various ratios and HPMCAS is, however, insoluble in pure EtOH. Since EtOH evaporates slower than ACE, EtOH concentration is expected to increase during droplet evaporation resulting in an early precipitation of HPMCAS. ACE:EtOH mixtures were used at the solvent ratios 95:5, 85:15 and 65:35 v/v. The samples prepared are shown in Table 5.7.

Table 5.7 List of CEL-loaded HPMCAS microparticle samples prepared.

Sample	Solvent volume ratio (ACE:EtOH:H_2O)	Solute conc. (%)	Polymer conc. (%)	Drug loading (%)	Flow rate (µL/min)
AE100:0	100:0:0	5	4.5	10	25
AE95:05	95:5:0	5	4.5	10	25
AE85:15	85:15:0	5	4.5	10	25
AE65:35	65:35:0	5	4.5	10	25
AH95:5	95:0:05	5	4.5	10	25
AH85:15	85:0:15	5	4.5	10	25
AH65:35	65:0:35	5	4.5	10	25
EH85:15	0:85:15	5	4.5	10	25
EH65:35	0:65:35	5	4.5	10	25
AEH70:15:15	70:15:15	5	4.5	10	25
AEH50:25:25	50:25:25	5	4.5	10	25

5.6 Water-soluble microparticles – Particle characteristics

5.6.1 Particle morphology

The morphology of CEL-loaded HPMCAS particles prepared using electrospraying was studies using SEM and selected images are shown in Figure 5.12. It is observed that particles with relatively different morphologies could be obtained by altering the solvent

systems used and all of the particles were relatively similar in size, being around 2-3 μm in diameter. It was seen that particle samples prepared with mixtures of ACE and EtOH (Figures 5.12 A-D) were similar in their appearance, all being disc shaped with no exceptions observed (see overview in Figure 5.12 L). This disc shape is believed to result from the collapse of hollow particles and could be due to the slow diffusion of HPMCAS during droplet drying or from impact of landing. In all samples the particles had a smooth surface indicating high solubility of HPMCAS in these mixtures.

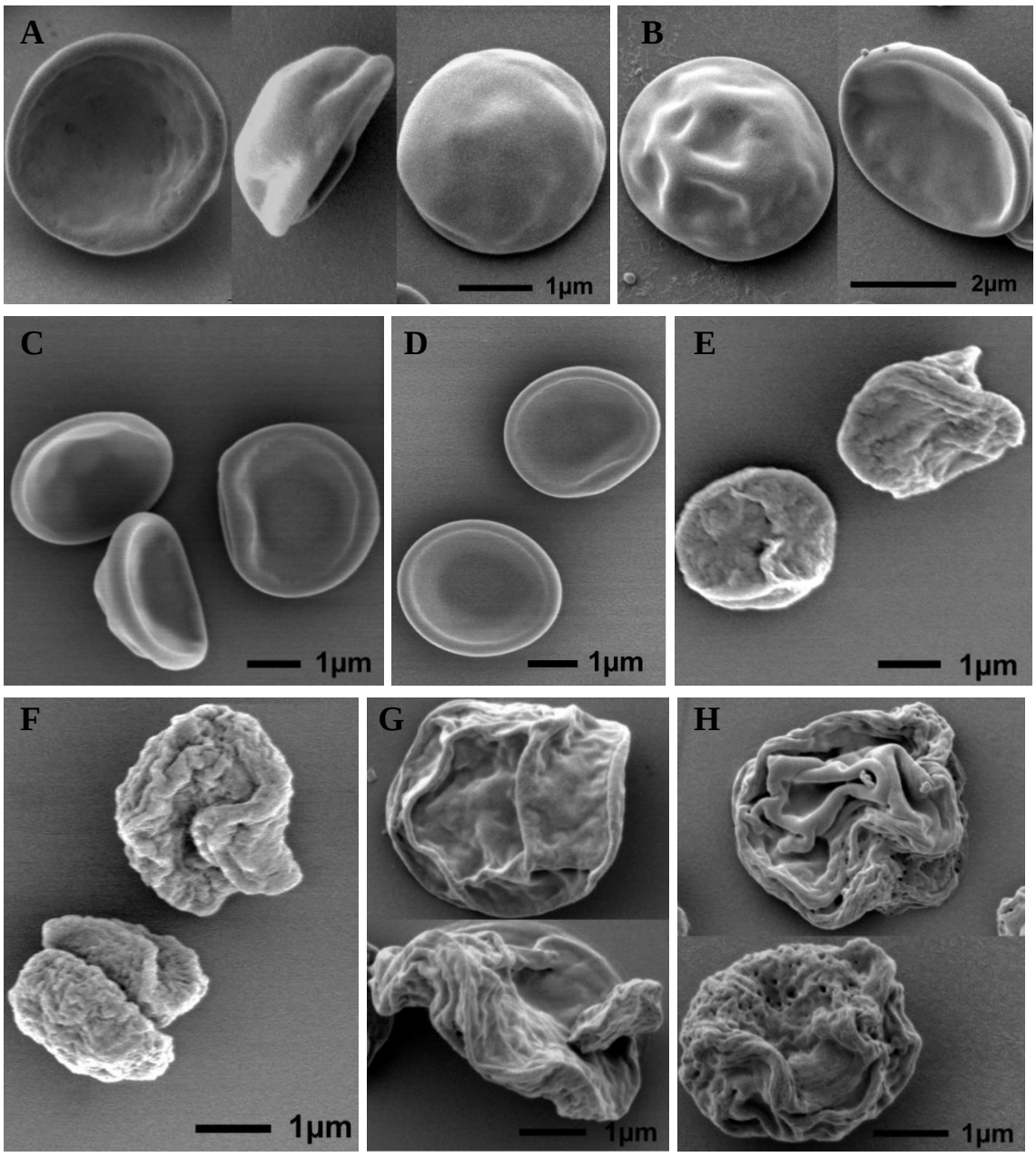

(Figure 5.12 Continued) →

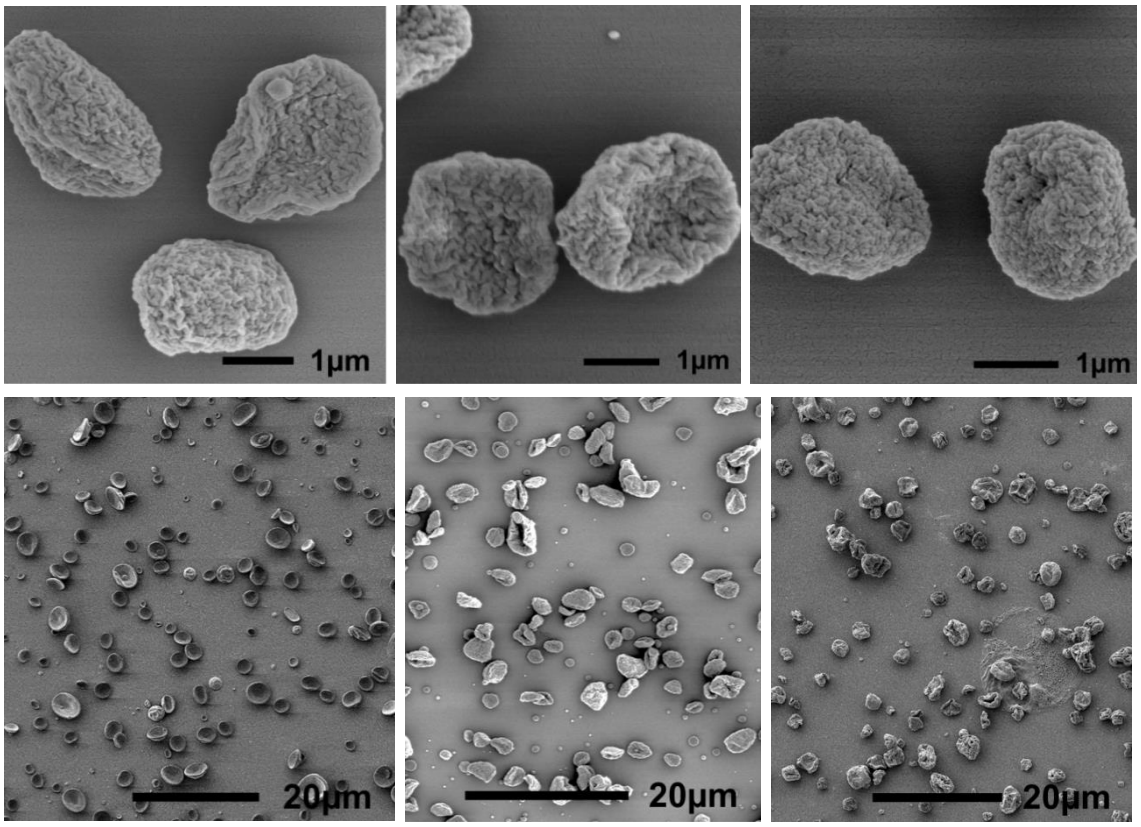

Figure 5.12 Representative SEM images of different microparticle samples: Samples AE100:0 (A), AE95:5 (B), AE85:15 (C), AE65:35 (D), AH95:5 (E), AH85:15 (F), AH65:35 (G), EH85:15 (H), EH65:35 (I), AEH70:15:15 (J), AEH50:25:25 (K), overview of sample AE85:15 (L) and overview of sample AH95:5 (M).

Figures 5.12 E-G show particles prepared using ACE:H_2O mixtures and particles here had a rougher appearance. These samples were again more disc shaped than spherical and were similar in morphology, but sample AH65:35 was slightly different seeming more wrinkled than the other two samples. The flattened appearance could be due to the collapse of porous or hollow particles during formation. The rough appearance indicated that solvent mixtures of ACE and H_2O did not have a high solubility for the solutes. Samples prepared with EtOH:H_2O mixtures (Figure 5.12 H+I) again have a rough appearance and whereas sample EH95:5 seemed to be wrinkled, EH85:15 seemed to be rough in a different way. Their morphology once again indicates that the solubility of

HPMCAS in the solvent mixtures was not very high. Particles prepared with a mixture of ACE, EtOH and H_2O (Figure 5.12 J+K) were very similar to the particles from sample EH85:15.

5.6.2 Physical form of drug

XRPD measurements of the particle powder samples showed a halo curve for all of the samples indicating that CEL was in an amorphous form in all of the samples (see Figure 5.13). However, for some of the samples (e.g. Figure 5.13 J and K) minor peaks were observed in the spectra, which could indicate a small presence of crystallinity in the samples.

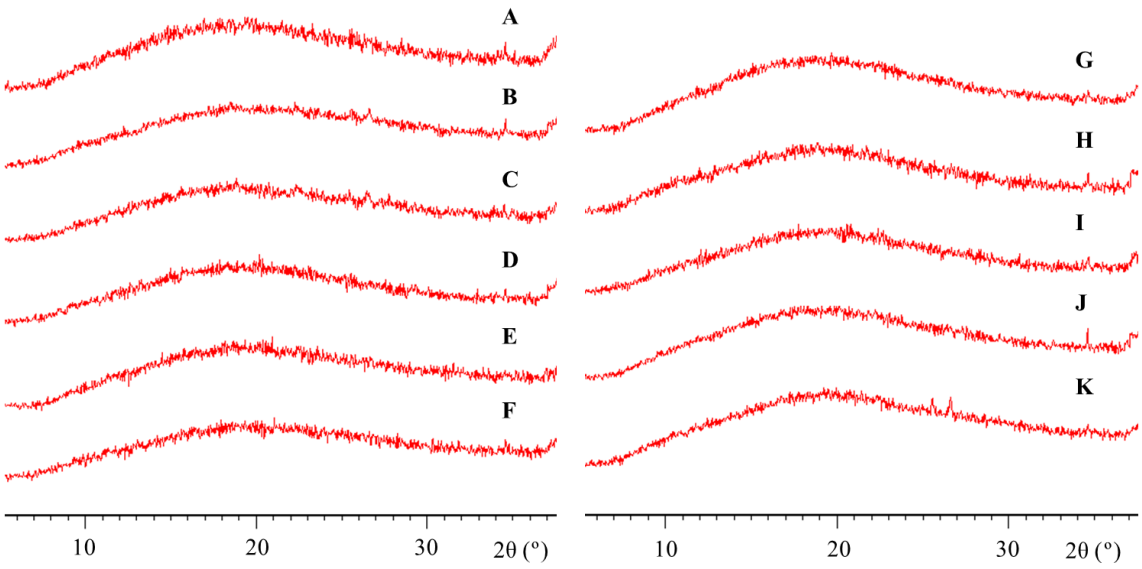

Figure 5.13 XRPD patterns of electrosprayed CEL-loaded HPMCAS particle samples, AE100:0 (A), AE95:05 (B), AE85:15 (C), AE65:35 (D), AH95:5 (E), AH85:15 (F), AH65:35 (G), EH85:15 (H), EH65:35 (I), AEH70:15:15 (J) and AEH50:25:25 (K).

The physical form of the CEL-loaded HPMCAS particle samples was also analysed using DSC and measured between 10 and 200 ºC at a heating rate of 10 ºC/min and measurements of selected samples are shown in Figure 5.14. The DSC curves of microparticle samples show no visible event while a small peak it is seen around 160 ºC

for the HPMCAS:CEL physical mixture. This could indicate that CEL was in an amorphous state in all microparticles samples but the signal from the glass transition event was not strong enough to detect. Also, no glass transition even was observed for HPMCAS neither in the particles, the physical mixture nor the pure HPMCAS sample although a halo was seen in the XRPD measurements. This could indicate that the T_g is above the measurement range. In the case that CEL was in a crystalline state in the particle sample it would be expected to see a melting endotherm around 160 ºC which was not seen in these measurements.

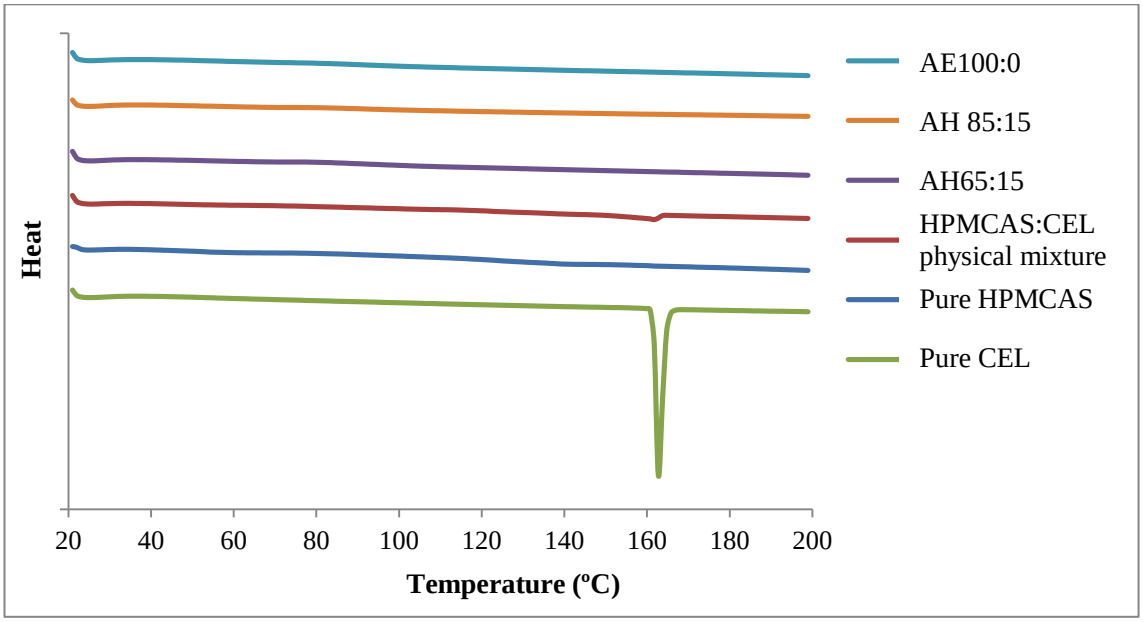

Figure 5.14 DSC curves of selected CEL-loaded HPMCAS particles.

5.6.3 Drug distribution

The surface concentration of CEL was analysed using XPS as in the previous studies. The concentration of CEL was again estimated directly from the atomic concentration of F, N and S atoms which are not present in the HPMCAS molecules. In order to eliminate the errors, ratios of N/F, S/F and F/C were used to calculate the CEL concentration at the surface of the microparticles. The surface concentration values of CEL as well as ratios of the three elements exclusive to CEL in these particles are

shown in Table 5.8. The CEL concentration on the surface of the microparticles ranged between 19-29% depending on the sample. It was observed that microparticles prepared using EtOH:H_2O mixtures had the lowest surface CEL concentration while samples AE65:35 and AH95:5 had the highest surface concentration of CEL. Further, for the samples prepared with ACE:EtOH mixtures the surface drug concentration increased consistently as a function of the EtOH concentration and for the samples prepared with ACE:H_2O mixtures it decreased as a function of the H_2O concentration.

Table 5.8 Surface chemical composition of CEL-loaded HPMCAS microparticles prepared at different drug loadings and with different solvent ratios.

Sample	N/F	S/F	F/C	CEL concentration
AE100:0	0.885	0.308	0.044	22.7 ± 0.3%
AE95:5	0.885	0.346	0.046	22.5 ± 0.6%
AE85:15	0.862	0.310	0.050	25.4 ± 1.9%
AE65:35	0.848	0.333	0.054	28.8 ± 1.0%
AH95:5	0.833	0.300	0.054	26.1 ± 0.6%
AH85:15	0.828	0.310	0.060	25.3 ± 2.1%
AH65:35	0.760	0.320	0.054	21.5 ± 2.0%
EH85:15	1.000	0.364	0.051	19.3 ± 1.5%
EH65:35	1.174	0.348	0.049	19.6 ± 1.2%
AEH70:15:15	0.815	0.346	0.050	22.5 ± 0.9%
AEH50:25:25	0.812	0.333	0.044	23.2 ± 0.8%

The surface drug content reached up to 28% for the particle samples, which were initially prepared with 20% drug loading, and two of the samples had a surface drug content slightly below the 20% initially loaded. This is different from the results obtained with CEL-loaded PLGA particles (see Table 5.6) where much higher drug

concentrations were measured. Further, the differences in surface drug concentration between the samples were not so great indicating only a small effect derived when using different solvent mixtures. This observation is explained by the differences in solubility of the solutes in the solvents (see Table 5.9), differences in evaporation of the solvents and the properties of the polymer.

Table 5.9 Solubility of CEL and HPMCAS in solvent mixtures. Values are based on solutions with approximately 5% solute concentration and 20% CEL loading.

Solvent mixture	Solubility of CEL	Solubility of HPMCAS
Pure ACE	Fully soluble	Fully soluble
ACE:EtOH	Fully soluble	EtOH < 90%
ACE:H_2O	H_2O < 50%	H_2O < 70%
EtOH:H_2O	H_2O < 25%	H_2O > 5%

For the samples prepared with ACE:EtOH mixtures both CEL and HPMCAS were soluble. During droplet evaporation, ACE will evaporate quicker than EtOH resulting in high EtOH concentrations, which would result in early precipitation of HPMCAS. This is similar to the case with CEL-loaded PLGA particles where an increase in MeOH concentrations leads to early polymer precipitation and migration of CEL to the surface. With HPMCAS microparticles an increase in the EtOH content in ACE:EtOH mixtures lead to an increase in the surface drug concentration, which correlates with the increased and quicker accumulation of EtOH during the process of particle formation and hence quicker precipitation of HPMCAS.

For the samples prepared with ACE:H_2O mixtures the HPMCAS has a good solubility until a certain point while the solubility of CEL is reduced when the H_2O content is

increased, and here a different trend was observed. During the process of particle formation, ACE would evaporate much quicker than H_2O resulting in higher H_2O concentrations, which results in precipitation of CEL early in the drying process. In this case it is likely that CEL molecules solidify before HPMCAS resulting in lower surface CEL concentration with increasing H_2O content. Such a trend was indeed observed although the general levels of surface drug concentration were not that low.

For the samples prepared with EtOH:H_2O mixtures the solubility of HPMCAS was intermediate to good depending on the EtOH content, while the solubility of CEL was low from the beginning and decreased as the H_2O content was increased. In this case, EtOH would evaporate quicker than H_2O, although both evaporating relatively slowly, and result in higher H_2O concentrations and early precipitation of CEL during droplet evaporation. Also, the solubility of HPMCAS increases as the H_2O content is increased and thus HPMCAS is expected to precipitate late in the droplet evaporation process. It is thus likely that CEL molecules solidify before HPMCAS resulting in lower surface CEL concentration with increasing H_2O content. In fact, the surface drug concentration measured here were slightly lower than the loaded concentration supporting the explanation.

5.8 Water-soluble microparticles – Drug release

Drug release from CEL-loaded HPMCAS microparticles were studied using a paddle dissolution device and were studied in different dissolution media. Since HPMCAS is soluble in water at a pH above 6 drug release takes place via a different process compared with the CEL-loaded PLGA particles. In this case, HPMCAS is likely to dissolve with time resulting in quicker release of drug. For this study, water was selected as one of the dissolution media and the release of CEL from the HPMCAS microparticles was also studied in phosphate buffer (pH 6.8). In addition, drug release

was tested under sink conditions, and here phosphate buffer (pH 6.8) + 0.5% SLS was used as the dissolution medium.

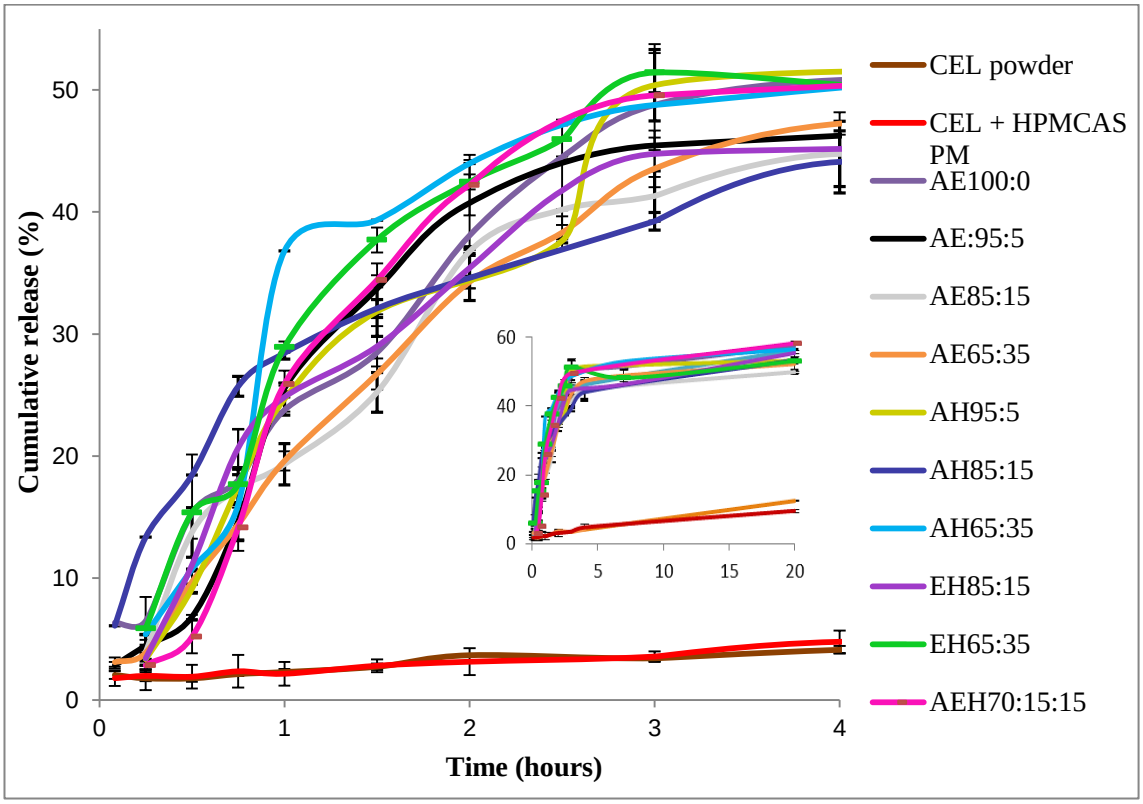

Figure 5.15 Drug release curves of CEL-loaded HPMCAS particles in H_2O. The smaller insert Figure shows drug release over a longer time interval.

Drug release profiles for microparticle samples in H_2O are shown in Figure 5.15. It is observed that all samples released between 44 and 52% of their drug load in 4 hours of exposure to the release medium. Further, it is seen with the pure CEL powder and the physical mixture of CEL and HPMCAS that only up to 5% was dissolved after 4 hours. This indicates that the solid dispersion microparticles result in a significant enhancement in drug dissolution rate compared with the pure drug and the physical mixtures, regardless of the microparticles produced from different solvent mixtures. This improved dissolution can be attributed to the smaller size of the particles as well as the amorphous form of the drug in the microparticles.

There was no clear relationship between the drug release profiles of the different samples and they were all relatively similar in their shape. Further, it is observed in the insert Figure that the drug was released continuously beyond the first 4 hours but the release rate slowed down after the first few hours plateauing at a maximum of 60% cumulative release. The released CEL molecules are presumably supersaturated in the medium but stay dissolved, most likely due to the precipitation inhibiting effect of HPCMAS. However, the cumulative drug release did pass beyond 60% due to the limited dissolution enhancement in water.

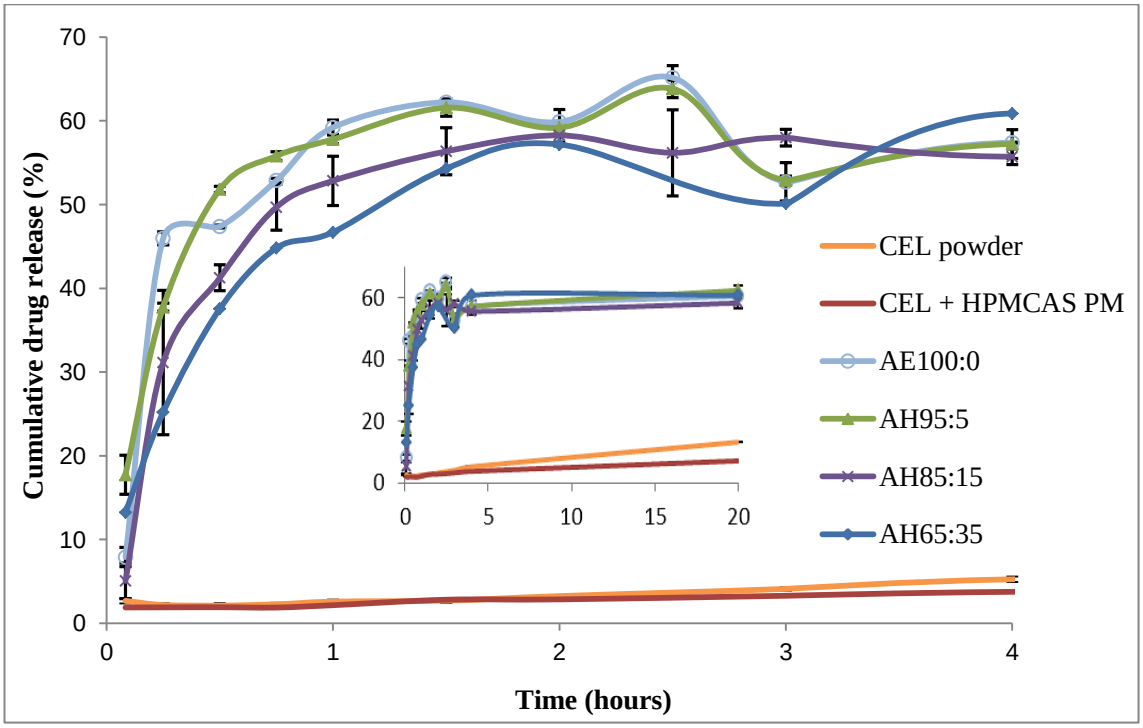

Figure 5.16 Drug release curves of CEL-loaded HPMCAS particles and in phosphate buffer pH 6.8.

The release study performed in phosphate buffer (pH 6.8) (see Figure 5.16) resulted in quicker release of CEL compared with release in H_2O but otherwise showed a similar trend as with H_2O. Pure CEL powder and physical mixture of CEL and HPMCAS again showed very limited dissolution indicating a much enhanced release from the electrosprayed particles. The maximum cumulative release was slightly higher than in

H_2O and was reached after 1-2 hours whereas it took much longer time when released in H_2O. With this Figure, there was a clearer trend in the drug release indicating that drug release rates decreased with increasing H_2O content in the ACE:H_2O for particle preparation. This finding correlated with the surface CEL concentration observed which also decreased as the H_2O concentration was increased. Also again the insert Figure indicated that CEL were kept dissolved for at least 20 hours probably due to the precipitation inhibition of HPMCAS.

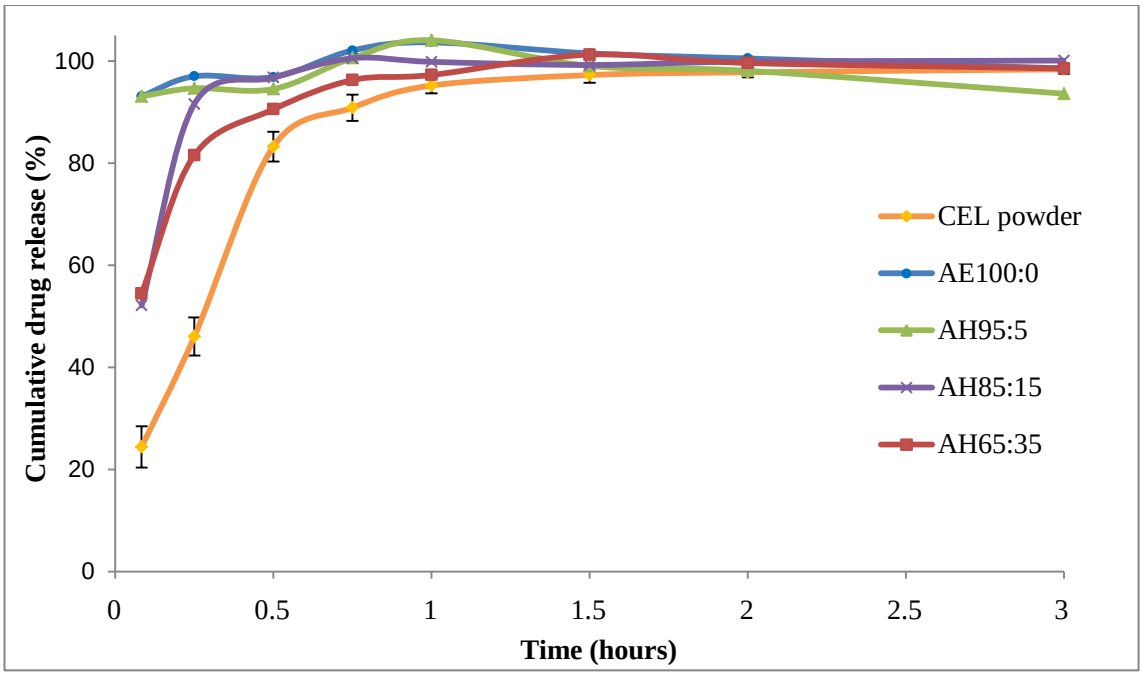

Figure 5.17 Drug release curves of CEL-loaded HPMCAS particles in phosphate buffer (pH 6.8) + 0.5% SLS.

Drug release from microparticle samples in phosphate buffer + 0.5% SLS is shown in Figure 5.17 and indicated much higher release rates as a consequence of the sink conditions provided. Here, all particle samples were fully dissolved, some almost immediately and some after an hour of release. The pure CEL powder was also fully dissolved but was clearly the slowest to be dissolved, once again indicating the dissolution enhancement from the electrosprayed microparticle formulations. Also, it

was observed that the drug release rate from the samples decreased with increasing H_2O content of the solvent mixtures used for particle preparation. This supports the observation in Figure 5.16 where the same trend was demonstrated indicating that the drug release was influenced by the solvent composition used and the resulting attributes of the particles, including their drug distribution. The influence of the size and morphology of particles from different samples on their drug release kinetics could not be seen from the drug release profiles in Figures 5.15-5.17 indicating that they were too similar to show distinctive release patterns. Thus, the small differences observed in the surface drug concentration indicate that the drug distribution was the main characteristic distinguishing the drug release profiles of the microparticles.

5.9 Summary

Microparticles of CEL molecularly embedded in a polymer matrix were prepared by electrospraying using different solvent mixtures and two different polymers to investigate the influence upon the resulting particle characteristics and release behaviour. The first set of mixtures studied consisted of a good solvent, ACE, and an anti-solvent, MeOH, for PLGA at different ratios. Particle formation, particle characteristics, drug distribution and drug release were examined and all of these were found to be influenced by the solvent composition.

Particle formation was strongly influenced by the polymer molecular conformation during droplet formation and by the anti-solvent concentration during droplet drying. A strong correlation was found between particle size and morphology, the solubility of the polymer in the solvent mixtures and the electrical conductivity of the solutions. The lack of chain entanglements in droplets containing anti-solvent resulted in compact polymer conformation and a grain-like appearance of the particles. Smaller particles were produced from the addition of anti-solvent as this produced smaller droplets and

compact polymer chains. Further, the early precipitation of polymer and low chain interaction with increasing content of anti-solvent resulted in surface enrichment of drug (from 10 and 20% up to 41 and 57% respectively), which was also demonstrated by the increasingly faster drug release rates observed.

A different polymer, HPMCAS, was introduced for the second set of studies, partly to examine whether a polymer with higher solubility than CEL in the solvents used would result in higher drug distribution towards the centre of the particles. Solvent mixtures of ACE, EtOH and H_2O were used, which can be a poor solvent for either of the solutes, CEL and HPMCAS, depending on the ratios used. It was expected that in different mixtures and ratios the solute with the poorer solubility in the mixture would precipitate first, leading to a lower concentration of that solute near the surface of the particles.

CEL-loaded HPMCAS microparticles were prepared with different shapes ranging from collapsed disc shape to compact particles with different surface roughness and appearance. The particle morphology was dependent on the solvent combinations and solubility of the solutes in the solvent mixtures. XRPD measurements indicated that CEL was amorphous in all particle samples and that it was finely dispersed in the polymer forming a solid dispersion. The surface drug concentrations of particles were similar among samples although samples prepared with EtOH and H_2O showed slightly lower concentration than initially loaded. The drug release studies showed improvement in dissolution rate and effective precipitation inhibition provided by HPMCAS. The differences in release rate was difficult to observe although some differences were observed under sink conditions.

The results all in all demonstrate the importance of solvent composition in particle preparation and indicate potential for exploiting this dependence to improve pharmaceutical particle design and performance.

Chapter 6

Spray drying of solid dispersions: The influence of mixed solvent systems on particle characteristics and comparisons with electrospraying

This chapter introduces the use of spray drying for preparing solid dispersion microparticles composed of Celecoxib and PLGA. The influence of process parameters, with specific focus on the solvent system, the particle characteristics as well as the drug release kinetics was examined. It was found that spherical particles were formed with a relatively broad size distribution from the spray drying process. The spray dried particles were prepared using the same solvents used in the electrospraying process, including mixed solvent systems with acetone and methanol, and the resulting particles were compared with the electrosprayed particles. The spray dried particles were similar in morphology regardless of the solvents used and generally showed a broad size distribution. They were less porous both on their surface and inside the particles and resulted in a more homogeneous drug distribution compared with the electrosprayed counterparts. Drug release from the spray dried particles varied depending on the solvent composition used but in general took place at a slower rate than the corresponding electrosprayed particles. Spray drying showed less control over particle characteristics compared with electrospraying for the studied setup and formulations.

6.1 Spray drying and particle preparation

The spray drying technology has commonly been used to prepare drug-loaded microparticles and solid dispersions and it is therefore prior knowledge that drug can be

highly dispersed in polymeric microparticles as a solid dispersion [Kojima *et al.* , Paudel *et al.*]. Drug-loaded PLGA particles have successfully been prepared by several researchers using laboratory scale spray-dryers and generally together with an inert loop device in order to use organic solvents [Meeus *et al.* 2012, Wang and Wang 2002]. In order to provide a reasonable basis for setting up comparisons between the electrosprayed and spray dried particles the operation parameters for the spray drying equipment was adjusted to obtain particles with similar diameter as the particles prepared with electrospraying, i.e. around 2-4 µm.

6.1.1 Introduction to setup and conditions with spray drying

The main adjustable operation parameters in spray drying are: the liquid feed rate, atomizing gas flow rate, drying gas flow rate, inlet temperature and outlet temperature, where outlet temperature is mainly controlled by the inlet temperature. A liquid feed rate of around 3 ml/min was selected based on previous studies done with the spray drier where polymeric particles around 1-5 µm were obtained depending on the remaining parameters. In order to prevent agglomeration and aggregation of particles during the drying process it is important to keep the outlet temperature well below the T_g of the processed materials. PLGA and CEL were both shown to have a T_g around 50 °C and thus initially an outlet temperature of 40 ºC was used to prepare the particles as demonstrated by O'Hara and Hickey [O'Hara and Hickey 2000].

Particles were prepared applying the above conditions and examined using SEM and it was observed that the particles had agglomerated forming bridges between the particles (see Figure 6.1). The surface morphology observed resulted from prolonged exposure to the electron beam and the particles had a smooth surface otherwise. The bridges between the particles are likely to have resulted from the close proximity of the outlet temperature to the T_g of PLGA, hence in the further studies an outlet temperature of

30 ºC was used in order to ensure temperatures below the T_g of PLGA during the whole spraying process. This required an inlet temperature of around 45 ºC. The disadvantage of using a low outlet temperature relative to the boiling point of the solvent is that the particle samples are likely to contain more residual solvent. Due to the low outlet temperature the maximum atomizing gas flow rate of 12.4 L/min and the maximum drying air aspiration rate of 375 L/min were used to best avoid residual moisture.

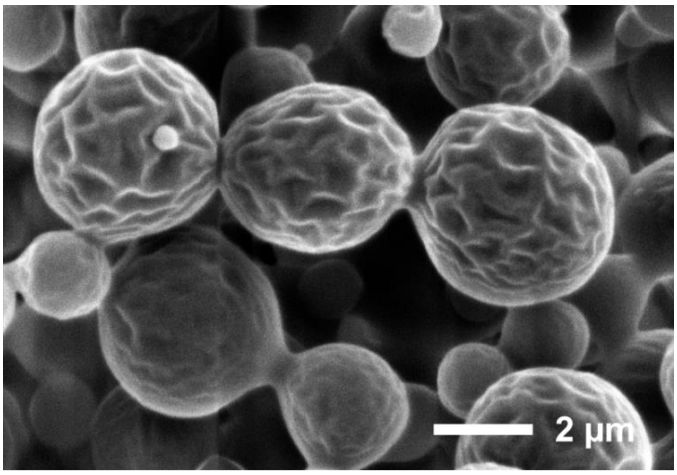

Figure 6.1 Particles prepared with ACE at 3 ml/min and 40 ºC outlet temperature.

6.1.2 Spray drying of CEL-loaded PLGA particles – solutions and setup

In order to study the effect of different solvents on the formation of microparticles in the spray drying process, microparticles were examined as a function of the solvent while the solute concentration and drug loading were kept constant at 5% w/v and 20% w/w, respectively. Particles were prepared in ACE and ACN again (see Table 6.1) similar to the electrosprayed particles to compare the particles and the process with electrospraying and the electrosprayed products. Since the composition of feed solution were identical to those used for some of the electrospraying experiments the characteristics of the solutions were the same as those once measured. Thus, the evaporation rate, solubility, dynamic viscosity, intrinsic viscosity and electrical conductivity can be seen on Tables 4.3-4.4 and Figures 4.8-4.9.

Table 6.1 Composition of feed solutions spray dried and the operational values applied.

Feed solutions	Drug loading	Feed rate	Atomizing gas flow rate	Aspiration rate	Inlet temp.	Outlet temp.
5% Solute conc. in ACN	20%	3 mL/min	12.4 L/min	375 L/min	43-47 ºC	30 ºC
5% Solute conc. in ACE	20%	3 mL/min	12.4 L/min	375 L/min	43-47 ºC	30 ºC

6.1.3 Characteristics of particles

SEM images of the spray dried microparticles prepared with ACN and ACE are presented in Figure 6.2 and it is observed that the particles were all spherical with smooth surfaces. None of the particles seemed to be fused together as a low outlet temperature was used. There were no visible differences in the morphology between the particle prepared using the two solvents and in both cases the mean diameter of the particles was around 2 µm. Both samples had a relatively broad particle size distribution (with a polydispersivity index of 42 and 38 for particles prepared with ACN and ACE respectively), compared with the electrosprayed samples prepared at similar conditions (see Table 4.6). The range of the particle diameters observed spanned from around 0.2 µm to around 5µm and the particles were thus in the same size range and the particles prepare with electrospraying using ACE and ACN, although particles below 1 µm were produced with spray drying. However, there were visible differences in particle morphology compared with microparticles prepared using electrospraying. The spray dried particles observed here were not porous on their surface and were in fact very smooth and spherical in appearance compared to their electrosprayed counterparts.

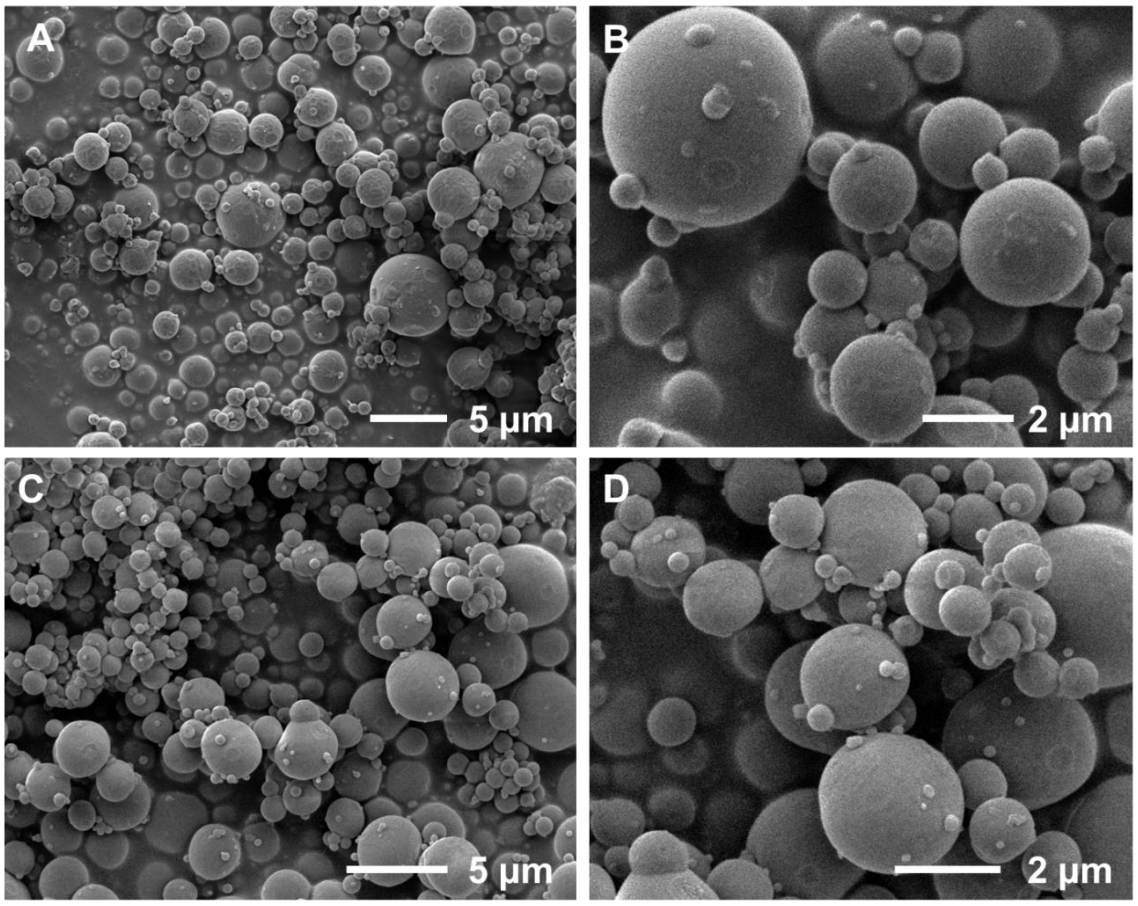

Figure 6.2 Representative SEM images of spray dried microparticles prepared in ACN (A, B) and ACE (C, D) prepared with an outlet temperature of 30 ºC.

The internal structure of the spray dried microparticles prepared using ACE and ACN was studied using FIB/SEM to also determine the porosity of the particles (see Figures 6.3 and 6.4). The images in Figure 6.3 show that particles of different size were sectioned and none of the particles show any visible porosity at any section of the particle. The images in Figure 6.4 also show no visible pores in the particles examined. The particles prepared with both solvents are thus assumed to be solid with little porosity and would thereby have a higher density compared with porous particles of the same diameter. Many of the particles prepared using electrospraying had an extensive porous network inside the particles and some were even hollow (see Figures 4.26 and 5.6). They therefore must have had a lower density than the spray dried particles. This

is, however, still to be confirmed quantitatively, for instance by measuring the differences between their geometric and aerodynamic diameters of the particles or by using a gas pycnometer.

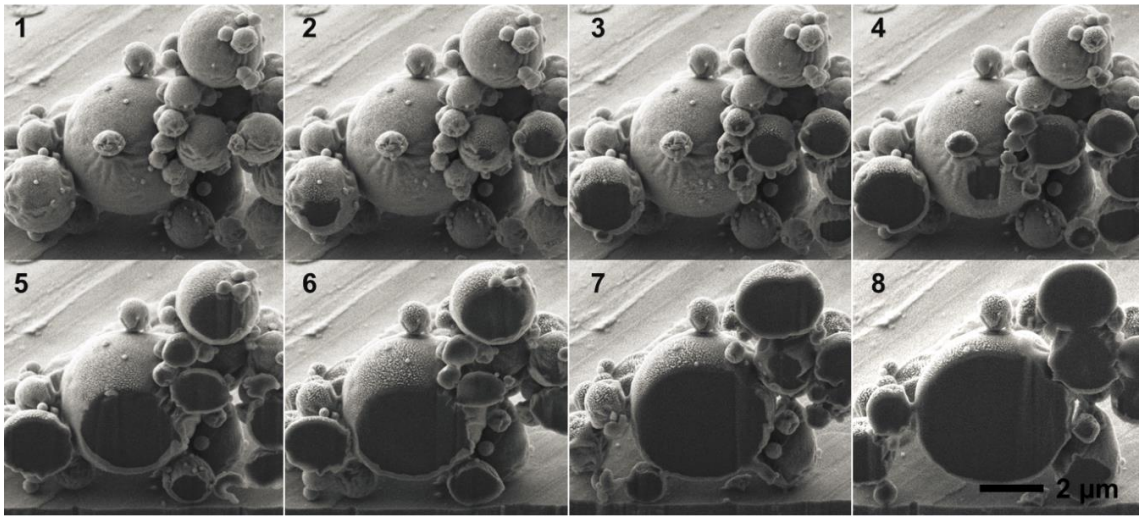

Figure 6.3 FIB/SEM images of spray dried microparticles prepared in ACN. The numbers indicate progression through the sample.

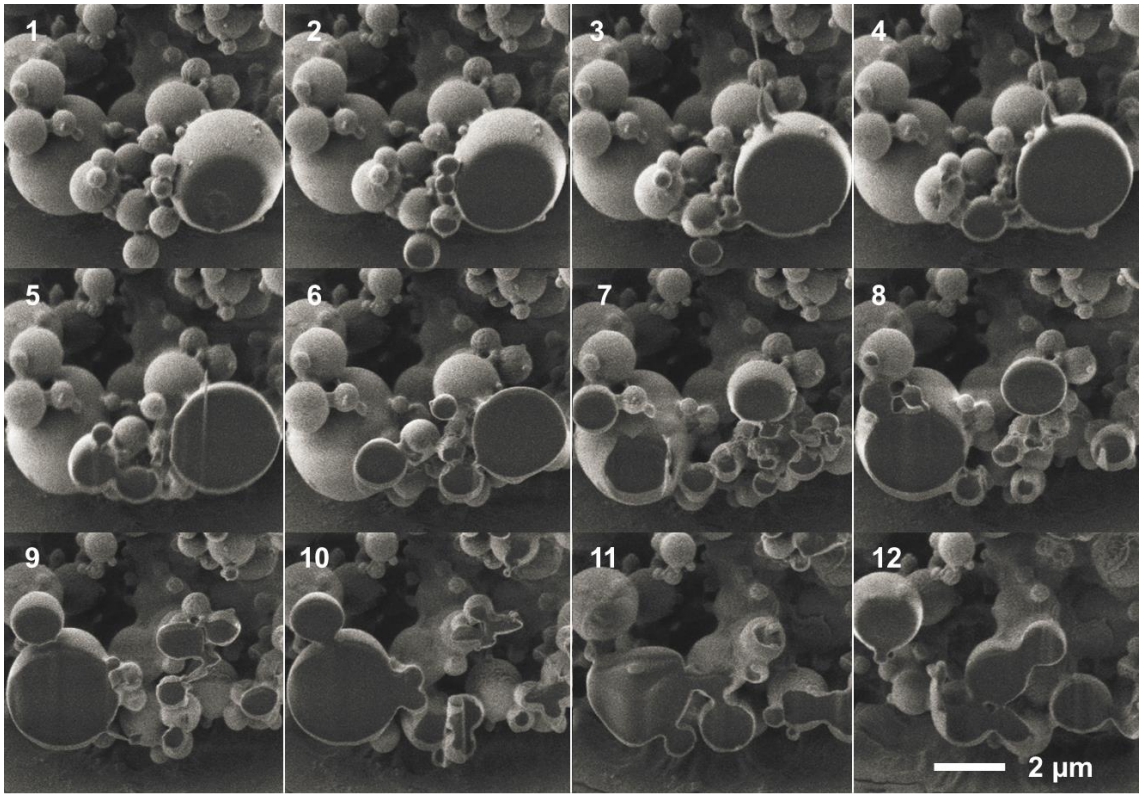

Figure 6.4 FIB/SEM images of spray dried microparticles prepared in ACE. The numbers indicate progression through the sample.

Analysis of the solid state form of CEL in the spray dried particles is shown in Figures 6.5 and 6.6. The DSC curves show that there is an endothermal peak around 57 ºC for both curves which is similar to the T_g of PLGA used in this study. A small endotherm event can be seen in Figure 6.5 A around 130 ºC, which could be due to a very small portion of crystalline CEL or a CEL solvate. However, due to its much smaller area compared with the glass transition event it is also likely to be a measurement error. Since no CEL melting peak was observed the DSC curves indicate that CEL was highly dispersed in the system in the amorphous state (see Figure 6.5).

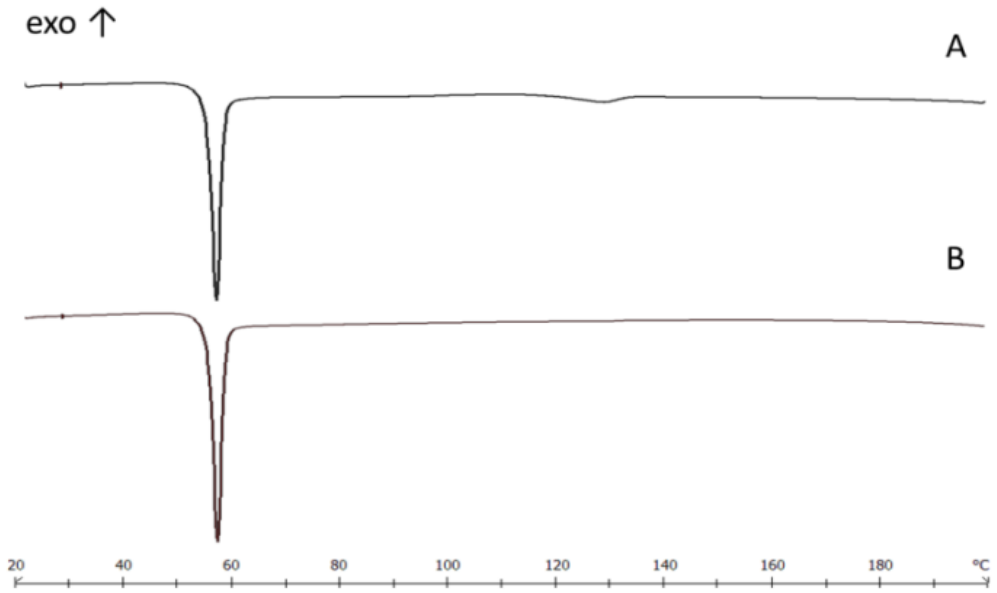

Figure 6.5 DSC curves of spray dried particles, prepared in ACE (A) and ACN (B).

The physical state of CEL in the spray dried particle was confirmed by XRPD analysis, in which both the spray dried samples prepared show no distinct peaks crystalline peaks, thus indicating that both CEL and PLGA were amorphous in the microparticles. The single T_g observed in DSC measurement suggests that CEL and PLGA were likely to be in a single amorphous phase with no noticeable difference in the shape or location of the peaks for the two curves. Further, no recrystallization was seen indicating that CEL was very well dispersed in the PLGA matrix or dissolved in molten PLGA. The T_g

found here is consistent with the ones observed for the electrosprayed samples (Figure 4.14) being in between the glass transition for particles with 10% and 30% drug loading.

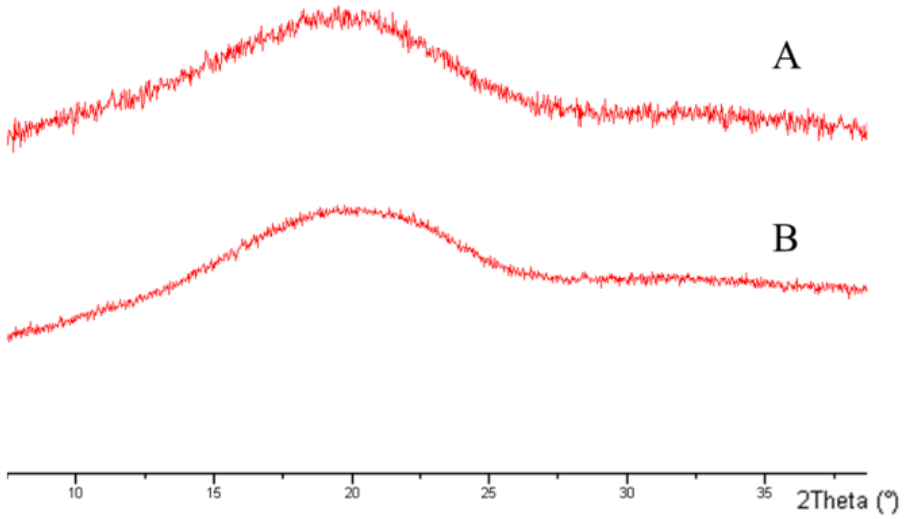

Figure 6.6 XRPD curves of spray dried particles prepared in ACE (A) and ACN (B).

6.1.4 Drug release from microparticles

Drug release from the spray dried particles prepared in ACE and ACN was studied using the same methodology as for the electrosprayed particles, a paddle dissolution apparatus with 500 mL of phosphate buffer (pH 6.8) + 1.5% SLS and analysed using HPLC (see section 3.12.2).

Also, it is worth mentioning that two types of spray dried samples were collected, a compact powder mass from the region between the cyclone and the collection vial, and a fine powder from the collection vial. Both types of powder samples were characterized to observe any differences and no noticeable differences were seen on XRPD and optical microscopy. The results in section 6.1.2-6.1.3 were collected and analysed using the fine powder. Drug release profiles of the compact and fine powder samples showed lower release rates (~50% release after 24 hours) for the compact

sample compared with the corresponding fine powder (~90% release after 24 hours) both prepared at 5% solute concentration, 20% drug loading in ACE. The lower release rates for the compact powder is not surprising due to their lower effective surface area to volume ratio from which the release can take place.

The drug release curves of the spray dried particles are presented in Figure 6.7 and show that drug release took place similarly to the electrosprayed particles prepared with the same formulation composition but with two quite different processes with different operational parameters.

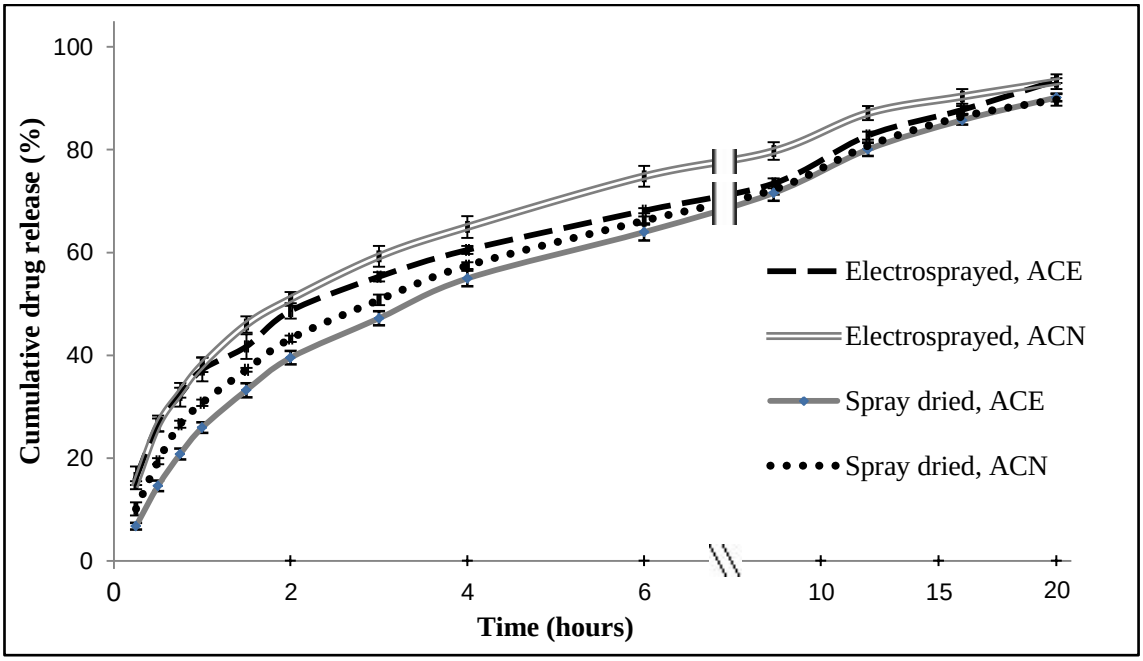

Figure 6.7 Drug release profile of microparticles prepared with 5% solute concentration and 20% drug loading in ACE or ACN, using spray drying and electrospraying, measured over 20 hours. Error bars indicate the standard deviation from the mean.

For both of the spray dried samples a small burst release was observed as with electrospraying but the burst release for the spray dried samples was smaller indicating less drug situated near the surface of the particles. Although the spray dried particles were smaller on average than the electrosprayed particles, with some of the particles

being significantly smaller, the release rates observed were similar. It was again observed that an extended release took place during the 20 hours the particles were exposed to release medium and between 89 and 93% of their drug content was released in this time. The particles prepared with ACE had a slightly lower release rate than those prepared with ACN, during the first 6 hours of release, and from then on their release curves were nearly indistinguishable. This could be explained by the broader size distribution observed for ACN where a larger population of small particles released their drug load early on.

6.2. Spray drying mixed solvent study and solution characteristics

6.2.1 Introduction to spray drying of mixed solvent systems

In continuation of the study on electrospraying of CEL-loaded PLGA particles using different solvent mixtures, the same solvent mixture composed of ACE (good solvent for PLGA) and MeOH (poor solvent for PLGA) were employed to vary the solvent power and the evaporation rate systematically. To further study the process of particle formation and influence of the solvent compositions on particle characteristics, the resulting microparticles were characterized using different analysis methods to examine the morphology, inner structure, surface chemistry, solid state properties and drug release rates. Moreover, the effect of polymer molecular conformation on processes that govern drug release from CEL-loaded PLGA microparticles prepared by spray drying were investigated similar to the studies performed electrospraying (section 5.1-5.5).

6.2.2 Setup and sample preparation

All microparticle samples were prepared at similar drying conditions (inlet temperature of 45 ℃, outlet temperature of 30 ℃, drying air flow rate of 375 L/min; atomizing air flow rate: 12.4 L/min and feed flow rate: 3 mL/min). The gentle drying conditions, and

in particular the low outlet temperature was again chosen due to the low glass transition temperatures of PLGA and CEL as explained in section 6.1.1.

Particle samples were prepared at four different ratios of solvent mixtures. The solute concentration was kept constant at 5% w/v and a drug loading of 10% was used. An overview of the samples prepared is presented in Table 6.2.

Table 6.2 Overview of solutions used for spray drying and their characteristics.

Sample	Drug loading (%w/w)	Polymer conc. (%w/v)	ACE:MeOH ratio (molar ratio)	Intrinsic viscosity
SD100:0	10	4.5	100:0	0.24
SD90:10	10	4.5	90:10	0.22
SD75:25	10	4.5	75:25	0.18
SD69:31	10	4.5	69:31	0.15

6.2.3 Solubility and polymer configuration

Polymer molecular conformation in feed solutions was evaluated by characterizing the rheological properties of feed solutions, which was done to study the polymer molecular conformation in solidified microparticles. It is assumed that droplet evaporation and particle formation take place so quick with spray drying that it does not provide enough time for polymer molecules to change their conformational structure from droplet formation to solidification. The solubility studies were performed as explained in section 5.1.4 and because the feed solutions used for the electrospraying (section 5.1) and spray drying (section 6.2) studies were exactly the same only the same set of solubility measurements are used (section 5.1.4).

6.2.4 Evaporation study

The evaporation profiles of the solvent mixtures and the feed solutions used for the spray drying studies are shown in Figure 6.8. The evaporation profiles were measured using TGA and the temperature was in this case kept constant at 30 °C to mimic the outlet temperature during the spray drying process. The weight loss was recorded as a function of time.

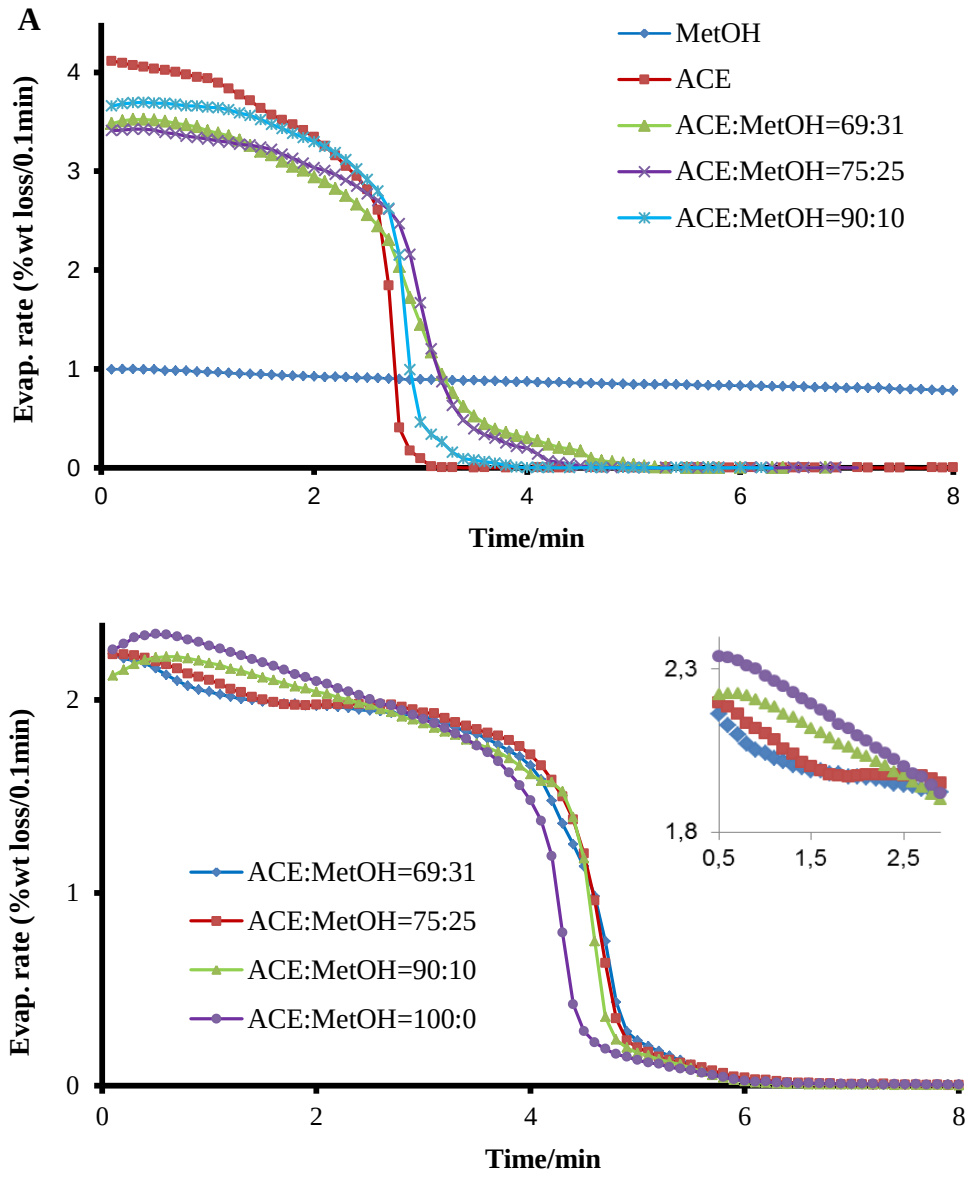

Figure 6.8 Estimation of the evaporation rates of the pure solvent mixtures (A) and the spraying solutions (B) performed at 30 °C. Results denote mean values for evaporation rate (n = 3).

The evaporation rate profiles of pure solvents (without CEL and PLGA) all showed reverse S-shaped curves representing three drying phases (Figure 6.8 A); a slowly declining evaporation rate in the beginning, a fast declining evaporation rate next and a slowly declining evaporation rate in the end. In the first phase, a loss in % solvent weight took place at a high rate, and the evaporation of solvent was mainly governed by the affinity between the solvent molecules. In the subsequent phase, the evaporation slowed down rapidly, indicating that the majority of the solvent had evaporated. In the final drying phase, the evaporation rate remained low as the residual solvents evaporated, possibly due to the reduced solvent volume.

The evaporation profiles of the solvents were changed when PLGA and CEL were added to the solvent systems (Figure 6.8 B). Four evaporation phases were observed at solvent ratios 69:31 and 75:25, whereas three phases were observed at solvent ratios 90:10 and 100:0. Further, a general decrease in the evaporation rates and an extended drying time were observed when PLGA and CEL were added to the solvent mixtures (compare Figures 6.8 A and 6.8 B). The slow final stage could be explained by the reduced solvent concentration and the closer interaction between solvents and solutes.

It was found that for solvent systems without solutes, a prolonged evaporation time was observed with an increase in the MeOH content of the systems (Figure 6.8 A), indicating the lower evaporation rate of MeOH. During the last part of the drying process, the evaporation rate approaches the rate of the solvent with the lowest volatility, in this case MeOH. The evaporation curves of the feed solutions containing PLGA and CEL showed lower evaporation rates compared with the pure solvent mixtures (Figure 6.8 A). The prolonged evaporation times with the feed solutions is explained by the interactions between the molecules of the solvent and the polymer, which could have led to a reduction in the rate of solvent evaporation. It has previously

been reported that the evaporation rate of a solvent in suspension is the same as the evaporation of the pure solvent while the evaporation of a solvent in a solution is different from the evaporation rate of the pure solvent [Charlesworth and Marshall 1960, Ranz and Marshall 1952]. The reduction in evaporation rate observed for the feed solutions could be explained by changes in the vapour pressure resulting from the addition of solutes.

The drying profiles of ACE:MeOH = 90:10 and ACE:MeOH = 100:0 were similar during the first drying phase, while in the second drying phase, ACE:MeOH = 90:10 showed a delayed drying profile (Figure 6.8 B). This indicates that addition of MeOH prolongs the drying time of the solution due to its lower evaporation rate. However, no clear differences were observed in the drying time by further increasing the MeOH content from 10% (90:10) to 31% (69:31) in the feed solution, even thought this was observed for the solvent mixtures (Figure 6.8 A). This could suggest that for all solutions containing MeOH, PLGA molecules begin precipitating according to their MeOH content and go from solution to form a suspension where the evaporation may be closer to that of the pure solvents, and hence faster. This increase in evaporation rate during precipitation may compensate for the decrease in evaporation rate experienced from the lower evaporation rate of MeOH.

Due to the lower evaporation of MeOH compared with ACE and the poor solubility of PLGA in MeOH, anti-solvent precipitation of PLGA will occur when the ACE:MeOH ratio decreases during evaporation and reaches the solvent saturation point for PLGA. This takes place at 65:35 ACE:MeOH molar ratio at 5% solute concentration and 10% drug loading, but this ratio becomes higher as the solute become more concentrated during solvent evaporation. CEL would still be dissolved at the saturation point of PLGA due to its better solubility in MeOH and its lower concentration in the solutions.

Also, considering the difference in molecular weight between CEL and PLGA, a difference in mass transfer is expected between the two molecules when the solutes move in the evaporating droplet. This is likely to have an influence on the distribution of the two molecules in the resulting microparticles.

6.3 Characteristics of spray dried particles

6.3.1 Drug entrapment and moisture content of particles

CEL-loaded PLGA microparticles were prepared with the 4 different solvent systems at 10% drug loading and otherwise at identical solute concentration and operation conditions. For all four particle formulations prepared, the entrapment efficiency was around 100% or slightly above 100% indicating good entrapment of the drug within the PLGA matrix (see Table 6.3). There was no obvious correlation between the processing conditions of the samples and the measured drug entrapment. The residual moisture in the particles was also measured after preparation of the spray dried samples. For all samples the residual moisture content was between 0.47% and 0.55% which can be regarded as low. There was again no correlation between the solvent composition of the solutions and the residual moisture observed although it was expected that SD69:31 would have a higher moisture content due to the higher MeOH content in these particles. Yet, possibly due to the small differences in boiling point and the rapid drying with the spray dryer no solvent related influence was observed. Further, the low residual moisture content in the microparticles suggests that the process parameters used in the present study were appropriate for effective drying of the PLGA microparticles.

6.3.2 Morphology and size of particles

SEM images of the particles prepared are presented in Figure 6.9. The microparticles were all spherical with smooth surfaces. The variation in solvent compositions did not

seem to have a visible influence on the morphology of the microparticles. All four microparticle samples exhibited similar morphology without fusion between the individual particles and could not be distinguished based on their appearance. The images indicate that the differences in properties between the two solvents used to form mixtures did not have detectable influence on the morphology of the particles. This could be explained by the rapid drying process of spray drying, which may not have allowed sufficient time for PLGA to change its structural conformation during drying of individual droplets at varying levels of ACE and MeOH. The PLGA chains may thus have stayed stretched out and well entangled resulting in smooth a surface morphology.

Table 6.3 Composition of feed solutions and physicochemical properties of CEL-loaded PLGA microparticles (5% solid concentration, 10% drug loading). Results denote mean ± SD (n = 3).

Sample	Mean diameter (μm)	Polydispersivity index (%)	Entrapment efficiency (%)	Surface CEL concentration (%)
SD100:0	2.0 ± 0.8	41.5	106.4 ± 1.0	14 ± 2
SD90:10	2.1 ± 0.7	31.6	106.9 ± 1.5	10 ± 1
SD75:25	1.8 ± 0.7	41.2	102.7 ± 0.0	18 ± 7
SD69:31	1.4 ± 0.5	32.2	101.4 ± 0.1	22 ± 1

The mean diameter of the microparticles was measured to be in the range of 1.4-2.2 μm (see Table 6.3), although many smaller and larger particles were prepared as seen in Figure 6.9. The particle size distribution was relatively wide with the polydispersivity index of the samples being in the range of 32-42% for all samples (see Table 6.3). Particles seemed to become smaller as the MeOH content was increased with particle from SD69:31 being the smallest and particles from SD 100:0 and SD 90:10 being the

largest. Although all of the samples were of similar size with a relatively large standard deviation, particles from SD69:31 were found to be significantly smaller compared with particles from SD100:0 and SD90:10.

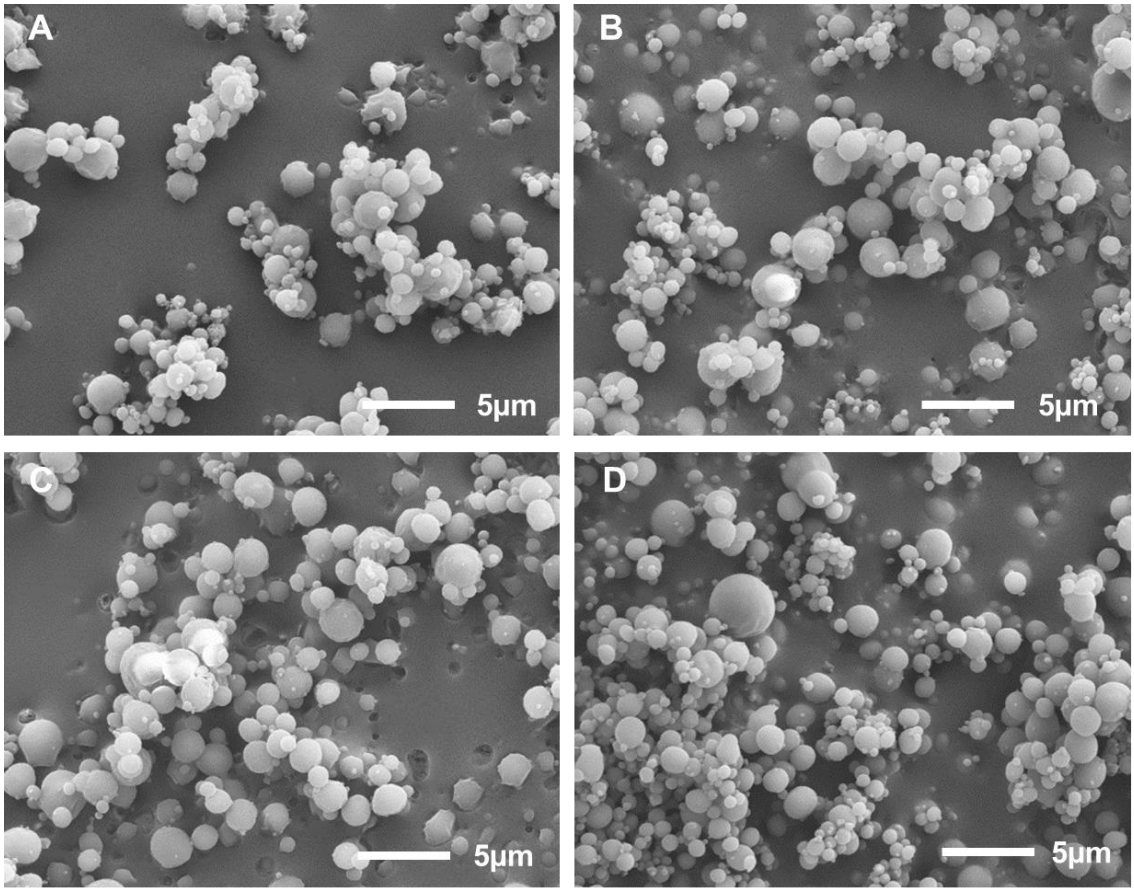

Figure 6.9 Representative SEM images of spray dried PLGA microparticles loaded CEL, samples SD100:0 (A), SD90:10 (B), SD75:25 (C) and SD69:31 (D).

With spray drying, it is known that a more viscous feed solution gives rise to larger particles. Figure 6.10 shows with at increasing PLGA concentrations solutions with high solvent power increase more in viscosity. Further, it was shown that the evaporation rate of the solvents decreased with increasing MeOH content, resulting in prolonged drying times of microparticles and possibly also smaller particles with denser inner structure (see Figure 6.8). It was thus expected that particles would become increasingly smaller as the MeOH content was increased and similar effect has

previously been reported [Shenoy *et al.* 2005a]. Such a trend was observed for the particles produced in this study, although the samples had a broad size distribution.

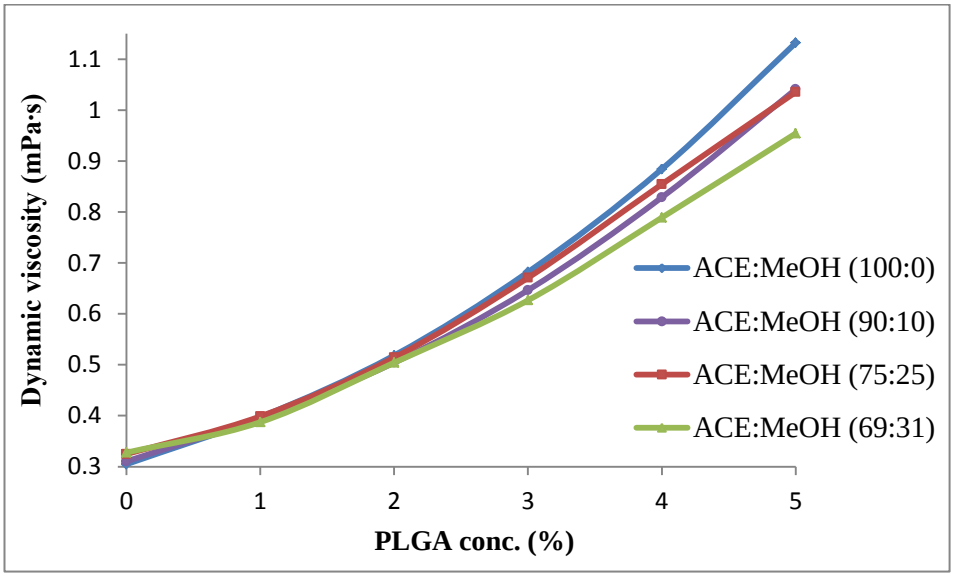

Figure 6.10 Viscosity of PLGA solutions with different solvent ratios as a function of concentration

6.3.3 Inner structure and porosity

Cross section images of the spray dried microparticles (see Figure 6.11) indicate that microparticles produced with high MeOH content (SD75:25 and SD69:31) exhibited a more solid inner structure compared to microparticles prepared with low MeOH content (SD90:10 and SD100:0). In the latter two samples particles containing visible pores were observed as seen on Figure 6.11 C and D. Although a majority of particles were solid in all four samples the presence of pores in two of the samples indicates a difference in the particle formation process.

The absence of visible pores in the majority of particles could be attributed to the high solute concentrations used in this study as well as the mild drying conditions applied in this study. The high solute concentration results in a denser polymer network at shell formation in the droplet evaporation process, while the low drying temperature gives

more time for the polymer to diffuse towards the core of the solidifying particle, both leading to denser particles (see section 2.3.3). This also correlates well with the observation in particle size, where the smaller particles were here the non-porous particles indicating that the particles are more densely arranged inside.

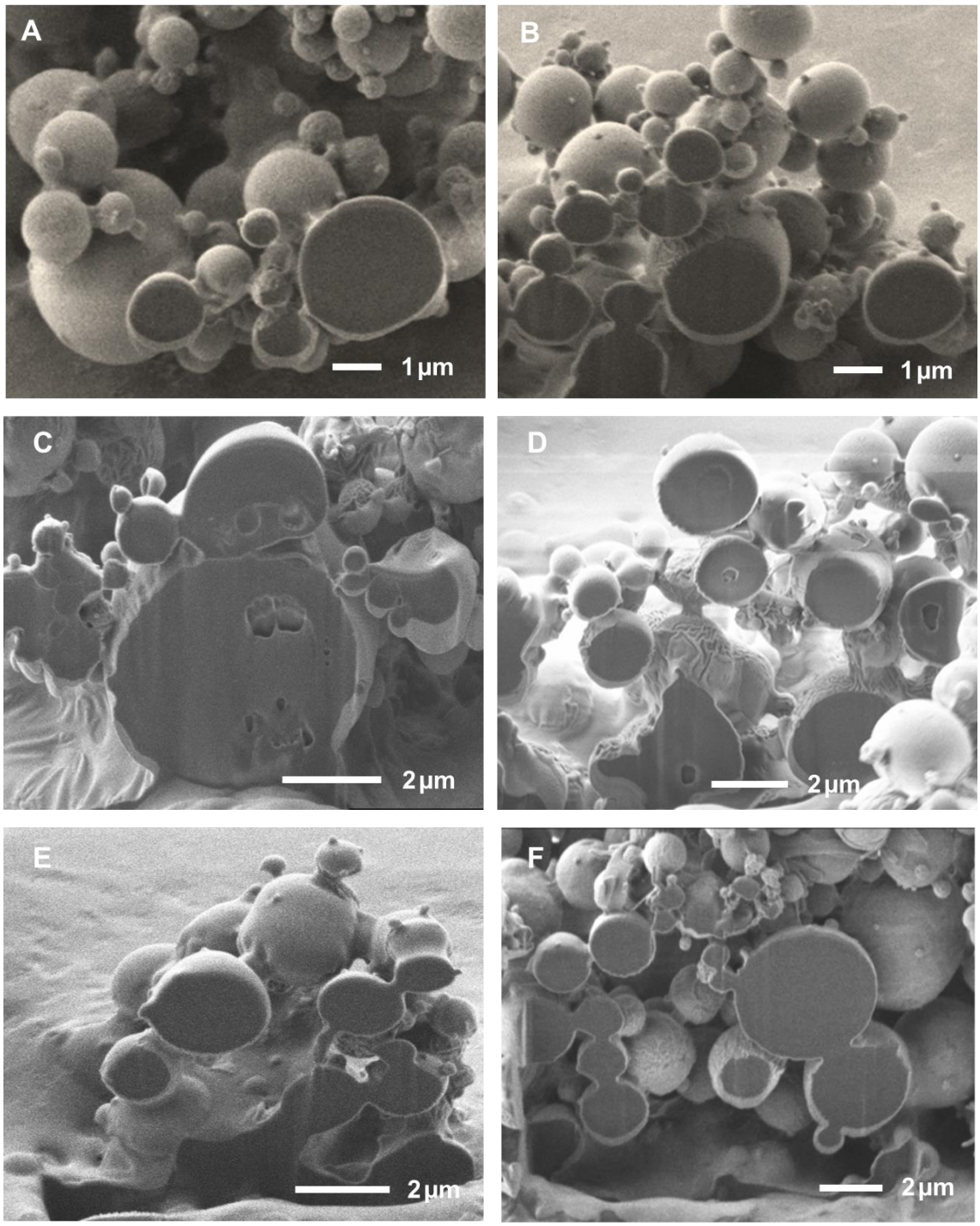

Figure 6.11 Representative FIB/SEM images of PLGA microparticles loaded with 10% (w/w) CEL, samples SD100:0 (A, C), SD90:10 (B, D), SD75:25 (E) and SD69:31 (F).

The pores observed in particles of samples SD100:0 and SD90:10 could be explained by the differences in evaporation rate and solubility measured for the four solvents compositions. The faster evaporation rate of pure ACE:MeOH = 100:0 and ACE:MeOH = 90:10 result in less time for the droplets to shrink due to earlier polymer precipitation and shell formation compared to ACE:MeOH = 75:25 and ACE:MeOH = 69:31 solvent mixtures. This could lead to a less dense inner structure and higher chance of getting pores. Moreover, the higher solubility of PLGA in solutions with ACE:MeOH = 100:0 and ACE:MeOH = 90:10 result in more stretched out PLGA structural conformation and more chain entanglement. This could result in slower polymer diffusion rate and therefore slower shrinking of the droplets, again leading to less dense and more porous particles. The same can be said for the higher viscosity of solutions with less MeOH which result in larger droplets and therefore also less dense particles.

6.3.4 Solid state characterization of particles

The physical state of CEL in the spray dried microparticles were studied using DSC and XRPD and the DSC curves are presented in Figure 6.12. All samples showed a single endothermic event at approximately 55 °C, indicating the glass transition of PLGA alone or PLGA and CEL combined. The absence of a recrystallization and melting event may further provide indication that the CEL was dispersed in the PLGA matrix in an amorphous state.

Results from the DSC curves are supported by the XRPD data presented in Figure 6.13, in which no crystalline peaks were observed in the diffractograms of the spray dried microparticles. All spray-dried microparticles formulations exhibited a halo shape characteristic for materials in their amorphous state.

The different solvent compositions used in this study did not result in detectable differences in the solid state properties of CEL in the PLGA matrix,

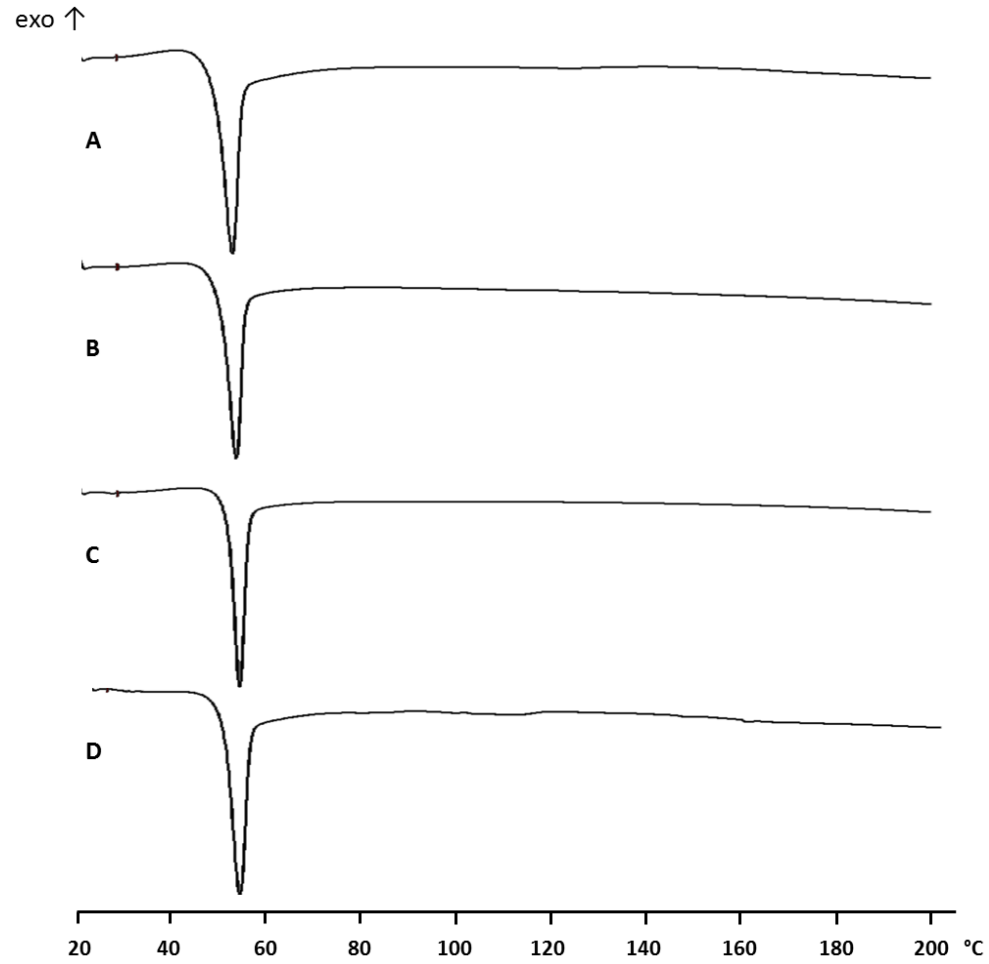

Figure 6.12 DSC thermogram of spray dried microparticles with 10% (w/w) CEL, samples SD100:0 (A), SD90:10 (B), SD75:25 (C) and SD69:31 (D).

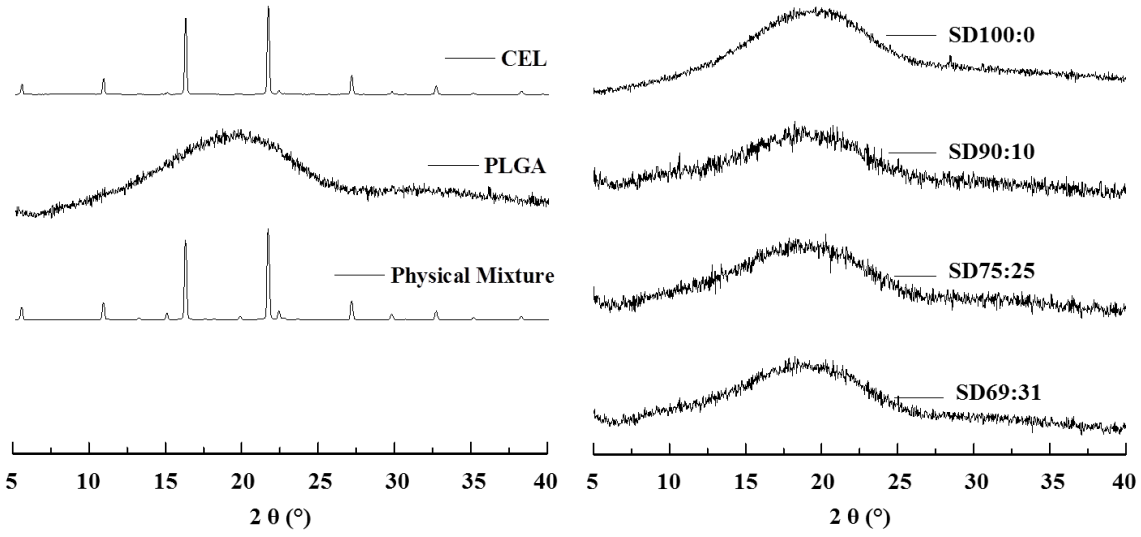

Figure 6.13 Representative XRPD profiles (B) of CEL-loaded microparticles with 10% (w/w) CEL, samples SD100:0, SD90:10, SD75:25 and SD69:31.

6.3.5 Drug distribution in particles

XPS was used to obtain the relative atomic concentrations (in %) of CEL on the surface of the spray dried particles. The surface CEL concentration was found to be in the range of 10-22% (see Table 6.3) whereas all samples were loaded with 10% drug. The results indicated a correlation between the solvent composition used to prepare the particles and the surface CEL concentration with the CEL concentration increasing as the MeOH content was increased. Again, as with the particles size sample SD90:10 did not quite follow the trend indicating that there could be an indirect correlation between the particle size and surface CEL concentration.

The increase in CEL concentration observed at high MeOH contents could be explained by differences in the diffusion rate of CEL and PLGA during the particle formation process (see section 2.3.3). For example, in the mixed solvent systems of ACE:MeOH = 75:25 and ACE:MeOH = 69:31, anti-solvent precipitation of PLGA is likely to occur prior to the precipitation of CEL due to the poor solubility of PLGA in both MeOH and ACE. Further, the PLGA molecules are much larger than the CEL molecules making them less mobile in the solution, especially when part of the solvent has evaporated. When PLGA has precipitated, part of the CEL molecules may still be dissolved moving around in the forming particles. When solvent escapes from inside of the particles the CEL molecules may thus migrate towards the particle surface together with the residual solvents (i.e. ACE and MeOH) resulting in the surface enrichment of CEL. This effect was, however, much less pronounced with the spray dried microparticles compared with the electrosprayed microparticles shown in Table 5.8.

6.4 Drug release from spray dried particles

The drug release behaviour of the CEL-loaded PLGA microparticles was investigated using the paddle dissolution method described in section 3.12.2. The release profiles of

CEL from the spray dried particles are shown in Figure 6.14. It was observed that all of the spray dried samples had a lower drug release rate relative to the dissolution of pure CEL and all of the samples showed a low burst release below 10% except for sample SD69:31. Further, the four microparticle samples exhibited different release profiles with an increase in release rate observed as the MeOH content was increased. Samples SD100:0 and SD90:10 were close with many of their corresponding points being within the standard deviation. The results correlated well both with the particle size data and with the XPS surface chemistry results all showing a trend between the solvent ratio used and their respective data.

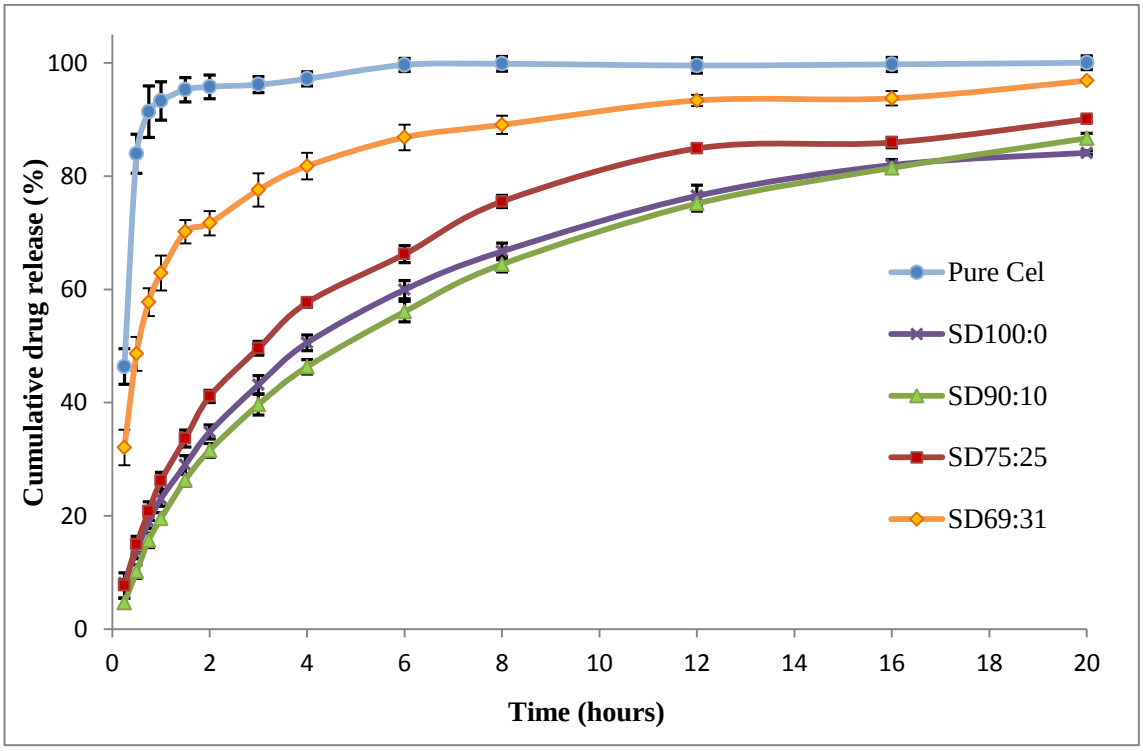

Figure 6.14 Drug release profile of spray dried microparticles prepared with different solvent ratios at 5% solute conc. and 10% drug loading, in phosphate buffer (pH 6.8) + 1.5% SLS, measured over 20 hours. Error bars indicate standard deviation (n=3-4).

Drug release from PLGA microparticle matrices will typically take place either via diffusion-driven or diffusion-driven followed by erosion-driven release due to the

hydrolysis of ester bond linkages in the PLGA molecules [Giteau *et al.* 2008]. For the uncapped PLGA such as the one used in this study, erosion of the PLGA matrix has been reported to take place after 15 days [Giteau *et al.* 2008] but would depend on the size and porosity of the particles as well as the release medium used. In the present study, the release from PLGA microparticles were investigated in a phosphate buffer solution (pH 6.8) containing SLS for 20 hours. Due to the negligible solubility of PLGA in phosphate buffer and the ability of the buffer to maintain the pH in a narrow range the drug release was most likely diffusion-driven. Release is further believed to have been mainly influenced by the PLGA matrix structure and the radial distribution of the drug in the microparticles.

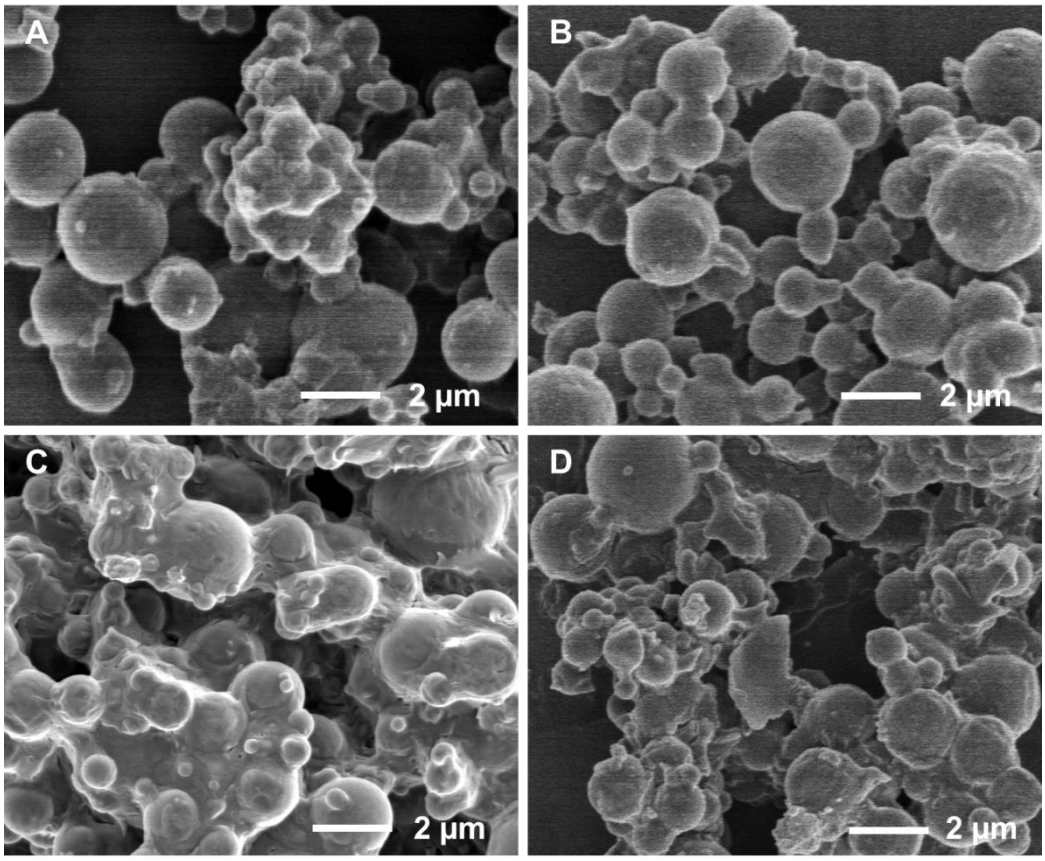

Figure 6.15 SEM images of spray dried microparticles after drug release in phosphate buffer + 1.5% SLS, samples SD100:0 (A), SD90:10 (B), SD75:25 (C) and SD69:31 (D).

The absence of critical erosion of the PLGA matrix structure could be supported by SEM images of the particles taken after the release studies (see Figure 6.15). The images show that particles were generally still intact after they had released most of their drug, which accounted for 10% of their mass. The connecting areas between some particles is most likely residual SLS from the release medium. Some of the particles in Figure 6.15 D seem to have lost their spherical structure possibly indicating that polymer molecules in SD69:31 were more loosely interconnected and thus lost their structure after releasing their drug load. This would make sense from the perspective of polymer structural conformation which was more compact and less entangled for SD:69:31 compared with the other samples.

The differences observed in the release profile of the particle samples could be attributed to the different physicochemical properties of the particles resulting from the spray drying process when using different solvent compositions. As expected, burst release was highest for sample SD69:31 (Figure 6.14), which also showed the highest surface CEL enrichment and the smallest particle size. The same trend was observed throughout the whole release curve and both the particle size and the surface CEL concentration correlated well with the release rate, which changed according to the MeOH content. The trends observed indicate that the increased surface area to volume ratio from the smaller particle size and the shifted radial drug distribution both have an influence on the drug release kinetics. Further, the structural conformation of PLGA in the microparticles may also have had an influence on the measured release rates. The fast precipitation of PLGA in the spray drying process for all of the solvent systems used may have resulted in different conformation of PLGA in the microparticles depending on the initial state within the solvents, which in turn influenced the CEL release profiles.

6.5 Comparison of spray dried and electrosprayed particles

In the previous sections the preparation of CEL-loaded PLGA microparticles using electrospraying and spray drying was described and the influence of various processing parameters on particle formation and the resulting particle characteristics was discussed. In this section some of the results obtained with electrospraying and spray drying are compared and the differences observed are discussed. The comparisons are mainly drawn on studies where similar formulation were used, that is formulations where CEL-loaded PLGA particles were prepared with 5% solute concentration, 10% drug loading and using the solvents ACE, ACN or solvent mixtures of ACE and MeOH.

6.5.1 Particle size and size distribution

In studies using electrospraying, mean particles sizes of 4.3 µm and 4.2 µm were observed for ACE and ACN, respectively, and generally particles prepared with ACN were slightly smaller than those prepared using ACE (see Table 4.6 and Figure 4.20). In studies using spray drying, mean particles sizes around 2 µm were observed for both ACE and ACN with no clear difference in the size of particles prepared with ACE and ACN. These results indicate that particles produced with electrospraying were generally larger than those prepared with spray drying at the same formulation condition. Yet, with both techniques the particle size could be altered by increasing or decreasing different parameters such as the viscosity of the solution, the flow rate of the feed solution, the electrical conductivity of the feed liquid (for electrospraying) and the drying settings (for spray drying).

Since the two techniques operate by different means and at very different mass outputs (high output for spray drying and low output for electrospraying) it is difficult to compare the resulting particle sizes based on a fixed set of formulation conditions. By increasing the liquid feed rate with spray drying, larger particles could have been

produced but would have required higher drying temperatures and would therefore be at the cost of inferior drying conditions for this specific PLGA/CEL system. Yet, it was observed with electrospraying that the solvents ACE and ACN resulted in slightly different particle size whereas no difference was observed with spray drying. The dynamic viscosities of the feed solutions were measured to be 1.01 mPa·s for the ACE solution and 0.97 mPa·s for the ACN solution, thereby being very close and possibly insignificant for the particle sizes. The differences in the electrical conductivity of ACE and ACN (see Table 4.3) are however, believed to have had an influence on the size of the electrosprayed particles but not on the spray dried particles. Thus more factors were involved with electrospraying determining the size of particles produced.

With the microparticles prepared using mixed solvents the same trend was observed with respect to particle size. Particles prepared with electrospraying were again larger than those prepared with spray drying but for both techniques the particles became smaller as the MeOH content was increased. Again, for electrospraying the influence of MeOH content on particle size was more pronounced, most likely due to the differences in electrical conductivity as well as the much slower drying process, which allowed longer time for droplet shrinking. However, as mentioned, electrospraying and spray drying are two different techniques and the two setups used have markedly different output and drying mechanisms. Therefore, the comparison in particle size was limited to observations made on the differences among samples for each of the two techniques and differences in the particle size distributions.

The size distribution measured for electrosprayed and spray dried particle samples were significantly different and was consistently observed throughout the studies performed. Whereas the electrosprayed particle samples had a polydispersivity index ranging between 6-24 (between 6-11 for 16 out of 25 samples measured) the spray dried

particles samples had a polydispersivity index between 32-42. This indicates that a more homogeneous population of microparticles can be achieved using electrospraying compared with the spray drying setup used in the present studies. Whereas electrospraying is known for its capability of producing near monodisperse particles this is not an easy task with spray drying. Some types of spray dryers are claimed to produce particles within a more narrow size distribution, for instance by using an internal mixing two-fluid nozzle (see Niro, http://www.niro.com/niro/cmsdoc.nsf/webdoc/ndkw653cl6) as opposed to the conventional two-fluid nozzle which was used in this study. Also, the Nano Spray Dryer produced by Buchi is claimed to produce smaller particles within a relatively narrow size range by utilizing a vibrating mesh in the spray dryer head (http://www.buchi.com/Nano-Spray-Dryer-B-90.12378.0.html). However, it is difficult and inappropriate to compare these spray drying setups with electrospraying at the current stage until a semi-commercial electrospraying setup is developed.

6.5.2 Morphology and Porosity of particles

In the studies using electrospraying several types of shapes were observed for the particles, ranging from spherical or elongated shapes to several types of collapsed shapes such as disc or bowl shaped particles. Further, different types of surface morphology were observed with electrospraying, such as smooth, porous, corrugated and grainy, all depending on the process parameters applied. In comparison, the spray dried particles all seemed to have similar shape and morphology. All of the particles produced were spherical with a smooth surface, regardless of changes in process parameters that were otherwise critical for particle shape and morphology with electrospraying.

The different shapes observed with electrospraying resulted either from changes in the solute concentration or from collapsing of the particles which in some way also was

determined by the solute concentration or viscosity of the solution. By modifying the viscosity of the feed solution, particles went from being collapsed (~2-3% PLGA) to spherical (~4-7% PLGA) and to elongated (~10% PLGA) and further increase in viscosity would have led to fibres being produced (electrospinning). That said, collapsed particles have also been demonstrated to be produced with spray drying by applying certain parametric values similar to electrospraying [Alamilla-Beltrán *et al.* 2005, Iskandar *et al.* 2003]. Elongated particles have also been produced [Corrigan *et al.* 2002, Gilani *et al.* 2005] but were generally not smooth as with electrospraying and formed via another mechanism, such as via crystallization.

The different morphologies observed with electrospraying were explained partly by the polymer conformation in the solvents used and due to heat and mass transfer mechanisms during particle formation, which resulted in several interesting morphologies. In the study with solvent mixtures using electrospraying, particle morphology could be modified depending on the solvent:anti-solvent ratio (see section 5.3.2). With spray drying no differences were observed in the resulting particle morphology when changing the solvent:anti-solvent ratio, although polymer precipitation and molecular level changes in the polymer conformation were expected to take place.

With electrospraying, PLGA began to precipitate during droplet evaporation, with a MeOH content of only 10% (ACE:MeOH 90:10), while with spray drying the polymer did not manage to precipitate even with a MeOH content of 31% (ACE:MeOH 69:31), despite being very close to the saturation point of PLGA (ACE:MeOH ~65:35). This is explained by the much quicker drying process with spray drying compared with electrospraying, which is believed to allow particles to solidify almost instantaneously before any changes can happen in the polymer matrix structure. The evaporation studies

using TGA showed that drying of drops at 25 ˚C and 30 ˚C were very similar in duration and indicate that the quick drying with spray drying results from higher mass and heat transfer, due to the warm drying gas and the high air circulation rate.

In the studies using electrospraying it was observed that most of the particles prepared were porous to some degree while some were hollow and others were solid. The spray dried samples were mainly absent of pores but in two of the samples prepared some pores were observed although not as porous as the electrosprayed particles. The differences observed in the porosity of spray dried and electrosprayed particles prepared using the same solutions can be attributed to differences in the particle formation process in the two techniques. Again, spray drying involves an active drying process with warm dry gas to dry droplets while the present electrospraying setup relies on passive drying. Thus, with spray drying the heat from the active drying could have reached into the core of the particles, at some point in the process, while with electrospraying solvent evaporation is likely to have only taken place at the surface, creating an imbalance in the radial distribution of solid material.

From the cross sectional images in Figure 4.22 it was observed that the particle porosity increased with increasing solvent concentration. Further, particles prepared with ACE were less porous than those prepared using ACN. These findings suggested that the porosity is influenced by the amount of solvent that needs to evaporate or escape to form the dry particle and the rate at which they dry. Solutions with low solute concentration (high solvent concentration), solvents with high boiling points and a passive, slow drying process would thus all result in increased porosity. This correlates well with the findings from this study. Moreover, in that case that the range of polymer concentrations at which electrospraying and spray drying form porous particles is different, pore formation could possibly be avoided for electrosprayed particles simply

by using higher solute concentrations. Yet, for mixed solvent solutions where early precipitation of PLGA took place, the particle formation process was different and resulted in less porous structures. It is believed that when PLGA precipitates in the droplet, the polymer interacts less with the solvent and shell formation does not take place. Instead, polymer nano-clusters move inwards towards the centre of the droplet and go together as the solvent evaporates (Figure 5.11).

Although it is obvious that the drying process in spray drying is much quicker than in electrospraying, this is somewhat contradicting with the common principle in spray drying that high drying rates result in a more porous particles than low drying rates [Vehring 2008; Yao *et al.* 2008]. Spray drying resulted in less porous particles even though it dried the particles at a quicker rate than with electrospraying. This further reaffirms that the drying process of the two techniques are not comparable. Also, although not investigated in this work, there is likely to be a difference in the density of the spray dried and electrosprayed particles given the differences in porosity and size of the particles. It is believed that the electrosprayed particles are generally less dense compared to the spray dried particles, based on the greater porosity and larger particles observed. This could be further investigated in future studies.

6.5.3 Solid state characteristics of the particle based solid dispersions

Comparing the solid state characteristics of microparticles produced with electrospraying and spray drying, both XRPD and DSC analysis showed similar data for the two techniques. DSC curves of electrosprayed particle samples (Figures 4.14) and spray drying particle samples (Figures 6.5 and 6.12) were absent of a melting endotherm around 162.7 ˚C, the measured melting endotherm for pure CEL. However, for some electrosprayed samples with higher drug loading (Figure 4.14B) and exothermal event indicating recrystallization and a shifted melting endotherm was

observed, which could also have been the case for spray dried samples at higher drug loading, had it been examined. Only a single glass transition event was observed, suggesting that the drug was highly dispersed in the polymer matrix. The presence of two nearby glass transition events would have indicated separate amorphous phases. Yet, in this case the individual T_g's for CEL and PLGA may have been too close to detect, as demonstrated by the single T_g observed for the physical mixture of CEL and PLGA (see Figure 4.6). Also, a relatively high solubility of CEL in PLGA, above the T_g of PLGA, was indicated by the small or shifted melting endotherm of the physical mixture. The absence of a melting peak for most of the electrosprayed and spray dried samples is thus partly attributed to the dissolution of CEL in PLGA before it reaches its melting point. Thus the solid state form of CEL within a PLGA matrix cannot be accurately determined only using DSC.

XRPD measurements for electrosprayed (Figure 4.23, 5.7) and spray dried samples (Figure 6.5, 6.13) all indicated that the samples were amorphous from the "halos" observed and the absence of sharp peaks. The diffractogram of electrosprayed samples and spray dried samples were very similar and could not be distinguished. However, the physical mixture of CEL and PLGA on Figure 4.10 showed clear peaks indicating crystallinity in the sample. Although the XRPD data strongly suggested that the samples were amorphous for both electrospraying and spray drying, differences in the solid dispersions produced could not be evaluated by this data. As with XRPD, observations made using polarized light microscopy did not indicate the presence of anisotropy in neither the electrosprayed nor the spray dried samples, which reaffirms the absence of crystallinity in the samples.

The results indicate that with both particle preparation processes CEL is well dispersed within the PLGA matrix preventing small crystals from forming at a drug concentration

up to 30% and perhaps also even higher. This, however, does not tell whether the drug is homogeneously distributed within the particles or more concentrated in some regions for either for the processes. Comparisons of drug release results suggest that some samples have a higher concentration of drug on their surface, with their faster release rates but this is not certain.

6.5.4 Drug distribution in particles

The surface chemistry of microparticle samples were studied to investigate the drug distribution and homogeneity of the solid dispersion prepared. XPS measurements of electrosprayed samples indicated that CEL was generally distributed towards the surface of the particles. All of the measured samples showed higher surface drug concentration than what was initially loaded into the particles. Further, the surface drug concentration increased with an increase in MeOH concentration for the binary solvent systems and also with an increase in drug loading. With the spray dried samples XPS measurements indicated that particles prepared mainly with ACE had similar surface drug concentration as initially loaded into the particles. Also for the spray dried samples the surface drug concentration increased with increasing MeOH concentration. The differences in the general surface drug concentration of particles prepared using the two techniques are seen in Tables 5.6 and 6.3 and shown together in Table 6.4.

For all of the four sample conditions the electrosprayed samples showed a higher surface drug concentration than the spray dried samples. This indicates that there are differences between the two processes which results in higher accumulation of drug towards the surface of the particles. For both techniques the increased migration of CEL towards the surface of the particles with increasing MeOH content was attributed to the small molecular weight and better solubility of CEL in MeOH. This would have allowed CEL molecules still dissolved in the droplet to move out through the polymer

network towards the forming particle surface together with the solvent. The higher surface drug concentrations observed for electrosprayed samples could thus be explained either by the slower solvent evaporation experienced with the passive drying process of electrospraying, or the influence of electrical charge on the molecular distribution of the particles. The electrical charge on the surface of droplets during particle formation could have attracted CEL molecules, slightly more than PLGA molecules, to distribute CEL molecules near the surface of the particles. This could be a result of polar groups in the CEL molecules although both molecules are generally nonpolar. The role of the electrical charge on the charging and distribution of individual molecules in droplet with electrospraying has not been reported but would be interesting to understand better.

Table 6.4 Surface drug concentration of electrosprayed and spray dried particle samples prepared with 10% drug loading using solvent mixtures of ACE and MeOH.

Sample	Electrosprayed samples	Spray dried samples
ACE:MeOH (100:0)	20 ± 1%	14 ± 2 %
ACE:MeOH (90:10)	31 ± 2%	10 ± 1 %
ACE:MeOH (75:25)	38 ± 1%	18 ± 7 %
ACE:MeOH (69:31)	41 ± 1%	22 ± 1 %

XPS analysis of electrosprayed CEL-loaded HPMCAS particles showed a relatively low surface drug concentration compared with the CEL-loaded PLGA particles. In fact, some of the samples had a surface drug concentration lower than initially loaded concentration (see Table 5.8). This could suggests that the drug distribution not only is determined by the solvent evaporation rate and electrical charge but also influenced by the solubility of solutes in the solvents and solvent mixtures used as well as the molecular mobility of the drug molecules in the given polymer matrix.

6.5.5 Drug release

Drug release curves for both electrosprayed and spray dried particle samples prepared with a single solvent showed diffusion mediated release taking place over several hours. The electrosprayed samples showed different degrees of burst release depending on the preparation conditions while the spray dried samples generally showed less burst release. Figure 6.16 presents a comparison of drug release for particles prepared with ACE and ACN using electrospraying and spray drying. It is seen that the electrosprayed particles had a slightly higher drug release rate than the spray dried particles and that for both techniques, particles prepared using ACN had a quicker release than those prepared using ACE. The differences in release rate from these particle samples is attributed to their differences in porosity, particle size and drug distribution. Particle size is considered as one of the main determinants of drug release from microparticles and this was also observed from Figures (4.26-4.31). Large particles have a lower surface to volume ratio than small particles and also have a longer diffusion distance to travel for the drug, both of which lead to slower drug release.

The spray dried samples were expected to release their drug quicker than the electrosprayed samples due to their smaller average size compared with electrosprayed particles prepared at similar conditions. Yet the spray dried samples showed slower drug release compared with the corresponding electrosprayed samples, which contradicts the theory. The electrosprayed particles were more porous than the spray dried counterparts and also had a higher surface drug concentration, which together could explain the results observed. An increase in particle porosity leads to an increase in surface to volume ratio as well as a reduction in the drug diffusion boundary, hence increasing the release rate. An increase in the surface drug concentration would result in

higher burst release and result in a general increase in release rate due to the shorter diffusion distances for drug molecules distributed near the particle surface.

Further, although not measured, the density of the solid regions of the particles may have been lower for electrosprayed particles, with the PLGA network perhaps being less packed judging from the higher porosity and larger particles observed. This could also have had an influence on the drug release rate, but all in all the release rates and the shape of the curves were not that different when considering two separate techniques were used to prepared the particles. A greater difference could have been expected considering the differences in particle size distributions and particle characteristics.

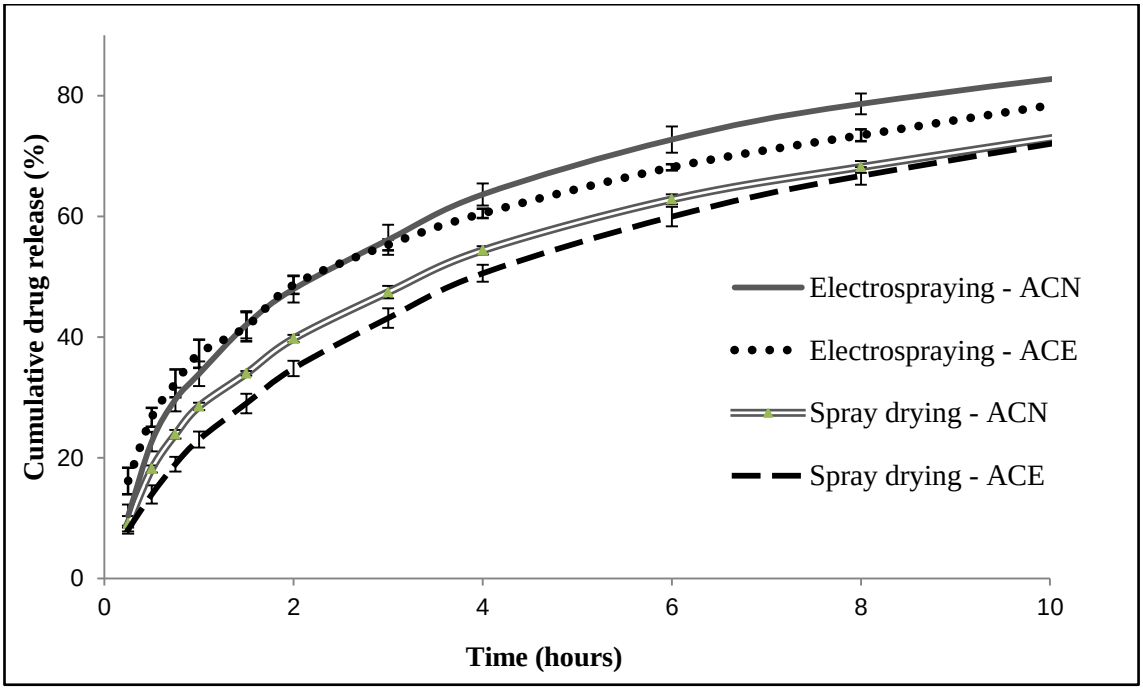

Figure 6.16 Drug release curves of electrosprayed and spray dried particles prepared with 5% solute concentration and 10% drug loading using ACN or ACE.

When comparing the drug release from particles prepared with ACE-MeOH mixtures using electrospraying and spray drying (see Figures 5.8 and 6.14), the difference is seen more clearly. Here, all of the samples prepared using electrospraying had higher release rates than the spray dried samples, although the general trend between the samples was

similar. For both techniques samples prepared with high MeOH content had the highest release rates. Also here, larger particles were observed, on average, for electrosprayed samples (see Tables 5.5 and 6.3) but did not correlate with the drug release rates. In this case the electrosprayed particles were again more porous than the spray dried particles (see Figures 5.6 and 6.11) and the surface drug concentration was generally considerably higher for electrosprayed samples. Both of these characteristics support the higher release rates observed for electrosprayed particles.

Moreover, the electrosprayed particles prepared with ACE:MeOH ratios, 90:10, 75:25 and 69:31 had all disintegrated when observed after drug release whereas the spray dried particles seemed to be structurally intact. The disintegration of microparticles into nanoparticles would result in much higher surface area to volume ratio and higher release rates, which supports the differences observes in Figures 5.8 and 6.14. Particles prepared using the two techniques can thus lead to significant differences in the drug release kinetics due to differences in their particles formation process and resulting particle characteristics. Such differences could be used to optimize the release profile of drug formulations prepared with either of these two techniques.

6.6 Additional remarks on electrospraying and spray drying

The particle formation process in both spray drying and electrospraying is of high interest to those who wish to design and engineer particles with special characteristics and function. Although much effort has been made to better understand the mechanisms behind the particle formation process with spray drying, the seemingly similar mechanisms in electrospraying are less understood and still needs to be investigated [Park and Lee 2009]. Nevertheless, some aspects in the process are clear and can be used to compare the two techniques and further some things have been discovered during the present work. To the best knowledge of the author of this thesis, only one

review article has set the two techniques up against each other, comparing the processes and their application for producing drug nanoparticles [Peltonen *et al.* 2010]. In this review Peltonen *et al.* discusses the advantages and disadvantages of each technique with focus on the scalability of the techniques, the producible particle size range and the compatibility of the techniques with different classes of materials. However, they do not go into detail with respect to the differences in the actual processes and do not explain the mechanism behind their respective particle formation process.

The advantages of electrospraying compared with spray drying is that it can fairly easily produce a near-monodisperse population of particles in the nano to micro range and can do this at ambient conditions with a large range of materials and solvents, given that the surface tension, electrical conductivity and viscosity of the liquid is kept within a certain window. Spray drying cannot produce particles with as narrow a size distribution and is further limited to non-thermolabile materials, but can still produce particles close to the nano range using a bench top system and is much easier to scale up than electrospraying. However, when scaled-up to commercial scale spray drying, currently, may not be able to produce particles with the same degree of control over their attributes as with a bench top system [Masters K 2002]. With electrospraying, a scale-up would likely involve having hundreds of parallel nozzles spraying simultaneously (see section 2.6.5) which would probably not affect the resulting particle characteristics.

In terms of particle formation the two techniques are known to have differences as they first of all employ different forces to atomise the liquid into droplets. Whereas spray drying mainly uses the pressure of a gas to part the liquid, electrospraying uses a high electric potential. Further, with spray drying an active heat/mass transfer takes place after droplet formation, while with the present electrospraying setup the droplets are

exposed to an electric field until they are discharged at collection. The electrospraying device can, however, be customized to control the environment (temperature and humidity) and also possibly incorporate a drying system similar to that used in spray drying setups. But for the current time the electrospraying is associated with a passive drying process. For both techniques small liquid filaments are ejected from the nozzle and quickly develop into spherical droplets which go through an evaporation process, finally resulting in dry particles. However, in the steps in between there may be significant differences resulting from the exposure to heated air and the exposure to an electric field.

A quantification of the typical time it takes for a droplet to form into a particle would be a useful measure to know for both techniques. Although this has not been measured, it can be speculated that the spray drying process should be quicker due to its active drying process. How much quicker it actually is, would need to be measured or extrapolated from indirect measurements and the influence of other factors on the particle formation and droplet evaporation processes should be elucidated. It has previously been reported that a liquid may evaporate at a higher rate when exposed to an electric field [Liu *et al*. 2005; Zheng *et al.* 2011]. Whether such an effect really takes place and plays a significant role during droplet evaporation in electrospraying is not currently known. The electric field in electrospraying may nevertheless have some influence at the droplet surface during particle formation. It is for instance plausible that a difference in electric charge between two materials suspended or dissolved in the droplet may lead to some sort of phase separation. Such a phenomenon would be interesting to look more into and may be useful to control the distribution of materials within the droplets.

Chapter 7

Conclusions and Future work

7.1 Conclusions

Developing an effective drug delivery system can be a complex and challenging task, but the opportunities and application of such systems are remarkable. Solid dispersion formulations have been widely studied and are promising for the development of oral dosages for poorly soluble drug compounds due to their dissolution enhancing ability. Moreover, extended release solid dispersions may further improve the performance of the formulations by providing less variation in the drug plasma concentration and less frequent dosages. Microparticle based delivery systems have shown a great potential to improve current treatments by tailoring their physicochemical attributes to the specific needs. Electrospraying was chosen for this purpose and specifically to improve the performance of solid dispersion formulations of poorly soluble drugs. Unlike spray drying, a well-established technique for pharmaceutical development, electrospraying is still in an experimental stage but has proven an attractive technology.

In the present study CEL-loaded PLGA microparticles were prepared with electrospraying with the aim to:

- obtain small particles in the lower micro-range
- the drug dispersed in the microparticles in a stable amorphous state
- good control of particle characteristics, size, morphology and porosity
- good control of drug release kinetics using the studied parameters.

With this in mind the influence of different processing parameters on the particle formation process, particle characteristics and drug release kinetics were investigated. This was done by studying a few different parameters which have previously been shown to have and important influence on the particle characteristics, including flow rate, solute concentration, drug loading and the composition of the solvent(s). The studies were focused on a single model drug, CEL, and the influence of different solvent mixtures on two drug-polymer combinations, CEL-PLGA and CEL-HPMCAS.

7.1.1 Electrospraying of solid dispersions

Solutions of CEL alone in different organic solvents demonstrated the sprayability of pure drug solution to form microparticles. CEL was then combined with PLGA, electrosprayed using a single nozzle setup and showed that they could be mixed and sprayed together in a single liquid phase to form microparticles with CEL molecules presumably dispersed within a PLGA matrix structure.

Generally, high collection yields and entrapment efficiencies were observed with the electrospraying process compared with conventional particle preparation techniques such as emulsion-based techniques and laboratory scale spray drying. Due to the simple collection process most of the output (>81%) was retained at collection and could easily be optimised by coating the nozzle or collecting in a closed chamber. The entrapment efficiencies were generally very high mainly due to the collection method and the single nozzle setup used. The particles were collected dry and were not washed in any way and further the drug was fully mixed with the polymer before and after spraying and thus prevented excessive loss in drug entrapment in the process.

7.1.2 Parametric study on particle characteristics

For the parametric study using CEL and PLGA, the particle size generally ranged between 2-8 μm and the size distribution was relatively narrow (polydispersivity indices

mostly between 6-16%). The applied flow rate had the most dominant influence on particle size with particle size increasing as the flow rate was increased. Also, solute concentration, drug loading and type of solvent influenced the particles size, mainly by either increasing or decreasing the viscosity or the electrical conductivity of the solution. An increase in viscosity resulted in an increase in particle size while an increase in electrical conductivity resulted in a decrease in particle size.

Particle morphology of drug-loaded PLGA particles ranged from being spherical with smooth or porous surface to raisin-like, grainy or collapsed. Elongated particles could also be produced by changing the viscosity of the solution to a higher range. Further, by using another polymer, HPMCAS, other types of surface morphologies were observed, mainly being collapsed with a shell or bowl shape or corrugated with different level of roughness. Particle surface morphology was influenced by the solvent(s) used and the presence of an anti-solvent to the polymer lead to significantly different morphologies. The results indicated that the evaporation rate and the solvent power of the solvents together had an important role in the particle formation process.

Cross sectional images of the particles showed a porous inner structure for most of the electrosprayed particles except for some particles prepared with ACE. It was further observed that the porosity increased as the solute concentration was decreased, indicating that the excess solvent in the droplets resulted in pore formation. This effect was explained by the solvent evaporation mechanism and the relatively low solute concentrations used with electrospraying.

XRPD and DSC analysis demonstrated that CEL was in an amorphous form for all PLGA-CEL particles studied, even at 30% drug loading, where no crystallinity was detected with XRPD. The absence of crystallinity indicated that CEL was molecularly dispersed in the PLGA matrix as a solid dispersion. Further, the physical stability of this

amorphous drug dispersion within the particles was measured over 8 months during storage in a desiccator. Yet, no signs of instability were observed both from XRPD measurements and visual inspection using SEM, indicating a relatively good physical stability of the prepared particle formulations.

Drug release studies were performed to predict the intestinal *in vivo* release profile and showed that under sink conditions the drug release could be controlled over a 20-24 hours period to provide either a rapid release over a short time or an extended release over the full 24 hours studied. Varying degrees of burst release was observed and is believed partly to be indicative of the surface CEL concentration. Further, particles that were either small or less compact also resulted in high burst release. Following the burst release a more sustained diffusion dependent release was observed until most of the drug had been released. Polymer erosion did not typically take place during the studied time span and thus did not affect the release. This was confirmed by taking SEM images of particles after dissolution and the release curves were fitted and correlated well with a standard Higuchi model for diffusion mediated release.

The studied parameters were all found to have some influence on the drug release profile with size, porosity, drug loading and solubility of PLGA in the solvent being the most significant factors. All of the studied parameters had an influence on particle size and an increase in particle size resulted in slower release due to a reduced surface to volume ratio. Further, an increase in porosity is believed to have led to similar effect via a reduction in the effective surface to volume ratio and possibly a density reduction in solid areas of the particles. Finally, the drug distribution in the particles also seemed to have a significant influence on drug release with higher drug concentrations at the surface resulting in a shorter diffusion boundary for the drug molecules and hence quicker release. Better control of the drug distribution within the particles could

eliminate the burst release observed in these studies and have a desirable impact on the drug release curves. It would also be useful to achieve delayed release by distributing the drug more towards the core of the particles and this may also further increase the drug stability of more unstable drugs, such as proteins.

Despite the fact that release mechanisms of PLGA-based controlled release systems have been extensively studied for over 20 years, the mechanism of drug release from PLGA microparticles is still not fully understood. This is partly due to the complexity of the processes and the interactions present in such a system but also because of the lack of full understanding on processes that govern drug release and the factors the influence the processes. In line with the Quality by Design (QbD) approach, the fundamental knowledge regarding these sophisticated processes and factors is necessary if we are to understand drug release in detail and gain better control of the drug release kinetics.

7.1.3 Mixed solvent studies with electrospraying

CEL-loaded PLGA and CEL-loaded HPMCAS microparticles were produced using mixed solvent systems at different solvent ratios using electrospraying to investigate the solvent interactions with the solutes and the influence of solvent compositions on the particle formation process. For the PLGA system mixtures of ACE and MeOH were used whereas for the HPMCAS system mixtures of ACE, EtOH and H_2O were used. The studies demonstrated that particle formation in the electrospraying process depended markedly on the solubility of the solutes in the solvent(s), as well as on the evaporation rate of the solvents. By using an anti-solvent or a poorer solvent for the polymers during particles formation, the molecular conformation of the polymer chains became more compact and less entangled and further resulted in early precipitation of the polymer during solvent evaporation.

For CEL-loaded PLGA particles, depending on the amount of the anti-solvent, different degrees of roughness were observed in the surface morphology and this also influenced the accumulation of CEL at the particle surface. A clear correlation was observed between the concentration of the anti-solvent in the solvent mixture and the surface content of CEL, which was also evident from the release rates observed in the drug release studies. The effect was less obvious with the CEL-loaded HPMCAS particles. Although HPMCAS is supposedly soluble in aqueous solutions with a pH above 5.5-6 as well as different organic solvents, there seems to be an unclear understanding whether a nano-suspension or an actual solution is formed. Further, it seems that a complex relationship exists between the solubility of HPMCAS in the solvent mixtures and the solubility during evaporation of the solvent. Here, CEL was less soluble than HPMCAS in some of the solvent mixtures and seemed to result in earlier precipitation of CEL and a lower surface drug concentration. Although there was some correlation between the solvent ratios, the particle morphologies, the surface CEL concentration and drug release, it was not as clear as for the PLGA-CEL system. The subtler differences in surface CEL concentration could also be explained by the lower molecular mobility of CEL in the HPMCAS matrix due to the higher viscosity of HPMCAS compared with PLGA. For these particles no crystallinity was measured despite the high surface CEL concentrations, which indicated that a phase separation is not likely to have happened. The mechanisms by which the different particle morphologies and drug distributions form different solvent mixtures are related to the balance between precipitation of solutes and evaporation of solvents.

7.1.4 Spray dried microparticles and comparisons with electrospraying

Spray dried particles were prepared at similar conditions as the electrosprayed particles to compare the two techniques. The spray dried particles appeared to be non-porous and

had a smooth surface under SEM observation making the different samples indistinguishable. The particles were generally smaller with a broader size distribution than the electrosprayed counterparts sprayed with the same solute concentration and drug loading. The drug was also highly dispersed in the polymeric matrix forming solid dispersions. For particles prepared with single solvents the release of CEL took place at slightly slower rates than with electrosprayed particles but not very differently, although the spray dried particles were smaller. This indicated that the spray dried particles were denser and therefore probably released their drug load slower than expected.

Further, for the mixed solvent system with ACE and MeOH it was observed that the surface drug concentration was much lower for spray dried particles when compared with electrosprayed particles, although the same trends were observed, indicating that the active drying process allowed less diffusion of drug molecules towards the surface. This also explains the differences observed in drug release rate of the particles prepared with ACE-MeOH mixtures where much faster release rates were observed for electrosprayed particles when MeOH was added to the solvent. The difference observed here is also explained by the disintegration of grainy electrosprayed particles which is likely to have resulted in much quicker release, while the spray dried particles remained structurally intact. It is believed that the main differences observed between the particles prepared using spray drying and electrospraying can be explained by differences in the droplet formation and droplet drying process and the resulting particle characteristics. This, however, needs to be further elucidated by careful observation of the two techniques.

At this point it is clear that there are certain differences between the electrospraying and spray drying processes for producing microparticles, mostly in the mechanisms involved in particle formation but also in the level of development of the technologies.

Whereas spray drying is a fully commercialized and optimized technology for pharmaceutical development and manufacturing, electrospraying is still at the experimental plan for formulation purposes, although the technology has become highly developed for mass spectrometer applications [Jaworek 2008; Takíts *et al.* 2004]. The difference in level of development makes it difficult to compare the two techniques due to the automated, commercial setups used for spray drying and the manual, customized setups available for electrospraying. In one way the automated functions and the convenient collection mechanisms of spray drying favour its use, and yet the high level of customization in electrospraying may also allow more flexibility with regards to experimentation and thereby favour the use of electrospraying. Also, although spray drying is automated and both humidity and temperature is controlled within the spraying chamber, it would still result in variation between the batches produced as it is not a continuous manufacturing process on its own.

Although some steps are being taken towards commercialization of electrospraying for pharmaceutical formulations, there are still many aspects of the electrospraying process that are unknown. Better understanding on the particle formation process as well as the influence of different processing parameters may provide ways of optimizing the overall particle preparation and design. Nevertheless, both electrospraying and spray drying are useful techniques in preparing microparticles with control of particle size and morphology and are believed to be suitable for producing functional drug delivery carrier systems with superior performance. Currently, drug delivery systems such as microparticle based carriers and solid dispersion formulations are finding their way into the product pipelines of many pharmaceutical and biotech companies. Such drug delivery systems should have a superior performance over conventional drug formulations with better control of drug release kinetics and additional features making

them perform better. In order to prepare such drug delivery system, a suitable particle engineering technology enabling control of such particle characteristics and functionality is necessary. Electrospraying was demonstrated to provide considerable control of important particle attributes such as size, morphology, shape, porosity and drug distribution as well as the resulting drug release kinetics. In this study electrospraying showed more room for tuning and control of particle characteristics compared with spray drying and can be further optimized to provide better control for particle engineering purposes. Nevertheless, both techniques can be considered suitable for generating drug-loaded particles intended for use as drug delivery carriers, each technique with its own advantages and limitations to be overcome.

7.2 Future work

Based on the research done in this project and the results obtained, several aspects of future work are recommended as follows:

7.2.1 Further investigation of the electrospraying particle formation process – A droplet study.

In this work, the electrospraying particle formation process was investigated by looking at the properties of the spraying solutions and the characteristics and drug release profile of the particles. To further build on the results of this project, droplet formation and the initial droplet drying stage could be looked further into by visualization using a high speed camera. This high speed camera would be used to capture images of electrosprayed droplets immediately after detachment from the cone-jet further downstream of the spray. By capturing images at different distances from the cone-jet it would be interesting to study different stages of droplet formation as well as mechanisms such as Coulomb fission. The studies could for instance be done using a

high speed camera incorporated with a microscope lens, and adjusted to capture the droplets at different positions. This study may give interesting and important new information on the particle formation process with electrospraying and the results can be compared with similar spray drying studies done by other researchers. Initial studies were performed testing a high speed camera with a frame rate of 1000 frames per second. The rapid movements in the cone-jet could be nicely visualised, however as this point a high magnification lens was not incorporated in the camera setup and the droplets have therefore not yet been visualized.

7.2.2 Electrospraying of protein drugs and control of drug distribution.

Electrospraying of protein drugs – particle characteristics and stability

Electrospraying of protein-based formulations could be studied using a model protein, such as lysozyme, to observe whether the protein remains stable and bioactive after being electrosprayed and also to examine the resulting particle characteristics. Lysozyme is a relatively stable protein with a net positive charge and a molecular weight of 14.3 kDa. Although a relatively common model protein it has not been used for electrospraying, to the best knowledge of the author, but provides a good protein for studying bioactivity and stability of proteins after electrospraying. The bioactivity can easily be measured using a standard kit with standard gram-negative bacteria, which should be lysed by the lysozyme if it is bioactive and the stability of the protein structure could be studied using spectroscopic techniques. Since lysozyme is water-soluble it could be electrosprayed either together with a water-soluble polymer such as HPMC or PVP or a sugar such as mannitol or trehalose using an aqueous and organic solvent mixture. Particles could also be prepared using electrospraying with a co-axial nozzle setup where proper encapsulation of the protein can be achieved. It is a common problem with spray drying of protein drugs that the proteins distribute towards the

surface of the particles due to their high surface activity and thus have a higher likelihood of denaturation caused by unfolding. By encapsulating the proteins within a polymer or sugar shell the protein molecules could be kept stable and bioactive for a longer time. This could perhaps also be done by controlling the drug distribution of particles to achieve higher drug concentration in the core of the particles.

Control of drug distribution in electrosprayed particles for drug delivery.

In the present project, CEL/PLGA and CEL/HPMCAS particles were prepared in binary solvent systems to study the influence of these solvents on the drug distribution in the particles. The study indicated solubility of the solutes in the solvents, molecular size of drug and polymer and the electrical charge of the solute may have had an influence on the drug distribution in electrosprayed particles. The influence of both the molecular size of solutes and their electrical charge would be interesting to further investigate by examining model proteins of similar molecular weight (14-17 kDa) with different net charge at a neutral pH. Lysozyme has a net positive charge (isoelectric point = 11), myoglobin has a net neutral charge (isoelectric point = 7.3) and alpha-lactalbumin has a net negative charge (isoelectric point = 4.2) and these proteins could be used and compared for this purpose. The differences in charge may result in different distribution of the proteins in the particles. These proteins could be electrosprayed using a polymer or sugar to study the distribution of the proteins in the resulting particles. In this case it may be advantageous to use a sugar such as trehalose, which has a molecular weight of 342 Da and is much smaller than the proteins and typically has a higher solubility. There may then be a good chance that trehalose distributes towards the surface of the particles assuming their superior molecular mobility compared with the proteins.

7.2.3 Drug release kinetics from particles loaded with different drug molecules.

In extension of the drug release studies performed in this project, where the influence of different particle characteristics on the drug release was studied, it would be interesting to examine the influence of drug molecular weight and drug water solubility on their drug release kinetics from PLGA particles. Although there are not many studies which report on the influence of drug properties on drug release from PLGA particles, it is believed that the molecular weight and solubility of the drug molecules have a great influence on drug release, provided that there are no strong interactions between the drug and the polymer. Since a large number of poorly water soluble drug compounds exist, some of these have similar molecular weight or similar aqueous solubility and can therefore be used to set up comparisons. The influence of the drug molecular weight on drug release rate could be established by looking at a few drugs compounds that are similar in solubility but different in molecular weight. The same could be done for the influence of drug solubility by studying drug compounds with similar molecular weight and different solubilities. It would be expected that diffusion mediated drug release from PLGA particles would take place at a higher rate for smaller molecules with a good solubility in the surrounding dissolution medium.

7.2.4 Drug transport studies and cellular uptake from microparticles

Caco-2 is a continuous cell line with origin from a human colon adenocarcinoma and is used extensively as a model of the intestinal barrier. These cells express many morphological and functional features that resemble that of intestinal enterocytes when grown in a monolayer [Pinto 1983]. Due to their similarity to small intestinal enterocytes Caco-2 cells are considered a representative model for the transport of drugs over the intestinal barrier. Caco-2 cells can be cultured on a permeable filter which allows them to act as a tight barrier between two compartments representing the apical

and basolateral sides of the cell monolayer (see Figure 7.1). Transport of different molecules across the monolayer can therefore be measured in both directions and the permeability of the cells to a specific substance can be determined [Sambuy *et al.* 2005].

It is of interest to test the drug release from electrosprayed microparticles and the transport of released drug by the Caco-2 intestinal cell model as this gives an indication of the *in vivo* performance of the drug formulations prepared. This drug transport model would then be used assess the permeability of the cells to drug molecules release from the microparticles in comparison to free drug crystals. Further, the differences in permeability between particles prepared with electrospraying and spray drying can be quantified to compare the performance of particles prepared with the two techniques. The particles would be suspended in the apical compartment of the system (see Figure 7.1) and samples would be taken from the basolateral compartment at given time intervals to estimate the transported drug. It is believed that the drug transport from the particles would be slower than for drug crystals due to the slower release rate from the particles, yet the total percentage of drug transported may be higher for the particles due to the molecular form of the drug at release. Drug loaded HPMCAS particles could be tested to examine the effect of precipitation inhibition, which could give additional improvement to the drug transport.

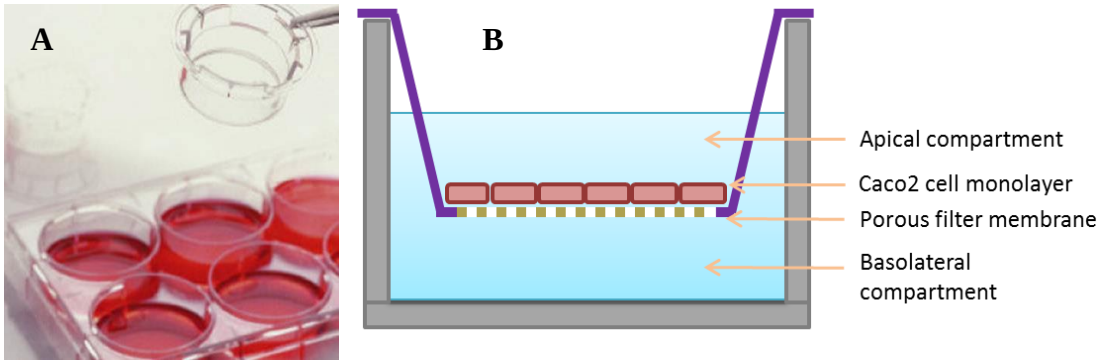

Figure 7.1 Caco-2 transwell plate (From Corning.com) (A) and sketch of components in a single well (B).

References

Aaltonen J., Allesø M., Mirza S., Koradia V., Gordon K. C. and Rantanen J. 2009. Solid form screening – A review. *European Journal of Pharmaceutics and Biopharmaceutics,* 71**,** 23-37.

Abebe W. 2002. Herbal medication: potential for adverse interactions with analgesic drugs. *Journal of Clinical Pharmacy and Therapeutics,* 27**,** 391-401.

Adams C. P. and Brantner V. V. 2006. Estimating The Cost Of New Drug Development: Is It Really $802 Million? *Health Affairs,* 25**,** 420-428.

Adams C. P. and Brantner V. V. 2010. Spending on new drug development1. *Health Economics,* 19**,** 130-141.

Adhikari B., Howes T., Bhandari B. R. and Truong V. 2000. Experimental studies and kinetics of single drop drying and their relevance in drying of sugar-rich foods: A review. *International Journal of Food Properties,* 3**,** 323-351.

Alamilla-Beltrán L., Chanona-Pérez J. J., Jiménez-Aparicio A. R. and Gutiérrez-López G. F. 2005. Description of morphological changes of particles along spray drying. *Journal of Food Engineering,* 67**,** 179-184.

Allison M. 2012. Reinventing clinical trials. *Nat Biotech,* 30**,** 41-49.

Almekinders J. C. and Jones C. 1999. Multiple jet electrohydrodynamic spraying and applications. *Journal of Aerosol Science,* 30**,** 969-971.

Almeria B., Deng W., Fahmy T. M. and Gomez A. 2010. Controlling the morphology of electrospray-generated PLGA microparticles for drug delivery. *Journal of Colloid and Interface Science,* 343**,** 125-133.

Almería B., Fahmy T. M. and Gomez A. 2011. A multiplexed electrospray process for single-step synthesis of stabilized polymer particles for drug delivery. *Journal of Controlled Release,* 154**,** 203-210.

Alonzo D., Zhang G., Zhou D., Gao Y. and Taylor L. 2010. Understanding the Behavior of Amorphous Pharmaceutical Systems during Dissolution. *Pharmaceutical Research,* 27**,** 608-618.

Alonzo D. E., Gao Y., Zhou D., Mo H., Zhang G. G. Z. and Taylor L. S. 2011. Dissolution and precipitation behavior of amorphous solid dispersions. *Journal of Pharmaceutical Sciences,* 100**,** 3316-3331.

Amidon G. L., Sinko P. J. and Fleisher D. 1988. Estimating Human Oral Fraction Dose Absorbed: A Correlation Using Rat Intestinal Membrane Permeability for Passive and Carrier-Mediated Compounds. *Pharmaceutical Research,* 5**,** 651-654.

Arya N., Chakraborty S., Dube N. and Katti D. S. 2009. Electrospraying: A facile technique for synthesis of chitosan-based micro/nanospheres for drug delivery applications. *Journal of Biomedical Materials Research Part B: Applied Biomaterials,* 88B**,** 17-31.

Ayal H., Gargallo L. and Radi D. 1993. Viscosity Behaviour of Dilute and Moderately Concentrated Solutions. 1. Poly(vinylpyrrolidone) in 2-propanol. *International Journal of Polymeric Materials,* 23**,** 47-55.

Bae S. E., Son J. S., Park K. and Han D. K. 2009. Fabrication of covered porous PLGA microspheres using hydrogen peroxide for controlled drug delivery and regenerative medicine. *Journal of Controlled Release,* 133**,** 37-43.

Baldinger A., Clerdent L., Rantanen J., Yang M. and Grohganz H. 2012. Quality by design approach in the optimization of the spray-drying process. *Pharmaceutical Development and Technology,* 17**,** 389-397.

Baldursdóttir S. G., Kjoniksen A. L., Karlsen J., Nyström B., Roots J. and Tannesen H. H. 2003. Riboflavin-Photosensitized Changes in Aqueous Solutions of Alginate. Rheological Studies. *Biomacromolecules,* 4**,** 429-436.

Bee T. R., M 2010. Using polymer technology to enhance bioavailability. *Pharmaceutical Technology***,** 37-42.

Beten D. B., Amighi K. and Moës A. J. 1995. Preparation of Controlled-Release Coevaporates of Dipyridamole by Loading Neutral Pellets in a Fluidized-Bed Coating System. *Pharmaceutical Research,* 12**,** 1269-1272.

Biedasek S., Abboud M., Moritz H.-U. and Stammer A. 2007. Online-Analysis on Acoustically Levitated Droplets. *Macromolecular Symposia,* 259**,** 390-396.

Bittner B. and Kissel T. 1999. Ultrasonic atomization for spray drying: a versatile technique for the preparation of protein loaded biodegradable microspheres. *Journal of Microencapsulation,* 16**,** 325-341.

Blagden N., de Matas M., Gavan P. T. and York P. 2007. Crystal engineering of active pharmaceutical ingredients to improve solubility and dissolution rates. *Advanced Drug Delivery Reviews,* 59**,** 617-630.

Bocanegra R., Galán D., Márquez M., Loscertales I. G. and Barrero A. 2005. Multiple electrosprays emitted from an array of holes. *Journal of Aerosol Science,* 36**,** 1387-1399.

Bock N., Woodruff M. A., Hutmacher D. W. and Dargaville T. R. 2011. Electrospraying a reproducible method for production of polymeric microspheres for biomedical applications. *Polymers,* 3**,** 131-149.

Boghra R. J., Kothawade P. C., Belgamwar V. S., Nerkar P. P., Tekade A. R. and Surana S. J. 2011. Solubility, Dissolution Rate and Bioavailability Enhancement of Irbesartan by Solid Dispersion Technique. *Chemical and Pharmaceutical Bulletin,* 59**,** 438-441.

Breitenbach J. 2002. Melt extrusion: from process to drug delivery technology. *European Journal of Pharmaceutics and Biopharmaceutics,* 54**,** 107-117.

Breitenbach J., Schrof W. and Neumann J. 1999. Confocal Raman-Spectroscopy: Analytical Approach to Solid Dispersions and Mapping of Drugs. *Pharmaceutical Research,* 16**,** 1109-1113.

Cal K. and Sollohub K. 2010. Spray drying technique. I: Hardware and process parameters. *Journal of Pharmaceutical Sciences,* 99**,** 575-586.

Cavalli R., Bisazza A., Bussano R., Trotta M., Civra A., Lembo D., Ranucci E. and Ferruti P. 2011. Poly(amidoamine)-Cholesterol Conjugate Nanoparticles Obtained by Electrospraying as Novel Tamoxifen Delivery System. *Journal of Drug Delivery,* 2011.

Chakraborty S., Liao I. C., Adler A. and Leong K. W. 2009. Electrohydrodynamics: A facile technique to fabricate drug delivery systems. *Advanced Drug Delivery Reviews,* 61**,** 1043-1054.

Champion J. A. and Mitragotri S. 2006. Role of target geometry in phagocytosis. *Proceedings of the National Academy of Sciences of the United States of America,* 103**,** 4930-4934.

Chan K. L. A. and Kazarian S. G. 2004. FTIR Spectroscopic Imaging of Dissolution of a Solid Dispersion of Nifedipine in Poly(ethylene glycol). *Molecular Pharmaceutics,* 1**,** 331-335.

Chang M. W., Stride E. and Edirisinghe M. 2010. Controlling the thickness of hollow polymeric microspheres prepared by electrohydrodynamic atomization. *J.R.Soc.Interface,* 7 Suppl 4**,** S451-S460.

Charlesworth D. H. and Marshall W. R. 1960. Evaporation from drops containing dissolved solids. *AIChE Journal,* 6**,** 9-23.

Chaumeil J. C. 1998. Micronization: a method of improving the bioavailability of poorly soluble drugs. *Methods Find.Exp.Clin.Pharmacol.,* 20**,** 211-215.

Chawla G. and Bansal A. K. 2007. A comparative assessment of solubility advantage from glassy and crystalline forms of a water-insoluble drug. *Eur.J.Pharm.Sci.,* 32**,** 45-57.

Chawla G., Gupta P., Thilagavathi R., Chakraborti A. K. and Bansal A. K. 2003. Characterization of solid-state forms of celecoxib. *Eur.J.Pharm.Sci.,* 20**,** 305-317.

Chen D.-R., Pui D. Y. H. and Kaufman S. L. 1995. Electrospraying of conducting liquids for monodisperse aerosol generation in the 4 nm to 1.8 µm diameter range. *Journal of Aerosol Science,* 26**,** 963-977.

Chen X. D. and Xie G. Z. 1997. Fingerprints of the Drying Behaviour of Particulate or Thin Layer Food Materials Established Using a Reaction Engineering Model. *Food and Bioproducts Processing,* 75**,** 213-222.

Chew N. Y. K., Tang P., Chan H. K. and Raper J. A. 2005. How Much Particle Surface Corrugation Is Sufficient to Improve Aerosol Performance of Powders? *Pharmaceutical Research,* 22**,** 148-152.

Chiou W. L. and Riegelman S. 1971. Pharmaceutical applications of solid dispersion systems. *Journal of Pharmaceutical Sciences,* 60**,** 1281-1302.

Chow A., Tong H., Chattopadhyay P. and Shekunov B. 2007. Particle Engineering for Pulmonary Drug Delivery. *Pharmaceutical Research,* 24**,** 411-437.

Cloupeau M. and Prunet-Foch B. 1994. Electrohydrodynamic spraying functioning modes: a critical review. *Journal of Aerosol Science,* 25**,** 1021-1036.

Cloupeau M. and Prunet-Foch B. 1989. Electrostatic spraying of liquids in cone-jet mode. *Journal of Electrostatics,* 22**,** 135-159.

Cloupeau M. and Prunet-Foch B. 1990. Electrostatic spraying of liquids: Main functioning modes. *Journal of Electrostatics,* 25**,** 165-184.

Corrigan D. O., Healy A. M. and Corrigan O. I. 2002. The effect of spray drying solutions of polyethylene glycol (PEG) and lactose/PEG on their physicochemical properties. *International Journal of Pharmaceutics,* 235**,** 193-205.

Costa P. and Sousa Lobo J. M. 2001. Modeling and comparison of dissolution profiles. *European Journal of Pharmaceutical Sciences,* 13**,** 123-133.

Craig D. Q. M. 2002. The mechanisms of drug release from solid dispersions in water-soluble polymers. *International Journal of Pharmaceutics,* 231**,** 131-144.

Craig D. Q. M. 1995. A review of thermal methods used for the analysis of the crystal form, solution thermodynamics and glass transition behaviour of polyethylene glycols. *Thermochimica Acta,* 248**,** 189-203.

Crowley M. M., Zhang F., Repka M. A., Thumma S., Upadhye S. B., Kumar Battu S., McGinity J. W. and Martin C. 2007. Pharmaceutical Applications of Hot-Melt Extrusion: Part I. *Drug Development and Industrial Pharmacy,* 33**,** 909-926.

Cui F., Yang M., Jiang Y., Cun D., Lin W., Fan Y. and Kawashima Y. 2003. Design of sustained-release nitrendipine microspheres having solid dispersion structure by quasi-emulsion solvent diffusion method. *Journal of Controlled Release,* 91**,** 375-384.

Curatolo W., Nightingale J. and Herbig S. 2009. Utility of Hydroxypropylmethylcellulose Acetate Succinate (HPMCAS) for Initiation and Maintenance of Drug Supersaturation in the GI Milieu. *Pharmaceutical Research,* 26**,** 1419-1431.

Dahlberg C., Millqvist-Fureby A. and Schuleit M. 2008. Surface composition and contact angle relationships for differently prepared solid dispersions. *European Journal of Pharmaceutics and Biopharmaceutics,* 70**,** 478-485.

Dahlberg C., Millqvist-Fureby A., Schuleit M. and Furó I. 2010. Relationships between solid dispersion preparation process, particle size and drug release – An NMR and NMR microimaging study. *European Journal of Pharmaceutics and Biopharmaceutics,* 76**,** 311-319.

Del Valle E. 2003. Cyclodextrins and their uses: A review. *Process Biochemistry*.

Deng W., Klemic J. F., Li X., Reed M. A. and Gomez A. 2006. Increase of electrospray throughput using multiplexed microfabricated sources for the scalable generation of monodisperse droplets. *Journal of Aerosol Science,* 37**,** 696-714.

Deng W., Waits C. M., Morgan B. and Gomez A. 2009. Compact multiplexing of monodisperse electrosprays. *Journal of Aerosol Science,* 40**,** 907-918.

Ding L., Lee T. and Wang C. H. 2005. Fabrication of monodispersed Taxol-loaded particles using electrohydrodynamic atomization. *J.Control Release,* 102**,** 395-413.

Dobry D., Settell D., Baumann J., Ray R., Graham L. and Beyerinck R. 2009. A Model-Based Methodology for Spray-Drying Process Development. *Journal of Pharmaceutical Innovation,* 4**,** 133-142.

Dokoumetzidis A. and Macheras P. 2006. A century of dissolution research: From Noyes and Whitney to the Biopharmaceutics Classification System. *International Journal of Pharmaceutics,* 321**,** 1-11.

Dravid V., Songsermpong S., Xue Z., Corvalan C. M. and Sojka P. E. 2006. Two-dimensional modeling of the effects of insoluble surfactant on the breakup of a liquid filament. *Chemical Engineering Science,* 61**,** 3577-3585.

Dubernet C. 1995. Thermoanalysis of microspheres. *Thermochimica Acta,* 248**,** 259-269.

Duft D., Achtzehn T., Muller R., Huber B. A. and Leisner T. 2003. Coulomb fission: Rayleigh jets from levitated microdroplets. *Nature,* 421**,** 128-128.

Edlund U. and Albertsson A. 2002. Degradable Polymer Microspheres for Controlled Drug Delivery. *Degradable Aliphatic Polyesters.* Springer Berlin / Heidelberg.

Emami J. 2006. In vitro–in vivo correlation: from theory to applications. *J Pharm Pharm Sci,* 9**,** 169-189.

Emara L. H., Badr R. M. and Abd Elbary A. 2002. Improving the Dissolution and Bioavailability of Nifedipine Using Solid Dispersions and Solubilizers. *Drug Development and Industrial Pharmacy,* 28**,** 795-807.

Enayati M., Ahmad Z., Stride E. and Edirisinghe M. 2010. One-step electrohydrodynamic production of drug-loaded micro- and nanoparticles. *J. R. Soc. Interface,* 7**,** 667-675.

Enayati M., Ahmad Z., Stride E. and Edirisinghe M. 2009. Preparation of polymeric carriers for drug delivery with different shape and size using an electric jet. *Curr. Pharm. Biotechnol.,* 10**,** 600-608.

Enayati M., Stride E., Edirisinghe M. and Bonfield W. 2012. Modification of the release characteristics of estradiol encapsulated in PLGA particles via surface coating. *Therapeutic Delivery,* 3**,** 209-226.

Fahr A. and Liu X. 2007. Drug delivery strategies for poorly water-soluble drugs. *Expert Opinion on Drug Delivery,* 4**,** 403-416.

Farid M. 2003. A new approach to modelling of single droplet drying. *Chemical Engineering Science,* 58**,** 2985-2993.

Feng A. L., Boraey M. A., Gwin M. A., Finlay P. R., Kuehl P. J. and Vehring R. 2011. Mechanistic models facilitate efficient development of leucine containing microparticles for pulmonary drug delivery. *International Journal of Pharmaceutics,* 409**,** 156-163.

Fouad E. A., El-Badry M., Mahrous G. M., Alanazi F. K., Neau S. H. and Alsarra I. A. 2011. The use of spray-drying to enhance celecoxib solubility. *Drug Development and Industrial Pharmacy,* 37**,** 1463-1472.

Freiberg S. and Zhu X. X. 2004. Polymer microspheres for controlled drug release. *International Journal of Pharmaceutics,* 282**,** 1-18.

Friesen D. T., Shanker R., Crew M., Smithey D. T., Curatolo W. J. and Nightingale J. A. S. 2008. Hydroxypropyl Methylcellulose Acetate Succinate-Based Spray-Dried Dispersions: An Overview. *Molecular Pharmaceutics,* 5**,** 1003-1019.

Fugh-Berman A. 2000. Herb-drug interactions. *The Lancet,* 355**,** 134-138.

Fukasawa M., Obara S. and eacute 2004. Molecular Weight Determination of Hypromellose Acetate Succinate (HPMCAS) Using Size Exclusion Chromatography with a Multi-Angle Laser Light Scattering Detector. *Chemical and Pharmaceutical Bulletin,* 52**,** 1391-1393.

Gañan-Calvo A. M. 1997. On the theory of electrohydrodynamically driven capillary jets. *Journal of Fluid Mechanics,* 335**,** 165-188.

Gañán-Calvo A. M. 1999. The surface charge in electrospraying: Its nature and its universal scaling laws. *Journal of Aerosol Science,* 30**,** 863-872.

Gañan-Calvo A. M., Davila J. and Barrero A. 1997. Current and droplet size in the electrospraying of liquids. Scaling laws. *Journal of Aerosol Science,* 28**,** 249-275.

Gershanik T. and Benita S. 2000. Self-dispersing lipid formulations for improving oral absorption of lipophilic drugs. *Eur.J.Pharm.Biopharm.,* 50**,** 179-188.

Gibson T. J., McCarty K., McFadyen I. J., Cash E., Dalmonte P., Hinds K. D., Dinerman A. A., Alvarez J. C. and Volkin D. B. 2011. Application of a high-throughput screening procedure with PEG-induced precipitation to compare relative protein solubility during formulation development with IgG1 monoclonal antibodies. *Journal of Pharmaceutical Sciences,* 100**,** 1009-1021.

Gilani K., Najafabadi A. R., Barghi M. and Rafiee-Tehrani M. 2005. The effect of water to ethanol feed ratio on physical properties and aerosolization behavior of spray dried cromolyn sodium particles. *Journal of Pharmaceutical Sciences,* 94**,** 1048-1059.

Giteau A., Venier-Julienne M. C., Aubert-Pouëssel A. and Benoit J. P. 2008. How to achieve sustained and complete protein release from PLGA-based microparticles? *Int J Pharm,* 350**,** 14-26.

Gomez A. and Tang K. 1994. Charge and fission of droplets in electrostatic sprays. *Physics of Fluids,* 6**,** 404-414.

Gorovoi B., Koval V., Gnilosyrov V. and Kashmanova Z. 1969. Quality of paint and varnish coatings of medical products and problems of raising it. *Biomedical Engineering,* 3**,** 209-212.

Grosberg A. Y., Khokhlov A. R. and Jelinski L. W. 1997. Giant Molecules: Here, There, and Everywhere. *American Journal of Physics,* 65**,** 1218-1219.

Guan J., Ferrell N., James Lee L. and Hansford D. J. 2006. Fabrication of polymeric microparticles for drug delivery by soft lithography. *Biomaterials,* 27**,** 4034-4041.

Gunawan L., Johari G. and Shanker R. 2006. Structural Relaxation of Acetaminophen Glass. *Pharmaceutical Research,* 23**,** 967-979.

Gursoy R. N. and Benita S. 2004. Self-emulsifying drug delivery systems (SEDDS) for improved oral delivery of lipophilic drugs. *Biomedicine & Pharmacotherapy,* 58**,** 173-182.

Hancock B. C. and Parks M. 2000. What is the true solubility advantage for amorphous pharmaceuticals? *Pharm. Res.,* 17**,** 397-404.

Hancock B. C., Shamblin S. L. and Zografi G. 1995. Molecular Mobility of Amorphous Pharmaceutical Solids Below Their Glass Transition Temperatures. *Pharmaceutical Research,* 12**,** 799-806.

Hartman R. P. A., Borra J. P., Brunner D. J., Marijnissen J. C. M. and Scarlett B. 1999a. The evolution of electrohydrodynamic sprays produced in the cone-jet mode, a physical model. *Journal of Electrostatics,* 47**,** 143-170.

Hartman R. P. A., Brunner D. J., Camelot D. M. A., Marijnissen J. C. M. and Scarlett B. 1999b. Electrohydrodynamic atomization in the cone-jet mode physical modeling of the liquid cone and jet. *Journal of Aerosol Science,* 30**,** 823-849.

Hartman R. P. A., Brunner D. J., Camelot D. M. A., Marijnissen J. C. M. and Scarlett B. 2000. Jet break-up in electrohydrodynamic atomization in the cone-jet mode *Journal of Aerosol Science,* 31**,** 65-95.

Higuchi T. 1963. Mechanism of sustained-action medication. Theoretical analysis of rate of release of solid drugs dispersed in solid matrices. *Journal of Pharmaceutical Sciences,* 52**,** 1145-1149.

Hong Y., Li Y., Yin Y., Li D. and Zou G. 2008. Electrohydrodynamic atomization of quasi-monodisperse drug-loaded spherical/wrinkled microparticles. *Journal of Aerosol Science,* 39**,** 525-536.

Hu L., Tang X. and Cui F. 2004. Solid lipid nanoparticles (SLNs) to improve oral bioavailability of poorly soluble drugs. *Journal of Pharmacy and Pharmacology,* 56**,** 1527-1535.

Huang X. and Brazel C. S. 2001. On the importance and mechanisms of burst release in matrix-controlled drug delivery systems. *Journal of Controlled Release,* 73**,** 121-136.

I Ré M. 1998. Microencapsulation by spray drying *Drying Technology,* 16**,** 1195-1236.

Ijsebaert J. C., Geerse K. B., Marijnissen J. C. M., Lammers J.-W. J. and Zanen P. 2001. Electro-hydrodynamic atomization of drug solutions for inhalation purposes. *Journal of Applied Physiology,* 91**,** 2735-2741.

Iskandar F., Gradon L. and Okuyama K. 2003. Control of the morphology of nanostructured particles prepared by the spray drying of a nanoparticle sol. *Journal of Colloid and Interface Science,* 265**,** 296-303.

Ivey J. W. and Vehring R. 2010. The use of modeling in spray drying of emulsions and suspensions accelerates formulation and process development. *Computers & Chemical Engineering,* 34**,** 1036-1040.

Janssens S., de Armas H. N., Roberts C. J. and Van den Mooter G. 2008. Characterization of ternary solid dispersions of itraconazole, PEG 6000, and HPMC 2910 E5. *Journal of Pharmaceutical Sciences,* 97**,** 2110-2120.

Janssens S. and Van den Mooter G. 2009. Review: physical chemistry of solid dispersions. *Journal of Pharmacy and Pharmacology,* 61**,** 1571-1586.

Jaworek A. 2008. Electrostatic micro- and nanoencapsulation and electroemulsification: A brief review. *Journal of Microencapsulation,* 25**,** 443-468.

Jaworek A. 2007. Micro- and nanoparticle production by electrospraying. *Powder Technology,* 176**,** 18-35.

Jaworek A. and Krupa A. 1999. Classification of the Modes of EHD Spraying. *Journal of Aerosol Science,* 30**,** 975.

Jaworek A. and Sobczyk A. T. 2008. Electrospraying route to nanotechnology: An overview. *Journal of Electrostatics,* 66**,** 197-219.

Jayasinghe S. N. and Edirisinghe M. J. 2002. Effect of viscosity on the size of relics produced by electrostatic atomization. *Journal of Aerosol Science,* 33**,** 1379-1388.

Jen Tsi Y. 1962. The Viscosity Of Macromolecules In Relation To Molecular Conformation. *In:* C. B. Anfinsen (ed.) *Advances in Protein Chemistry.* Academic Press.

Juppo A. M., Boissier C. and Khoo C. 2003. Evaluation of solid dispersion particles prepared with SEDS. *International Journal of Pharmaceutics,* 250**,** 385-401.

Kanig J. L. 1964. Properties of fused mannitol in compressed tablets. *Journal of Pharmaceutical Sciences,* 53**,** 188-192.

Kaushal A. M., Gupta P. and Bansal A. K. 2004. Amorphous drug delivery systems: molecular aspects, design, and performance. *Crit Rev.Ther.Drug Carrier Syst.,* 21**,** 133-193.

Ke P., Hasegawa S., Al-Obaidi H. and Buckton G. 2012. Investigation of preparation methods on surface/bulk structural relaxation and glass fragility of amorphous solid dispersions. *International Journal of Pharmaceutics,* 422**,** 170-178.

Keck C. M. and Müller R. H. 2006. Drug nanocrystals of poorly soluble drugs produced by high pressure homogenisation. *European Journal of Pharmaceutics and Biopharmaceutics,* 62**,** 3-16.

Kennedy J. P. and Niebergall P. J. 1996. Development and Optimization of a Solid Dispersion Hot-Melt Fluid Bed Coating Method. *Pharmaceutical Development and Technology,* 1**,** 51-62.

Kennedy M., Hu J., Gao P., Li L., Ali-Reynolds A., Chal B., Gupta V., Ma C., Mahajan N., Akrami A. and Surapaneni S. 2008. Enhanced Bioavailability of a Poorly Soluble VR1 Antagonist Using an Amorphous Solid Dispersion Approach: A Case Study. *Molecular Pharmaceutics,* 5**,** 981-993.

Kim H. K., Chung H. J. and Park T. G. 2006. Biodegradable polymeric microspheres with "open/closed" pores for sustained release of human growth hormone. *J.Control Release,* 112**,** 167-174.

Klose D., Siepmann F., Elkharraz K., Krenzlin S. and Siepmann J. 2006. How porosity and size affect the drug release mechanisms from PLGA-based microparticles. *Int.J.Pharm.,* 314**,** 198-206.

Klose D., Siepmann F., Elkharraz K. and Siepmann J. 2008. PLGA-based drug delivery systems: importance of the type of drug and device geometry. *Int.J.Pharm.,* 354**,** 95-103.

Kohane D. S. 2007. Microparticles and nanoparticles for drug delivery. *Biotechnology and Bioengineering,* 96**,** 203-209.

Kojima Y., Ohta T., Shiraki K., Takano R., Maeda H. and Ogawa Y. Effects of spray drying process parameters on the solubility behavior and physical stability of solid dispersions prepared using a laboratory-scale spray dryer. *Drug Development and Industrial Pharmacy,* 0**,** 1-10.

Kumar Naraharisetti P., Yung Sheng Ong B., Wei Xie J., Kam Yiu Lee T., Wang C.-H. and Sahinidis N. V. 2007. In vivo performance of implantable biodegradable preparations delivering Paclitaxel and Etanidazole for the treatment of glioma. *Biomaterials,* 28**,** 886-894.

Lastow O. and Balachandran W. 2006. Numerical simulation of electrohydrodynamic (EHD) atomization. *Journal of Electrostatics,* 64**,** 850-859.

Leane M. M., Sinclair W., Qian F., Haddadin R., Brown A., Tobyn M. and Dennis A. B. Formulation and process design for a solid dosage form containing a spray-dried amorphous dispersion of ibipinabant. *Pharmaceutical Development and Technology,* 0**,** 1-8.

Lemaire V., B+©lair J. and Hildgen P. 2003. Structural modeling of drug release from biodegradable porous matrices based on a combined diffusion/erosion process. *International Journal of Pharmaceutics,* 258**,** 95-107.

Leuenberger H. 2002. Spray Freeze-drying – The Process of Choice for Low Water Soluble Drugs? *Journal of Nanoparticle Research,* 4**,** 111-119.

Leuner C. and Dressman J. 2000. Improving drug solubility for oral delivery using solid dispersions. *Eur. J. Pharm. Biopharm.,* 50**,** 47-60.

Lin J.-C. and Gentry J. W. 2003. Spray Drying Drop Morphology: Experimental Study. *Aerosol Science and Technology,* 37**,** 15-32.

Lindfors L., Skantze P., Skantze U., Westergren J. and Olsson U. 2007. Amorphous Drug Nanosuspensions. 3. Particle Dissolution and Crystal Growth. *Langmuir,* 23**,** 9866-9874.

Lipinski C. 2002. Poor aqueous solubility-an industry wide problem in drug discovery. *Am. Pharm. Rev.,* 5**,** 82-85.

Lipinski C. A. 2000. Drug-like properties and the causes of poor solubility and poor permeability. *Journal of Pharmacological and Toxicological Methods,* 44**,** 235-249.

Liversidge G. G. and Cundy K. C. 1995. Particle size reduction for improvement of oral bioavailability of hydrophobic drugs: I. Absolute oral bioavailability of nanocrystalline danazol in beagle dogs. *International Journal of Pharmaceutics,* 125**,** 91-97.

Löbmann K., Laitinen R., Grohganz H., Gordon K. C., Strachan C. and Rades T. 2011. Coamorphous Drug Systems: Enhanced Physical Stability and Dissolution Rate of Indomethacin and Naproxen. *Molecular Pharmaceutics,* 8**,** 1919-1928.

López-Jerrera J. M. and Gañan-Calvo A. M. 2004. A note on charged capillary jet breakup of conducting liquids: experimental validation of a viscous one-dimensional model. *Journal of Fluid Mechanics,* 501**,** 303-326.

Lu G. W., Hawley M., Smith M., Geiger B. M. and Pfund W. 2006. Characterization of a novel polymorphic form of celecoxib. *Journal of Pharmaceutical Sciences,* 95**,** 305-317.

Lu Y. and Chen S. C. 2004. Micro and nano-fabrication of biodegradable polymers for drug delivery. *Advanced Drug Delivery Reviews,* 56**,** 1621-1633.

Luo C. J., Stoyanov S. D., Stride E., Pelan E. and Edirisinghe M. 2012. Electrospinning versus fibre production methods: from specifics to technological convergence. *Chemical Society Reviews,* 41**,** 4708-4735.

Maa Y. F., Costantino H. R., Nguyen P. A. and Hsu C. C. 1997. The Effect of Operating and Formulation Variables on the Morphology of Spray-Dried Protein Particles. *Pharmaceutical Development and Technology,* 2**,** 213-223.

Maa Y. F., Nguyen P. A. and Hsu S. W. 1998. Spray-drying of air-liquid interface sensitive recombinant human growth hormone. *Journal of Pharmaceutical Sciences,* 87**,** 152-159.

Majerik V., Charbit G., Badens E., Horváth G., Szokonya L., Bosc N. and Teillaud E. 2007. Bioavailability enhancement of an active substance by supercritical antisolvent precipitation. *The Journal of Supercritical Fluids,* 40**,** 101-110.

Masters K. 2002. *Spray Drying in Practice*, SprayDryConsult International.

Meeus J., Chen X., Scurr D. J., Ciarnelli V., Amssoms K., Roberts C. J., Davies M. C. and Den Mooter G. v. 2012. Nanoscale surface characterization and miscibility study of a spray-dried injectable polymeric matrix consisting of poly(lactic-co-glycolic acid) and polyvinylpyrrolidone. *Journal of Pharmaceutical Sciences,* 101**,** 3473-3485.

Megelski S., Stephens J. S., Chase D. B. and Rabolt J. F. 2002. Micro- and Nanostructured Surface Morphology on Electrospun Polymer Fibers. *Macromolecules,* 35**,** 8456-8466.

Merisko-Liversidge E. and Liversidge G. G. 2011. Nanosizing for oral and parenteral drug delivery: A perspective on formulating poorly-water soluble compounds using wet media milling technology. *Advanced Drug Delivery Reviews,* 63**,** 427-440.

Midhun B. S., KT; Manzoor, K; Jayakumar, R; Nair SC; Deepthy M 2011. Preparation of Budesonide-Loaded Polycaprolactone Nanobeads by Electrospraying for Controlled Drug Release. *Journal of Biomaterials Science, Polymer Edition,* 22**,** 2431-44.

Moretti M. D. L., Gavini E., Juliano C., Pirisino G. and Giunchedi P. 2001. Spray-dried microspheres containing ketoprofen formulated into capsules and tablets. *Journal of Microencapsulation,* 18**,** 111-121.

Moustafine R. I., Kabanova T. V., Kemenova V. A. and Van den Mooter G. 2005. Characteristics of interpolyelectrolyte complexes of Eudragit E100 with Eudragit L100. *Journal of Controlled Release,* 103**,** 191-198.

Mu L. and Feng S. S. 2001. Fabrication, characterization and in vitro release of paclitaxel (Taxol) loaded poly (lactic-co-glycolic acid) microspheres prepared by spray drying technique with lipid/cholesterol emulsifiers. *J.Control Release,* 76**,** 239-254.

Müller R. H., Mäder K. and Gohla S. 2000. Solid lipid nanoparticles (SLN) for controlled drug delivery – a review of the state of the art. *European Journal of Pharmaceutics and Biopharmaceutics,* 50**,** 161-177.

Müllertz A., Ogbonna A., Ren S. and Rades T. 2010. New perspectives on lipid and surfactant based drug delivery systems for oral delivery of poorly soluble drugs. *Journal of Pharmacy and Pharmacology,* 62**,** 1622-1636.

Nandiyanto A. B. D. and Okuyama K. 2011. Progress in developing spray-drying methods for the production of controlled morphology particles: From the nanometer to submicrometer size ranges. *Advanced Powder Technology,* 22**,** 1-19.

Nešić S. and Vodnik J. 1991. Kinetics of droplet evaporation. *Chemical Engineering Science,* 46**,** 527-537.

Noyes A. A. and Whitney W. R. 1897. The rate of solution of solid substances in their own solutions *Journal of the American Chemical Society,* 19**,** 930-934.

Nyholm D., Askmark H., Gomes-Trolin C., Knutson T., Lennernäs H., Nyström C. and Aquilonius S.-M. 2003. Optimizing Levodopa Pharmacokinetics: Intestinal Infusion Versus Oral Sustained-Release Tablets. *Clinical Neuropharmacology,* 26**,** 156-163.

O'Hara P. and Hickey A. 2000. Respirable PLGA Microspheres Containing Rifampicin for the Treatment of Tuberculosis: Manufacture and Characterization. *Pharmaceutical Research,* 17**,** 955-961.

Ohara T., Kitamura S., Kitagawa T. and Terada K. 2005. Dissolution mechanism of poorly water-soluble drug from extended release solid dispersion system with ethylcellulose and hydroxypropylmethylcellulose. *International Journal of Pharmaceutics,* 302**,** 95-102.

Okuyama K., Abdullah M., Lenggoro I. W. and Iskandar F. 2006. Preparation of functional nanostructured particles by spray drying. *Advanced Powder Technology,* 17**,** 587-611.

Okuzono T., Ozawa K. and Doi M. 2006. A simple model of skin formation caused by solvent evaporation in polymer solutions. *Phys. Rev. Lett.,* 97.

Panchagnula R. and Thomas N. S. 2000. Biopharmaceutics and pharmacokinetics in drug research. *International Journal of Pharmaceutics,* 201**,** 131-150.

Paradkar A., Ambike A. A., Jadhav B. K. and Mahadik K. R. 2004. Characterization of curcumin–PVP solid dispersion obtained by spray drying. *International Journal of Pharmaceutics,* 271**,** 281-286.

Pareta R. and Edirisinghe M. J. 2006. A novel method for the preparation of biodegradable microspheres for protein drug delivery. *Journal of The Royal Society Interface,* 3**,** 573-582.

Park C. H. and Lee J. 2009. Electrosprayed polymer particles: Effect of the solvent properties. *Journal of Applied Polymer Science,* 114**,** 430-437.

Park Y.-J., Kwon R., Quan Q., Oh D., Kim J., Hwang M., Koo Y., Woo J., Yong C. and Choi H.-G. 2009. Development of novel ibuprofen-loaded solid dispersion with improved bioavailability using aqueous solution. *Archives of Pharmacal Research,* 32**,** 767-772.

Passerini N. and Craig D. Q. M. 2001. An investigation into the effects of residual water on the glass transition temperature of polylactide microspheres using modulated temperature DSC. *Journal of Controlled Release,* 73**,** 111-115.

Patterson J. E., James M. B., Forster A. H., Lancaster R. W., Butler J. M. and Rades T. 2007. Preparation of glass solutions of three poorly water soluble drugs by spray drying, melt extrusion and ball milling. *International Journal of Pharmaceutics,* 336**,** 22-34.

Paudel A. and Van den Mooter G. 2012. Influence of Solvent Composition on the Miscibility and Physical Stability of Naproxen/PVP K 25 Solid Dispersions Prepared by Cosolvent Spray-Drying. *Pharmaceutical Research,* 29**,** 251-270.

Paudel A., Worku Z. A., Meeus J., Guns S. and Van den Mooter G. Manufacturing of solid dispersions of poorly water soluble drugs by spray drying: Formulation and process considerations. *International Journal of Pharmaceutics*.

Peltonen L., Valo H., Kolakovic R., Laaksonen T. and Hirvonen J. 2010. Electrospraying, spray drying and related techniques for production and formulation of drug nanoparticles. *Expert Opinion on Drug Delivery,* 7**,** 705-719.

Percy S. 1872. Improvement in drying and concentrating liquid substances by atomizing.

Pinon-Segundo E., Ganem-Quintanar A., Alonso-Perez V. and Quintanar-Guerrero D. 2005. Preparation and characterization of triclosan nanoparticles for periodontal treatment. *Int.J.Pharm.,* 294**,** 217-232.

Pinto M. 1983. Enterocyte-like differentiation and polarization of the human colon carcinoma cell line Caco-2 in culture. *Biol. Cell,* 47**,** 323-330.

Pouton C. W. 2000. Lipid formulations for oral administration of drugs: non-emulsifying, self-emulsifying and self-microemulsifying drug delivery systems. *European Journal of Pharmaceutical Sciences,* 11, Supplement 2**,** S93-S98.

Qian F., Huang J. and Hussain M. A. 2010. Drug–polymer solubility and miscibility: Stability consideration and practical challenges in amorphous solid dispersion development. *Journal of Pharmaceutical Sciences,* 99**,** 2941-2947.

Qian F., Wang J., Hartley R., Tao J., Haddadin R., Mathias N. and Hussain M. 2012. Solution Behavior of PVP-VA and HPMC-AS-Based Amorphous Solid Dispersions and Their Bioavailability Implications. *Pharmaceutical Research***,** 1-11.

Ranade V. V. 1991. Drug delivery systems 5A. Oral drug delivery. *The Journal of Clinical Pharmacology,* 31**,** 2-16.

Ranganath S., Kee I., Krantz W., Chow P. and Wang C.-H. 2009. Hydrogel Matrix Entrapping PLGA-Paclitaxel Microspheres: Drug Delivery with Near Zero-Order Release and Implantability Advantages for Malignant Brain Tumour Chemotherapy. *Pharmaceutical Research,* 26**,** 2101-2114.

Ranz W. and Marshall W. 1952. Evaporation from drops. *Chem. Eng. Prog,* 48**,** 141-146.

Rasenack N. and Müller B. W. 2004. Micron-Size Drug Particles: Common and Novel Micronization Techniques. *Pharmaceutical Development and Technology,* 9**,** 1-13.

Raula J., Eerikainen H. and Kauppinen E. I. 2004. Influence of the solvent composition on the aerosol synthesis of pharmaceutical polymer nanoparticles. *International Journal of Pharmaceutics,* 284**,** 13-21.

Rautio J., Kumpulainen H., Heimbach T., Oliyai R., Oh D., Jarvinen T. and Savolainen J. 2008. Prodrugs: design and clinical applications. *Nat Rev Drug Discov,* 7**,** 255-270.

Rayleigh L. 1882. On the equilibrium of liquid conducting masses charged with electricity. *Philos. Mag.,* 184.

Regele J. D., Papac M. J., Rickard M. J. A. and Dunn-Rankin D. 2002. Effects of capillary spacing on EHD spraying from an array of cone jets. *Journal of Aerosol Science,* 33**,** 1471-1479.

Reneker D. and Chun I. 1996. Nanometre diameter fibres of polymer, produced by electrospinning. *Nanotechnology,* 7**,** 216.

Riis T., Bauer-Brandl A., Wagner T. and Kranz H. 2007. pH-independent drug release of an extremely poorly soluble weakly acidic drug from multiparticulate extended release formulations. *European Journal of Pharmaceutics and Biopharmaceutics,* 65**,** 78-84.

Rizi K. G., RJ; Donaldson, M; Williams, AC 2011. Production of pH-responsive microparticles by spray drying investigation of experimental paramter effects on morphological and release properties. *Journal of Pharmaceutical Science,* 100**,** 14.

Rodríguez-Spong B., Price C. P., Jayasankar A., Matzger A. J. and Rodríguez-Hornedo N. r. 2004. General principles of pharmaceutical solid polymorphism: A supramolecular perspective. *Advanced Drug Delivery Reviews,* 56**,** 241-274.

Rowe R. S., PJ; Quinn, ME 2009. *Handbook of Pharmaceutical Excipients,* Grayslake, IL, Pharmaceutical Press.

Rumondor A., Stanford L. and Taylor L. 2009. Effects of Polymer Type and Storage Relative Humidity on the Kinetics of Felodipine Crystallization from Amorphous Solid Dispersions. *Pharmaceutical Research,* 26**,** 2599-2606.

Saharan V. A., Kukkar V., Kataria M., Gera M. and Choudhury P. K. 2009. Dissolution Enhancement of Drugs. Part I: Technologies and Effect of Carriers. *International Journal of Health Research,* 2**,** 107-124.

Sambuy Y., De Angelis I., Ranaldi G., Scarino M. L., Stammati A. and Zucco F. 2005. The Caco-2 cell line as a model of the intestinal barrier: influence of cell and culture-related factors on Caco-2 cell functional characteristics. *Cell biology and toxicology,* 21**,** 1-26.

Santesson S., Johansson J., Taylor L. S., Levander I., Fox S., Sepaniak M. and Nilsson S. 2003. Airborne Chemistry Coupled to Raman Spectroscopy. *Analytical Chemistry,* 75**,** 2177-2180.

Sastry S. V., Nyshadham J. R. and Fix J. A. 2000. Recent technological advances in oral drug delivery - a review. *Pharmaceutical Science & Technology Today,* 3**,** 138-145.

Schiffter H. and Lee G. 2007. Single-droplet evaporation kinetics and particle formation in an acoustic levitator. Part 1: Evaporation of water microdroplets assessed using boundary-layer and acoustic levitation theories. *Journal of Pharmaceutical Sciences,* 96**,** 2274-2283.

Scoutaris N., Hook A., Gellert P., Roberts C., Alexander M. and Scurr D. 2012. ToF-SIMS analysis of chemical heterogenities in inkjet micro-array printed drug/polymer formulations. *Journal of Materials Science: Materials in Medicine,* 23**,** 385-391.

Sekiguchi K. O., U 1964. Studies on absorption of eutectic mixture. II. Absorption of fused agglomerated of chloramphenicol urea in rabbits. *Chem. Pharm. Bull.,* 12**,** 134-136.

Serajuddin A. T. 1999. Solid dispersion of poorly water-soluble drugs: early promises, subsequent problems, and recent breakthroughs. *Journal of Pharmaceutical Sciences,* 88**,** 1058-1066.

Serajuddin A. T. M. 2007. Salt formation to improve drug solubility. *Advanced Drug Delivery Reviews,* 59**,** 603-616.

Sethia S. and Squillante E. 2004. Solid dispersion of carbamazepine in PVP K30 by conventional solvent evaporation and supercritical methods. *International Journal of Pharmaceutics,* 272**,** 1-10.

Shegokar R. and Müller R. H. 2010. Nanocrystals: Industrially feasible multifunctional formulation technology for poorly soluble actives. *International Journal of Pharmaceutics,* 399**,** 129-139.

Shenoy S., Bates W., Frisch H. and Wnek G. 2005a. Role of chain entanglements on fiber formation during electrospinning of polymer solutions: good solvent, non-specific polymer?polymer interaction limit. *Polymer,* 46**,** 3372-3384.

Shenoy S. L., Bates W. D., Frisch H. L. and Wnek G. E. 2005b. Role of chain entanglements on fiber formation during electrospinning of polymer solutions: good solvent, non-specific polymer-polymer interaction limit. *Polymer,* 46**,** 3372-3384.

Simonelli A. P., Mehta S. C. and Higuchi W. I. 1969. Dissolution Rates of High Energy Polyvinylpyrrolidone (PVP)-Sulfathiazole Coprecipitates. *Journal of Pharmaceutical Sciences,* 58**,** 538-549.

Six K., Murphy J., Weuts I., Craig D. Q. M., Verreck G., Peeters J., Brewster M. and Van den Mooter G. 2003. Identification of Phase Separation in Solid Dispersions of Itraconazole and Eudragit® E100 Using Microthermal Analysis. *Pharmaceutical Research,* 20**,** 135-138.

Six K., Verreck G., Peeters J., Brewster M. and Mooter G. V. d. 2004. Increased physical stability and improved dissolution properties of itraconazole, a class II drug, by solid dispersions that combine fast- and slow-dissolving polymers. *Journal of Pharmaceutical Sciences,* 93**,** 124-131.

Smallwood I. M. 1996. *Handbook of organic solvent properties*, Arnold.

Smith J. N., Flagan R. C. and Beauchamp J. L. 2002. Droplet Evaporation and Discharge Dynamics in Electrospray Ionization. *The Journal of Physical Chemistry A,* 106**,** 9957-9967.

Sollohub K. and Cal K. 2010. Spray drying technique: II. Current applications in pharmaceutical technology. *Journal of Pharmaceutical Sciences,* 99**,** 587-597.

Soppimath K. S., Aminabhavi T. M., Kulkarni A. R. and Rudzinski W. E. 2001. Biodegradable polymeric nanoparticles as drug delivery devices. *Journal of Controlled Release,* 70**,** 1-20.

Srinivasarao M., Collings D., Philips A. and Patel S. 2001. Three-Dimensionally Ordered Array of Air Bubbles in a Polymer Film. *Science,* 292**,** 79-83.

Strachan C. J., Rades T., Gordon K. C. and Rantanen J. 2007. Raman spectroscopy for quantitative analysis of pharmaceutical solids. *Journal of Pharmacy and Pharmacology,* 59**,** 179-192.

Sweetana S. and Akers M. J. 1996. Solubility principles and practices for parenteral drug dosage form development. *PDA journal of pharmaceutical science and technology / PDA,* 50**,** 330-342.

Takáts Z., Wiseman J. M., Gologan B. and Cooks R. G. 2004. Mass Spectrometry Sampling Under Ambient Conditions with Desorption Electrospray Ionization. *Science,* 306**,** 471-473.

Tanaka N., Imai K., Okimoto K., Ueda S., Tokunaga Y., Ibuki R., Higaki K. and Kimura T. 2006. Development of novel sustained-release system, disintegration-controlled matrix tablet (DCMT) with solid dispersion granules of nilvadipine (II): In vivo evaluation. *Journal of Controlled Release,* 112**,** 51-56.

Tang K. and Gomez A. 1996. Monodisperse Electrosprays of Low Electric Conductivity Liquids in the Cone-Jet Mode. *Journal of Colloid and Interface Science,* 184**,** 500-511.

Taylor G. 1964. Disintegration of water drops in an electric field. *Proceedings of the Royal Society, London,* A 280**,** 383-397.

Taylor L. S. and Zografi G. 1997. Spectroscopic Characterization of Interactions Between PVP and Indomethacin in Amorphous Molecular Dispersions. *Pharmaceutical Research,* 14**,** 1691-1698.

Teberekidis V. I. and Sigalas M. P. 2007. Theoretical study of hydrogen bond interactions of felodipine with polyvinylpyrrolidone and polyethyleneglycol. *Journal of Molecular Structure: THEOCHEM,* 803**,** 29-38.

Testa B. 2009. Prodrugs: bridging pharmacodynamic/pharmacokinetic gaps. *Current Opinion in Chemical Biology,* 13**,** 338-344.

Tsapis N., Bennett D., Jackson B., Weitz D. A. and Edwards D. A. 2002. Trojan particles: Large porous carriers of nanoparticles for drug delivery. *Proceedings of the National Academy of Sciences,* 99**,** 12001-12005.

Tsapis N., Dufresne E. R., Sinha S. S., Riera C. S., Hutchinson J. W., Mahadevan L. and Weitz D. A. 2005. Onset of Buckling in Drying Droplets of Colloidal Suspensions. *Physical Review Letters,* 94**,** 018302.

Tuckermann R., Puskar L., Zavabeti M., Sekine R. and McNaughton D. 2009. Chemical analysis of acoustically levitated drops by Raman spectroscopy. *Analytical and Bioanalytical Chemistry,* 394**,** 1433-1441.

Urbanetz N. A. and Lippold B. C. 2005. Solid dispersions of nimodipine and polyethylene glycol 2000: dissolution properties and physico-chemical characterisation. *European Journal of Pharmaceutics and Biopharmaceutics,* 59**,** 107-118.

Valo H., Peltonen L., Vehvilainen S., Karjalainen M., Kostiainen R., Laaksonen T. and Hirvonen J. 2009. Electrospray encapsulation of hydrophilic and hydrophobic drugs in poly(L-lactic acid) nanoparticles. *Small,* 5**,** 1791-1798.

Van den Mooter G., Weuts I., De Ridder T. and Blaton N. 2006. Evaluation of Inutec SP1 as a new carrier in the formulation of solid dispersions for poorly soluble drugs. *International Journal of Pharmaceutics,* 316**,** 1-6.

Van den Mooter G., Wuyts M., Blaton N., Busson R., Grobet P., Augustijns P. and Kinget R. 2001. Physical stabilisation of amorphous ketoconazole in solid dispersions with polyvinylpyrrolidone K25. *European Journal of Pharmaceutical Sciences,* 12**,** 261-269.

Van Drooge D. J., Hinrichs W. L. J., Visser M. R. and Frijlink H. W. 2006. Characterization of the molecular distribution of drugs in glassy solid dispersions at the nano-meter scale, using differential scanning calorimetry and gravimetric water vapour sorption techniques. *International Journal of Pharmaceutics,* 310**,** 220-229.

Van Eerdenbrugh B. and Taylor L. S. 2010. Small Scale Screening To Determine the Ability of Different Polymers To Inhibit Drug Crystallization upon Rapid Solvent Evaporation. *Molecular Pharmaceutics,* 7**,** 1328-1337.

Van Nijlen T., Brennan K., Van den Mooter G., Blaton N., Kinget R. and Augustijns P. 2003. Improvement of the dissolution rate of artemisinin by means of supercritical fluid technology and solid dispersions. *International Journal of Pharmaceutics,* 254**,** 173-181.

Vasconcelos T., Sarmento B. and Costa P. 2007. Solid dispersions as strategy to improve oral bioavailability of poor water soluble drugs. *Drug Discov. Today,* 12**,** 1068-1075.

Vehring R. 2008. Pharmaceutical particle engineering via spray drying. *Pharm. Res.,* 25**,** 999-1022.

Vehring R., Foss W. R. and Lechuga-Ballesteros D. 2007. Particle formation in spray drying. *Journal of Aerosol Science,* 38**,** 728-746.

Verreck G., Chun I., Peeters J., Rosenblatt J. and Brewster M. E. 2003. Preparation and Characterization of Nanofibers Containing Amorphous Drug Dispersions Generated by Electrostatic Spinning. *Pharmaceutical Research,* 20**,** 810-817.

Vippagunta S. R., Wang Z., Hornung S. and Krill S. L. 2007. Factors affecting the formation of eutectic solid dispersions and their dissolution behavior. *Journal of Pharmaceutical Sciences,* 96**,** 294-304.

Walton D. E. and Mumford C. J. 1999. The morphology of spray-dried particles: The effect of process variables upon the morphology of spray-dried particles. *Chemical engineering reseach & design,* 77.

Wang F. J. and Wang C. H. 2002. Sustained release of etanidazole from spray dried microspheres prepared by non-halogenated solvents. *Journal of Controlled Release,* 81**,** 263-280.

Warren D. B., Benameur H., Porter C. J. H. and Pouton C. W. 2010. Using polymeric precipitation inhibitors to improve the absorption of poorly water-soluble drugs: A mechanistic basis for utility. *Journal of Drug Targeting,* 18**,** 704-731.

Washington C. 1990. Drug release from microdisperse systems: a critical review. *International Journal of Pharmaceutics,* 58**,** 1-12.

Weiler C., Egen M., Trunk M. and Langguth P. 2010. Force control and powder dispersibility of spray dried particles for inhalation. *Journal of Pharmaceutical Sciences,* 99**,** 303-316.

Wendorf J., Chesko J., Kazzaz J., Ugozzoli M., Vajdy M., O'Hagan D. and Singh M. 2008. A comparison of anionic nanoparticles and microparticles as vaccine delivery systems. *Human Vaccines,* 4**,** 44-49.

Weuts I., Kempen D., Verreck G., Decorte A., Heymans K., Peeters J., Brewster M. and Mooter G. V. d. 2005. Study of the physicochemical properties and stability of solid dispersions of loperamide and PEG6000 prepared by spray drying. *European Journal of Pharmaceutics and Biopharmaceutics,* 59**,** 119-126.

Wong S. M., Kellaway I. W. and Murdan S. 2006. Enhancement of the dissolution rate and oral absorption of a poorly water soluble drug by formation of surfactant-containing microparticles. *International Journal of Pharmaceutics,* 317**,** 61-68.

Wu Y. and Clark R. L. 2007. Controllable porous polymer particles generated by electrospraying. *Journal of Colloid and Interface Science,* 310**,** 529-535.

Wu Y., MacKay J. A., McDaniel R., Chilkoti A. and Clark R. L. 2008. Fabrication of Elastin-Like Polypeptide Nanoparticles for Drug Delivery by Electrospraying. *Biomacromolecules,* 10**,** 19-24.

Xie J., Lim L. K., Phua Y., Hua J. and Wang C.-H. 2006a. Electrohydrodynamic atomization for biodegradable polymeric particle production. *Journal of Colloid and Interface Science,* 302**,** 103-112.

Xie J., Marijnissen J. C. and Wang C. H. 2006b. Microparticles developed by electrohydrodynamic atomization for the local delivery of anticancer drug to treat C6 glioma in vitro. *Biomaterials,* 27**,** 3321-3332.

Xie J., Tan R. S. and Wang C.-H. 2008. Biodegradable microparticles and fiber fabrics for sustained delivery of cisplatin to treat C6 glioma in vitro. *Journal of Biomedical Materials Research Part A,* 85A**,** 897-908.

Xu J., Bovet L. L. and Zhao K. 2008. Taste masking microspheres for orally disintegrating tablets. *International Journal of Pharmaceutics,* 359**,** 63-69.

Xu Y. and Hanna M. A. 2006. Electrospray encapsulation of water-soluble protein with polylactide. Effects of formulations on morphology, encapsulation efficiency and release profile of particles. *Int. J. Pharm.,* 320**,** 30-36.

Xue L., Mao L., Cai Q., Yang X. and Jin R. 2010. Preparation of amino acid ester substituted polyphosphazene microparticles via electrohydrodynamic atomization. *Polymers for Advanced Technologies,* 22**,** 2009-2016.

Yang Y. Y., Chung T. S., Bai X. L. and Chan W. K. 2000. Effect of preparation conditions on morphology and release profiles of biodegradable polymeric microspheres containing protein fabricated by double-emulsion method. *Chemical Engineering Science,* 55**,** 2223-2236.

Yao J., Kuang Lim L., Xie J., Hua J. and Wang C. H. 2008. Characterization of electrospraying process for polymeric particle fabrication. *Journal of Aerosol Science,* 39**,** 987-1002.

York P. 1999. Strategies for particle design using supercritical fluid technologies. *Pharmaceutical Science & Technology Today,* 2**,** 430-440.

Yu D.-G., Branford-White C., Shen X.-X., Zhang X.-F. and Zhu L.-M. 2010a. Solid Dispersions of Ketoprofen in Drug-Loaded Electrospun Nanofibers. *Journal of Dispersion Science and Technology,* 31**,** 902-908.

Yu D.-G., Branford-White C., White K., Li X.-L. and Zhu L.-M. 2010b. Dissolution Improvement of Electrospun Nanofiber-Based Solid Dispersions for Acetaminophen. *AAPS PharmSciTech,* 11**,** 809-817.

Yu D.-G., Williams G. R., Yang J.-H., Wang X., Yang J.-M. and Li X.-Y. 2011. Solid lipid nanoparticles self-assembled from electrosprayed polymer-based microparticles. *Journal of Materials Chemistry,* 21**,** 15957-15961.

Yu D.-G., Yang J.-M., Branford-White C., Lu P., Zhang L. and Zhu L.-M. 2010c. Third generation solid dispersions of ferulic acid in electrospun composite nanofibers. *International Journal of Pharmaceutics,* 400**,** 158-164.

Yu D., Shen X., Branford-White C., White K., Zhu L. and Bligh A. 2009. Oral fast-dissolving drug delivery membranes prepared from electrospun polyvinylpyrrolidone ultrafine fibers. *Nanotechnology,* 20**,** 055104.

Yüksel N., Karataş A., Özkan Y., Savaşer A., Özkan S. A. and Baykara T. 2003. Enhanced bioavailability of piroxicam using Gelucire 44/14 and Labrasol: in vitro and in vivo evaluation. *European Journal of Pharmaceutics and Biopharmaceutics,* 56**,** 453-459.

Zeleny J. 1917. Instability of Electrified Liquid Surfaces. *Physical Review,* 10**,** 1-6.

Zeleny J. 1915. On the conditions of instability of liquid drops, with applications to the electrical discharge from liquid points. *Proceedings of the Cambridge Philosophical Society,* 18**,** 71-93.

Zerrouk N., Chemtob C., Arnaud P., Toscani S. and Dugue J. 2001. In vitro and in vivo evaluation of carbamazepine-PEG 6000 solid dispersions. *International Journal of Pharmaceutics,* 225**,** 49-62.

Zhang W., Chen M., Zha B. and Diao G. 2012. Correlation of polymer-like solution behaviors with electrospun fiber formation of hydroxypropyl-[small beta]-cyclodextrin and the adsorption study on the fiber. *Physical Chemistry Chemical Physics,* 14**,** 9729-9737.

Zhou D., Grant D. J. W., Zhang G. G. Z., Law D. and Schmitt E. A. 2007. A calorimetric investigation of thermodynamic and molecular mobility contributions to the physical stability of two pharmaceutical glasses. *Journal of Pharmaceutical Sciences,* 96**,** 71-83.

Zhou X. D., Zhang S. C., Huebner W., Ownby P. D. and Gu H. 2001. Effect of the solvent on the particle morphology of spray dried PMMA. *Journal of Materials Science,* 36**,** 3759-3768.

Zhu Q., Harris M. T. and Taylor L. S. 2012. Modification of Crystallization Behavior in Drug/Polyethylene Glycol Solid Dispersions. *Molecular Pharmaceutics,* 9**,** 546-553.